Understanding the role of mitochondrial Haemoglobin- an *in-silico* approach

Gunjan Katyal

Thesis submitted to the University of Nottingham for the degree of Doctor of Philosophy

December 2021

Supervisory team: Professor Lisa Chakrabarti, Doctor Reinhard Stoger and Professor Richard Emes

School of Veterinary Medicine and Science

University of Nottingham

Vice Chancellor's Scholarship for Research Excellence (International)
2018-2021

Abstract

About 60 years ago, Nobel Laureate, Max F. Perutz, who discovered the structure of the globular protein Haemoglobin (Hb), suggested that changes in the molecule were seen in neurodegenerative diseases and argued its role as a drug receptor. Neurodegeneration is more likely to be affected by a fundamental yet inevitable phenomenon of ageing. There has been sufficient evidence that changes in the powerhouse of the cell, mitochondria dysfunction, is one of the hallmarks of ageing and neurodegeneration. Yet we are still far off from deciphering direct links and pathways conclusively leading to it. The project was aimed to find that, if Hb is localised in the mitochondria, it must influence the proteins situated there. Hence to validate the theory the project entailed working on the unique and mysterious icefish that are the only vertebrate organisms without Hb and acted as a model to understand the differences observed in the presence/absence of this protein.

In general protein-protein interactions (PPI) can influence many biological processes, metabolic pathways and, cell-to-cell interactions [1]. These interactions could be transient or permanent [2], where transient interactions would form signalling pathways and permanent interactions will form a stable protein complex. New functionality of a characterised protein or a new protein can be predicted on the evidence of their interaction with well characterised proteins in the proteome.

PPI data can be categorised into three types,
-*in vitro*, which includes liquid chromatography (LC), gel-electrophoresis, western blots, coimmunoprecipitation, mass spectrophotometry (MS), X-ray crystallographic, NMR techniques,
-*in vivo*, where the techniques are involved with the whole organism,
-*in silico*, techniques involving, sequence and structural based approaches, chromosome proximity, phylogenetic tree, and proteins/gene expression data.

The thesis entails *in vitro* and *in silico* approaches combined to decipher a Hb interactome. The three result chapters were primarily focussed on important mitochondrial proteins associated with mitochondrial Hb. (i) First, new insights on the ATP synthase mitochondrial encoded F_o motor subunits, ATP6 and ATP8 in the icefish were established using sequential and structural comparison of the nucleotide and protein sequences, where changes were observed in the Hb-less icefish *C. gunnari*. The changes in protein expression were also observed for ATP6 protein in the icefish using immunoblotting (ii) Second, changes in the mitochondrial proteome of the icefish were observed when compared to closely related red-blooded fish, in two different muscle tissues, red and white, using LC/LC-MS and network analysis. The changes were observed in important pathways such as citric acid cycle, ribosome machinery and fatty acid degradation. (iii) Finally, the last chapter aimed at understanding the sequential and structural changes in the 3' remnant haemoglobin alpha (HbA) protein in the icefish. A plausible new role for HbA was suggested, where interaction between natural inhibitor of ATP synthase, ATPIF1 and HbA was established using molecular docking and simulations and supported by *in vitro* co-immunoprecipitation/immunoblotting. In summary the thesis adds onto our understanding of mitochondrial Hb and its putative role in the mitochondria.

List of Publications:

1) **Sequence and structure comparison of ATP synthase F0 subunits 6 and 8 in notothenioid fish.**
Gunjan Katyal[1], *Brad Ebanks*[1], *Magnus Lucassen*[2], *Chiara Papetti*[3], *Lisa Chakrabarti*[1,4]
doi: https://doi.org/10.1371/journal.pone.0245822
[1]*School of Veterinary Medicine and Science, University of Nottingham, Sutton Bonington, LE12 5RD, UK*
[2] *Alfred Wegener Institute, Bremerhaven, Germany*
[3]*Biology Department, University of Padova, via U. Bassi, 58/b, 35121, Padova, Italy*
[4] *MRC-Versus Arthritis Centre for Musculoskeletal Ageing Research, UK,*
Corresponding author: lisa.chakrabarti@nottingham.ac.uk

2) **Proteomes of icefish muscle mitochondria point to important differences in ATP synthase sub-units compared with closely related red blooded species. (Submitted, under review)**
Gunjan Katyal[1], *Brad Ebanks*[1], *Freya Shephard*[1], *Chiara Papetti*[2], *Magnus Lucassen*[3], *Lisa Chakrabarti*[1,4]
[1]*School of Veterinary Medicine and Science, University of Nottingham, Sutton Bonington, LE12 5RD, UK*
[2]*Biology Department, University of Padova, via U. Bassi, 58/b, 35121, Padova, Italy*
[3]*Alfred Wegener Institute, Bremerhaven, Germany*
[4] *MRC-Versus Arthritis Centre for Musculoskeletal Ageing Research, UK,*
Corresponding author: lisa.chakrabarti@nottingham.ac.uk

3) **The dysregulated Pink1- Drosophila mitochondrial proteome is partially corrected with exercise**
Brad Ebanks[1], *, *Thomas L. Ingram*[1], *, ***Gunjan Katyal***[1], *John R. Ingram*[1], *Nicoleta Moisoi*[2], *Lisa Chakrabarti*[1,3]
Aging (Albany NY). 2021 Jun 1;13 (11):14709-14728
https://doi.org/10.18632/aging.203128
[1]*School of Veterinary Medicine and Science, University of Nottingham, Sutton Bonington, LE12 5RD, UK*
[2]*Leicester School of Pharmacy, Leicester Institute for Pharmaceutical Innovation, De Montfort University, The Gateway, Leicester LE1 9BH, UK*
[3]*MRC-Versus Arthritis Centre for Musculoskeletal Ageing Research, UK,*
Corresponding author: lisa.chakrabarti@nottingham.ac.uk

4) **Mitochondrial homeostasis in cellular models of Parkinson's Disease**
Nina Krako Jakovljevic[1], *Brad Ebanks*[2], ***Gunjan Katyal***[2], *Lisa Chakrabarti*[2,3], *Ivanka Markovic*[4], *Nicoleta Moisoi*[5]
Journal: ***Bioenergetics Communications***
[1]*Clinic for Endocrinology, Diabetes and Metabolic Diseases, University Clinical Center of Serbia, Faculty of Medicine, University of Belgrade Dr Subotica 13, 11000 Belgrade, Serbia*
[2]*School of Veterinary Medicine and Science, University of Nottingham, Sutton Bonington, LE12 5RD, UK*
[3]*MRC-Versus Arthritis Centre for Musculoskeletal Ageing Research, UK,*
[4]*Institute for Medical and Clinical Biochemistry, Faculty of Medicine, University of 13 Belgrade, Pasterova 2, 11000 Belgrade, Serbia*
[5]*Leicester School of Pharmacy, Leicester Institute for Pharmaceutical Innovation, De Montfort University, The Gateway, Leicester LE1 9BH, UK*
Corresponding authors: nicoleta.moisoi@dmu.ac.uk and ivanka.markovic@med.bg.ac.rs

5) **Exercising D. melanogaster Modulates the Mitochondrial Proteome and Physiology - The Effect on Lifespan Depends Upon Age and Sex**
Brad Ebanks[1], *, *Ying Wang*[1], *, ***Gunjan Katyal***[1], *Chloe Sargent*[2], *Thomas Ingram*[1], *Antonia Bowman*[1], *Nicoleta Moisoi*[3], *Lisa Chakrabarti*[1,4]
Int. J. Mol. Sci. 2021, 22 (21), 11606; https://doi.org/10.3390/ijms222111606
[1]*School of Veterinary Medicine and Science, University of Nottingham, Sutton Bonington, LE12 5RD, UK*

[2] *School of Bioscience, University of Nottingham, Sutton Bonington, LE12 5RD, UK*
[3]*Leicester School of Pharmacy, Leicester Institute for Pharmaceutical Innovation, De Montfort University, The Gateway, Leicester LE1 9BH, UK*
[4]*MRC-Versus Arthritis Centre for Musculoskeletal Ageing Research, UK,*
Corresponding author: lisa.chakrabarti@nottingham.ac.uk

Acknowledgements

First and foremost, I am extremely grateful to my supervisor Professor Lisa Chakrabarti, for giving me an opportunity to work in her lab, consistently pushing me to thrive for the best, for her invaluable advice, support, and patience. A mentor who not only pushes you to do the best, but also makes you believe in the best, that you didn't know existed before.

There are few lines in Hindi by famous Indian poet Kabir Das, that I would like to dedicate to my supervisor:

गुरु कुम्हार शिष कुंभ है, गढ़ि गढ़ि काढ़े खोट ।

अंतर हाथ सहार दै, बाहर बाहै चोट ॥

which translates to, "*a mentor is like a skilled potter who can identify an unbaked earthen pot and being a skilled artisan, turns it into a final fully shaped pot. To ensure the final product, the potter has one palm inside of the pot while the other hand shapes it from outside to make sure the pot does not break or shatter and turns into an immaculate flawless pot*!"

Secondly, I would like to thank the University of Nottingham Vice Chancellor's Scholarship for Research Excellence (International) 2018-2021, without which this Ph.D. would haven't been possible. I am very thankful to the University for providing an excellent multi-cultural environment and active support for the mental health of its student. As a mental health advocate, I cannot thank enough for this, because the PhD journey though very learning, can be extremely stressful.

I also like to extend my gratitude to my second supervisor Dr. Reinhard Stoger, and my third supervisor, Professor Richard Emes, for their invaluable advice as and when I needed it. I would also like to thank ever smiling and very supportive Dr. Catrin Rutland for being my internal examiner and helping me to do better in my Ph.D.

I would like to thank my wonderful parents who have graciously supported me in all my endeavours, my pillar of strength my mother Mrs. Shashi Katyal, and my father, late Mr. Sudhir Katyal whom I lost during the very start of my Ph.D., but I am certain that he must be super proud today wherever he is. Nothing would have been possible without my sister, Rupali's constant support from across the globe, whom I have messaged every day and cried with, and my brother-in-law, Dr. Varun, who has been a constant motivator and inspiration in my life. I would like to mention a little fire and constant support, my youngest cousin Bhavini, who to date sends me motivational messages and is my personal cheerleader. I also dedicate this to my two aunts who are teachers themselves, Dimple and Meeta, thank you for your guidance and support! And lastly, my grandparents, JC Khanna and Usha who sent their blessings to me every single day.

Nothing would have been closely possible without the support of my close friends, the list is long but it's worth mentioning every one of them who supported me dearly during my Ph.D., and the most difficult times, first losing my dad, and then through the pandemic. My friends from India, Jaya, Shefali, Megha, Shweta, Prakhar,

Vaibhav, thank you for constantly checking on me and pushing me to do my best. My Nottingham friends, Vivek, Amar, William, Vicky and Neelima. I would also like to acknowledge and thank Benjamin for all the kindness and encouragement.

To my Vet school friends, Anitha and Emma, for sharing the best and the worst times of Ph.D. together.

Special shout out, to my colleague, Brad Ebanks, who has been a great lab mate, a young man full of ideas and dedication, so very inspiring to see. Also, all the other people I came across in this wonderful journey of three years. Thank you!

Hypothesis

The dynamic location of haemoglobin in mitochondria plays an important role in regulation of mitochondrial function and overall metabolic health.

AIM

To establish and understand more about mitochondrial haemoglobin using insights gained from the Antarctic icefish which are natural knockouts for haemoglobin.

Table of contents

Chapter 1 : Introduction

1.1 Mitochondria

Mitochondria are organelles that produce adenosine triphosphate (ATP) via oxidative phosphorylation (OxPhos), a process that involves the transfer of electrons between multi-subunit complexes (I to IV) of the electron transport chain (ETC) coupled with the reduction of molecular oxygen. They are thought to have originated from a bacterial ancestor and are known to maintain their own genome[3]. Having a small genome, in the form of mitochondrial DNA that encodes thirteen mitochondrial proteins in humans involved in oxidative phosphorylation complexes, out of which two are part of the complex V, ATP8 and ATP6. Nevertheless, most mitochondrial proteins are encoded in the nucleus and are imported into mitochondria. Mitochondria are also known for their involvement in many vital cellular activities such as apoptosis, calcium homeostasis and regulation of cell homeostasis. The electrochemical proton gradient across the inner mitochondrial membrane required by ATP synthase is maintained by the electron transport chain proton-pumping complexes I, III and IV.

Complex I is the proton pumping complex of the mitochondrial respiratory chain and is one of the largest complexes. Complex I couples electron transfer from NADH (reduced nicotinamide adenine dinucleotide) to ubiquinone to the translocation of four protons from the mitochondrial matrix to the intermembrane space (IMS), that provides much of the proton-motive force for adenosine triphosphate synthesis[4]. Mammalian complex I is built of 45 (44 unique) subunits. There are 14 central subunits forming the core of the complex [5].

Complex II, also known as the succinate dehydrogenase, accepts electrons from succinate which is also an intermediate in citric acid cycle. Succinate is oxidised to fumarate and two electrons are accepted by FAD within complex II, which are transferred to Fe-S clusters and subsequently to coenzyme Q. But unlike complex I, no protons are transferred across the membrane by complex II[6]. Coenzyme Q transfers electrons to complex III.

Complex III or cytochrome c reductase is made up of cytochrome b, Rieske subunits (containing two Fe-S clusters) and cytochrome c proteins. The haem containing complex alternates between two ferrous states during electron transfer. Unlike in complex I and complex II, cytochrome c can only accept one electron at a time hence the process occurs in two steps, releasing four protons into the intermembrane space at the end of the cycle[7,8].

Complex IV or cytochrome c oxidase, oxidises cytochrome c and transfers the electrons to oxygen which is the final electron carrier in aerobic cellular respiration. The bound dioxygen species are converted into molecules of water and release four protons into the intermembrane space[9].

Complex V or ATP synthase (ATPase), utilises the ETC generated proton gradient across the inner mitochondrial membrane to form ATP. This complex is discussed in detail in the subsequent sections.

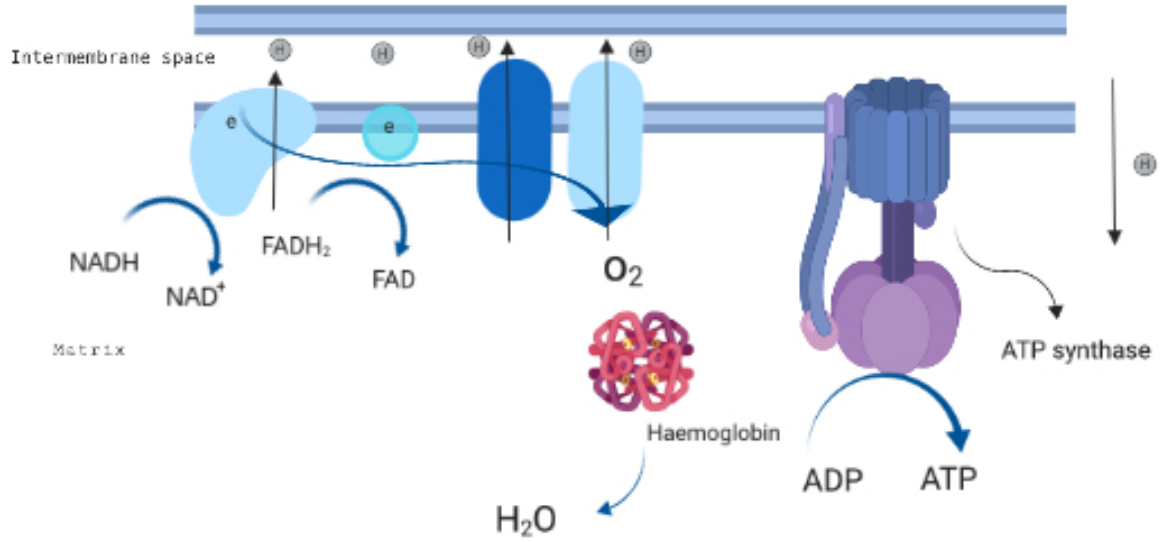

Figure 1-1 Representation of the mitochondrial respiratory chain complexes and the oxidative phosphorylation system, showing plausible localisation and the role of haemoglobin in mitochondria.

Mitochondria play an important role in multiple functions in addition to ATP production which makes it highly complex and crucial to understand mitochondrial dynamics and pathways involved in it[10].Due to this, there has been an increasing interest in the structure and function of mitochondrial proteins [11–14]. Efforts have been made to decipher the structure, assembly process, coupling mechanism and associated pathologies of respiratory chain complexes[15,16]. However, the exact organisation of the many proteins and super-complexes involved is still a challenge due to changes in stoichiometry that vary with different physiological conditions and cell types[17,18].

1.1.1 Mitochondrial DNA

Mitochondria maintain a small genome that encodes 13 mitochondrial proteins and 24 RNAs in humans. The human mtDNA genome compromises 16, 569 base pairs, with an inner 'light' strand and outer 'heavy' strand[19]. The replication machinery of mtDNA consists of mtDNA polymerase γ (Pol γ), a helicase (Twinkle or PEO1), topoisomerase I, mtDNA single-stranded DNA-binding protein and others. There are two models of DNA replication that have been proposed, 'stand-displacement' model and strand-coupled replication. In strand-displacement model, replication is initiated by transcription within non-coding mtDNA displacement loop and proceeds clockwise from the origin of heavy strand replication until the origin of light-strand replication is exposed leading to light-strand synthesis[20]. Stranded-

coupled replication only occurs in certain circumstances[21]. Overall mtDNA is extremely compact where each protein and rRNA genes are immediately flanked by at least one tRNA gene[19]. And yet even though the overall genetic content and gene order is remarkedly conserved among vertebrates, the nucleotide sequence and organisation of mtDNA regulatory elements of the genome vary considerably.

The mitochondrial mRNA translation is controlled by several regulatory proteins that eventually also regulate the assembly of OxPhos machinery. The proteins encoded by mtDNA are part of complex I, complex III, complex IV and complex V. NADH dehydrogenase 1 (MTND1)-MTND6 and MTND4L of complex I are encoded by mtDNA. Cytochrome b, a central subunit of the cytochrome c reductase complex (complex III) is encoded by mtDNA[22]. The core of the cytochrome c complex (complex IV) comprises three mtDNA encoded proteins CO1, CO2 and CO3 part of cytochrome c oxidase I[23]. ATP6, ATP8 and ATP9 of complex V are encoded by mtDNA where ATP6 and ATP8 are encoded on bicistronic mRNA transcript, that is encoding both the proteins by a single mRNA transcript [24]. In cold environments, protective mtDNA lineages seem to have arisen including relative uncoupling of mitochondria to increase heat generation at the expense of ATP production [25,26].

Defects in *mtDNA* results in impaired synthesis of mtDNA encoded ETC complex subunits, ultimately resulting in an impaired OxPhos and energy deficiency[27]. Defects in the mtDNA are more common than in nuclear DNA, such as basal mutations. mtDNA lies close to the ETC complexes in the mitochondrial matrix and is usually subjected to reactive oxygen species (ROS) which could result in mtDNA mutations and contribute in the process of ageing[28]. Since mtDNA and mitochondria are ubiquitous it can affect every tissue in the body. There are three types of mtDNA mutations, namely, single deletions, point mutations in tRNA genes and point mutations in protein coding genes. mtDNA variation affects our physiology and our ability to adapt to environmental change such as adjustment to thermal stress and activity demands[29].

1.1.2 Mitochondria Role in signalling

Mitochondria are not isolated organelles but form a dynamic network within the cell and are continuously fusing and dividing. Mitochondria have about 1500 proteins that perform multiple functions originating from two genomes, mitochondrial and nuclear[30]. Most functions are encoded in the nucleus and imported to the cytosol for translation. This requires the mitochondrial gene expression to be tightly connected with inter-compartmental crosstalk with the cell and other organelles for proper mitochondrial function. Mitochondria are known to regulate the different genes to facilitate different cellular functions. There are four main mechanisms, regulation of TCA metabolites[31], mitochondrial ROS[32], regulation of calcium uptake[33,34], and ATP concentration subsequently membrane potential[35] through which mitochondria use to communicate with the rest of the cell.

1.1.3 Mitochondria in ageing and neurodegeneration

Ageing can be defined as a complex process of molecular, cellular and organ damage leading to loss of function increasing vulnerability and ultimately death. The consequence of ageing can result in pathological conditions such as cancer, neurodegeneration, cardiovascular disorders, to name a few[36]. A lot of studies suggest mitochondria are a hallmark for ageing caused by mitochondrial abnormalities including accumulation of reactive oxygen species (ROS) that can cause defects in the mitochondrial DNA and structural components[37–39]. Hence, it's important to understand the changes that occur in mitochondria to have a better understanding of the pathophysiology of the diseases.

Major changes occur in the brain during ageing and neurodegeneration, leading to conditions such as dementia, Alzheimer's disease (AD), Parkinson's disease (PD), and Huntington's disease (HD)[40]. The brain is a highly active organ with high energy requirements and about 20 % of body's oxygen is required to cater for the brain's energy needs for many important mechanisms, including maintaining cell's membrane potential, re-establishing ion-balance, and to trigger release of neurotransmitters. Hence mitochondria play an important role in neuronal cells in response to high metabolic demands [41].

Mitochondrial dysfunction within the neurons of substantia nigra (SN) neurons is prominent in both ageing and Parkinson's disease. Alpha-synuclein protein is known to cause synaptic dysfunction in PD, which interacts with mitochondria causing their dysfunction, and also impair the mitochondrial protein import [42] indicating direct changes in the organelle. A decrease in the protein import activity is linked to reduced protein levels of various OxPhos subunits [43]. Another study has shown that the axons of SN neurons in PD cases show a very high expression of porin per axonal volume, suggesting and increase in mitochondrial density per axon [44].In AD as well changes in the mitochondrial trafficking are observed[45].

Impairment of certain mitochondrial respiratory components has been linked to neurodegenerative diseases[46]. Complex I (NADH: ubiquinone oxidoreductase) is the first of the five complexes of the respiratory chain and oxidative phosphorylation [47]. Studies carried out in humans, using post-mortem brain regions from older people compared with brain regions from young people, have shown a rise in nitration and oxidation with a decrease in superoxide dismutase (SOD), catalase, GSH reductase activity and complex I activity in hippocampus and frontal cortex [41]. This causes redox imbalance and negatively impacts mitochondrial function. A defective complex I is observed in Parkinson's disease [47], as shown in a study that inhibition of Complex I, leads to disruption of OPA1 oligomeric complexes that maintain the cristae structure in mitochondria, as a consequence, major structural abnormalities are observed similar to the defects observed in PD [48]. Alpha synuclein oligomers, discussed previously, interact with and impair complex I respiration, inducing the opening of permeability transition pore and increasing the permeability of the inner mitochondria membrane[49]. This leads to swelling of matrix, cristae unfolding, rupturing of outer mitochondrial membrane, increase ROS and ultimately cell death.[49,50].

Reduced activity of Complex II and Complex III have been observed in Huntingtin Disease (HD), where it has been seen that huntingtin gene knock-in mouse

embryos, show significant impair of mitochondrial respiration and ATP production [51] . Cytochrome c and Complex IV mediate the transfer of electrons to oxygen in ETC [52]. A decreased level of cytochrome oxidase activity was found in transgenic mouse models of AD[53]. Even though mitochondrial calcium accumulation is tightly controlled yet sometimes due to abnormal accumulation of calcium various pathways are triggered that dysfunction of mitochondria. Calcium ions also stimulate nitric oxide synthase which is known to inhibit complex IV and produce more ROS [54]. A calcium dys-homeostasis has been found in patients with Huntington's disease [55]. Calcium homeostasis is essential for normal neuronal function[56]. A cross talk is observed between the calcium ions (Ca^{2+}) and reactive oxygen species, where ROS are regulated by Ca^{2+} dependent pathways [57]. The free intracellular calcium plays a signalling role through the membranes of mitochondria. With ageing, a gradual increase in the calcium ion levels is a threat for the cell and lead to its dismal by activation of proteases and phospholipases [58].A negative correlation has been found between brain cytochrome oxidase activity and increased point mutation levels in cytochrome oxidase gene [59]. This can be correlated to with cytochrome oxidase deficiency in substantia nigra contributing to PD [60].

Reductions in OxPhos is a hallmark of neurodegenerative diseases causing energy crises in neurons. Complex V, which is discussed later in the chapter, has been suggested to regulate cell life and death in neurodegenerative diseases[61].Mutations in complex V of OxPhos subunit ATP6, have been observed to be in the maternally inherited neurodegenerative disease Leigh's syndrome [62].

Mitochondrial DNA (mtDNA) has a high mutation rate in vertebrates[63,64], and mutations have been linked with many diseases[65,66]. In general, mtDNA, accumulates mutations with ageing, such as large-scale deletions and point mutations that correlates with decline in mitochondrial function [25]. As mtDNA lies very close in proximity to the sites of OxPhos, its prone to oxidative damage, especially with ageing[67]. Neuronal cells are very prone to oxidative damage which makes mitochondria and subsequently mtDNA susceptible to the damage[68].

1.2 ATP Synthase

ATP synthase (ATPase/Complex V) is a molecular machine that uses chemical and mechanical aspects of enzyme function[69]. Complex V of the electron transport chain, ATP synthase, is responsible for the production of intracellular ATP from ADP and inorganic phosphate[70]. ATP synthase not only synthesizes ATP but is also crucial for the architecture of the mitochondrial inner membrane[71]. Structurally these enzymes in lower organisms consist of four distinct features, a headpiece, a base piece, a central stalk and a second stalk extending from the base piece to the head of the headpiece[72–74]. In higher vertebrates, there is an additional ring like structure surrounding the central stalk.

There are two components that are defined biochemically, an F_0 and F_1 component, the F_0 component is responsible for channelling protons from the intermembrane space across the inner mitochondrial membrane and into the mitochondrial matrix([75–77] (See **Figure 1-2).** The F_1 component of the enzyme is water soluble

and contains five subunit types in the ratio a3b3gde whereas the F_o component is detergent soluble and has three subunits in bacteria (a1b2c12) and about eleven subunits in animal[78,79]. Additional to the two subunits the enzyme also has a regulatory subunit, IF1. The F_1 motor is driven by ATP binding and hydrolysis whereas the F_o motor is driven by the proton gradient[80].

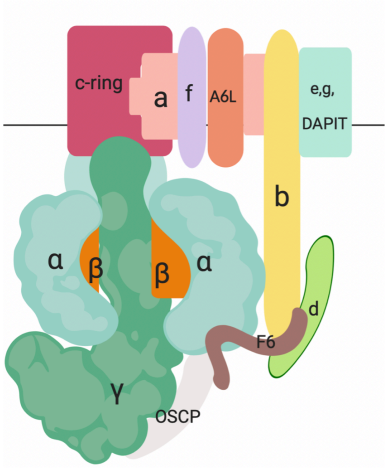

Figure 1-2. Human mitochondrial ATP synthase. Complex V consists of two functional domains, F_1 and F_o. F_1 comprises 5 different subunits (three α, three β, and one γ, δ and ε) and is situated in the mitochondrial matrix. F_o contains subunits c, a (ATP6), b, d, F6, OSCP and the accessory subunits e, f, g and 8/A6L. F_1 subunits γ, δ and ε constitute the central stalk of complex V. Subunits b, d, F6 and OSCP form the peripheral stalk.

The ATP synthesis F_o motor is composed of components c and a is believed to drive the F1 motor in reverse through the central stalk or rotor F_1-gamma subunit[81]. The g- and e-subunits of the F_1 core are linked to the c12 ring through interactions with the polar loop of subunit c[82,83] and would rotate in concert with the c12 ring [84,85].

Many studies suggest dysregulation of the ATP synthase enzyme in ageing and neurodegeneration[86–88]. Previously it has been reported that overexpression of anti-apoptotic protein Bcl-xL in neurons increases the production of ATP production, as it directly binds to the enzyme indicating a neuroprotective role. Thus the enzyme has a role beyond oxidative phosphorylation and such emerging roles suggest the enzyme might be involved in new pathways and have more interacting partners than already known [89].

1.2.1 Fo Motor

The F_o component of ATPase spans the inner mitochondria membrane and functions as a proton transporter[90]. The motor unit F_o is composed of subunits b, OSCP (oligomycin sensitivity conferring protein), d, e, f, g, h, i/j, k which are encoded by nuclear genes and subunits a (ATP6) and 8 (ATP8), which are encoded by mitochondrial genes[91].

A study suggested that the F_1 region of ATP synthase is shielded by F_o which has a functional significance, making the study of the structural units of F_o subunit quite important in the context of ATP synthesis[92]. Despite the structure of the complex having been first resolved decades ago, and hypotheses of the chemical mechanism were developed over half a century ago, significant breakthroughs continue to be made in our understanding of both the structure and function of the enzyme and its F_o component[93–96].

Subunit *a* of the F_o subunit is largely hydrophobic and folds in the membrane with five transmembrane helices[97,98], at least two of which interact with subunit *c* during proton transport[99]. The two hydrophobic transmembrane a-helices are joined by a more polar loop region that is exposed to the F_1 binding side of the membrane, where helix-2 is thought to be the site of H^+ binding during transport[100]. Subunit *b* is a single transmembrane helix that is connected to a polar elongated cytoplasmic domain which plays a key role in fixing F_1 to F_o. Subunit *c* folds in the membrane in a hairpin-like structure[101,102]. The proton translocation through F_o involves residues Asp 61 of subunit *c* and Arg 210 of subunit *a*. Since Asp 61 is buried in the membrane bilayer it requires a hydrophilic access pathway from both sides of membrane[103]. This is achieved by set of polar residues Gln 252, Asn 214, Asn 148, Asn 119, His 245, Glu 219, Ser 144 and Asn 238 forming a hydrophilic path between Arg 210 and periplasmic membrane surface[103]. During the synthesis of ATP, the transmembrane H^+ electrochemical potential is high at the periplasmic face and low towards F_1 face (cytoplasmic) and this drives protonation of Asp 61 through the subunit *a* and causes the c-terminal helix of subunit *c* to rotate (clockwise) and adopt a stable protonated conformation[104].

1.2.2 ATP8-ATP6

The genes encoding the F_o subunits ATP6 and ATP8 are in the mitochondrial genome[105]. Both ATP synthase subunit *a* (ATP6) and subunit 8 (ATP8) are proteins that function as part of the F_o component of ATP synthase and unusually they are encoded by genes that overlap within the mitochondrial genome[105]. This overlap is over a short, but variable between species, base pair sequence where the translation initiation site of subunit 8 is contained within the coding region of subunit 6.

ATP6 protein with the c-ring is known to form the proton-conducting channel of the F_o region[103]. A study with high-resolution cryo-electron microscopic structure of the dimeric F_o region of yeast ATP synthase also showed that the subunits ATP6 and i/j form the contact sites between two ATP synthase monomers which supported by interaction between subunits e and k[106]. Subunits e, g and f help in the integration of the subunits ATP6 and ATP8 which subsequently helps for the proton conduction channel between ATP6 and c-ring[107]. This is followed by the inhibitory protein IF1 is released and in the final step DAPIT (diabetes associated protein in insulin-sensitive tissue) is added to the assembly line to promote dimerization and oligomerization of the ATP synthase.

ATP8 is an integral transmembrane component of the peripheral stalk, serving an important role in the assembly of the complex[108]. The peripheral stalk is a crucial

component of the F_o component, forming a physical connection between the membrane sector of the complex and the catalytic core. It provides flexibility, aids in the assembly and stability of the complex, and forms the dimerization interface between ATP synthase pairs[109]. The C-terminus of ATP8 extends 70 Å from the surface and makes contacts with subunits b, d and F_6, while the N-terminus has been reported to make connections with subunits b, f and 6 in the intermembrane space[110,111]. Subunit 8 is also known to play a role in the activity of the enzyme complex[112]. ATP6 is an α-helical protein embedded within the inner mitochondrial membrane and it interacts closely with the c-ring of F_o, providing aqueous half-channels that shuttle protons to and from the rotating c-ring[76,113]. It has previously been reported that ATP6 has at least five hydrophobic transmembrane spanning α helices domain, where two of the helices h4 and h5 are well conserved across many species[114].

mtDNA is subjected to a number of mutations ultimately causing reduction in the OxPhos capacity[115,116]. Since ATP8 and ATP6 are overlapping genes, mutation in one gene can affect either or both. Mutations in ATP8 have been previously reported in neurological disorders, cardiovascular diseases schizophrenia and autism[67,117–120]. Mutations in ATP6 have been observed in patients with NARP or MILS syndrome, where ATP production was severely compromised[121,122]. This was due to either a block in proton translocation, less sufficient coupling or defects in the assembly and stability of ATP synthase[123–126]. Hence, diseases associated with mutations in ATP6 and ATP8 are challenging to study due to factors such as complex inheritance and interactions with nuclear genes. Overall, changes in these proteins affect the ATP synthase structure and mechanism.

1.2.3 ATP-IF1

The ATP synthase Inhibitory Factor 1 (ATPIF1/IF1), is the natural inhibitor of the enzyme and a nuclear encoded mitochondrial protein.[127]. It is an α-helical protein that contains inhibitory domain at the N-terminus and a dimerization domain at the C-terminus[128].

The inhibitory protein IF1 is expressed to prevent ATP hydrolysis by the uncoupled ATPase. ATP synthase can function in reverse, acting as an ATP hydrolase for maintaining the proton motive force and this process is regulated by the inhibitor peptide of IF1, which is a highly conserved protein[129,130]. When the mitochondrial matrix pH drops (<6.5), IF1 becomes activated and binds between the α and β-F1-ATPase reaching the γ subunit of the central stalk with its N-terminus[128], blocking ATP hydrolysis and preventing a waste of energy[131]. IF1 is regulated by pH acting upon the histidine present in the C-terminal forming inactive tetramers, dimers or at times even as monomers[132]. IF1 plays a role in limiting oxidative phosphorylation and promoting glycolysis[133]. Studies show that the mitochondrial content of IF1 controls the activity of oxidative phosphorylation mediating the shift of cancer cells to an enhanced aerobic glycolysis.

IF1 has previously reported to be associated with cardiovascular disease, anaemia and visual impairment in different animal models[134–136]. The protein is also overexpressed in numerous cancers due to high oxidative stress[137]. IF1 is also

highly expressed in neurons, probably in a protective role to prevent ATP depletion and cellular damage during ischaemia[138,139]. The protein lies at the crossroad between mitochondrial dynamics and energy balance yet very little has been discussed about this protein in the literature.

1.3 Haemoglobin

1.3.1 Haemoglobin – The tetramer

Haemoglobin (Hb) is composed of four polypeptide globin chains (tetramer). Each globin chain contains a haem moiety which has an organic part (a protoporphyrin ring made up of four pyrrole rings) and central iron ion in the ferrous state (Fe^{2+})[140]. Haem synthesis occurs in both the cytosol and mitochondria, where protoporphyrin is synthesised from the condensation of glycine and succinyl coenzyme A. Eight molecules of each cyclises into protoporphyrin ring, which binds to a Fe^{2+} ion to form haem[141]. The Fe^{2+} forms 6 bonds to the haem moiety out of which, 4 binds to nitrogen atoms and one binds to histidine residue at position 87 (proximal) on α-globin chain and last bond to a histidine at position 89 on the same chain at position 89 (distal)[142].

The adult human Hb is in the form of two α-globin (HbA)and two β-globin (HbB) chains. Each α- chain has 141 amino acids and each β- chain has 146 amino acids. Genes for the α- chain are found on chromosome 16 and those for β- chain are on chromosome 11[143–145]. Globin chains are synthesised in the cytosol. There are three clusters of hydrophobic residues near the haem: one on the side of His E7, another on the side of His F8, and the third at the bottom of the haem. There are two metal binding sites, 59 and 88 in the α- chain. The β-chain of haemoglobin has two metal binding sites, 64 & 93, positions 2,3, 83, 144 are binding sites for 2,3-bisphosphoglycerate. These conserved positions are especially important for the function of the haemoglobin molecule. Several of them, such as histidine His87 and His63 are directly involved in the oxygen-binding site. Phenylalanine Phe43 and leucine F4 (Leu83) are also in direct contact with the haem group. Tyrosine Tyr140 stabilizes the molecule by forming a hydrogen bond between the H and F helices. Proline Pro37 is important because it terminates the C helix.

The tetramer has multiple functions; oxygen transport, carbon dioxide transport, buffering of hydrogen ions, anti-oxidant functions[146] and nitric oxide metabolism[147,148]. Hb is an allosteric protein, that is the binding of oxygen of one haem group increases the oxygen affinity within the remaining haem groups; which means oxyhaemoglobin has a different quaternary structure than deoxyhaemoglobin[149]. It has been suggested previously that the globins or derived peptide fragments have additional physiological functions, where the presence of α- and β- globin chains was found in cells other than erythrocytes, including human brain and peripheral tissues[150–152]. Hb also plays a role in several neurological conditions, including superficial siderosis[153], Alzheimer disease and progressive multiple sclerosis[154].

Single amino acid substitutions in proteins can lead to disorders and diseases. In haemolytic anaemia, sickle cell anaemia[155] an amino acid substitution at the sixth position of β-chain of Hbs results in loss of negative charge and a gain in hydrophobicity that alters the Hbs dimer-tetramer assembly, resulting in the instability and polymerisation of the protein. The residue changes at key sites within a protein may result in a series of conformation changes, including the breakage of salt bridges, alteration of interaction network and disruption of hydrogen bonds, which in turn may perturb the energy landscape[156].

1.3.2 Dynamic Location of Haemoglobin

There is a wide range of evidence that suggests that Hb has dynamic locations in cell, neurons, endothelial cells, mitochondria, and vascular expression[157–161]. This leads to the argument that Hb has roles other than that of transporting oxygen and carbon dioxide. Haem, the major component of haemoglobin, is incorporated in several other protein groups including the cytochrome family, peroxidase and NO synthase [162]. Ferrochelatase and other enzymes involved in haemoglobin biosynthesis, are located in mitochondria and haem is manufactured entirely within the mitochondrion; it is reasonable to suggest that haem-containing proteins may also reside in the organelle where they are constructed [163] .

Hb has also been seen expressed in brain tissues, where it is speculated to play protective role against oxidative and nitrostative stresses, as Hb is known to bind to NO, the strongest ligand of the ferrous haem iron of HB[164,165]. The presence of Hb in brain tissue acts as a sensor of the energy status of neurons and as an oxygen storage reservoir to regulate mitochondrial function[159,166].

Hb is seen to localise in the inter-membrane space of mitochondria, in the regions where a continuous supply of oxygen is critical for survival. The presence of haemoglobin in mitochondria is attributed as a protective mechanism in circulating leukocytes [26]. Hb β-chain has been found to interact with subunits of ATP synthase which could also be seen as regulation of OxPhos [167]. Another study has shown the presence of HbA in the endothelium walls of the retina of, Antarctic icefish, that has been speculated to play an uncharacterised role[161]. HbA has also been observed to modulate endothelial NO flux. This evidence of Hbs having a dynamic location highlight towards an additional role as a regulator of different cellular mechanisms in various cellular locations.

1.3.3 Role of Mitochondria Haemoglobin in Ageing/Neurodegeneration

A decrease in the levels of Hb can have an impact on the respiratory chain which is a hallmark of ageing and neurodegeneration [168]. A decrease in haem synthesis with an increase in age causes mitochondrial complex IV inhibition, oxidative stress, iron accumulation and cell death [162]. Haem breakdown is catalysed by the enzyme haem oxygenase-1 (HO1) which has been shown to bring about the oxidative neurotoxicity of haemoglobin in cortical neurons. The overexpression of HO1 in the substantia nigra (mid-brain), in the affected mice has significantly shown to increase in survival of dopaminergic neurons [162]. An increase in HbB has been seen in normal ageing with a simultaneous increase in an amyloid precursor protein/PS1 as a compensatory mechanism for hypoxia[169].
It has been observed that mitochondrial haemoglobin is reduced in neurons in Parkinson's disease by interacting with alpha-synuclein by the regulation of AKT [160]. A study showed changes in the distribution of alpha and beta haemoglobin proteins in the degenerating brain [160]. Neuronal haemoglobin is known to play a critical role in maintaining normal mitochondrial functioning in the brain. In AD

brains Hb expression has been found to be increased[170] and there is good evidence that anaemia is a risk factor for dementia and AD[171–173]. There have been studies on neuronal HbB playing a role in neuroprotection by being part of neuronal energetics in patients with multiple sclerosis (MS)[174,175]. These findings about Hb can help improve therapeutics for diseases and new insights in disease pathophysiology.

1.3.4 Haemoglobin Null mutants

Antarctic Icefishes (Antarctic white fish), belonging to family Channichthyidae, suborder Notothenioidei are the only vertebrates that lack functional haemoglobin genes and red blood cells [176,177]. All notothenioid species, except the 16 icefish species have red blood and express haemoglobin. This makes them the only reported vertebrates to completely devoid of oxygen transporting proteins[178], despite the fact that all other vertebrates have the same general mechanism for getting oxygen to the cells, via RBCs which contain Hb. The loss of Hb in the Antarctic Icefish is postulated to be due to a mutational process, which has resulted in the loss of the β-globin gene and partial omission of the α-globin gene from α-/β-globin leading to the locus becoming functionally inactive. 15 out of the 16 icefish species are known to retain only a 3'fragment of an α- globin gene[179]. The sixteenth species, *Neopagetopsis ionah* retained an intact but unexpressed HbA gene fused to two β-pseudogenes [180]. Previously, it has also been shown that excess of β- chain produced is capable of contributing β- chains to newly synthesised haemoglobin A[181].

The icefish make an excellent model organism for studying adaptations in vertebrates. Many species within the Channichthyid family also lack Mb, an intracellular oxygen-binding protein found in muscle. In total, six out of 16 icefish species lack Mb expression in their heart ventricles, a loss that has occurred through four different mutational events [182]. The fish have high mitochondrial densities in order to counter the pressures of a cold environment. This is a likely compensation for the lack of Hb and Mb and to enhance oxygen storage and diffusion[183]. An overall increase in mitochondrial phospholipids may be attributable to an upregulation in the glycerol-lipid synthesis pathway, yet it is unknown how the synthesis of phospholipids is integrated into mitochondrial biogenesis in either fish or mammals[184]. The other adaptations suggested to compensate for the lack of Hb are large hearts containing more mitochondria than hearts of similar-sized Hb- expressing fishes[185]. Interestingly, the hearts of icefishes lack the mitochondrial isoform of creatine kinase, an enzyme that plays a pivotal role in energy flux by catalysing the reversible transfer of phosphate between creatine and ADP [186].

Mitochondria play a central role in defining the thermal responses of aerobic energy metabolism of ectothermic animals[187], little is known about the biochemical mechanisms involved [188].Thermal range and upper limits of mitochondrial function in ice fish fall well below values predicted based on temperate organisms, indicating that stenothermy and cold specialization detected in Antarctic fish are reflected at the cellular and molecular level [189]. Maximal enzyme activities of citrate synthase (CS) and lactate dehydrogenase (LDH) in brain homogenates of Antarctic and tropical fishes, showed a partial temperature compensation of ATP-

generating capacity in notothenioids[190], consistent with earlier observations of partial compensation in the brain oxygen consumption rate observed in these fish.

A lot of attention has been given to the mitochondrial NADH dehydrogenase subunit 6 gene (ND6). ND6 is involved in the assembly and function of ETC complex I, where certain changes in this protein's amino acid composition may have a role in the thermal sensitivity of mitochondrial ATP synthesis[187,191,192]. Thus, these linkages make it interesting and essential to study the mitochondrial proteome for this sub order. It is important to look at the mitochondria of these fish, as Antarctic notothenioid fish are characterised by their evolutionary adaptation to the cold, which is associated with unique physiological adaptations in mitochondria to withstand the cold and reduce energetic requirements. There are many other biochemical and cellular adaptations that have helped Icefish to survive sub-zero temperatures. The loss ability to up-regulate key chaperoning molecules such as heat shock proteins, which functions to maintain protein homeostasis in the cold and lack of an inducible HSR under thermal stress are favoured in these fish regardless of it being evolutionarily advantageous or not [193]. Antarctic species are similar in terms of their ecology, but strongly differ in their geographical distribution, and therefore environmental temperature exposure[194].

We have samples from four species of the Notothenioid sub-order, *Champsocephalus gunnari* (*C. gunnari*) (common name: Mackerel icefish) and *Chionodraco rastorspinosus* (*C. rastrospinosus*) (common name: Ocellated icefish) are devoid of haemoglobin, whereas the species, *Notothenia* coriiceps (*N. coriiceps)* (common name: Marbled rockcod) and *Trematomus bernacchii* (*T. bernacchii)* (common name: Black rockcod) are species that express haemoglobin.

1.4 METHODS

The thesis combines *in vitro* and *in silico* approaches to predict a Hb interactome.

1.4.1 *In vitro* Methods

Proteins extracted from tissues/cells can be separated using SDS-PAGE and detecting proteins using western blots by transferring the proteins to a membrane and using antibodies to detect antigen for the specific protein of interest. The subcellular fractionations can be confirmed using specific protein markers.
Liquid chromatography–mass spectrometry (LC/MS) gives qualitative summary of the proteins identified from the sample as well as it provides a label-free, intensity-based quantification for comparing relative protein amounts between samples and for determining significant differences.
Coimmunoprecipitation is a well-established method that uses an immobilised antibody, the protein in question, in a pull-down assay to detect stable complexes.

Antarctic Fish Muscle tissue used in this thesis.
SVMS Clinical Ethical Review, University of Nottingham, (ref # 2744 190509). White and red muscle samples of Antarctic notothenioid fish, *N. rossii*, *T. bernacchii* (red-blooded species – Cruise PS112, Weddell Sea in 2013-2014), *C. gunnari* and *C. rastrospinosus* [icefish species – Cruise ANTXXVIII (PS79), Antarctic Peninsula in 2012].

1.4.2 *In silico* Methods- Sequence and Structure Homology

In silico methods and webservers have developed to predict function and structure of proteins and genes alike[195]. Although the amino acid sequence determines the three-dimensional structure and the biochemical function of the protein, the specific relation as how the proteins work in a cohort are still not known in many cases[196]. The extensive data set of amino acid sequences, three-dimensional structures, biochemical and biological functions of gene products proteins can potentially explain the pathophysiology of many disease conditions[197]. The propensity of protein sites to be occupied by any of the 20 amino acids, is known as site specific amino acid preferences. A general consequence of amino acid substitutions is the changes in biophysical and evolutionary forces that correlates with the changes in molecular structure and function of the protein, thermodynamic stability, protein-folding, protein-protein interactions, and protein expression[198].
In bioinformatics, the sequence alignments are used to show evolutionary relationships by constructing phylogenetic trees. A multiple sequence alignment describes the mode of arrangement of three or more protein sequences, in order to distinguish the areas of similarity among them, where alignment refers to matching as many characters as possible from each sequence[199]. The sequence alignment is applied to infer the functional, morphological and evolutionary relationship between the protein sequences[200]. To solve multiple sequence alignment problems by using dynamic programming, the current tools use the iterative

algorithms with the progressive approach[201]. Some commonly used methods that employ progressive and iterative approaches are Clustal Omega[202], DIALIGN [203], M-Coffee [204].

Gene expression method is used for the quantification of the level at which a particular gene is expressed within a cell, tissue or organism under varied disease or experimental conditions. The genes can be clustered together according to their expression levels and develop functional relationships among them.

1.4.3 *In silico* Methods- Computational Analysis of PPI network

A PPI network is a mathematical graph consisting of nodes and edges where proteins are nodes that are joined by different interactions as edges. The network can show a various thing such as a, a neighbouring protein in a graph may share same functionality, a densely connected subgraph could predict formation of protein complexes. The protein function can be predicted from the topology or the connectivity of the PPI network[205]. There are several protein interaction databases that are available to curate and organise the biological relevant data. Some commonly used databases are, BioGRID[206], DIP[207], BIND[208], MINT[209], STRING[210].

Currently, although large-scale mitochondrial comparative proteomic data have been accumulated, mitochondrial proteomics still faces the challenge of how to investigate biofunctions of the identified uncommented mitochondrial proteins and how to build mitochondria specific signalling networks.

1.4.4 *In silico* Methods- Molecular Docking and MD Simulations

All proteins exert their functions by recognising other molecular components[211]. Molecular docking techniques aim to predict best binding or interacting of proteins to either the ligand or another macromolecule. This requires an experimentally solved structure such as X-ray crystallography or NMR or through homology modelling. The docking can be broadly described into two main steps, one the production of conformations or docking pose, and second a scoring function which is associated with each predicted conformation[212,213]. There are three types of docking, rigid docking, semi-flexible docking, and flexible docking. We have used automated protein-protein docking software PatchDock, that uses a rigid docking, considering both the protein entities as rigid bodies[214], verified by the Critical Assessment of Prediction of Interactions (CAPRI)[215]. A protein-protein docking entails prediction of residue-residue contacts involved in the target interaction. The server aims to find best docking transformation with good molecular shape complementarity. Each transformation is evaluated by scoring function that considers both geometric fit and desolvation energy[216]. Desolvation energy is described as the free energy changes accompanying movement of water molecules into the binding pocket of a protein[217]. An RMSD clustering is applied to discard redundant solutions[214]. FireDock (Fast Interaction REfinement in molecular DOCKing) refinement tool for rigid body docking solutions was also used, where

the refinement rearranges the interface side chains and adjusts relative orientation of the molecules[218].

Understanding how biological macromolecules work requires knowledge of their structure and dynamics. Molecular Dynamics (MD) is a computational technique for simulating the dynamic behaviour of molecular systems as a function of time where all entities in a simulation box are considered flexible[211]. MD computes the movement of atoms along time by using classical Newton's mechanics[219]. MD simulation and constructive interplay between experiments can help in refinement of methodologies for structural biologist. MD is highly used for to predict and validate unreported interactions between proteins. Some widely used MD simulation software are NAMD, GROMACS and AMBER. I have used GROMACS for the current work[220]. There are multiple steps involved in an MD simulation, where first step is to get the knowledge of the initial system with respect to its positional coordinates. A simulation will then replicate experimental conditions, taking in account temperature, pressure, density, which is then solvated with an explicit solvent[221]. The whole system is energy minimised with respect to the position of side chains, assuming the net attractive charge on each atom as maximum. The system is then equilibrated and heated at a desired temperature. The final step encompasses a time scale trajectory of protein complex in compliance to equilibrated conditions. The analysis of an MD simulation using total energy of the system, RMSD differences between two structures before and after simulation, radius of gyration to gather the stability of the structure throughout the simulation [222,223].

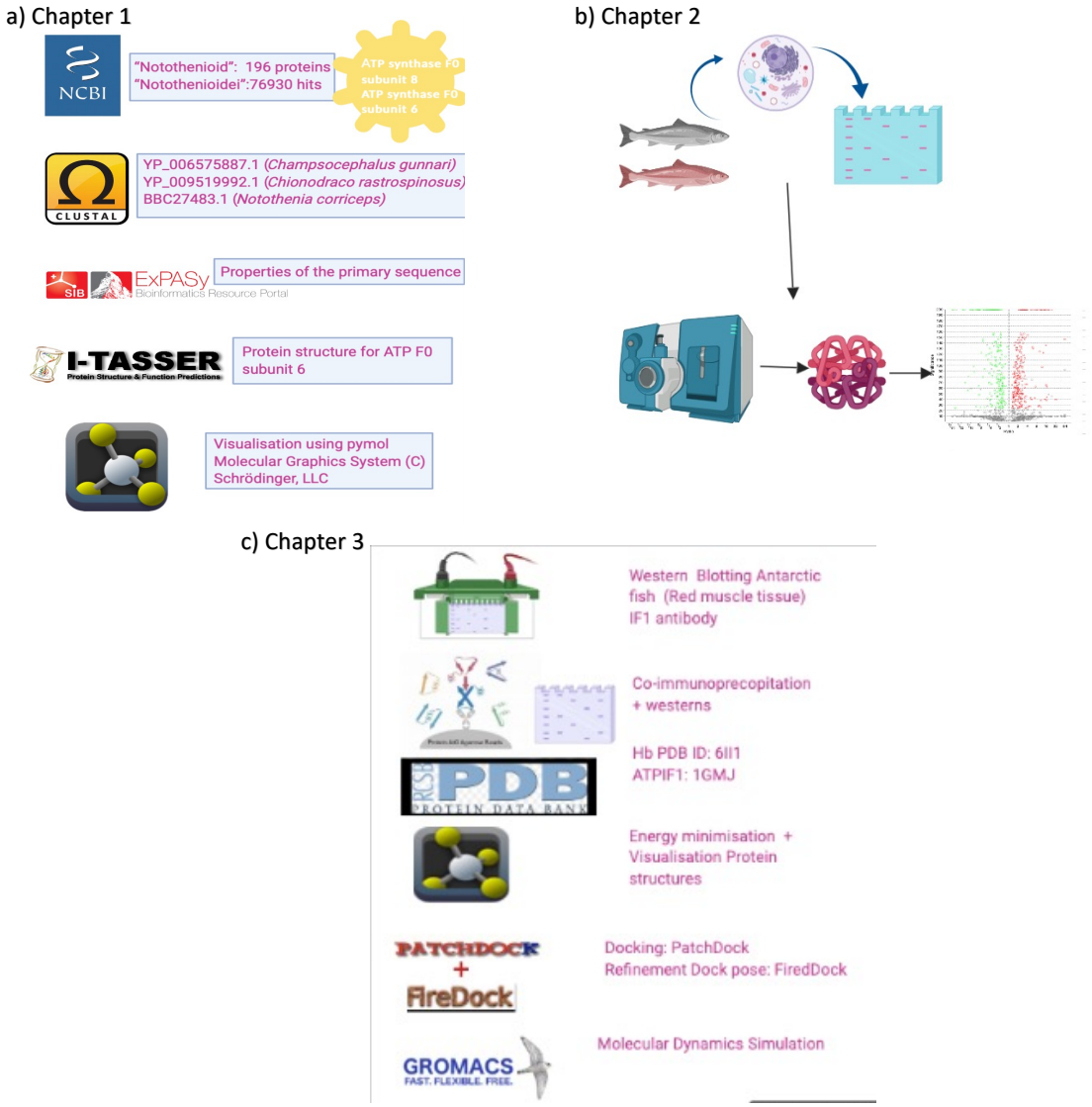

Figure 1-3 Schematic representation of the methodology used in this thesis.

Cellular level life is a finely orchestrated interplay of many different proteins interacting with each other and their environment. Thus, the work in this PhD focuses on studying the protein-protein interactions of dynamically localised haemoglobin using the various techniques described above **(Figure 1-3)**. The first chapter focusses on adaptation of two mitochondrial encoded proteins that are part of the ATP synthase complex, involved in energy mechanisms in the oxidative phosphorylation in Hb-less Antarctic fish. It explores the sequence and structural changes in the proteins ATP8 and ATP6. The second chapter highlights proteins seen differentially regulated in the mitochondria of the Antarctic fish, a direct comparison among the fish that has retained globins, retained only myoglobin but lost Hb, and a complete loss of all globins using LC/LC-MS and network analysis. The final chapter combines experimental and docking/molecular dynamic simulations to explore interactions of energy modulator, the inhibitory protein of ATP synthase, Inhibitory Factor 1 and Hb. In summary, I focussed on deciphering a haemoglobin interactome that emphasises on a plausible role of haemoglobin as a modulator of the energy mechanism in the mitochondria.

1.5 Bibliography

1. Braun P, Gingras A-C. History of protein-protein interactions: from egg-white to complex networks. Proteomics. 2012;12: 1478–1498. doi:10.1002/pmic.201100563
2. Nooren IMA, Thornton JM. Diversity of protein–protein interactions. EMBO J. 2003;22: 3486–3492. doi:https://doi.org/10.1093/emboj/cdg359
3. Gray MW, Burger G, Lang BF. Mitochondrial Evolution. Science (80-). 1999;283: 1476 LP – 1481. doi:10.1126/science.283.5407.1476
4. Hirst J. Towards the molecular mechanism of respiratory complex I. Biochem J. 2009;425: 327–339. doi:10.1042/BJ20091382
5. Wirth C, Brandt U, Hunte C, Zickermann V. Structure and function of mitochondrial complex I. Biochim Biophys Acta - Bioenerg. 2016;1857: 902–914. doi:https://doi.org/10.1016/j.bbabio.2016.02.013
6. Yankovskaya V, Horsefield R, Törnroth S, Luna-Chavez C, Miyoshi H, Léger C, et al. Architecture of succinate dehydrogenase and reactive oxygen species generation. Science. 2003;299: 700–704. doi:10.1126/science.1079605
7. Trumpower BL. The protonmotive Q cycle. Energy transduction by coupling of proton translocation to electron transfer by the cytochrome bc1 complex. J Biol Chem. 1990;265: 11409–11412.
8. Sun C, Benlekbir S, Venkatakrishnan P, Wang Y, Hong S, Hosler J, et al. Structure of the alternative complex III in a supercomplex with cytochrome oxidase. Nature. 2018;557: 123–126. doi:10.1038/s41586-018-0061-y
9. Calhoun MW, Thomas JW, Gennis RB. The cytochrome oxidase superfamily of redox-driven proton pumps. Trends Biochem Sci. 1994;19: 325–330. doi:10.1016/0968-0004(94)90071-x
10. Van Der Bliek AM, Sedensky MM, Morgan PG. Cell biology of the mitochondrion. Genetics. 2017;207: 843–871. doi:10.1534/genetics.117.300262
11. Murphy MP. How mitochondria produce reactive oxygen species. Biochem J. 2009;417: 1–13. doi:10.1042/BJ20081386
12. Giorgi C, Agnoletto C, Bononi A, Bonora M, de Marchi E, Marchi S, et al. Mitochondrial calcium homeostasis as potential target for mitochondrial medicine. Mitochondrion. 2012;12: 77–85. doi:10.1016/j.mito.2011.07.004
13. Tait, S.W., and Green DR. Mitochondrial regulation of cell death. Cold Spring Harb. Perspect. Cold Spring Harb Perspect Biol. 2013; a008706. doi:10.1016/j.yapd.2006.04.010
14. Chu Q, Martinez TF, Novak SW, Donaldson CJ, Tan D, Vaughan JM, et al. Regulation of the ER stress response by a mitochondrial microprotein. Nat Commun. 2019;10: 1–13. doi:10.1038/s41467-019-12816-z
15. Azuma K, Ikeda K, Inoue S. Functional mechanisms of mitochondrial respiratory chain supercomplex assembly factors and their involvement in muscle quality. Int J Mol Sci. 2020;21: 1–17. doi:10.3390/ijms21093182
16. Guo R, Gu J, Zong S, Wu M, Yang M. Structure and mechanism of mitochondrial electron transport chain. Biomed J. 2018;41: 9–20. doi:10.1016/j.bj.2017.12.001
17. Genova ML, Lenaz G. Functional role of mitochondrial respiratory supercomplexes. Biochim Biophys Acta - Bioenerg. 2014;1837: 427–443. doi:10.1016/j.bbabio.2013.11.002
18. Ikeda K, Shiba S, Horie-Inoue K, Shimokata K, Inoue S. A stabilizing factor

for mitochondrial respiratory supercomplex assembly regulates energy metabolism in muscle. Nat Commun. 2013;4. doi:10.1038/ncomms3147
19. Anderson S, Bankier AT, Barrell BG, de Bruijn MHL, Coulson AR, Drouin J, et al. Sequence and organization of the human mitochondrial genome. Nature. 1981;290: 457–465. doi:10.1038/290457a0
20. Shadel GS, Clayton DA. MITOCHONDRIAL DNA MAINTENANCE IN VERTEBRATES. Annu Rev Biochem. 1997;66: 409–435. doi:10.1146/annurev.biochem.66.1.409
21. Yasukawa T, Yang M-Y, Jacobs HT, Holt IJ. A Bidirectional Origin of Replication Maps to the Major Noncoding Region of Human Mitochondrial DNA. Mol Cell. 2005;18: 651–662. doi:https://doi.org/10.1016/j.molcel.2005.05.002
22. Islas-Osuna MA, Ellis TP, Marnell LL, Mittelmeier TM, Dieckmann CL. Cbp1 is required for translation of the mitochondrial cytochrome b mRNA of Saccharomyces cerevisiae. J Biol Chem. 2002;277: 37987–37990. doi:10.1074/jbc.M206132200
23. Tavares-Carreón F, Camacho-Villasana Y, Zamudio-Ochoa A, Shingú-Vázquez M, Torres-Larios A, Pérez-Martínez X. The pentatricopeptide repeats present in Pet309 are necessary for translation but not for stability of the mitochondrial COX1 mRNA in yeast. J Biol Chem. 2008;283: 1472–1479. doi:10.1074/jbc.M708437200
24. Rak M, Su CH, Xu JT, Azpiroz R, Singh AM, Tzagoloff A. Regulation of mitochondrial translation of the ATP8/ATP6 mRNA by Smt1p. Mol Biol Cell. 2016;27: 919–929. doi:10.1091/mbc.E15-09-0642
25. Federico A, Cardaioli E, Da Pozzo P, Formichi P, Gallus GN, Radi E. Mitochondria, oxidative stress and neurodegeneration. J Neurol Sci. 2012;322: 254–62. doi:10.1016/j.jns.2012.05.030
26. Shephard F, Greville-Heygate O, Liddell S, Emes R, Chakrabarti L. Analysis of Mitochondrial haemoglobin in Parkinson's disease brain. Mitochondrion. 2016;29: 45–52. doi:10.1016/j.mito.2016.05.001
27. Ballinger SW, Patterson C, Yan CN, Doan R, Burow DL, Young CG, et al. Hydrogen peroxide- and peroxynitrite-induced mitochondrial DNA damage and dysfunction in vascular endothelial and smooth muscle cells. Circ Res. 2000;86: 960–966. doi:10.1161/01.res.86.9.960
28. Larsson N-G. Somatic mitochondrial DNA mutations in mammalian aging. Annu Rev Biochem. 2010;79: 683–706. doi:10.1146/annurev-biochem-060408-093701
29. Douglas C. Mitochondrial DNA in evolution and disease. Nature. 2016;535.
30. Pfanner N, Warscheid B, Wiedemann N. Mitochondrial proteins: from biogenesis to functional networks. Nat Rev Mol Cell Biol. 2019;20: 267–284. doi:10.1038/s41580-018-0092-0
31. Martínez-Reyes I, Chandel NS. Mitochondrial TCA cycle metabolites control physiology and disease. Nat Commun. 2020;11: 1–11. doi:10.1038/s41467-019-13668-3
32. Sena LA, Chandel NS. Physiological roles of mitochondrial reactive oxygen species. Mol Cell. 2012;48: 158–167. doi:10.1016/j.molcel.2012.09.025
33. Patron M, Raffaello A, Granatiero V, Tosatto A, Merli G, Stefani D De, et al. The mitochondrial calcium uniporter (MCU): Molecular identity and physiological roles. J Biol Chem. 2013;288: 10750–10758. doi:10.1074/jbc.R112.420752
34. Haynes CM, Fiorese CJ, Lin YF. Evaluating and responding to mitochondrial

dysfunction: The mitochondrial unfolded-protein response and beyond. Trends Cell Biol. 2013;23: 311–318. doi:10.1016/j.tcb.2013.02.002
35. Veatch JR, McMurray MA, Nelson ZW, Gottschling DE. Mitochondrial Dysfunction Leads to Nuclear Genome Instability via an Iron-Sulfur Cluster Defect. Cell. 2009;137: 1247–1258. doi:10.1016/j.cell.2009.04.014
36. López-Otín C, Blasco MA, Partridge L, Serrano M, Kroemer G. The Hallmarks of Aging. Cell. 2013;153: 1194–1217. doi:https://doi.org/10.1016/j.cell.2013.05.039
37. Sun N, Youle RJ, Finkel T. The Mitochondrial Basis of Aging. Mol Cell. 2016;61: 654–666. doi:10.1016/j.molcel.2016.01.028
38. Beal MF. Mitochondria take center stage in aging and neurodegeneration. Ann Neurol. 2005;58: 495–505. doi:10.1002/ana.20624
39. Cabral-Costa J V., Kowaltowski AJ. Neurological disorders and mitochondria. Mol Aspects Med. 2020;71: 100826. doi:10.1016/j.mam.2019.10.003
40. Mattson MP, Arumugam T V. Hallmarks of Brain Aging: Adaptive and Pathological Modification by Metabolic States. Cell Metab. 2018;27: 1176–1199. doi:https://doi.org/10.1016/j.cmet.2018.05.011
41. Grimm A, Eckert A. Brain aging and neurodegeneration: from a mitochondrial point of view. J Neurochem. 2017;143: 418–431. doi:10.1111/jnc.14037
42. Nakamura K, Nemani VM, Azarbal F, Skibinski G, Levy JM, Egami K, et al. Direct membrane association drives mitochondrial fission by the Parkinson disease-associated protein α-synuclein. J Biol Chem. 2011;286: 20710–20726. doi:10.1074/jbc.M110.213538
43. Franco-Iborra S, Cuadros T, Parent A, Romero-Gimenez J, Vila M, Perier C. Defective mitochondrial protein import contributes to complex I-induced mitochondrial dysfunction and neurodegeneration in Parkinson's disease. Cell Death Dis. 2018;9. doi:10.1038/s41419-018-1154-0
44. Reeve AK, Grady JP, Cosgrave EM, Bennison E, Chen C, Hepplewhite PD, et al. Mitochondrial dysfunction within the synapses of substantia nigra neurons in Parkinson's disease. npj Park Dis. 2018;4: 1–10. doi:10.1038/s41531-018-0044-6
45. Wang W, Zhao F, Ma X, Perry G, Zhu X. Mitochondria dysfunction in the pathogenesis of Alzheimer's disease: Recent advances. Mol Neurodegener. 2020;15: 1–22. doi:10.1186/s13024-020-00376-6
46. Moreira PI, Santos MS, Oliveira CR. Alzheimer's disease: a lesson from mitochondrial dysfunction. Antioxid Redox Signal. 2007;9: 1621–1630. doi:10.1089/ars.2007.1703
47. Schapira AH V. Complex I: Inhibitors, inhibition and neurodegeneration. Exp Neurol. 2010;224: 331–335. doi:10.1016/j.expneurol.2010.03.028
48. Ramonet D, Perier C, Recasens A, Dehay B, Bové J, Costa V, et al. Optic atrophy 1 mediates mitochondria remodeling and dopaminergic neurodegeneration linked to complex i deficiency. Cell Death Differ. 2013;20: 77–85. doi:10.1038/cdd.2012.95
49. Ludtmann MHR, Angelova PR, Horrocks MH, Choi ML, Rodrigues M, Baev AY, et al. α-synuclein oligomers interact with ATP synthase and open the permeability transition pore in Parkinson's disease. Nat Commun. 2018;9. doi:10.1038/s41467-018-04422-2
50. Stefanis L. α-Synuclein in Parkinson's disease. Cold Spring Harb Perspect Med. 2012;2: a009399–a009399. doi:10.1101/cshperspect.a009399

51. Gu M, Gash MT, Mann VM, Javoy-Agid F, Cooper JM, Schapira AHV. Mitochondrial defect in Huntington's disease caudate nucleus. Ann Neurol. 1996;39: 385–389. doi:10.1002/ana.410390317
52. Mammucari C, Rizzuto R. Signaling pathways in mitochondrial dysfunction and aging. Mech Ageing Dev. 2010;131: 536–543. doi:10.1016/j.mad.2010.07.003
53. Pinto M, Moraes CT. Mechanisms linking mtDNA damage and aging. Free Radic Biol Med. 2015;85: 250–258. doi:10.1016/j.freeradbiomed.2015.05.005
54. Zu G, Reiser G. 2011_Ca. 2011;14. doi:10.1089/ars.2010.3359
55. Kolobkova YA, Vigont VA, Shalygin A V., Kaznacheyeva E V. Huntington's disease: Calcium dyshomeostasis and pathology models. Acta Naturae. 2017;9: 34–46.
56. Lee K-S, Huh S, Lee S, Wu Z, Kim A-K, Kang H-Y, et al. Altered ER–mitochondria contact impacts mitochondria calcium homeostasis and contributes to neurodegeneration in vivo in disease models. Proc Natl Acad Sci. 2018;115: E8844–E8853. doi:10.1073/pnas.1721136115
57. Valko M, Leibfritz D, Moncol J, Cronin MTD, Mazur M, Telser J. Free radicals and antioxidants in normal physiological functions and human disease. Int J Biochem Cell Biol. 2007;39: 44–84. doi:10.1016/j.biocel.2006.07.001
58. Wieckowski MR, Marchi S, Pinton P, Poletti F, De Marchi E, Agnoletto C, et al. Calcium signaling around Mitochondria Associated Membranes (MAMs). Cell Commun Signal. 2011;9: 19. doi:10.1186/1478-811X-9-19
59. Lin MT. High aggregate burden of somatic mtDNA point mutations in aging and Alzheimer's disease brain. Hum Mol Genet. 2002;11: 133–145. doi:10.1093/hmg/11.2.133
60. Kraytsberg Y, Kudryavtseva E, McKee AC, Geula C, Kowall NW, Khrapko K. Mitochondrial DNA deletions are abundant and cause functional impairment in aged human substantia nigra neurons. Nat Genet. 2006;38: 518–520. doi:10.1038/ng1778
61. Mnatsakanyan N, Jonas EA. The new role of F1Fo ATP synthase in mitochondria-mediated neurodegeneration and neuroprotection. Exp Neurol. 2020;332: 113400. doi:10.1016/j.expneurol.2020.113400
62. Moslemi A-R, Darin N, Tulinius M, Oldfors A, Holme E. Two new mutations in the MTATP6 gene associated with Leigh syndrome. Neuropediatrics. 2005;36: 314–318. doi:10.1055/s-2005-872845
63. Nabholz B, Glémin S, Galtier N. The erratic mitochondrial clock: Variations of mutation rate, not population size, affect mtDNA diversity across birds and mammals. BMC Evol Biol. 2009;9: 1–13. doi:10.1186/1471-2148-9-54
64. Allio R, Donega S, Galtier N, Nabholz B. Large variation in the ratio of mitochondrial to nuclear mutation rate across animals: Implications for genetic diversity and the use of mitochondrial DNA as a molecular marker. Mol Biol Evol. 2017;34: 2762–2772. doi:10.1093/molbev/msx197
65. Greaves LC, Turnbull DM. Mitochondrial DNA mutations and ageing. Biochim Biophys Acta - Gen Subj. 2009;1790: 1015–1020. doi:https://doi.org/10.1016/j.bbagen.2009.04.018
66. Greaves LC, Reeve AK, Taylor RW, Turnbull DM. Mitochondrial DNA and disease. J Pathol. 2012;226: 274–286. doi:10.1002/path.3028
67. Sharma P, Sampath H. Mitochondrial DNA Integrity: Role in Health and Disease. Cells . 2019. doi:10.3390/cells8020100
68. Garza-Lombó C, Posadas Y, Quintanar L, Gonsebatt ME, Franco R.

Neurotoxicity Linked to Dysfunctional Metal Ion Homeostasis and Xenobiotic Metal Exposure: Redox Signaling and Oxidative Stress. Antioxid Redox Signal. 2018;28: 1669–1703. doi:10.1089/ars.2017.7272
69. Oster G, Wang H. Reverse engineering a protein: the mechanochemistry of ATP synthase. Biochim Biophys Acta - Bioenerg. 2000;1458: 482–510. doi:https://doi.org/10.1016/S0005-2728(00)00096-7
70. Capaldi RA, Aggeler R, Turina P, Wilkens S. Coupling between catalytic sites and the proton channel in F1F0-type ATPases. Trends Biochem Sci. 1994;19: 284–289. doi:10.1016/0968-0004(94)90006-x
71. Strauss M, Hofhaus G, Schröder RR, Kühlbrandt W. Dimer ribbons of ATP synthase shape the inner mitochondrial membrane. EMBO J. 2008;27: 1154–1160. doi:10.1038/emboj.2008.35
72. McEnery MW, Buhle Jr. EL, Aebi U, Pedersen PL. Proton ATPase of rat liver mitochondria. Preparation and visualization of a functional complex using the novel zwitterionic detergent 3-[(3-cholamidopropyl)dimethylammonio]-1-propanesulfonate. J Biol Chem. 1984;259: 4642–4651. doi:10.1016/S0021-9258(17)43095-X
73. Wilkens S, Dunn SD, Capaldi RA. A cryoelectron microscopy study of the interaction of the Escherichia coli F1-ATPase with subunit b dimer. FEBS Lett. 1994;354: 37–40. doi:10.1016/0014-5793(94)01059-5
74. Wilkens S, Capaldi RA. ATP synthase's second stalk comes into focus. Nature. 1998;393: 29. doi:10.1038/29908
75. Dimroth P. Operation of the F0 motor of the ATP synthase. Biochimica et Biophysica Acta - Bioenergetics. 2000. pp. 374–386. doi:10.1016/S0005-2728(00)00088-8
76. Angevine CM, Fillingame RH. Aqueous access channels in subunit a of rotary ATP synthase. J Biol Chem. 2003;278: 6066–6074. doi:10.1074/jbc.M210199200
77. Aksimentiev A, Balabin IA, Fillingame RH, Schulten K. Insights into the Molecular Mechanism of Rotation in the F o Sector of ATP Synthase. Biophys J. 2004;86: 1332–1344. doi:10.1016/S0006-3495(04)74205-8
78. Altendorf K, Stalz W, Greie J, Deckers-Hebestreit G. Structure and function of the F(o) complex of the ATP synthase from Escherichia coli. J Exp Biol. 2000;203: 19–28.
79. Weber J, Senior AE. Catalytic mechanism of F1-ATPase. Biochim Biophys Acta. 1997;1319: 19–58. doi:10.1016/s0005-2728(96)00121-1
80. Noji H, Yasuda R, Yoshida M, Kinosita K. Direct observation of the rotation of F1-ATPase. Nature. 1997;386: 299–302. doi:10.1038/386299a0
81. Hausrath AC, Grüber G, Matthews BW, Capaldi RA. Structural features of the γ subunit of the Escherichia coli F1 ATPase revealed by a 4.4-Å resolution map obtained by x-ray crystallography. Proc Natl Acad Sci U S A. 1999;96: 13697–13702. doi:10.1073/pnas.96.24.13697
82. Fillingame RH, Jiang W, Dmitriev OY. Coupling H+ transport to rotary catalysis in F-type ATP synthases: Structure and organization of the transmembrane rotary motor. J Exp Biol. 2000;203: 9–17. doi:10.1242/jeb.203.1.9
83. Hermolin J, Dmitriev OY, Zhang Y, Fillingame RH. Defining the Domain of Binding of F1 Subunit ε with the Polar Loop of F0 Subunit c in theEscherichia coli ATP Synthase*. J Biol Chem. 1999;274: 17011–17016. doi:https://doi.org/10.1074/jbc.274.24.17011
84. Howitt SM, Rodgers AJW, Hatch LP, Gibson F, Cox GB. The coupling of the

relative movement of thea andc subunits of the F0 to the conformational changes in the F1-ATPase. J Bioenerg Biomembr. 1996;28: 415–420. doi:10.1007/BF02113983
85. Junge W, Lill H, Engelbrecht S. ATP synthase: an electrochemical ransducer with rotatory mechanics. Trends Biochem Sci. 1997;22: 420–423. doi:https://doi.org/10.1016/S0968-0004(97)01129-8
86. Terni B, Boada J, Portero-Otin M, Pamplona R, Ferrer I. Mitochondrial ATP-synthase in the entorhinal cortex is a target of oxidative stress at stages I/II of alzheimer's disease pathology. Brain Pathol. 2010;20: 222–233. doi:10.1111/j.1750-3639.2009.00266.x
87. Beck SJ, Guo L, Phensy A, Tian J, Wang L, Tandon N, et al. Deregulation of mitochondrial F1FO-ATP synthase via OSCP in Alzheimer's disease. Nat Commun. 2016;7: 11483. doi:10.1038/ncomms11483
88. Chen R, Park H-A, Mnatsakanyan N, Niu Y, Licznerski P, Wu J, et al. Parkinson's disease protein DJ-1 regulates ATP synthase protein components to increase neuronal process outgrowth. Cell Death Dis. 2019;10: 469. doi:10.1038/s41419-019-1679-x
89. Mnatsakanyan N, Jonas EA. The new role of F1Fo ATP synthase in mitochondria-mediated neurodegeneration and neuroprotection. Exp Neurol. 2020;332: 113400. doi:10.1016/j.expneurol.2020.113400
90. Watt IN, Montgomery MG, Runswick MJ, Leslie AGW, Walker JE. Bioenergetic cost of making an adenosine triphosphate molecule in animal mitochondria. Proc Natl Acad Sci U S A. 2010;107: 16823–16827. doi:10.1073/pnas.1011099107
91. Artika IM. Current understanding of structure, function and biogenesis of yeast mitochondrial ATP synthase. J Bioenerg Biomembr. 2019;51: 315–328. doi:10.1007/s10863-019-09809-4
92. Ko YH, Hullihen J, Hong S, Pedersen PL. Mitochondrial F_0F_1 ATP Synthase: SUBUNIT REGIONS ON THE F_1 MOTOR SHIELDED BY F_0, FUNCTIONAL SIGNIFICANCE, AND EVIDENCE FOR AN INVOLVEMENT OF THE UNIQUE F_0 SUBUNIT F_6*. J Biol Chem. 2000;275: 32931–32939. doi:10.1074/jbc.M004453200
93. Mitchell P. Coupling of phosphorylation to electron and hydrogen transfer by a chemi-osmotic type of mechanism. Nature. 1961;191: 144–148. doi:10.1038/191144a0
94. Abrahams JP, Leslie AGW, Lutter R, Walker JE. Structure at 2.8 Â resolution of F1-ATPase from bovine heart mitochondria. Nature. 1994;370: 621–628. doi:10.1038/370621a0
95. Klusch N, Murphy BJ, Mills DJ, Yildiz Ö, Kühlbrandt W. Structural basis of proton translocation and force generation in mitochondrial ATP synthase. Elife. 2017;6: 1–16. doi:10.7554/eLife.33274
96. Kubo S, Niina T, Takada S. Molecular dynamics simulation of proton-transfer coupled rotations in ATP synthase FO motor. Sci Rep. 2020;10: 1–16. doi:10.1038/s41598-020-65004-1
97. Long JC, Wang S, Vik SB. Membrane topology of subunit a of the F1F0 ATP synthase as determined by labeling of unique cysteine residues. J Biol Chem. 1998;273: 16235–16240. doi:10.1074/jbc.273.26.16235
98. Valiyaveetil FI, Fillingame RH. Transmembrane topography of subunit a in the Escherichia coli F1F0 ATP synthase. J Biol Chem. 1998;273: 16241–16247. doi:10.1074/jbc.273.26.16241
99. Kühlbrandt W, Davies KM. Rotary ATPases: A New Twist to an Ancient

Machine. Trends Biochem Sci. 2016;41: 106–116. doi:https://doi.org/10.1016/j.tibs.2015.10.006
100. Fillingame RH. Coupling H+ transport and ATP synthesis in F1F0-ATP synthases: glimpses of interacting parts in a dynamic molecular machine. J Exp Biol. 1997;200: 217–224. doi:10.1242/jeb.200.2.217
101. Ogilvie I, Aggeler R, Capaldi RA. Cross-linking of the δ Subunit to One of the Three α Subunits Has No Effect on Functioning, as Expected if δ Is a Part of the Stator That Links the F1 and F0 Parts of the Escherichia coli ATP Synthase*. J Biol Chem. 1997;272: 16652–16656. doi:https://doi.org/10.1074/jbc.272.26.16652
102. Lill H, Hensel F, Junge W, Engelbrecht S. Cross-linking of Engineered Subunit δ to (αβ)3 in Chloroplast F-ATPase*. J Biol Chem. 1996;271: 32737–32742. doi:https://doi.org/10.1074/jbc.271.51.32737
103. Rastogi VK, Girvin ME. Structural changes linked to proton translocation by subunit c of the ATP synthase. Nature. 1999;402: 263–268. doi:10.1038/46224
104. picture story How proton pumps make ATP The discovery of chaperonins. 1999;6: 1999.
105. Fearnley IM, Walker JE. Two overlapping genes in bovine mitochondrial DNA encode membrane components of ATP synthase. EMBO J. 1986;5: 2003–2008. doi:10.1002/j.1460-2075.1986.tb04456.x
106. Hahn A, Parey K, Bublitz M, Mills DJ, Zickermann V, Vonck J, et al. Structure of a Complete ATP Synthase Dimer Reveals the Molecular Basis of Inner Mitochondrial Membrane Morphology. Mol Cell. 2016;63: 445–456. doi:10.1016/j.molcel.2016.05.037
107. Hutcheon ML, Duncan TM, Ngai H, Cross RL. Energy-driven subunit rotation at the interface between subunit a and the c oligomer in the F0 sector of Escherichia coli ATP synthase. Proc Natl Acad Sci U S A. 2001;98: 8519–8524. doi:10.1073/pnas.151236798
108. Devenish RJ, Papakonstantinou T, Galanis M, Law RH, Linnane AW, Nagley P. Structure/function analysis of yeast mitochondrial ATP synthase subunit 8. Ann N Y Acad Sci. 1992;671: 403–14. doi:10.1111/j.1749-6632.1992.tb43814.x
109. Colina-Tenorio L, Dautant A, Miranda-Astudillo H, Giraud MF, González-Halphen D. The peripheral stalk of rotary ATPases. Front Physiol. 2018;9: 1–19. doi:10.3389/fphys.2018.01243
110. Stephens AN, Khan MA, Roucou X, Nagley P, Devenish RJ. The molecular neighborhood of subunit 8 of yeast mitochondrial F1F0-ATP synthase probed by cysteine scanning mutagenesis and chemical modification. J Biol Chem. 2003;278: 17867–17875. doi:10.1074/jbc.M300967200
111. Lee J, Ding SJ, Walpole TB, Holding AN, Montgomery MG, Fearnley IM, et al. Organization of subunits in the membrane domain of the bovine F-ATPase revealed by covalent cross-linking. J Biol Chem. 2015;290: 13308–13320. doi:10.1074/jbc.M115.645283
112. GRANDIER-VAZEILLE X, OUHABI R, GUÉRIN M. Antibodies against subunits of F0 sector of ATP synthase from Saccharomyces cerevisiae Stimulation of ATP synthase by subunit-8-reactive antibodies and inhibition by subunit-9-reactive antibodies. Eur J Biochem. 1994;223: 521–528. doi:10.1111/j.1432-1033.1994.tb19021.x
113. Allegretti M, Klusch N, Mills DJ, Vonck J, Kühlbrandt W, Davies KM. Horizontal membrane-intrinsic α-helices in the stator a-subunit of an F-type

ATP synthase. Nature. 2015;521: 237–240. doi:10.1038/nature14185
114. Gu J, Zhang L, Zong S, Guo R, Liu T, Yi J, et al. Cryo-EM structure of the mammalian ATP synthase tetramer bound with inhibitory protein IF1. 2019;1075: 1068–1075.
115. Ng YS, Turnbull DM. Mitochondrial disease: genetics and management. J Neurol. 2016;263: 179–191. doi:10.1007/s00415-015-7884-3
116. Xu T, Pagadala V, Mueller DM. Understanding structure, function, and mutations in the mitochondrial ATP synthase. Microb cell (Graz, Austria). 2015;2: 105–125. doi:10.15698/mic2015.04.197
117. Galimberti CA, Diegoli M, Sartori I, Uggetti C, Brega A, Tartara A, et al. Brain pseudoatrophy and mental regression on valproate and a mitochondrial DNA mutation. Neurology. 2006;67: 1715 LP – 1717. doi:10.1212/01.wnl.0000242882.58086.9a
118. Auré K, Dubourg O, Jardel C, Clarysse L, Sternberg D, Fournier E, et al. Episodic weakness due to mitochondrial DNA MT-ATP6/8 mutations. Neurology. 2013;81: 1810 LP – 1818. doi:10.1212/01.wnl.0000436067.43384.0b
119. Tansel T, Paçal F, Ustek D. A novel ATP8 gene mutation in an infant with tetralogy of Fallot. Cardiol Young. 2013/06/05. 2014;24: 531–533. doi:DOI: 10.1017/S1047951113000668
120. Sequeira A, Rollins B, Magnan C, Van Oven M, Baldi P, Myers RM, et al. Mitochondrial Mutations in Subjects with Psychiatric Disorders. PLoS One. 2015;10: 1–17. doi:10.1371/journal.pone.0127280
121. Jonckheere AI, Smeitink JAM, Rodenburg RJT. Mitochondrial ATP synthase: Architecture, function and pathology. J Inherit Metab Dis. 2012;35: 211–225. doi:10.1007/s10545-011-9382-9
122. Uziel G, Moroni I, Lamantea E, Fratta GM, Ciceri E, Carrara F, et al. Mitochondrial disease associated with the T8993G mutation of the mitochondrial ATPase 6 gene: a clinical, biochemical, and molecular study in six families. J Neurol Neurosurg & Psychiatry. 1997;63: 16 LP – 22. doi:10.1136/jnnp.63.1.16
123. Baracca A, Sgarbi G, Mattiazzi M, Casalena G, Pagnotta E, Valentino ML, et al. Biochemical phenotypes associated with the mitochondrial ATP6 gene mutations at nt8993. Biochim Biophys Acta - Bioenerg. 2007;1767: 913–919. doi:https://doi.org/10.1016/j.bbabio.2007.05.005
124. Carrozzo R, Rizza T, Stringaro A, Pierini R, Mormone E, Santorelli FM, et al. Maternally-inherited Leigh syndrome-related mutations bolster mitochondrial-mediated apoptosis. J Neurochem. 2004;90: 490–501. doi:https://doi.org/10.1111/j.1471-4159.2004.02505.x
125. Cortés-Hernández P, Vázquez-Memije ME, García JJ. ATP6 homoplasmic mutations inhibit and destabilize the human F 1F0-ATP synthase without preventing enzyme assembly and oligomerization. J Biol Chem. 2007;282: 1051–1058. doi:10.1074/jbc.M606828200
126. Tatuch Y, Christodoulou J, Feigenbaum A, Clarke JTR, Wherret J, Smith C, et al. Heteroplasmic mtDNA mutation (T→G) at 8993 can cause Leigh disease when the percentage of abnormal mtDNA is high. Am J Hum Genet. 1992;50: 852–858.
127. PULLMAN ME, MONROY GC. a Naturally Occurring Inhibitor of Mitochondrial Adenosine. J Biol Chem. 1963;238: 3762–3769.
128. Gledhill JR, Montgomery MG, Leslie AGW, Walker JE. How the regulatory protein, IF1, inhibits F1-ATPase from bovine mitochondria. Proc Natl Acad

Sci U S A. 2007;104: 15671–15676. doi:10.1073/pnas.0707326104
129. Cabezón E, Montgomery MG, Leslie AGW, Walker JE. The structure of bovine F1-ATPase in complex with its regulatory protein IF1. Nat Struct Biol. 2003;10: 744–750. doi:10.1038/nsb966
130. Boyer PD. The ATP synthase--a splendid molecular machine. Annu Rev Biochem. 1997;66: 717–749. doi:10.1146/annurev.biochem.66.1.717
131. Isidoro A, Casado E, Redondo A, Acebo P, Espinosa E, Alonso AM, et al. Breast carcinomas fulfill the Warburg hypothesis and provide metabolic markers of cancer prognosis. Carcinogenesis. 2005;26: 2095–2104. doi:10.1093/carcin/bgi188
132. Genoux A, Pons V, Radojkovic C, Roux-Dalvai F, Combes G, Rolland C, et al. Mitochondrial inhibitory factor 1 (IF1) is present in human serum and is positively correlated with HDL-cholesterol. PLoS One. 2011;6. doi:10.1371/journal.pone.0023949
133. Sánchez-Aragó M, Chamorro M, Cuezva JM. Selection of cancer cells with repressed mitochondria triggers colon cancer progression. Carcinogenesis. 2010;31: 567–576. doi:10.1093/carcin/bgq012
134. Maierean S, Serban MC, Rizzo M, Lippi G, Sahebkar A, Banach M. The potential role of mitochondrial ATP synthase inhibitory factor 1 (IF1) in coronary heart disease: a literature review. Lipids Health Dis. 2017;16: 1–7. doi:10.1186/s12944-017-0430-9
135. García-Bermúdez J, Cuezva JM. The ATPase Inhibitory Factor 1 (IF1): A master regulator of energy metabolism and of cell survival. Biochim Biophys Acta - Bioenerg. 2016;1857: 1167–1182. doi:10.1016/j.bbabio.2016.02.004
136. Martín-Jiménez R, Faccenda D, Allen E, Reichel HB, Arcos L, Ferraina C, et al. Reduction of the ATPase inhibitory factor 1 (IF1) leads to visual impairment in vertebrates. Cell Death Dis. 2018;9: 669. doi:10.1038/s41419-018-0578-x
137. Solaini G, Sgarbi G, Baracca A. The F1Fo-ATPase inhibitor, IF1, is a critical regulator of energy metabolism in cancer cells. Biochem Soc Trans. 2021;49: 815–827. doi:10.1042/BST20200742
138. Campanella M, Parker N, Tan CH, Hall AM, Duchen MR. IF1: setting the pace of the F1Fo-ATP synthase. Trends Biochem Sci. 2009;34: 343–350. doi:https://doi.org/10.1016/j.tibs.2009.03.006
139. Campanella M, Casswell E, Chong S, Farah Z, Wieckowski MR, Abramov AY, et al. Regulation of Mitochondrial Structure and Function by the F1Fo-ATPase Inhibitor Protein, IF1. Cell Metab. 2008;8: 13–25. doi:https://doi.org/10.1016/j.cmet.2008.06.001
140. Lukin JA, Kontaxis G, Simplaceanu V, Yuan Y, Bax A, Ho C. Quaternary structure of hemoglobin in solution. Proc Natl Acad Sci U S A. 2003;100: 517–520. doi:10.1073/pnas.232715799
141. Mense SM, Zhang L. Heme: A versatile signaling molecule controlling the activities of diverse regulators ranging from transcription factors to MAP kinases. Cell Res. 2006;16: 681–692. doi:10.1038/sj.cr.7310086
142. Bhagavan NV, Ha C-E. Metabolism of Iron and Heme. Essentials Med Biochem. 2015; 511–529. doi:10.1016/b978-0-12-416687-5.00027-0
143. Miele AE, Draghi F, Vallone B, Boffi A. The carbon monoxide derivative of human hemoglobin carrying the double mutation LeuB10 → Tyr and HisE7 → Gln on α and β chains probed by infrared spectroscopy. Arch Biochem Biophys. 2002;402: 59–64. doi:10.1016/S0003-9861(02)00061-9
144. Altamentova SM, Marva E, Shaklai N. Oxidative interaction of unpaired

hemoglobin chains with lipids and proteins: A key for modified serum lipoproteins in thalassemia. Arch Biochem Biophys. 1997;345: 39–46. doi:10.1006/abbi.1997.0224
145. Abdullah UYH, Ibrahim HM, Jassim HM, Salleh MZ, Kek TL, Fakhruzzaman bin Noorizhab MN, et al. Relative proteome quantification of alpha, beta, gamma and delta globin chains in early eluting peaks of Bio-Rad variant II® CE-HPLC of hemoglobin from healthy and beta-thalassemia subjects in Malaysia. Biochem Biophys Reports. 2019;18: 100635. doi:10.1016/j.bbrep.2019.100635
146. Vitturi DA, Sun CW, Harper VM, Thrash-Williams B, Cantu-Medellin N, Chacko BK, et al. Antioxidant functions for the hemoglobin β93 cysteine residue in erythrocytes and in the vascular compartment in vivo. Free Radic Biol Med. 2013;55: 119–129. doi:10.1016/j.freeradbiomed.2012.11.003
147. Rong Z, Wilson MT, Cooper CE. A model for the nitric oxide producing nitrite reductase activity of hemoglobin as a function of oxygen saturation. Nitric Oxide - Biol Chem. 2013;33: 74–80. doi:10.1016/j.niox.2013.06.008
148. Meyer C, Heiss C, Drexhage C, Kehmeier ES, Balzer J, Mühlfeld A, et al. Hemodialysis-Induced Release of Hemoglobin Limits Nitric Oxide Bioavailability and Impairs Vascular Function. J Am Coll Cardiol. 2010;55: 454–459. doi:10.1016/j.jacc.2009.07.068
149. Shibayama N. Allosteric transitions in hemoglobin revisited. Biochim Biophys Acta - Gen Subj. 2020;1864: 2019. doi:10.1016/j.bbagen.2019.03.021
150. Newton DA, Rao KMK, Dluhy RA, Baatz JE. Hemoglobin is expressed by alveolar epithelial cells. J Biol Chem. 2006;281: 5668–5676. doi:10.1074/jbc.M509314200
151. Slemmon JR, Hughes CM, Campbell GA, Flood DG. Increased levels of hemoglobin-derived and other peptides in Alzheimer's disease cerebellum. J Neurosci. 1994;14: 2225–2235. doi:10.1523/jneurosci.14-04-02225.1994
152. Gomes I, Dale CS, Casten K, Geigner MA, Gozzo FC, Ferro ES, et al. Hemoglobin-derived peptides as novel type of bioactive signaling molecules. AAPS J. 2010;12: 658–669. doi:10.1208/s12248-010-9217-x
153. Koeppen AH, Michael SC, Li D, Chen Z, Cusack MJ, Gibson WM, et al. The pathology of superficial siderosis of the central nervous system. Acta Neuropathol. 2008;116: 371–382. doi:10.1007/s00401-008-0421-z
154. Lewin A, Hamilton S, Witkover A, Langford P, Nicholas R, Chataway J, et al. Free serum haemoglobin is associated with brain atrophy in secondary progressive multiple sclerosis. Wellcome Open Res. 2017;1: 1–23. doi:10.12688/wellcomeopenres.9967.1
155. Eaton WA, Bunn HF. Treating sickle cell disease by targeting HbS polymerization. Blood. 2017;129: 2719–2726. doi:10.1182/blood-2017-02-765891
156. Wang Z, Moult J. SNPs, protein structure, and disease. Hum Mutat. 2001;17: 263–270. doi:10.1002/humu.22
157. Lechauve C, Butcher JT, Freiwan A, Biwer LA, Keith JM, Good ME, et al. Endothelial cell α-globin and its molecular chaperone α-hemoglobin-stabilizing protein regulate arteriolar contractility. J Clin Invest. 2018;128: 5073–5082. doi:10.1172/JCI99933
158. Straub AC, Lohman AW, Billaud M, Johnstone SR, Dwyer ST, Lee MY, et al. Endothelial cell expression of haemoglobin α regulates nitric oxide signalling. Nature. 2012;491: 473–477. doi:10.1038/nature11626

159. Brown N, Alkhayer K, Clements R, Singhal N, Gregory R, Azzam S, et al. Neuronal Hemoglobin Expression and Its Relevance to Multiple Sclerosis Neuropathology. J Mol Neurosci. 2016;59: 1–17. doi:10.1007/s12031-015-0711-6
160. Shephard F, Greville-Heygate O, Marsh O, Anderson S, Chakrabarti L. A mitochondrial location for haemoglobins—Dynamic distribution in ageing and Parkinson's disease. Mitochondrion. 2014;14: 64–72. doi:10.1016/J.MITO.2013.12.001
161. Corliss BA, Delalio LJ, Stevenson Keller TC, Keller AS, Keller DA, Corliss BH, et al. Vascular Expression of Hemoglobin Alpha in Antarctic Icefish Supports Iron Limitation as Novel Evolutionary Driver. Front Physiol. 2019;10. doi:10.3389/fphys.2019.01389
162. Freed J, Chakrabarti L. Defining a role for hemoglobin in Parkinson's disease. npj Park Dis. 2016;2: 1–4. doi:10.1038/npjparkd.2016.21
163. Shephard F, Greville-Heygate O, Marsh O, Anderson S, Chakrabarti L. A mitochondrial location for haemoglobins-Dynamic distribution in ageing and Parkinson's disease. Mitochondrion. 2014. pp. 64–72. doi:10.1016/j.mito.2013.12.001
164. Bellelli A, Brunori M, Miele AE, Panetta G, Vallone B. The Allosteric Properties of Hemoglobin: Insights from Natural and Site Directed Mutants. Curr Protein Pept Sci. 2006;7: 17–45. doi:10.2174/138920306775474121
165. Saha D, Patgaonkar M, Shroff A, Ayyar K, Bashir T, Reddy KVR. Hemoglobin Expression in Nonerythroid Cells: Novel or Ubiquitous? Cavaillon J-M, editor. Int J Inflam. 2014;2014: 803237. doi:10.1155/2014/803237
166. Codrich M, Bertuzzi M, Russo R, Francescatto M, Espinoza S, Zentilin L, et al. Neuronal hemoglobin affects dopaminergic cells' response to stress. Cell Death Dis. 2018;8: e2538–e2538. doi:10.1038/cddis.2016.458
167. Shephard F, Greville-Heygate O, Liddell S, Emes R, Chakrabarti L. Analysis of Mitochondrial haemoglobin in Parkinson's disease brain. Mitochondrion. 2016;29: 45–52. doi:10.1016/j.mito.2016.05.001
168. Bibbin T. Paul1, David H. Manz1, Frank M. Torti SVT. Mitochondria and Iron: Current Questions Bibbin. 2016;10: 95–118. doi:10.1080/17474086.2016.1268047.Mitochondria
169. Chuang JY, Lee CW, Shih YH, Yang T, Yu L, Kuo YM. Interactions between amyloid-β and hemoglobin: Implications for amyloid plaque formation in alzheimer's disease. PLoS One. 2012;7. doi:10.1371/journal.pone.0033120
170. Wu CW, Liao PC, Yu L, Wang ST, Chen ST, Wu CM, et al. Hemoglobin promotes Aβ oligomer formation and localizes in neurons and amyloid deposits. Neurobiol Dis. 2004;17: 367–377. doi:10.1016/j.nbd.2004.08.014
171. Atti AR, Palmer K, Volpato S, Zuliani G, Winblad B, Fratiglioni L. Anaemia increases the risk of dementia in cognitively intact elderly. Neurobiol Aging. 2006;27: 278–284. doi:https://doi.org/10.1016/j.neurobiolaging.2005.02.007
172. Pandav RS, Chandra V, Dodge HH, DeKosky ST, Ganguli M. Hemoglobin Levels and Alzheimer Disease: An Epidemiologic Study in India. Am J Geriatr Psychiatry. 2004;12: 523–526. doi:https://doi.org/10.1097/00019442-200409000-00011
173. Faux NG, Rembach A, Wiley J, Ellis KA, Ames D, Fowler CJ, et al. An anemia of Alzheimer's disease. Mol Psychiatry. 2014;19: 1227–1234. doi:10.1038/mp.2013.178
174. Särkijärvi S, Kuusisto H, Paalavuo R, Levula M, Airla N, Lehtimäki T, et al.

Gene expression profiles in Finnish twins with multiple sclerosis. BMC Med Genet. 2006;7: 11. doi:10.1186/1471-2350-7-11
175. Broadwater L, Pandit A, Clements R, Azzam S, Vadnal J, Sulak M, et al. Analysis of the mitochondrial proteome in multiple sclerosis cortex. Biochim Biophys Acta - Mol Basis Dis. 2011;1812: 630–641. doi:https://doi.org/10.1016/j.bbadis.2011.01.012
176. Johan T. Ruud. Vertebrates without Erythrocytes and Blood Pigment. Nature. 1954;173: 848–850.
177. Kim BM, Amores A, Kang S, Ahn DH, Kim JH, Kim IC, et al. Antarctic blackfin icefish genome reveals adaptations to extreme environments. Nat Ecol Evol. 2019;3: 469–478. doi:10.1038/s41559-019-0812-7
178. Beers JM, Jayasundara N. Antarctic notothenioid fish: what are the future consequences of "losses" and "gains" acquired during long-term evolution at cold and stable temperatures? J Exp Biol. 2015;218: 1834–45. doi:10.1242/jeb.116129
179. Di Prisco G, Cocca E, Parker SK, Detrich HW. Tracking the evolutionary loss of hemoglobin expression by the white-blooded Antarctic icefishes. Gene. 2002;295: 185–191. doi:10.1016/S0378-1119(02)00691-1
180. Near TJ, Parker SK, Detrich HW. A genomic fossil reveals key steps in hemoglobin loss by the Antarctic icefishes. Mol Biol Evol. 2006;23: 2008–2016. doi:10.1093/molbev/msl071
181. Weatherall DJ, Clegg JB. Haemoglobin synthesis in thalassaemia. Biochem J. 1970;119: 1241–1243. doi:10.1042/bj1190068pb
182. Borley KA, Sidell BD. Evolution of the myoglobin gene in Antarctic Icefishes (Channichthyidae). Polar Biol. 2011;34: 659–665. doi:10.1007/s00300-010-0921-x
183. Sidell BD, O'Brien KM. When bad things happen to good fish: The loss of hemoglobin and myoglobin expression in Antarctic icefishes. J Exp Biol. 2006;209: 1791–1802. doi:10.1242/jeb.02091
184. O'Brien KM, Mueller IA. The unique mitochondrial form and function of antarctic channichthyid icefishes. Integr Comp Biol. 2010;50: 993–1008. doi:10.1093/icb/icq038
185. Wujcik JM, Wang G, Eastman JT, Sidell BD. Morphometry of retinal vasculature in Antarctic fishes is dependent upon the level of hemoglobin in circulation. J Exp Biol. 2007;210: 815–824. doi:10.1242/jeb.001867
186. O'Brien KM, Mueller IA, Orczewska JI, Dullen KR, Ortego M. Hearts of some Antarctic fishes lack mitochondrial creatine kinase. Comp Biochem Physiol - Part A Mol Integr Physiol. 2014;178: 30–36. doi:10.1016/j.cbpa.2014.08.003
187. Mark FC, Lucassen M, Strobel A, Barrera-Oro E, Koschnick N, Zane L, et al. Mitochondrial function in antarctic nototheniids with ND6 translocation. PLoS One. 2012;7. doi:10.1371/journal.pone.0031860
188. Strobel A, Graeve M, Poertner HO, Mark FC. Mitochondrial Acclimation Capacities to Ocean Warming and Acidification Are Limited in the Antarctic Nototheniid Fish, Notothenia rossii and Lepidonotothen squamifrons. PLoS One. 2013;8. doi:10.1371/journal.pone.0068865
189. Weinstein RB, Somero GN. Effects of temperature on mitochondrial function in the Antarctic fish Trematomus bernacchii. J Comp Physiol - B Biochem Syst Environ Physiol. 1998;168: 190–196. doi:10.1007/s003600050136
190. Kawall HG, Torres JJ, Sidell BD, Somero GN. Metabolic cold adaptation in Antarctic fishes: Evidence from enzymatic activities of brain. Mar Biol. 2002;140: 279–286. doi:10.1007/s002270100695

191. Papetti C, Liò P, Rüber L, Patarnello T, Zardoya R. Antarctic fish mitochondrial genomes lack ND6 gene. J Mol Evol. 2007;65: 519–528. doi:10.1007/s00239-007-9030-z
192. Zhuang X, Cheng CHC. ND6 Gene "lost" and found: Evolution of mitochondrial gene rearrangement in antarctic notothenioids. Mol Biol Evol. 2010;27: 1391–1403. doi:10.1093/molbev/msq026
193. Sleadd IM, Lee M, Hassumani DO, Stecyk TMA, Zeitz OK, Buckley BA. Sub-lethal heat stress causes apoptosis in an Antarctic fish that lacks an inducible heat shock response. J Therm Biol. 2014;44: 119–125. doi:10.1016/j.jtherbio.2014.06.007
194. Franklin CE, Davison W, Seebacher F. Antarctic fish can compensate for rising temperatures: Thermal acclimation of cardiac performance in Pagothenia borchgrevinki. J Exp Biol. 2007;210: 3068–3074. doi:10.1242/jeb.003137
195. Altelaar AFM, Munoz J, Heck AJR. Next-generation proteomics: Towards an integrative view of proteome dynamics. Nat Rev Genet. 2013;14: 35–48. doi:10.1038/nrg3356
196. Kovács IA, Luck K, Spirohn K, Wang Y, Pollis C, Schlabach S, et al. Network-based prediction of protein interactions. Nat Commun. 2019;10: 1–8. doi:10.1038/s41467-019-09177-y
197. Ideker T, Sharan R. Protein networks in disease 10.1101/gr.071852.107. Genome Res. 2008;18: 644–652. doi:10.1101/gr.071852.107.Freely
198. Sikosek T, Chan HS. Biophysics of protein evolution and evolutionary protein biophysics. J R Soc Interface. 2014;11. doi:10.1098/rsif.2014.0419
199. Le Q, Sievers F, Higgins DG. Protein multiple sequence alignment benchmarking through secondary structure prediction. Bioinformatics. 2017;33: 1331–1337. doi:10.1093/bioinformatics/btw840
200. Dalal A, Atri A. An Introduction to Sequence and Series. Int J Res. 2014;1: 1286–1292. doi:10.1002/0471250953.bi0301s42.An
201. Das S, Biswas A, Dasgupta S, Abraham A. Bacterial Foraging Optimization Algorithm: Theoretical Foundations, Analysis, and Applications. In: Abraham A, Hassanien A-E, Siarry P, Engelbrecht A, editors. Foundations of Computational Intelligence Volume 3: Global Optimization. Berlin, Heidelberg: Springer Berlin Heidelberg; 2009. pp. 23–55. doi:10.1007/978-3-642-01085-9_2
202. Madeira F, Park YM, Lee J, Buso N, Gur T, Madhusoodanan N, et al. The EMBL-EBI search and sequence analysis tools APIs in 2019. Nucleic Acids Res. 2019;47: W636–W641. doi:10.1093/nar/gkz268
203. Subramanian AR, Kaufmann M, Morgenstern B. DIALIGN-TX: Greedy and progressive approaches for segment-based multiple sequence alignment. Algorithms Mol Biol. 2008;3: 1–11. doi:10.1186/1748-7188-3-6
204. Wallace IM, O'Sullivan O, Higgins DG, Notredame C. M-Coffee: Combining multiple sequence alignment methods with T-Coffee. Nucleic Acids Res. 2006;34: 1692–1699. doi:10.1093/nar/gkl091
205. Nooren IMA, Thornton JM. Diversity of protein-protein interactions. EMBO J. 2003;22: 3486–3492. doi:10.1093/emboj/cdg359
206. Stark C, Breitkreutz B-J, Reguly T, Boucher L, Breitkreutz A, Tyers M. BioGRID: a general repository for interaction datasets. Nucleic Acids Res. 2006;34: D535–D539. doi:10.1093/nar/gkj109
207. Xenarios I, Rice DW, Salwinski L, Baron MK, Marcotte EM, Eisenberg D. DIP: the database of interacting proteins. Nucleic Acids Res. 2000;28: 289–

291. doi:10.1093/nar/28.1.289
208. Bader GD, Betel D, Hogue CW V. BIND: the Biomolecular Interaction Network Database. Nucleic Acids Res. 2003;31: 248–250. doi:10.1093/nar/gkg056
209. Chatr-aryamontri A, Ceol A, Palazzi LM, Nardelli G, Schneider MV, Castagnoli L, et al. MINT: the Molecular INTeraction database. Nucleic Acids Res. 2006/11/29. 2007;35: D572–D574. doi:10.1093/nar/gkl950
210. Szklarczyk D, Gable AL, Lyon D, Junge A, Wyder S, Huerta-Cepas J, et al. STRING v11: Protein-protein association networks with increased coverage, supporting functional discovery in genome-wide experimental datasets. Nucleic Acids Res. 2019;47: D607–D613. doi:10.1093/nar/gky1131
211. Salmaso V, Sturlese M, Cuzzolin A, Moro S. DockBench as docking selector tool: the lesson learned from D3R Grand Challenge 2015. J Comput Aided Mol Des. 2016;30: 773–789. doi:10.1007/s10822-016-9966-4
212. Huang S-Y, Zou X. Advances and Challenges in Protein-Ligand Docking. International Journal of Molecular Sciences . 2010. doi:10.3390/ijms11083016
213. Abagyan R, Totrov M. High-throughput docking for lead generation. Curr Opin Chem Biol. 2001;5: 375–382. doi:https://doi.org/10.1016/S1367-5931(00)00217-9
214. Schneidman-Duhovny D, Inbar Y, Nussinov R, Wolfson HJ. PatchDock and SymmDock: Servers for rigid and symmetric docking. Nucleic Acids Res. 2005;33: 363–367. doi:10.1093/nar/gki481
215. Inbar Y, Schneidman-Duhovny D, Halperin I, Oron A, Nussinov R, Wolfson HJ. Approaching the CAPRI challenge with an efficient geometry-based docking. Proteins Struct Funct Bioinforma. 2005;60: 217–223. doi:https://doi.org/10.1002/prot.20561
216. Zhang C, Vasmatzis G, Cornette JL, DeLisi C. Determination of atomic desolvation energies from the structures of crystallized proteins11Edited by B. Honig. J Mol Biol. 1997;267: 707–726. doi:https://doi.org/10.1006/jmbi.1996.0859
217. Young T, Abel R, Kim B, Berne BJ, Friesner RA. Motifs for molecular recognition exploiting hydrophobic enclosure in protein–ligand binding. Proc Natl Acad Sci. 2007;104: 808 LP – 813. doi:10.1073/pnas.0610202104
218. Sanchez G. Las instituciones de ciencia y tecnología en los procesos de aprendizaje de la producción agroalimentaria en Argentina. El Sist argentino innovación Inst Empres y redes El desafío la creación y apropiación Conoc. 2013; 659–664. doi:10.1002/prot
219. Adcock SA, McCammon JA. Molecular Dynamics: Survey of Methods for Simulating the Activity of Proteins. Chem Rev. 2006;106: 1589–1615. doi:10.1021/cr040426m
220. Abraham MJ, Murtola T, Schulz R, Páll S, Smith JC, Hess B, et al. GROMACS: High performance molecular simulations through multi-level parallelism from laptops to supercomputers. SoftwareX. 2015;1–2: 19–25. doi:https://doi.org/10.1016/j.softx.2015.06.001
221. Toosi K. 基因的改变NIH Public Access. Bone. 2014;23: 1–7. doi:10.1021/bi800894u.Simulations
222. Lobanov MY, Bogatyreva NS, Galzitskaya O V. Radius of gyration as an indicator of protein structure compactness. Mol Biol. 2008;42: 623–628. doi:10.1134/S0026893308040195

223. Kufareva I, Abagyan R. Methods of protein structure comparison. Methods Mol Biol. 2012;857: 231–257. doi:10.1007/978-1-61779-588-6_10

Chapter 2 : Sequence and structure comparison of ATP synthase F0 subunits 6 and 8 in notothenioid fish

PLOS ONE

DataAvailabilityStatement: All relevant data are within the manuscript and its Supporting information files.

Funding: Gunjan Katyal was supported by Vice Chancellor's International Scholarship for Research RESEARCH ARTICLE

Sequence and structure comparison of ATP synthase F_0 subunits 6 and 8 in notothenioid fish

Gunjan Katyal[1], Brad Ebanks[1], Magnus Lucassen[2], Chiara Papetti[3], Lisa Chakrabarti[1,4]*

1 School of Veterinary Medicine and Science, University of Nottingham, Sutton Bonington, United Kingdom,
2 Alfred Wegener Institute, Bremerhaven, Germany, **3** Biology Department, University of Padova, Padova, Italy, **4** MRC-Versus Arthritis Centre for Musculoskeletal Ageing Research, Nottingham, United Kingdom

* lisa.chakrabarti@nottingham.ac.uk

OPEN ACCESS

Citation: Katyal G, Ebanks B, Lucassen M, Papetti C, Chakrabarti L (2021) Sequence and structure comparison of ATP synthase F_0 subunits 6 and 8 in notothenioid fish. PLoS ONE 16 (10): e0245822. https://doi.org/10.1371/journal.pone.0245822

Editor: Benedetta Ruzzenente, Imagine Institute for genetic diseases, FRANCE

Received: January 7, 2021

Accepted: September 9, 2021

Published: October 6, 2021

PeerReviewHistory: PLOS recognizes the benefits of transparency in the peer review process; therefore, we enable the publication of all of the content of peer review and author responses alongside final, published articles. The editorial history of this article is available here: https://doi.org/10.1371/journal.pone.0245822

Abstract

Mitochondrial changes such as tight coupling of the mitochondria have facilitated sustained oxygen and respiratory activity in haemoglobin-less icefish of the Channichthyidae family. We aimed to characterise features in the sequence and structure of the proteins directly involved in proton transport, which have potential physiological implications. ATP synthase subunit a (*ATP6*) and subunit 8 (*ATP8*) are proteins that function as part of the F_0 component (proton pump) of the F_0F_1complex. Both proteins are encoded by the mitochondrial genome and involved in oxidative phosphorylation. To explore mitochondrial sequence variation for ATP6 and ATP8 we analysed sequences from *C. gunnari* and *C. rastrospinosus* and compared them with their closely related red-blooded species and eight other vertebrate species. Our comparison of the amino acid sequence of these proteins reveals important differences that could underlie aspects of the unique physiology of the icefish. In this study we find that changes in the sequence of subunit a of the icefish *C. gunnari* at position 35 where there is a hydrophobic alanine which is not seen in the other notothenioids we analysed. An amino acid change of this type is significant since it may have a structural impact. The biology of the haemoglobin-less icefish is necessarily unique and any insights about these animals will help to generate a better overall understanding of important physiological pathways.

2.1 Introduction

The oceans which surround Antarctica, and their sub-zero temperatures provide a home to fish of the suborder Notothenioidei—a prime example of a marine species flock.

Notothenioids are renowned for their physiological adaptations to cold temperatures. This includes the ability to synthesise antifreeze glycoproteins (AFGP) and antifreeze-potentiating proteins (AFPP) [1]. The capacity to synthesise antifreeze glycopeptides (AFGPs) is a biochemical adaptation that enabled the Notothenioidei to colonize and thrive in the extreme polar environment [2]. These proteins are largely composed of a Thr-Ala-Ala repeat with a conjugated disaccharide via the hydroxyl group of the Thr residue and reduce the freezing point of the animals internal fluids [3,4].

Channichthyidae, contained within the Notothenioid suborder, are remarkable due to the absence of haemoglobin and, in some species, myoglobin too [5–7]. The sub-zero temperatures of the water they inhabit allow the highest levels of oxygen solubility, which is suggested to facilitate their survival despite the loss of globin proteins [7].

Myoglobin is absent in the oxidative skeletal muscle in all icefish, but the absence of myoglobin in cardiac muscle has been reported in only six of the species of the Channichthyinae [8,9]. While the molecular genetics of how myoglobin expression has been lost have been studied, the physiological differences between those that express and those that do not express myoglobin are not fully understood. Small intracellular diffusion distances to mitochondria and a greater percentage of cell volume occupied by mitochondria are two evolutionary adaptations that might compensate for the absence of myoglobin [10,11]. In the particular case of *Champsocephalus gunnari*, the mRNA transcript of myoglobin is present in the cardiac tissue but a 5-bp frameshift insertion hinders the synthesis of protein from the mRNA transcript
[8,12].

Notothenioidei have high densities of mitochondria in muscle cells, versatility in mitochondrial biogenesis and a unique lipidomic profile [13–15]. These features have also been hypothesised to facilitate sustained oxygen consumption and respiratory activity in the absence of haemoglobin and myoglobin.

Complex V of the electron transport chain, ATP synthase, is responsible for the production of intracellular ATP from ADP and inorganic phosphate. Composed of an F_o and F_1 component, the F_o component is responsible for channelling protons from the intermembrane space across the inner mitochondrial membrane and into the mitochondrial matrix [16–18]. The rotation of the c-ring in F_o, and with this the γ-subunit of the central stalk, facilitates the translocation of protons across the inner mitochondrial membrane that ultimately drives the catalytic mechanism of the F_1 component [19,20].

The motor unit F_o, embedded in the inner membrane of mitochondria, is composed of subunits b, OSCP (oligomycin sensitivity conferring protein), d, e, f, g, h, i/j, k which are encoded by nuclear genes and subunits a (ATP6) and

8 (ATP8), which are encoded by mitochondrial genes [21]. Despite the structure of the complex having been first resolved decades ago, and hypotheses of the chemical mechanism were developed over half a century ago, significant breakthroughs continue to be made in our understanding of both the structure and function of the enzyme and its F_o component [22–25]. Both ATP synthase subunit a (ATP6) and subunit 8 (ATP8) are proteins that function as part of the F_o component of ATP synthase, encoded by genes that overlap within the mitochondrial genome [26]. This overlap is over a short, but variable between species, base pair sequence where the translation initiation site of subunit 8 is contained within the coding region of subunit 6.

The peripheral stalk is a crucial component of the F_o component forming a physical connection between the membrane sector of the complex and the catalytic core. It provides flexibility, aids in the assembly and stability of the complex, and forms the dimerization interface between ATP synthase pairs [27]. ATP8 is an integral transmembrane component of the peripheral stalk, serving an important role in the assembly of the complex [28]. The C-terminus of ATP8 extends 70 Å from the surface of the makes contacts with subunits b, d and F_6, while the N-terminus has been reported to make connections with subunits b, f and 6 in the intermembrane space [29,30]. Subunit 8 is also known to play a role in the activity of the enzyme complex [31].

ATP6 is an α-helical protein embedded within the inner mitochondrial membrane and it interacts closely with the c-ring of F_o, providing aqueous half-channels that shuttle protons to and from the rotating c-ring [17,32]. It has previously been reported that ATP6 has at least five hydrophobic transmembrane spanning α helices domain, where two of the helices h4 and h5 are well conserved across many species [33].

Proteins coded by mitochondrial DNA (mtDNA) are involved in oxidative phosphorylation and can directly influence the metabolic performance of this pathway. Evaluating the selective pressures acting on these proteins can provide insights in their evolution, where mutations in the mtDNA can be favourable, neutral, or harmful. The amino acid changes can cause inefficiencies in the electron transfer chain, causing oxidative damage by excess production of reactive oxygen species and eventually interrupting the production of mitochondrial energy. Due to the tight coupling of icefish mitochondria relative to their red-blooded relatives, any changes in the structure of ATP Synthase subunits, particularly those directly involved in the transport of protons across the membrane, could result in significant physiological outcomes [34].

In this work, we combine sequence analyses and secondary structure prediction analyses to explore mitochondrial genetic variation for ATP6 and ATP8 in the Notothenioidei suborder species as well as other vertebrate species. The species considered include *Champsocephalus gunnari*, *Chionodraco rastrospinosus* and *Chaenocephalus aceratus* from the

Channichthyidae family, *Notothenia coriiceps* and *Trematomus bernacchii* from the Nototheniidae family and the sub-Antarctic *Eleginops maclovinus* from family Eleginopsidae, all the broader Notothenioidei suborder. The species of suborder Notothenioidei are further compared with the following eight vertebrates: *Homo sapiens (*family: Hominidae), *Nothobranchius furzeri (*family: Nothobranchiidae), *Danio rerio (*family: Cyprinidae), *Anolis carolinensis (*family: Dactyloidae), *Cavia porcellus (*family: Caviidae), *Balaena mysticetus (*family: Balaenidae), *Heterocephalus glaber (*family: Heterocephalidae), and Lasiurus *borealis (*family: Vespertilionidae) to shed light on the changes of these proteins in the notothenioid species by comparing them to better characterised diverse vertebrate species. These species choices help us decipher amino acid changes specific to notothenioids and those that are potentially species specific (S1 Fig).

2.2 Methodology

2.2.1 Extraction of gene and protein sequences of ATP8 and ATP6 suborder Notothenioidei and other vertebrates

The list of complete coding sequences (CDS) and protein sequences of the proteins were obtained from the National Centre for Biotechnology Information (NCBI) protein database search, we chose only the Refseq (provides a comprehensive, integrated, non-redundant, wellannotated set of sequences, including genomic DNA, transcripts, and proteins) sequence queries (https://www.ncbi.nlm.nih.gov/ lMSast searched:17th August 2020). Though these sequences have been taken from highly reliable Refseq database [35] validated by different sources it is important to recognise they could still be prone to error.

2.2.2 Multiple protein sequence alignment (MSA)

(-/-) indicates absence of both haemoglobin and myoglobin genes, whereas (-/+) indicate absence of haemoglobin but presence of myoglobin. The sequences for the Notothenioidei suborder species *C. gunnari (*-/-), *C. rastrospinosus (*-/+), *C. aceratus (*-/-), *N. coriiceps (*+/+), *T. bernacchii*, *E. maclovinus (*+/+), and eight other vertebrate species, *N. furzeri*, *D. rerio*, *A. carolinensis*, *C. porcellus*, *B. mysticetus*, *H. glaber*, *L. borealis*, *H. sapiens* were aligned using Clustal omega [36] to prepare the initial alignment of ATP6 protein under the criteria of the presence and the absence of haemoglobin and myoglobin proteins in the species, the alignments were also verified using the other two progressive methods, MAFFT [37] and MUSCLE [36]. The same method was applied for protein ATP8. The MSA was visualised and edited using JALVIEW [38]. The eight vertebrate species were selected as well known and sequenced representative of different groups under vertebrate: fish (*N. furzeri* and *D. rerio*), reptiles (*A.*

carolinesis), mammals (*C. porcellus*, *H. glaber*, *L. borealis*, *H. sapiens*, *B. mysticetus*). *H.sapiens* sequences have been included in our analyses since much of what is known about these proteins has previously been characterised in humans. The selection of these different species shows the conservation of these mitochondrial proteins across vertebrate species, including *H. sapiens*.

2.2.3 Codon alignment

Complete nucleotide coding sequences for genes *ATP6* and *ATP8* from the fourteen vertebrate species were retrieved from NCBI GenBank database (see Table 1). The sequences were aligned using Clustal omega [36] and were manually edited and visualised as codons using MATLAB version R2018b (9.5.0).

2.2.4 Comparison of properties of amino acids among the sequence from the above-mentioned species

Using the ExPASy [39] tool ProtScale [40], different amino acid properties such as the molecular weight of amino acids across the sequence, hydrophobicity trend of amino acids, α—helix forming amino acids, average flexibility trend and mutability for the protein ATP6 were compared graphically among the seven fish species (5 Antarctic, 1 sub-Antarctic, *D. rerio* and *N. furzeri*) (https://web.expasy.org/protscale/).

2.2.5 Structure prediction for protein sequences

The MSA was structurally validated using the structure prediction tool I-TASSER [41] (Iterative Threading ASSEmbly Refinement) a hierarchical approach to protein structure and function prediction, to generate the protein structure for AT6 from different species (https://zhanglab.ccmb.med.umich.edu/I-TASSER/). The structures were validated using SAVES v6.0 (https://saves.mbi.ucla.edu/), using ERRAT [42], PROCHECK [43,44] and ProSA-web [45].
(Figures in supplementary files).

2.2.6 Figures

Protein structure images were produced with PyMOL v. 2.3.2. (The PyMOL Molecular Graphics System, Version 2.0 Schro¨dinger, LLC.) Graphs were produced with MATLAB version R2018b (9.5.0). Sequence logos were created using the webserver WebLogo using alignment of 5947 vertebrate (NCBI:txid7742) protein sequences for the protein ATP6 (http://weblogo. threeplusone.com/). Using RefSeq sequences with custom range of sequence length of 224– 231 to obtain full sequences only (searched: 3rd May 2021).

2.3 Results

2.3.1 Codon alignment

MSA of all the sequences of ATP8 (see Fig 1) and ATP6 (see Fig 2) from the different vertebrate s

pecies (see Table 1) for both nucleotide (codon) and proteins identified several

Species/Features	*C. gunnari*	*C. rastrospinosus*	*C. aceratus*	*N. corriceps*	*T. bernacchii*	*E. maclovinus*	*N. furzeri*	*D. rerio*	*A. carolinensis*	*L. borealis*	*H. glaber*	*C. porcellus*	*B. mysticetus*	*H. sapiens*
Common Name	Mackerelicefis	Ocellatedicefis	Blackfindicefis	Marbledrockcoc	Emeraldrockcoc	Rockcod	Killifish	Zebrafis	Lizard	Easternredbat	Nakedmoleral	GuineaPig	Bowhea Whale	Humans
Accession No. ATP6 protein	YP_00657588	YP_009519992	AEH05456	BBC27483.	ANN44664.	YP_009340791	YP_00245626	NP_059336	ACD81888.	YP_005255232	YP_00422267	QIQ22938.	AWM99473.	YP_00302403
Accession No. ATP6 nucleotide	NC_018340	NC_039543	NC_015654.	NC_015653.	KU16686	NC_033386	NC_011814.	NC_002333	NC_016873.	NC_001573.	NC_015112.	NC_000884	NC_005268	NC_012920
Accession No. ATP8 protein	YP_00657588	YP_009519991	YP_004581501	YP_00458148	ANN44663.	YP_009340792	YP_00245626	NP_059335	ACD81887.1	YP_005255232	YP_00422261	NP_008755	NP_944611.	NC_012920.
Haemoglobin	-	-		+	+	+	+	+	+	+	+	+	+	+
Myoglobin	-	+	-	+	+	+	+	+	+	+	+	+	+	+
Length of nucleotide ATP6	683	695	695	695	695	695	682	683	680	683	680	680	680	680
5 ' flanking region ATP8	74nt	nt 75	nt 75	nt 75	nt 75	nt 75	nt 74	nt 73	nt-1rn 67 Lysine	nt 71	nt 73	nt 68	nt 71	nt 71
ATP6-Start codon	atg	gtg	gtg	gtg	atg	gtg	atg	atg	ag	atg	atg	atg	atg	atg
_nucleotides at 'end c	-	+ GTG-AAC-CTG-ACC	+ GTG-AAC-CTG-ACC	+ GTG-GTC-CTG-ACC	+ ATG-AAC-TTG-GCC	+ GTG-AAC-CTG-ACC	-	-	-	-	-	-	-	-
_amino acid at 'end c	-	MNLT +	MNLT +	MVLT +	MNLA +	MNLT +	-	-	-	-	-	-	-	-
Codon pliaing at position 37 nucleotide	GCT	TCT	TCT	TCT	TCC	TCT	CTT	ACA	AAT	ACC	CCC	CCC	CCA	CCA
Residue Alignin at positio 35 protein	Alanine	Serine	Serine	Serine	Serine	Serine	Leucine	Threonin	Asparagin	-	-	-	-	-
Residues 35 positions 38 43 aligned 37 42 residues	Valine-Isoleucin	Valine-Isoleucir	Valine-Isoleucir	Valine-Isoleucir	Valine-Valin	Valine-Valin	Tryptophan Leucine	Tryptophan Isoleucine	Leucine-Valine	Isoleucine Asparagin	Isoleucine Asparagin	Isoleucine Asparagin	Isoleucine Asparagin	Isoleucine Asparagin
Properties of substitution	Non-Pola	Non-Pola	Non-Pola	Non-Pola	Non-Pola	Non-Pola	Non-polar aromaticAA Hydrophobic branchedAA	Non-polar aromaticAA Hydrophobic branchedAA	Hydrophobi AA	HydrophobicAA —Polar,non-chargedAA	HydrophobicAA —Polar,non-chargedAA	Hydrophobi AA—Polar, non-charge AA	Hydrophobi AA—Polar, non-charge AA	HydrophobicAA —Polar,non-chargedAA
Structural change 39 position 38 43 aligned 37 42 residues	strand-stran	coil-coil	coil-coil	coil-coil	strand-stran	strand-stran	strand-stran	strand-stran	strand-stran	coil-coil	coil-coil	coil-coil	coil-coil	coil-coil

Table 1. Features of nucleotide and protein sequencesfor ATP synthase F_0 subunit 6 and 8.

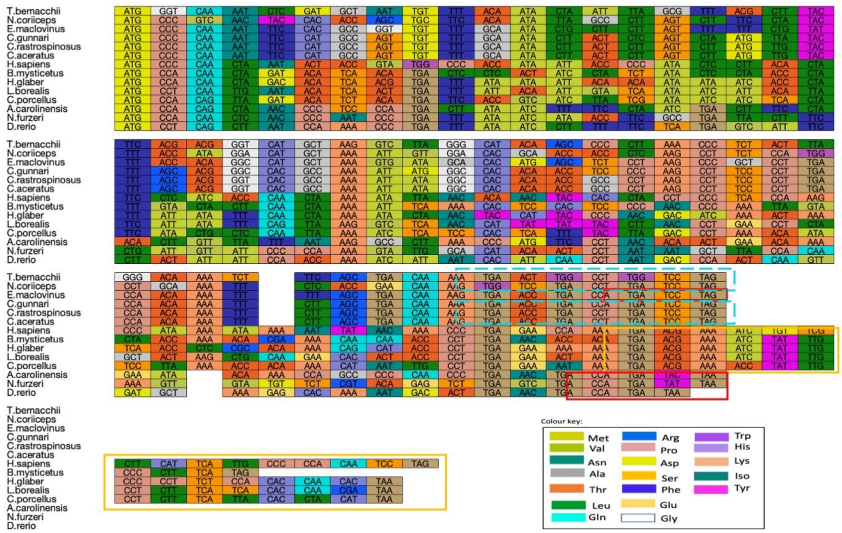

Fig 1. Multiple sequence alignment for nucleotide sequences of ATP synthase subunit 8. Multiple codon alignment of nucleotide sequences of ATP synthase subunit 8 was created using the Clustal omega alignment of nucleotides we screened five Antarctic and one sub-Antarctic fish species and eight vertebrate outgroups same as ATP6 MSA (See Fig 1 for colour key). The highlighted boxes show the overlap of the ATP8 and ATP6 sequences for different species where different colour of the boxes correspond to the different lengths of overlap.

https://doi.org/10.1371/journal.pone.0245822.g001

conserved codons and amino acid residues. The sequence knowledge was gathered from curated entries in RefSeq which nevertheless could be subject to error.

Five of the six Antarctic fish species have twelve nucleotides (four codons) at the 5' end of the gene sequence which are not found in the other eight vertebrate species. The codon alignment ATP6 for species *E. maclovinus*, *N. coriiceps*, *C. rastrospinosus* and *C. aceratus* show that GTG codes for methionine, as the start codon for the protein. GTG which is originally known for coding the amino acid valine has been accepted as a mitochondrion start codon for invertebrate mitogenomes [46–48]. A common feature with the species that have GTG as a start codon is that *N. coriiceps*, *E. maclovinus*, *C. rastrospinosus* have genes coding for myoglobin, where the latter is devoid of haemoglobin. *C. aceratus* do not express myoglobin due to a 15 bp sequence insertion, other than that difference, their myoglobin gene sequence is identical to that of *C. rastrospinosus* [9]. The only exception to this is the red-blooded species *T. bernacchii*, but this may be attributed to the unverified source of its sequence submission.

Another trend that has been observed through sequence alignment is that the species that are more similar and have the same amino acid for a particular position also have codons with the same nucleotide (nt) at the third position. 'TGA' codons or 'stop codons' are found within the translated sequence, here these code for tryptophan, as seen in human and yeast mitochondria [49]. A variation in the length of the sequences was observed, with

an average length for *ATP6* nt sequence of 683 and 74 nt for *ATP8* gene sequences. The *ATP6* sequence ends with a TAA stop codon in all species except the two red blooded Antarctic fish species, *N. coriiceps* and *E. maclovinus*.

2.3.2 Overlapping genes

The overlap between genes is encoded on the same strand (Table 1). The length of overlap was 22 nt in ATP8-ATP6 for the five of the six species of Notothenioidei suborder, that is excluding

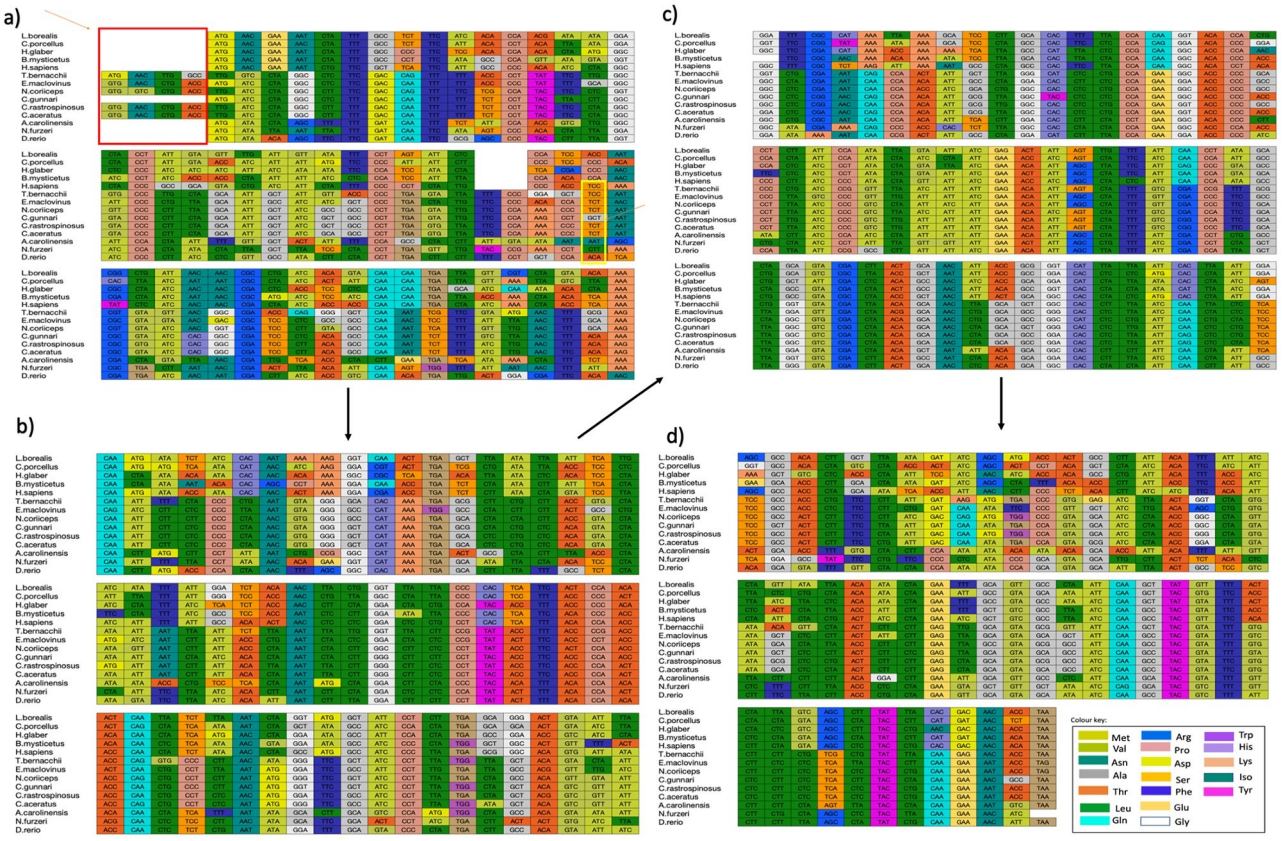

Fig 2. (a-d) Multiple sequence alignment for nucleotide sequences of ATP synthase subunit 6. Multiple codon alignment of nucleotide sequences of ATP synthase subunit 6 was created using the Clustal omega alignment of nucleotides for five Antarctic and one sub-Antarctic fish species and eight vertebrate outgroups and visualised) using MATLAB. The colour of the codon boxes corresponds to the respective amino acid (See colour key).

https://doi.org/10.1371/journal.pone.0245822.g002

icefish *C. gunnari* where the overlap was of 10nt. Species *H. sapiens*, *H. glaber*, *L. borealis* and *C. porcellus* had an overlap of 43nt between ATP6 and ATP8. The shortest overlap between the two genes were observed in the species *A. carolinesis* has an overlap of 10nt and *N. furzeri* and *D. rerio*, have an overlap of 7nts.

2.3.3 Protein alignment and structural changes in ATP6

The complete amino acid sequences for ATP8 and ATP6 were aligned separately for the fourteen vertebrate species (see Figs 3 & 4). Protein sequence alignment showed conserved residues across the species based on identity and similarity. Four Antarctic fish species, *N. coriiceps*, *T. bernacchii*, *C. rastrospinosus*, *C. aceratus* and the sub-Antarctic *E. maclovinus* have four amino acids at the N-terminal with a total of 231 residues. As previously mentioned, the only exception to this, is the species *C. gunnari* with 227 residues similar to that of other fish species, *N. furzeri* and *D. rerio*. Species *H. sapiens*, *A. carolinesis*, *L. borealis*, *H. glaber* and *C. porcellus* have 226 residues and *B. mysticetus* has 225 residues. The protein ATP6 in vertebrates is known to have 226–228 residues. In humans, four point mutations in the ATP6 gene account for 82% of disease associated with this gene, suggesting point mutations could have physiological relevance [50,51]. Common features in all fourteen species were as follows: (1) several hydrophobic amino acids (light pink) were observed to be conserved across the sequences in

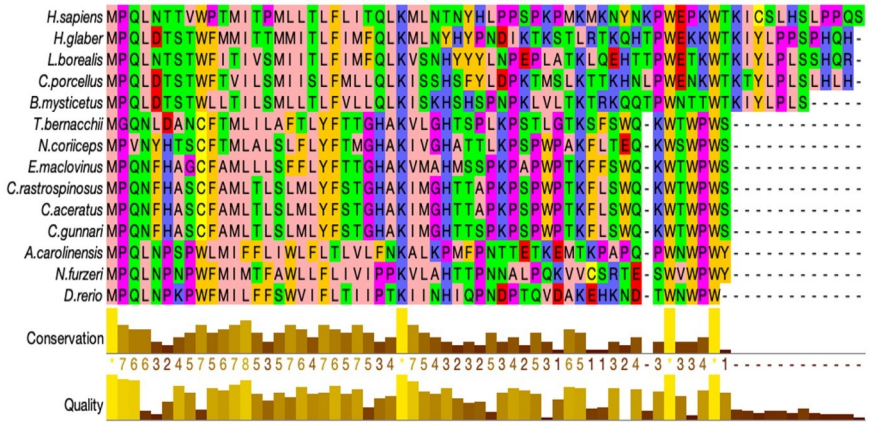

Fig 3. Multiple sequence alignment of ATP8 protein sequences. The ATP8 protein sequences were aligned using Clustal omega and edited using zappo colour scheme in JalView. Notothenioidei are grouped together in blue; all species are displayed to the colour corresponding to their phylogenetic closeness. (Colours according to physiochemical properties of amino acids; Aliphatic/hydrophobic-A, I, L, M, V- light pink; Aromatic-F, W, Y- mustard;
Conformationally special- Glycine, P- magenta; C-yellow; Hydrophilic- N, Q, S, Q, T- light green; Negatively charged/ D,E-Red; Positively charged/R,H,K-Blue) in jalview. The bar-graphs below represent a quantitative measure of conservation at each position. The figure was created using JalView.

https://doi.org/10.1371/journal.pone.0245822.g003

the species, (2) insertions and deletions of amino acids occurred more frequently near N-termini, and (3) the C-terminal of the protein sequence is hydrophilic. Dashes in the amino acid sequence represent gaps which may be an insertion or deletion of a residue. The gap in the alignment is observed for the species *H. sapiens*, *L. borealis*, *C. porcellus*, *B. mysticetus* and *H. glaber* at position 35, and at the C-terminal end for *A. carolinesis* and *B. mysticetus*, at position 226 and 225 respectively.

The amino acid at position 35 has predominantly hydrophilic residues except in the two species *C. gunnari* and *N. furzeri*, where it is substituted with alanine or leucine respectively.

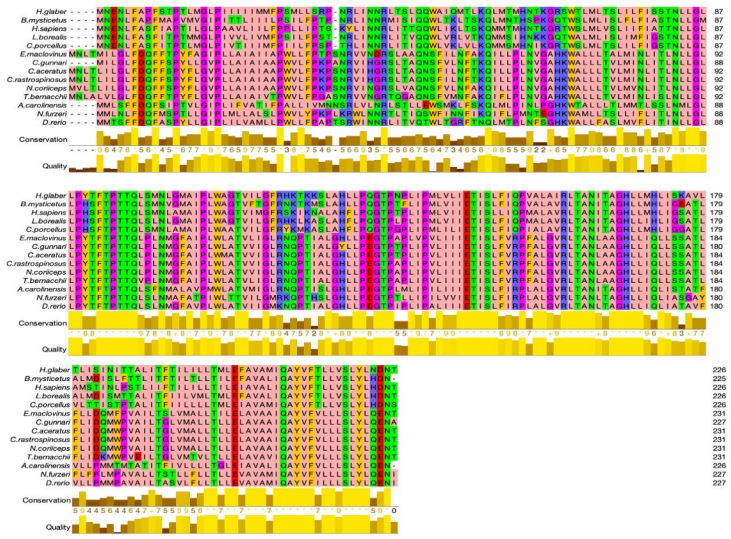

Fig 4. Multiple sequence alignment for protein sequences of ATP synthase F_0 subunit 6. The ATP6 protein sequences were aligned using Clustal omega and edited using zappo colour scheme.

https://doi.org/10.1371/journal.pone.0245822.g004

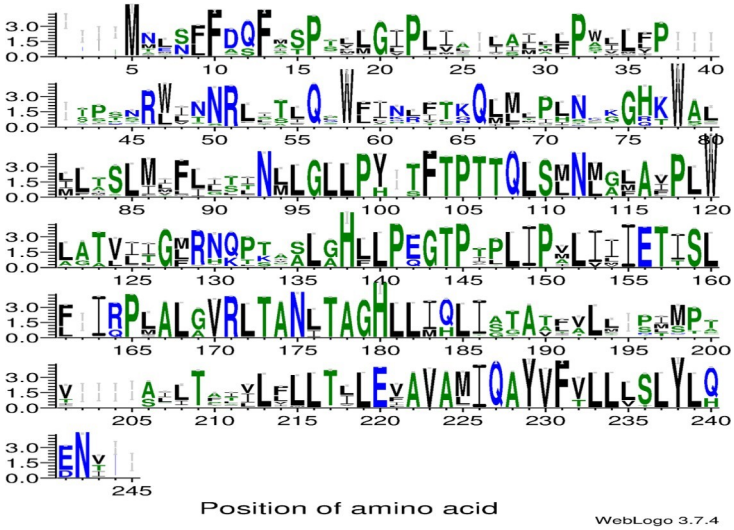

Fig 5. Sequence logos displaying conservation of residues created for all aligned blocks of the MSA for protein ATP synthase F_0 subunit 6 for 5947 vertebrate species from NCBI using webserver WebLogo (http://weblogo. threeplusone.com/) the y axis represents probability of the residue occurring at that position from the MSA.

https://doi.org/10.1371/journal.pone.0245822.g005

All the Antarctic species except *C. gunnari*, the sub-Antarctic species, *E. maclovinus* and surprisingly *H. sapiens* from the mammalian species have a serine at this position. When we look

at the codon alignment of the ATP6 gene, serine is encoded by codon TCT predominantly at position 39 for all the species except *T. bernacchii* and *H. sapiens* and the alanine for the species *C. gunnari* is encoded by GCT (see Fig 2).

The logo (see Fig 5) displays the conserved amino acids in the protein ATP6 for a particular position for 5947 vertebrate species. The protein is overall very conserved in the vertebrates, and position 38–39 show conservation for amino acids serine and threonine as also seen in the Antarctic species (except *C. gunnari*) and *E. maclovinus*.

A similar pattern was found in the amino acid alignment of ATP8, where the species, *H. sapiens*, *B. mysticetus*, *H. glaber*, *C. porcellus* and *L. borealis*, that showed a gap in the previous alignment have hydrophilic residues whereas the other species have a gap at the position 47. This observation could be attributed to the overlapping nature of the nucleotide sequences coding for the two proteins. The protein sequence of ATP6 was observed to be more conserved than ATP8. The amino acid sequences at the N- terminal are more diverse, and the methionine residues are usually followed by amino acids with short polar side chains [52]. Alanine is a non-polar amino acid whereas serine is a polar amino acid. The hydrophobicity plot, average flexibility, mutability, and coil prediction across the sequences has shown that *T. bernacchii* and *E. maclovinus* show similar trends in their physico-chemical properties across the sequence. *Notothenia coriiceps*, *C. aceratus* and *C. rastrospinosus* follow this trend. *Champsocephalus gunnari* is the only species out of the seven fish species compared, that is different from the others (see Fig 6).

Protein structure differences were predicted at position 38–39 for species *C. gunnari (*icefish), *N. furzeri*, *D. rerio* and *A. carolinesis*, where a strand-strand structure is found at that position. All other species have coil structures at those positions (see Fig 7). For species *T. bernacchii* and *E. maclovinus* there is also a prediction for a strand structure at positions 42–43.

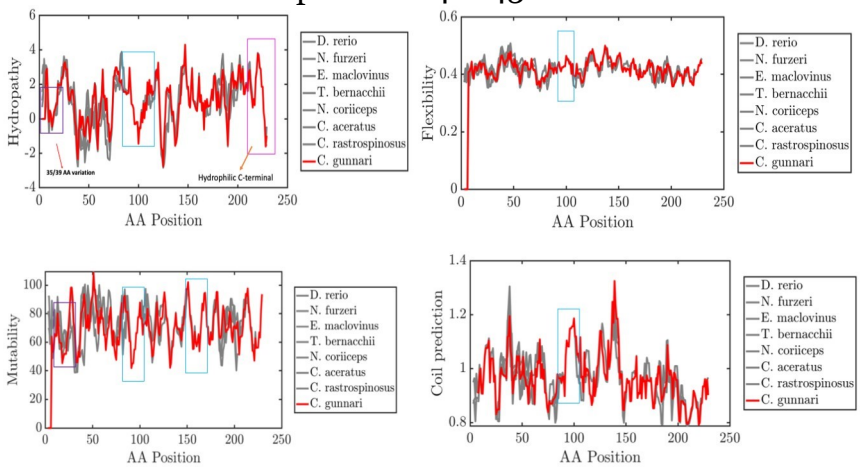

Fig 6. Primary sequence features of ATP Synthase F_0 subunit 6 in species *C. gunnari (*red), *C. rastrospinosus*, *C. aceratus*, *N. coriiceps*, *T. bernacchii*, *E. maclovinus*, *N. furzeri* and *D. rerio*. Red Box: N-terminal property changes, Purple Box: Changes in properties observed at 35/39 variation, blue box: Conserved regions 90–170 (Active site 160– 169), Pink Box: C-terminal low hydrophobicity. A

difference in the peaks have been observed for different properties (highlighted) such as molecular weight and hydrophobicity of amino acid residues across the sequence and other properties such as tendency of amino acid residues towards beta-sheet, bulkiness and flexibility.

https://doi.org/10.1371/journal.pone.0245822.g006

2.4 Discussion

We present our analyses highlighting differences in sequence and structure observed in the two proteins of complex V, ATP8 and ATP6, encoded by mtDNA between the red- and white blooded species of suborder Notothenioidei. Our analyses are based on the current genome annotation available which is subject to change as more information becomes available. We have only selected *RefSeq* sequences as these are reviewed by NCBI and represent a compilation of the current knowledge of a gene and protein products and is synthesised using information integrated from multiple sources. *RefSeq* is used as a reference standard for a variety of purposes such as genome annotation and reporting locations of sequence variation. It is important to acknowledge however that database information is regularly updated and may change. Currently, the RefSeq and GenBank entries available for a ATP6 sequences for the Antarctic/sub-Antarctic fish, NC_015653.1, AP006021.1 (*N. coriiceps*), NC_039543.1, MF622064.1 (*C. rastrospinosus*), NC_033386.1, KY038381.1 (*E. maclovinus*), NC_015654.1, YP_004581502.1 (*C. aceratus*), which are submitted by different authors, have the start codon as GTG for the five species of Notothenioidei suborder. The protein length of ATP6 has been consistent in all the entries, 231 amino acids.

It has previously been shown that mitochondria from icefish are more tightly coupled than those of their red-blooded counterparts [34]. Mitochondria that are tightly coupled usually have competent membranes and protons can only get into the matrix by passing through complex V. The red-blooded species *N. coriiceps*, *E. maclovinus*, *T. bernacchii*, the two icefish *C. rastrospinosus (*devoid of hb, have mb), *C. aceratus (*devoid of hb, do not express mb but have a nearly identical gene to that of C. rastrospinosus for mb), have an additional 12 nucleotides at the N-terminal. The only exception to this is the icefish *C. gunnari* which is completely devoid of both hb and mb. Since *C. gunnari* is the extreme of all the species of Notothenioidei suborder in question in terms of loss of globins, the change observed could be an altered variation for the gene.

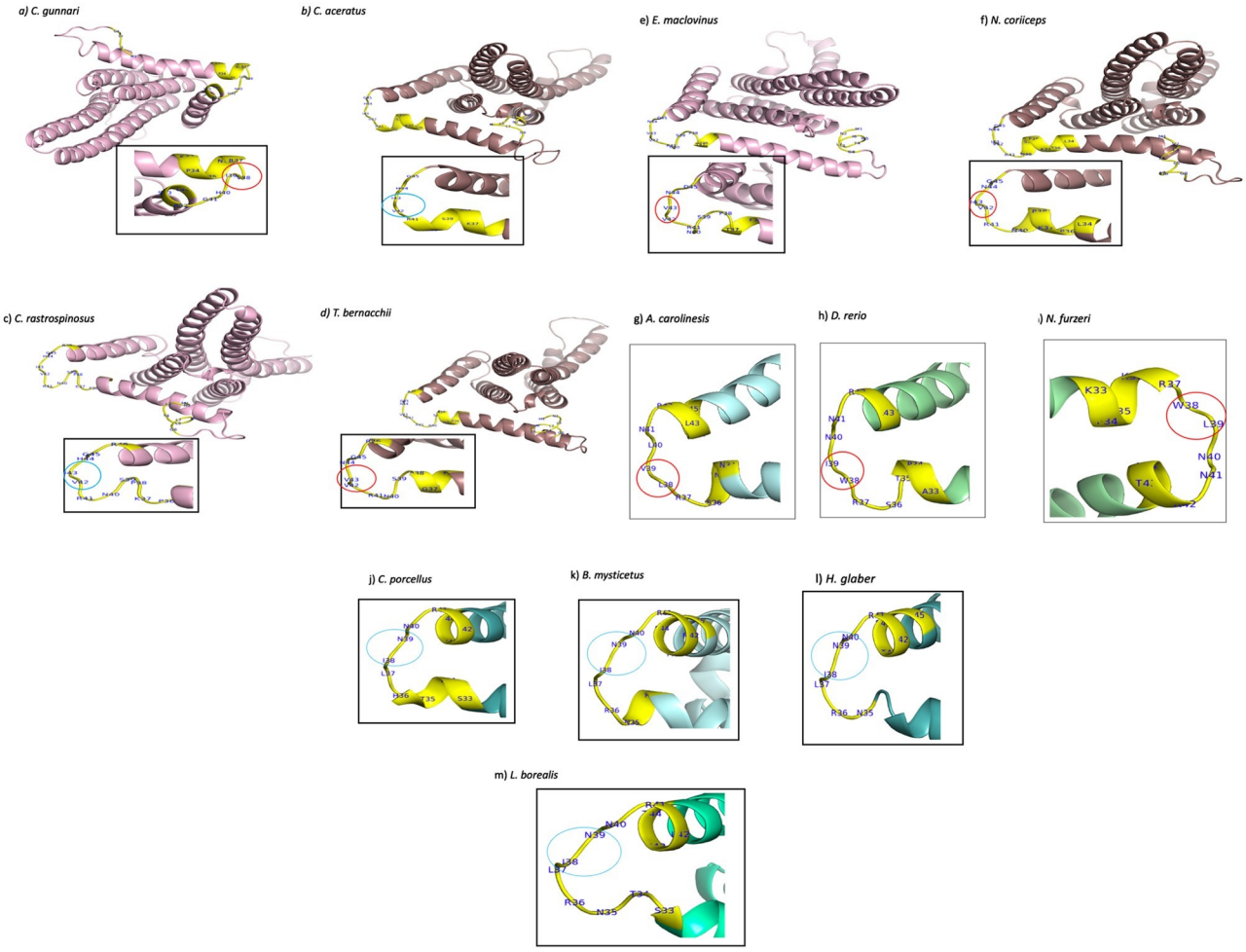

Fig 7. Representative structures of ATP synthase F_0 subunit 6 for the fourteen vertebrate species created using I-TASSER [41] suite and visualised and edited using PyMOL v. 2.3.2. a) *C. gunnari* (-/-) residues 38 (valine) and 39 (isoleucine) shows strand structure b) *C. aceratus* (-/-) residues 42 (valine) and 43 coil (isoleucine), aligning with 38/39 in MSA, show a coil structure c) *C. rastrospinosus* (-/+) residues 42-Valine and 43-Isoleucine has a coil structure d) *T. bernacchii* (+/+) residues 42-Valine and 43-Valine show a strand structure e) *E. maclovinus* (+/+) residues 42
-Valine and 43-Valine show a strand structure f) *N. coriiceps* (+/+) residues 42 (Valine) 43 (isoleucine) has a coil structure. g) *A. carolinesis* residues 38 (Leucine) and 39 (Valine) show a strand structure h) *D. rerio* residues 38 (tryptophan) and 39 (Isoleucine) show a strand structure i) *N. furzeri* residues 38 (Tryptophan) and 39 (Leucine) show a strand structure. j) *C. porcellus* residues 38 (Isoleucine) and 39 (Asparagine) show a coil structure k) *B. mysticetus* residues 38 (Isoleucine) and 39 (Asparagine) show a coil structure. l) *H. glaber* residues 38 (Isoleucine) and 39 (Asparagine) show a coil structure—m) *L. borealis* residues 38 (Isoleucine) and 39 (Asparagine) show a coil structure.

https://doi.org/10.1371/journal.pone.0245822.g007

2.4.1 GTG as an alternative start codon

The biosynthesis of proteins encoded by their respective mRNA requires an initiation codon for their translation. ATG is the usual initiation codon but GTG has been reported as initiation codon in some lower organisms, the frequency of annotated alternate codon in higher organisms is found to be less than 1% [53]. An *in-vitro* study of GTG-mediated translation of enhanced green fluorescent protein suggested that initiation with GTG codon regulates expression of lower levels of the protein and a similar observation was made for the protein endopin 2B-2 [54]. It has

also been observed in a few human diseases that a mutation of the ATG initiation codon to a GTG are associated with diseases such as beta-thalassemia and Norrie disease, where GTG mutation leads to inactivation of the gene [55,56]. Another example is a disruption caused by GTG as the initiation codon in the gene CYP2C19, which resulted in poor metabolism of a drug, mephenytoin, when compared to the gene with an ATG initiation codon [57]. Numerous studies on bacteria and lower organisms show GTG as a start codon, where the non-methionine codon is initially coded for, however, when they act as a start codon the initial amino acid is substituted with a methionine [54,58]. There is only a single report of a vertebrate species, rat, where GTG is the start codon in mtDNA [59]. An ATG to GTG exchange in human gene *FRMD7 (*FERM Domain Containing 7) has been found as a first base transversion of the start codon that accounts for a mutation, causing morphological changes in the optic nerve head [60]. The level of corresponding protein expression has been shown to be lower when initiated using an alternative codon such as GTG rather than ATG [54,61]. GTG was observed as a start codon for ATP8 in fish *Philomycus bilineatus*, which adds onto the show GTG as an acceptable start codon [62].

A few but increasing number of mammalian genes have been found to give rise to an alternative initiation codon in regulatory proteins such as transcription factors, growth factors and a few kinases in humans and rats. The finding in all these studies have shown a similar trend of a lower level of protein production when compared to an ATG start codon [63–65]. It has been shown that the fish inhabiting colder climates had undergone stronger selective constraints in order to avoid deleterious mutations [66,67]. MtDNA coding genes such as ATP6, could be placed under selective pressures by low environmental temperatures. A larger ratio of substitution for different sites could indicate proteins undergoing adaptations [68]. A decrease in ATP6 activity previously reported, shows incomplete ATPase complexes that are capable of ATP hydrolysis but not ATP synthesis. ATPase complexes completely lacking subunit a, were capable of maintaining structural interactions between F1 and F0 parts of the enzyme but the interactions were found to be weaker [69].

The GTG initiation for protein ATP6 in these fish species could suggest a common parallel evolution of the translation machinery. The favouring of GTG as a start codon could also mean a higher stability of the protein as GC base pair has higher thermal stability when compared to the AT base pair which is attributed from stronger stacking interaction between GC bases and a presence of triple bond compared to that of AT double bond [70].

2.4.2Overlap of ATP8 and ATP6 genes

Protein coding genes ATP8 and ATP6 are located adjacent to each other and are overlapping on the same strand in humans and other vertebrates, with an overlap of 44 nt (NCBI:

NC_012920.1) observed in the humans for the gene. It has been previously reported that ATP8-ATP6 overlap is generally of 10 nt in the fish genome [71]. Species *T. bernacchii*, *E. maclovinus*, *N. coriiceps*, *C. rastrospinosus* and *C. aceratus* show an overlap of 22 nts and *C. gunnari* has a 10 nt overlap, as reported previously in other fish genomes mentioned above. The overlap for the four out of six species of suborder Notothenioidei start from the third nucleotide for codon AAG coding for amino acid lysine whereas for the other two species, *T. bernacchii* and *C. gunnari*, it is encoded by AAA. It is hypothesised that overlaps are a mechanism for reduction of genome size and regulation of gene expression [72,73], which is seen in the species *C. gunnari* and the eight vertebrate outgroups.

The gene coding ATP8 ends with the stop codon TAG for all species of suborder Notothenioidei and TAA for the other vertebrate species, a single exception to this was *H. glaber* that ends with a TAG stop codon. It has been previously hypothesised that TAG is a sub-optimal stop codon which is less likely to be selected. A study showed that the protein encoding genes that end with TAA stop codons are, on average more abundant than those with genes ending with TGA or TAG and further shows that a switch of stop codon TAG from TGA might pass through the mutational path of TAA stop codon which could be subject to positive selection in several groups [74].

2.4.3 Protein alignment and structural changes in ATP6

The four Antarctic fish species, *N. coriiceps*, *T. bernacchii*, *C. rastrospinosus*, *C. aceratus* and the sub-Antarctic *E. maclovinus* have four amino acids at the N-terminal of ATP6 and a total of 231 residues. As previously mentioned, the only exception to this is the species *C. gunnari* with 227 residues similar to *N. furzeri* and *D. rerio*. N-terminal addition of amino acids can influence the properties of the protein, as it can change the molecular weight of the protein, the charge, hydrophobicity, and this has been seen in the yeast meta-caspase prion protein Mca1 [75].

Amino acid position 35 is populated with predominantly hydrophilic residues, apart for the two species *C. gunnari* and *N. furzeri*, where respectively, alanine and leucine are found. All the other Antarctic fish species and *E. maclovinus* have a serine at this position. When we look at the codon alignment of the ATP6 gene, serine is encoded by codon TCT at position 39 for all the species except *T. bernacchii (*encoded by TCC) and the alanine for the species *C. gunnari* is encoded by GCT. Serine is the only amino acid that is encoded by two codon sets. A common example of a missense mutation is where the single base pair can alter the corresponding codon to a different amino acid. This base substitution even though affecting a single codon can still have a significant effect on the protein production. It has been recently discovered that serine at a highly conserved position is more often encoded in TCN fashion and will tend to substitute non-

synonymously to proline and alanine, which shows that codon for which serine is coded indicate different types of selection for amino acid and its acceptable substitutions [76]. This may be suggested as a reason for the presence of hydrophobic alanine observed in *C. gunnari* at position 35.

The weblogo for protein ATP6 shows overall conservation across the sequence for the vertebrates where the C-terminal of the protein is more conserved than the N-terminal. High conservation is observed from residues 85–112 and 165–185, as also seen in our MSA for the fourteen species. The position 35 is seen to be conserved preferably for threonine or serine as in the weblogo (Fig 5).

The hydrophobicity plot, average flexibility, mutability, and coil prediction across the sequences highlights differences in the physiochemical properties across the sequence of protein ATP6 in the species *C. gunnari*.

The secondary structure of a protein is the way in which protein molecules are coiled and folded in a certain way according to the primary sequence. Beta-strands give stability to the structure of a protein, its intrinsic flexibility can sometimes return it to coil configuration in order for the protein to perform other functions. Structural changes were observed at position 38–39 for species *C. gunnari*, *N. furzeri*, *D. rerio* and *A. carolinesis*, where strand-strand structure was predicted at that position. All other species are predicted to have coil structures at those positions (Figs 6 & 7). Species *T. bernacchii* and *E. maclovinus* are predicted to have strand structures at positions 42–43.

Protein structure, dynamics and function are all interlinked and it is vital to understand the structure of a protein in relation to function to comprehend molecular processes [77]. We have used the unique biology of the icefish to gain a better understanding of the variability of ATP6 and ATP8 sequence and structure which has importance for mitochondrial function.

2.5 Conclusions

In this study we suggest that mitochondrial encoded protein ATP6 has an alternative start codon GTG in the species of suborder Notothenioidei except for the hb-less *C. gunnari*. This could be related to a higher thermal stability with altered expression of this protein. Another striking difference observed only in *C. gunnari* for the protein, was a substitution of hydrophilic amino acid serine (TCT) to hydrophobic amino acid alanine (GCT). This could be a base substitution for thymine to guanine at N1 position of the codon that might have a structural impact on the protein. Our predictions based on the available curated sequence data now point to the need for targeted experimentation to understand the full physiological impact of our findings.

2.6 Supporting information

S1 Fig. A pictographic representation of the relatedness of 'ATP6 protein' sequence for notothenioids to other species using NJ-phylogenetic tree (Clustal omega[35]) analysed by taking alignment data that shows similarity in the amino acid composition of the protein for different vertebrate species (pictures source: Wikipedia.com, human skull: Bonesclones.com, naked mole rat: Wikiwand.com, *E. maclovinus*: Scanndposters.com). (DOCX)

S2 Fig. Protein structure evaluations of ATP6 for fish species C. aceratus, C. gunnari, C. rastrospinosus, E. maclovinus, N. corriceps, T. bernacchii, D. rerio and N. furzeri (A-I) using SAVES v6.0 (https://saves.mbi.ucla.edu/), using ERRAT[41], PROCHECK[42,43] and ProSA-web[44]. (DOCX)

2.7 Author Contributions

Conceptualization: Gunjan Katyal, Magnus Lucassen, Chiara Papetti, Lisa Chakrabarti.

Data curation: Gunjan Katyal, Brad Ebanks.

Formal analysis: Gunjan Katyal.

Funding acquisition: Lisa Chakrabarti.

Investigation: Gunjan Katyal.

Methodology: Gunjan Katyal, Lisa Chakrabarti.

Resources: Magnus Lucassen, Chiara Papetti.

Supervision: Lisa Chakrabarti.

Writing – original draft: Gunjan Katyal, Brad Ebanks, Lisa Chakrabarti.

Writing – review & editing: Gunjan Katyal, Brad Ebanks, Magnus Lucassen, Chiara Papetti, Lisa Chakrabarti.

2.8 References

1. Duman JG. Animal ice-binding (antifreeze) proteins and glycolipids: An overview with emphasis on physiological function. J Exp Biol. 2015; 218: 1846–1855. https://doi.org/10.1242/jeb.116905 PMID: 26085662
2. Devries AL. Role of glycopeptides and pepddes in inhibition of crystallization of water in polar fishes. Philos Trans R Soc London B, Biol Sci. 1984; 304: 575–588. https://doi.org/10.1098/rstb.1984.0048
3. Chen L, Devries AL, Cheng CHC. Evolution of antifreeze glycoprotein gene from a trypsinogen gene in Antarctic notothenioid fish. Proc Natl Acad Sci U S A. 1997; 94: 3811–3816. https://doi.org/10.1073/ pnas.94.8.3811 PMID: 9108060
4. Harding MM, Anderberg PI, Haymet ADJ. "Antifreeze" glycoproteins from polar fish. European Journal of Biochemistry. 2003. pp. 1381–1392. https://doi.org/10.1046/j.1432-1033.2003.03488.x PMID: 12653993
5. Ruud Johan T. Vertebrates without Erythrocytes and Blood Pigment. Nature. 1954; 173: 848–850. https://doi.org/10.1038/173848a0 PMID: 13165664
6. Hamoir G. Biochemical adaptation of the muscles of the channichthyidae to their lack in hemoglobin and myoglobin. Comp Biochem Physiol—Part B Biochem. 1988; 90: 557–559. https://doi.org/10.1016/ 0305-0491 (88)90295-7
7. Sidell BD, O'Brien KM. When bad things happen to good fish: The loss of hemoglobin and myoglobin expression in Antarctic icefishes. J Exp Biol. 2006; 209: 1791–1802. https://doi.org/10.1242/jeb.02091 PMID: 16651546
8. Sidell BD, Vayda ME, Small DJ, Moylan TJ, Londraville RL, Yuan ML, et al. Variable expression of myoglobin among the hemoglobinless Antarctic icefishes. Proc Natl Acad Sci U S A. 1997; 94: 3420–3424. https://doi.org/10.1073/pnas.94.7.3420 PMID: 9096409
9. Small DJ, Moylan T, Vayda ME, Sidell BD. The myoglobin gene of the Antarctic icefish, Chaenocephalus aceratus, contains a duplicated TATAAAA sequence that interferes with transcription. J Exp Biol.
2003; 206: 131–139. https://doi.org/10.1242/jeb.00067 PMID: 12456703
10. O'Brien KM, Xue H, Sidell BD. Quantification of diffusion distance within the spongy myocardium of hearts from antarctic fishes. Respir Physiol. 2000; 122: 71–80. https://doi.org/10.1016/s0034-5687 (00) 00139-0 PMID: 10936602
11. O'Brien KM, Sidell BD. The interplay among cardiac ultrastructure, metabolism and the expression of oxygen-binding proteins in Antarctic fishes. J Exp Biol. 2000; 203: 1287–1297. PMID: 10729278
12. Small DJ, Vayda ME, Sidell BD. A novel vertebrate myoglobin gene containing three A+T-rich introns is conserved among antarctic teleost species which differ in myoglobin expression. J Mol Evol. 1998; 47:
156–166. https://doi.org/10.1007/pl00006372 PMID: 9694664
13. Archer SD, Johnston IA. Density of Cristae and Distribution of Mitochondria in the Slow Muscle Fibers of Antarctic Fish. Physiol Zool. 1991; 64: 242–258. https://doi.org/10.1086/physzool.64.1.30158522
14. O'Brien KM. Mitochondrial biogenesis in cold-bodied fishes. J Exp Biol. 2011; 214: 275–285. https://doi. org/10.1242/jeb.046854 PMID: 21177947
15. Biederman AM, Kuhn DE, O'Brien KM, Crockett EL. Mitochondrial membranes in cardiac muscle from Antarctic notothenioid fishes vary in phospholipid composition and membrane fluidity. Comp Biochem Physiol Part—B Biochem Mol Biol. 2019; 235: 46–53. https://doi.org/10.1016/j.cbpb.2019.05.011 PMID: 31176865
16. Dimroth P. Operation of the F0 motor of the ATP synthase. Biochimica et Biophysica Acta—Bioenergetics. 2000. pp. 374–386. https://doi.org/10.1016/S0005-2728 (00)00088-8
17. Angevine CM, Fillingame RH. Aqueous access channels in subunit a of rotary ATP synthase. J Biol Chem. 2003; 278: 6066–6074. https://doi.org/10.1074/jbc.M210199200 PMID: 12473663
18. Aksimentiev A, Balabin IA, Fillingame RH, Schulten K. Insights into the Molecular Mechanism of Rotation in the F o Sector of ATP Synthase. Biophys J. 2004; 86: 1332–1344. https://doi.org/10.1016/ S0006-3495 (04)74205-8 PMID: 14990464
19. Noji H, Yasuda R, Yoshida M, Kinosita K. Direct observation of the rotation of F1-ATPase. Nature.
1997; 386: 299–302. https://doi.org/10.1038/386299a0 PMID: 9069291

20. Ma J, Flynn TC, Cui Q, Leslie AGW, Walker JE, Karplus M. A dynamic analysis of the rotation mechanism for conformational change in F1-ATPase. Structure. 2002; 10: 921–931. https://doi.org/10.1016/ s0969-2126 (02)00789-x PMID: 12121647

21. Artika IM. Current understanding of structure, function and biogenesis of yeast mitochondrial ATP synthase. J Bioenerg Biomembr. 2019; 51: 315–328. https://doi.org/10.1007/s10863-019-09809-4 PMID: 31418131

22. Mitchell P. Coupling of phosphorylation to electron and hydrogen transfer by a chemi-osmotic type of mechanism. Nature. 1961; 191: 144–148. https://doi.org/10.1038/191144a0 PMID: 13771349

23. Abrahams JP, Leslie AGW, Lutter R, Walker JE. Structure at 2.8 Aˆ resolution of F1-ATPase from bovine heart mitochondria. Nature. 1994; 370: 621–628. https://doi.org/10.1038/370621a0 PMID: 8065448

24. Klusch N, Murphy BJ, Mills DJ, Yildiz O¨ , Ku¨hlbrandt W. Structural basis of proton translocation and force generation in mitochondrial ATP synthase. Elife. 2017; 6: 1–16. https://doi.org/10.7554/eLife. 33274 PMID: 29210357

25. Kubo S, Niina T, Takada S. Molecular dynamics simulation of proton-transfer coupled rotations in ATP synthase FO motor. Sci Rep. 2020; 10: 1–16.

26. Fearnley IM, Walker JE. Two overlapping genes in bovine mitochondrial DNA encode membrane components of ATP synthase. EMBO J. 1986; 5: 2003–2008. https://doi.org/10.1002/j.1460-2075.1986. tb04456.x PMID: 2875870

27. Colina-Tenorio L, Dautant A, Miranda-Astudillo H, Giraud MF, Gonza´lez-Halphen D. The peripheral stalk of rotary ATPases. Front Physiol. 2018; 9: 1–19.

28. Devenish RJ, Papakonstantinou T, Galanis M, Law RH, Linnane AW, Nagley P. Structure/function analysis of yeast mitochondrial ATP synthase subunit 8. Ann N Y Acad Sci. 1992; 671: 403–14. https://doi. org/10.1111/j.1749-6632.1992.tb43814.x PMID: 1288337

29. Stephens AN, Khan MA, Roucou X, Nagley P, Devenish RJ. The molecular neighborhood of subunit 8 of yeast mitochondrial F1F0-ATP synthase probed by cysteine scanning mutagenesis and chemical modification. J Biol Chem. 2003; 278: 17867–17875. https://doi.org/10.1074/jbc.M300967200 PMID: 12626501

30. Lee J, Ding SJ, Walpole TB, Holding AN, Montgomery MG, Fearnley IM, et al. Organization of subunits in the membrane domain of the bovine F-ATPase revealed by covalent cross-linking. J Biol Chem.
2015; 290: 13308–13320. https://doi.org/10.1074/jbc.M115.645283 PMID: 25851905

31. Grandier-Vazeille X, Ouhabi R, Gue´rin M. Antibodies against subunits of F0 sector of ATP synthase from Saccharomyces cerevisiae Stimulation of ATP synthase by subunit-8-reactive antibodies and inhibition by subunit-9-reactive antibodies. Eur J Biochem. 1994; 223: 521–528. https://doi.org/10.1111/j. 1432-1033.1994.tb19021.x PMID: 8055922

32. Allegretti M, Klusch N, Mills DJ, Vonck J, Ku¨hlbrandt W, Davies KM. Horizontal membrane-intrinsic αhelices in the stator a-subunit of an F-type ATP synthase. Nature. 2015; 521: 237–240. https://doi.org/
10.1038/nature14185 PMID: 25707805

33. Gu J, Zhang L, Zong S, Guo R, Liu T, Yi J, et al. Cryo-EM structure of the mammalian ATP synthase tetramer bound with inhibitory protein IF1. 2019; 1075: 1068–1075.

34. Mueller IA, Grim JM, Beers JM, Crockett EL, O'Brien KM. Inter-relationship between mitochondrial function and susceptibility to oxidative stress in red-And white-blooded Antarctic notothenioid fishes. J Exp Biol. 2011; 214: 3732–3741. https://doi.org/10.1242/jeb.062042 PMID: 22031737

35. O'Leary NA, Wright MW, Brister JR, Ciufo S, Haddad D, McVeigh R, et al. Reference sequence
(RefSeq) database at NCBI: Current status, taxonomic expansion, and functional annotation. Nucleic Acids Res. 2016; 44: D733–D745. https://doi.org/10.1093/nar/gkv1189 PMID: 26553804

36. Madeira F, Park YM, Lee J, Buso N, Gur T, Madhusoodanan N, et al. The EMBL-EBI search and sequence analysis tools APIs in 2019. Nucleic Acids Res. 2019; 47: W636–W641. https://doi.org/10. 1093/nar/gkz268 PMID: 30976793

37. Rozewicki J, Li S, Amada KM, Standley DM, Katoh K. MAFFT-DASH: Integrated protein sequence and structural alignment. Nucleic Acids Res. 2019; 47: W5–W10. https://doi.org/10.1093/nar/gkz342 PMID: 31062021

38. Waterhouse AM, Procter JB, Martin DMA, Clamp M, Barton GJ. Jalview Version 2-A multiple sequence alignment editor and analysis workbench. Bioinformatics. 2009; 25: 1189–1191. https://doi.org/10. 1093/bioinformatics/btp033 PMID: 19151095

39. Gasteiger E, Gattiker A, Hoogland C, Ivanyi I, Appel RD, Bairoch A. ExPASy: The proteomics server for in-depth protein knowledge and analysis. Nucleic Acids Res. 2003; 31: 3784–3788. https://doi.org/10. 1093/nar/gkg563 PMID: 12824418

40. Gasteiger E, Hoogland C, Gattiker A, Duvaud S, Wilkins MR, Appel RD, et al. The Proteomics Protocols Handbook. Proteomics Protoc Handb. 2005; 571–608. https://doi.org/10.1385/1592598900

41. Yang J, Zhang Y. I-TASSER server: New development for protein structure and function predictions. Nucleic Acids Res. 2015; 43: W174–W181. https://doi.org/10.1093/nar/gkv342 PMID: 25883148

42. Colovos C, Yeates TO. Verification of protein structures: Patterns of nonbonded atomic interactions. Protein Sci. 1993; 2: 1511–1519. https://doi.org/10.1002/pro.5560020916 PMID: 8401235

43. Laskowski RA, MacArthur MW, Moss DS, Thornton JM. PROCHECK: a program to check the stereochemical quality of protein structures. J Appl Crystallogr. 1993; 26: 283–291. https://doi.org/10.1107/ s0021889892009944

44. Sippl MJ. Recognition of errors in three-dimensional structures of proteins. Proteins Struct Funct Bioinforma. 1993; 17: 355–362. https://doi.org/10.1002/prot.340170404 PMID: 8108378

45. Wiederstein M, Sippl MJ. ProSA-web: Interactive web service for the recognition of errors in threedimensional structures of proteins. Nucleic Acids Res. 2007; 35: 407–410. https://doi.org/10.1093/nar/ gkm290 PMID: 17517781

46. Guo J, Yang H, Zhang C, Xue H, Xia Y, Zhang JE. Complete mitochondrial genome of the apple snail Pomacea diffusa (Gastropoda, Ampullariidae) with phylogenetic consideration. Mitochondrial DNA Part B Resour. 2017; 2: 865–867. https://doi.org/10.1080/23802359.2017.1407683 PMID: 33474014

47. Lin GM, Xiang P, Sampurna BP, Der Hsiao C. Genome skimming yields the complete mitogenome of Chromodoris annae (Mollusca: Chromodorididae). Mitochondrial DNA Part B Resour. 2017; 2: 609–610. https://doi.org/10.1080/23802359.2017.1372715 PMID: 33473918

48. Yang T, Xu G, Gu B, Shi Y, Mzuka HL, Shen H. The complete mitochondrial genome sequences of the Philomycus bilineatus (Stylommatophora: Philomycidae) and phylogenetic analysis. Genes (Basel). 2019; 10: 1–13. https://doi.org/10.3390/genes10030198 PMID: 30841657

49. Fox TD. Five TGA "stop" codons occur within the translated sequence of the yeast mitochondrial gene for cytochrome c oxidase subunit II. Proc Natl Acad Sci U S A. 1979; 76: 6534–6538. https://doi.org/10. 1073/pnas.76.12.6534 PMID: 230513

50. Verny C, Guegen N, Desquiret V, Chevrollier A, Prundean A, Dubas F, et al. Hereditary spastic paraplegia-like disorder due to a mitochondrial ATP6 gene point mutation. Mitochondrion. 2011; 11: 70–75. https://doi.org/10.1016/j.mito.2010.07.006 PMID: 20656066

51. Pfeffer G, Frcpc CM, Blakely EL, Alston CL, Boggild M, Horvath R, et al. Europe PMC Funders Group Adult-onset spinocerebellar ataxia syndromes due to MTATP6 mutations. 2014; 83: 883–886.

52. Arnesen T, Van Damme P, Polevoda B, Helsens K, Evjenth R, Colaert N, et al. Proteomics analyses reveal the evolutionary conservation and divergence of N-terminal acetyltransferases from yeast and humans. Proc Natl Acad Sci U S A. 2009; 106: 8157–8162. https://doi.org/10.1073/pnas.0901931106 PMID: 19420222

53. Donath A, Ju¨hling F, Al-Arab M, Bernhart SH, Reinhardt F, Stadler PF, et al. Improved annotation of protein-coding genes boundaries in metazoan mitochondrial genomes. Nucleic Acids Res. 2019; 47: 10543–10552. https://doi.org/10.1093/nar/gkz833 PMID: 31584075

54. Hwang SR, Garza CZ, Wegrzyn JL, Hook VYH. Demonstration of GTG as an alternative initiation codon for the serpin endopin 2B-2. Biochem Biophys Res Commun. 2005; 327: 837–844. https://doi. org/10.1016/j.bbrc.2004.12.053 PMID: 15649421

55. Villalobos-ar AR, Casas-casta M, Guti E, Perea FJ, Thein SL, Ibarra B. Globin gene haplotypes in Mexican mestizos. 1997; 498–500. PMID: 9262381

56. Isashiki Y, OHbA N, Yanagita T, Hokita N, Doi N, Nakagawa M, et al. Novel mutation at the initiation codon in the Norrie disease gene in two Japanese families. Hum Genet. 1995; 95: 105–108. https://doi. org/10.1007/BF00225085 PMID: 7814011

57. Ferguson RJ, De Morais SMF, Benhamou S, Bouchardy C, Blaisdell J, Ibeanu G, et al. A new genetic defect in human CYP2C19: Mutation of the initiation codon is responsible for poor metabolism of Smephenytoin. J Pharmacol Exp Ther. 1998; 284: 356–361. PMID: 9435198

58. Kitamoto T, Wang W, Salvaterra PM. Structure and organization of the Drosophila cholinergic locus. J Biol Chem. 1998; 273: 2706–2713. https://doi.org/10.1074/jbc.273.5.2706 PMID: 9446576

59. Gadaleta G, Pepe G, De Candia G, Quagliariellol C, Sbisa E, Saccone C, et al. Nucleic Acids Research Nucleotide sequence of rat nitochondrial NADH dehydrogenase subunit 1. GTG, a new initiator codon in vertebrate mitochondrial genome We have determined the nucleotide sequence of cloned fragments that contain with ATT. However th. 1988;22: 6233.

60. Choi JH, Shin JH, Seo JH, Jung JH, Choi KD. A start codon mutation of the FRMD7 gene in two Korean families with idiopathic infantile nystagmus. Sci Rep. 2015; 5: 5–10. https://doi.org/10.1038/srep13003 PMID: 26268155

61. Panicker IS, Browning GF, Markham PF. The effect of an alternate start codon on heterologous expression of a PhoA fusion protein in mycoplasma gallisepticum. PLoS One. 2015; 10: 1–10. https://doi.org/ 10.1371/journal.pone.0127911 PMID: 26010086

62. Yang T, Xu G, Gu B, Shi Y, Mzuka HL, Shen H. The complete mitochondrial genome sequences of the Philomycus bilineatus (Stylommatophora: Philomycidae) and phylogenetic analysis. Genes (Basel). 2019; 10: 1–14. https://doi.org/10.3390/genes10030198 PMID: 30841657

63. Short JD, Pfarr CM. Translational regulation of the JunD messenger RNA. J Biol Chem. 2002; 277: 32697–32705. https://doi.org/10.1074/jbc.M204553200 PMID: 12105216

64. Claus P, Do¨ring F, Gringel S, Mu¨ller-Ostermeyer F, Fuhlrott J, Kraft T, et al. Differential intranuclear localization of fibroblast growth factor-2 isoforms and specific interaction with the survival of motoneuron protein. J Biol Chem. 2003; 278: 479–485. https://doi.org/10.1074/jbc.M206056200 PMID: 12397076

65. Rhee S, Yang SJ, Lee SJ, Park D. βPix-bL, a novel isoform of βPix, is generated by alternative translation. Biochem Biophys Res Commun. 2004; 318: 415–421. https://doi.org/10.1016/j.bbrc.2004.04.039 PMID: 15120616

66. Silva G, Lima FP, Martel P, Castilho R. Thermal adaptation and clinal mitochondrial DNA variation of European anchovy. Proc R Soc B Biol Sci. 2014; 281. https://doi.org/10.1098/rspb.2014.1093 PMID: 25143035

67. Sun YB, Shen YY, Irwin DM, Zhang YP. Evaluating the roles of energetic functional constraints on teleost mitochondrial-encoded protein evolution. Mol Biol Evol. 2011; 28: 39–44. https://doi.org/10.1093/ molbev/msq256 PMID: 20924083

68. Deng Z, Wang X, Xu S, Gao T, Han Z. Population genetic structure and selective pressure on the mitochondrial ATP6 gene of the Japanese sand lance Ammodytes personatus Girard. J Mar Biol Assoc United Kingdom. 2019; 99: 1409–1416. https://doi.org/10.1017/S0025315419000225

69. Jesˇina P, Tesařova´ M, Fornůskova´ D, Vojtı´sˇkova´ A, Pecina P, Kaplanova´ V, et al. Diminished synthesis of subunit a (ATP6) and altered function of ATP synthase and cytochrome c oxidase due to the mtDNA 2 bp microdeletion of TA at positions 9205 and 9206. Biochem J. 2004; 383: 561–571. https://doi.org/ 10.1042/BJ20040407 PMID: 15265003

70. Yakovchuk P, Protozanova E, Frank-Kamenetskii MD. Base-stacking and base-pairing contributions into thermal stability of the DNA double helix. Nucleic Acids Res. 2006; 34: 564–574. https://doi.org/10. 1093/nar/gkj454 PMID: 16449200

71. Satoh TP, Miya M, Mabuchi K, Nishida M. Structure and variation of the mitochondrial genome of fishes. BMC Genomics. 2016; 17. https://doi.org/10.1186/s12864-016-3054-y PMID: 27604148

72. Krakauer DC. Evolutionary Principles of Genomic Compression. Comments Theor Biol. 2002; 7: 215– 236.

73. Johnson ZI, Chisholm SW. Properties of overlapping genes are conserved across microbial genomes. Genome Res. 2004; 14: 2268–2272. https://doi.org/10.1101/gr.2433104 PMID: 15520290

74. Belinky F, Babenko VN, Rogozin IB, Koonin EV. Purifying and positive selection in the evolution of stop codons. Sci Rep. 2018; 8: 1–11.

75. Erhardt M, Wegrzyn RD, Deuerling E. Extra N-terminal residues have a profound effect on the aggregation properties of the potential yeast prion protein Mca1. PLoS One. 2010; 5. https://doi.org/10.1371/ journal.pone.0009929 PMID: 20360952

76. Schwartz GW, Shauli T, Linial M, Hershberg U. Serine substitutions are linked to codon usage and differ for variable and conserved protein regions. Sci Rep. 2019; 9: 1–9.

77. Garcia-Manero Guillermo, Yang Hui, Kuang Shao-Qing, O'Brien Susan, Thomas Deborah and K H. 基因的改变NIH Public Access. Bone. 2005; 23: 1–7.

2.9 APENDIX A

2.9.1 Methods: Western Blotting

1. Antarctic Fish Muscle tissue. SVMS Clinical Ethical Review, University of Nottingham, (ref # 2744 190509). White and red muscle samples of Antarctic notothenioid fish, *N. rossii*, *T. bernacchii* (red-blooded species – Cruise PS112, Weddell Sea in 2013-2014), *C. gunnari* and *C. rastrospinosus* [icefish species – Cruise ANTXXVIII (PS79), Antarctic Peninsula in 2012] *N. rossii* and *T. bernacchii* have 30-45 % of haematocrit and 18-28 % haematocrit respectively.
2. Subcellular fractionation. The liver tissues were stored at -80°C and while obtaining the fractions were put on ice throughout. The tissues were cut with a sterile blade and then homogenised using Dounce homogeniser, in 2 mL mitochondria extraction buffer (50 mM Tris-Cl pH 7.4, 100 mM KCl, 1.5 mM MgCl2, 1 mM EGTA, 50 mM HEPES and 100mM sucrose). The whole cell fractions were used for western blotting. Western blotting was performed as follow: 18 µl sample x 9 µl DTT x 9 µl LDS buffer were added and the samples were boiled for 10 mins and vortex before loading onto precast 12 well NuPage 12% Bis-Tris Gels (Novex, Life Technologies) and run at 200 V for 35 min. Gels were transferred at 30 V for 60 min to 0.45 µm Nitrocellulose membrane (Novex, Life Technologies). Membrane was blocked in 3% (w/v) milk powder in TBS-T (Tris-Buffered Saline and 0.1% Tween-20) for 1 h at room temperature, then incubated at 4 °C overnight in primary antibodies (ATP6 – abcam, ab192423; 1:5000 dilution). Membrane was washed 3 × 5 min at room temperature in TBS-T and incubated in peroxidase conjugate goat anti-rabbit for 1h at room temp, at a 1:2500 dilution in 3% milk powder (w/v) in TBS-T. Membrane was further washed 3 × 5 min in TBS-T and developed using ECL Plus for 5 min (Pierce ThermoFisher) and imaged using ChemiDoc (BioRad)_. The membranes are re-probed with GAPDH (abcam ab8245; 1:5000) and was left overnight at 4 °C and the same steps were repeated. Membranes were washed 3 × 5 min at room temperature in TBS-T and incubated in peroxidase conjugate anti-mouse (1:25000) for 1h at room temperature. Membrane was washed 3 × 5 min in TBS-T and developed using ECL Plus for 5 min and imaged using ChemiDoc.

2.9.2 RESULTS:

The isolated whole cell fractions of liver samples isolated from four notothenioid species, *N. rossii* and *T. bernacchii* (the red-blooded species) and *C. rastrospinosus* and *C. gunnari* (the icefish) were subjected to western blotting. The ATP6 protein was seen significantly lowered for icefish *C. gunnari* in comparison to the other species. This might be correlated with the changes observed for alternate start codons

for the other species and specific amino acid substitution. GAPDH was used as a loading control for the samples.

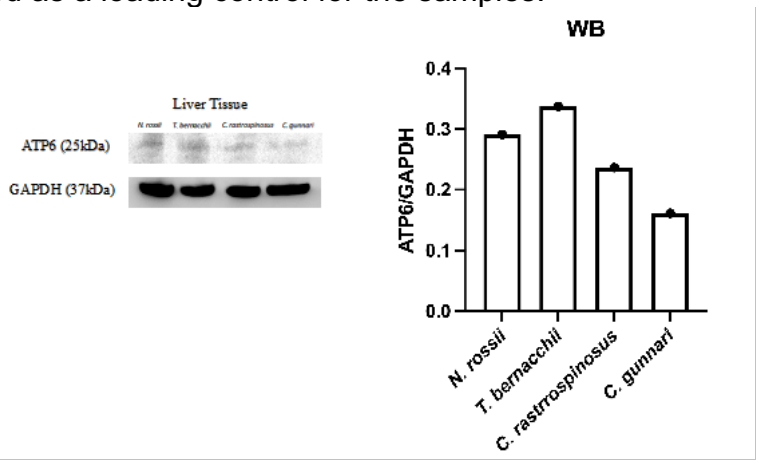

Figure 2-1. Liver tissues from N. rossii, T. bernacchii, C. rastrospinosus and C. gunnari whole cell lysate separated on SDS-PAGE and analysed by Western blotting using antibody against 25-kD subunit of ATP synthase, ATP6 using GAPDH as a loading control.

On performing westerns with ATP6 on liber tissue, we saw variable expression of ATP6 in the icefish and red-blooded fish, with GAPDH as a control. The expression of ATP6 was seen the lowest in icefish *C. gunnari*, and highest in *T. bernacchii*. Despite of having a comparable expression of ATP6 in the two red-blooded fish, T. bernacchii, is the only red-blooded Antarctic fish that has ATG start codon unlike GTG in the other Antarctic fish.

2.9.3 RESULTS

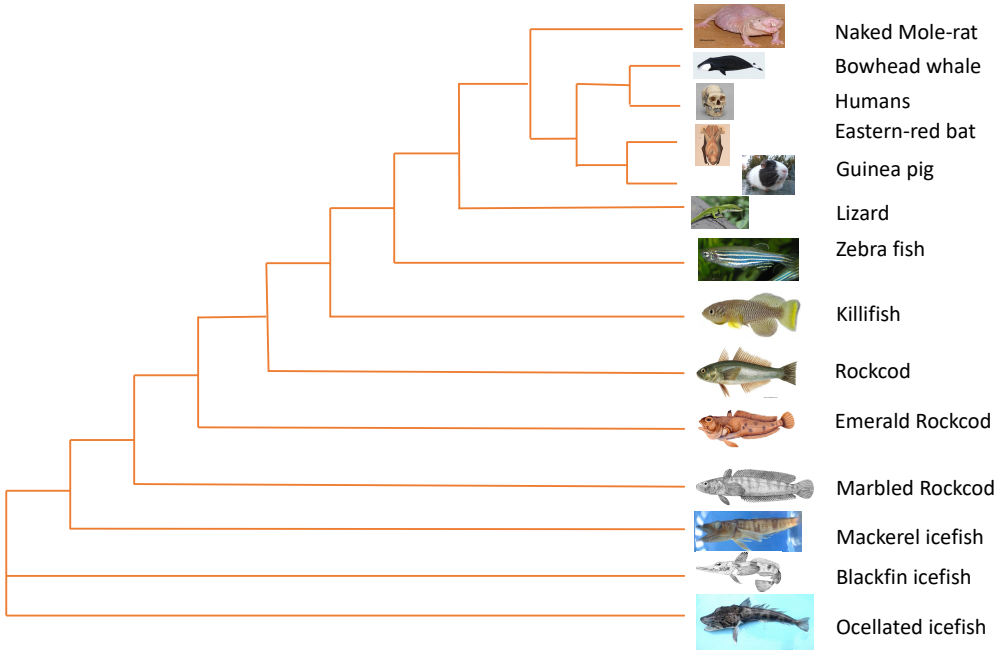

Supplementary Figure 2-2. A pictographic representation of the relatedness of 'ATP6 protein' sequence for notothenioids to other species using NJ-phylogenetic tree (Clustal omega (Madeira *et al.*, 2019)) analysed by taking alignment data that shows similarity in the

amino acid composition of the protein for different vertebrate species (pictures source: wikipedia.com, human skull: bonesclones.com, naked mole rat: wikiwand.com, *E. maclovinus*: scanndposters.com).

In the study we have aligned the nucleotide and protein sequences for ATP6. The choice of different vertebrate species as outgroups apart from the notothenioids (Supplementary Fig 2.2) for the protein allow us to highlight changes in the amino acid sequences that may be specific to the notothenioid fish and those changes that may be species specific.

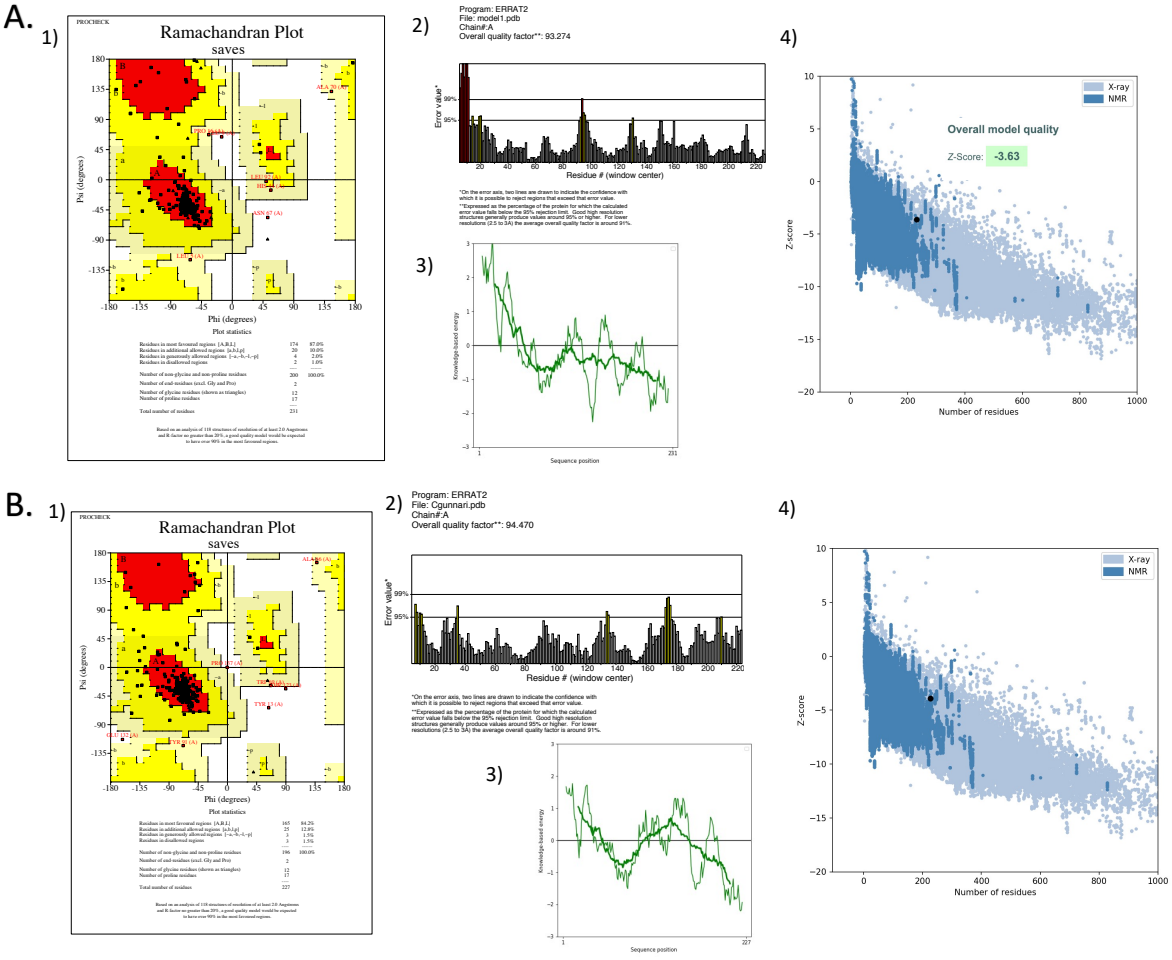

C.

1)

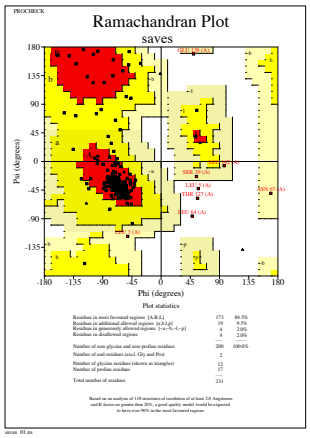

2)

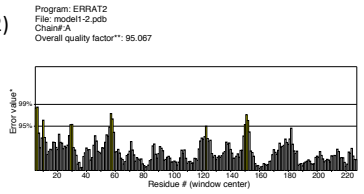

3)

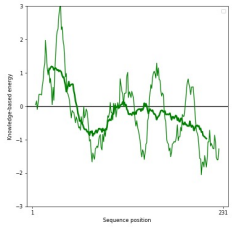

4)

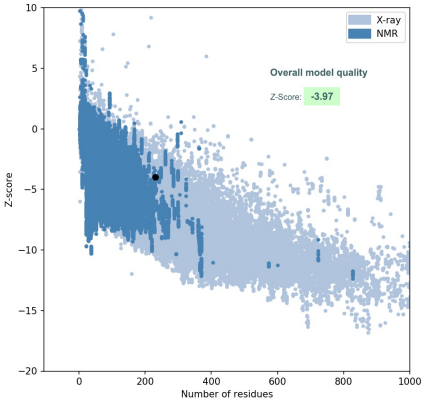

D.

1)

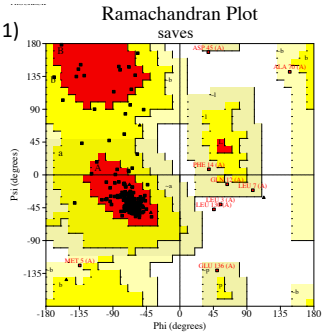

2)

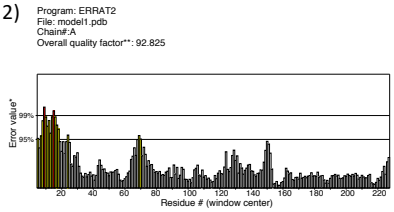

3)

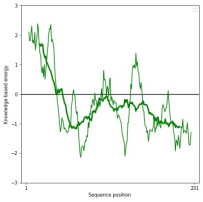

4)

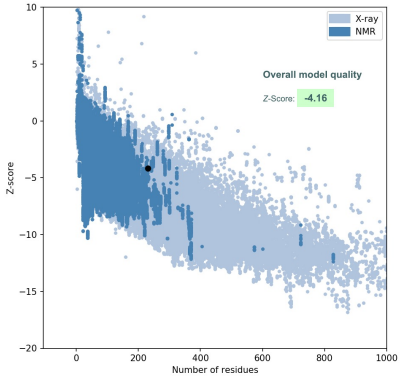

E.

1)

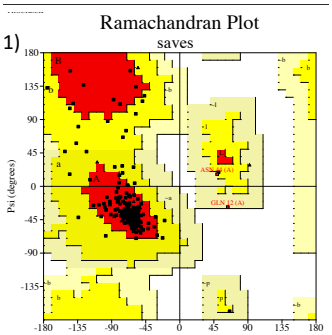

2)

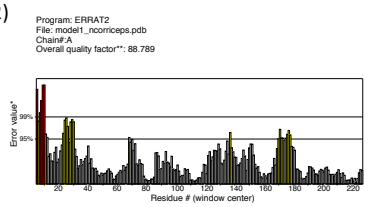

3)

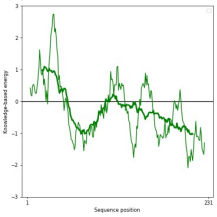

4)

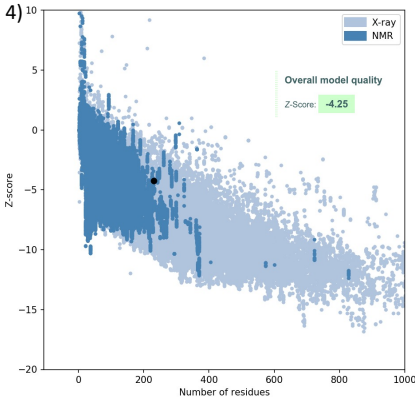

F.

1)

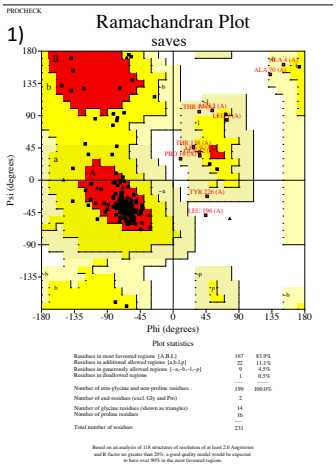

2)

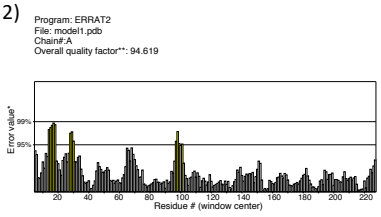

3)

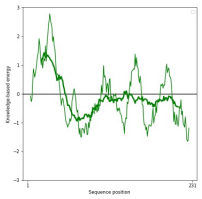

4)

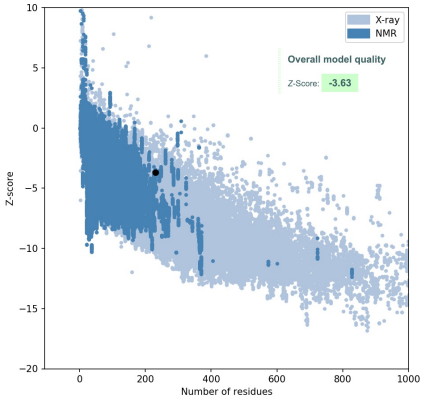

G

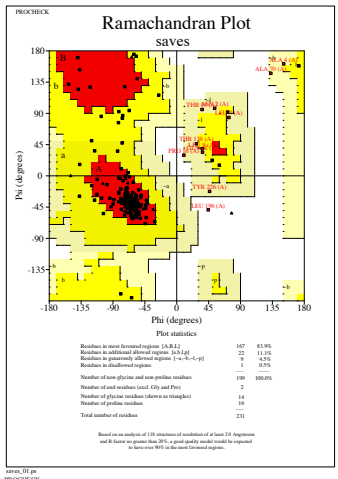

2)

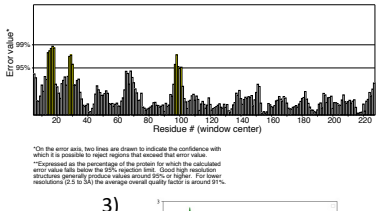

3)

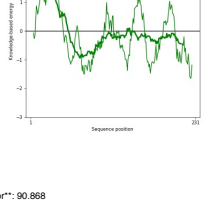

4)

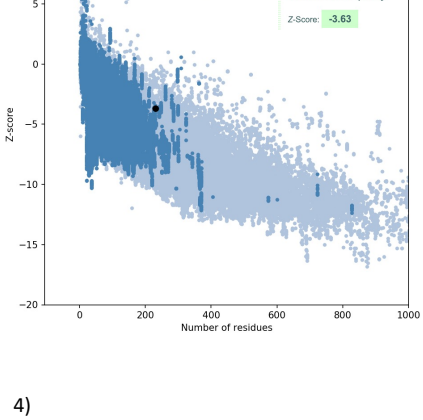

H.

1)

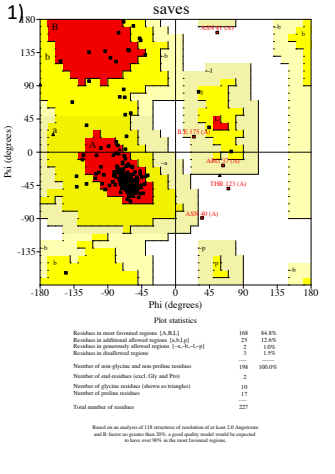

2)

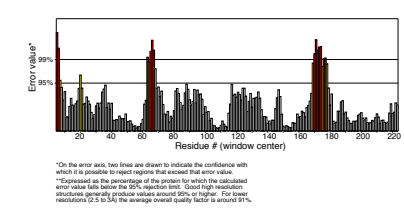

3)

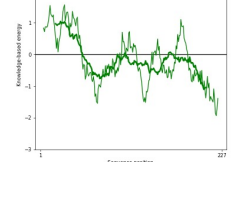

4)

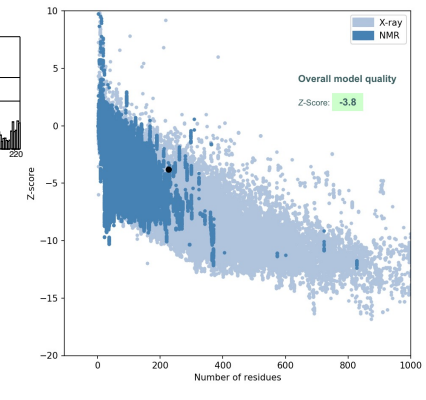

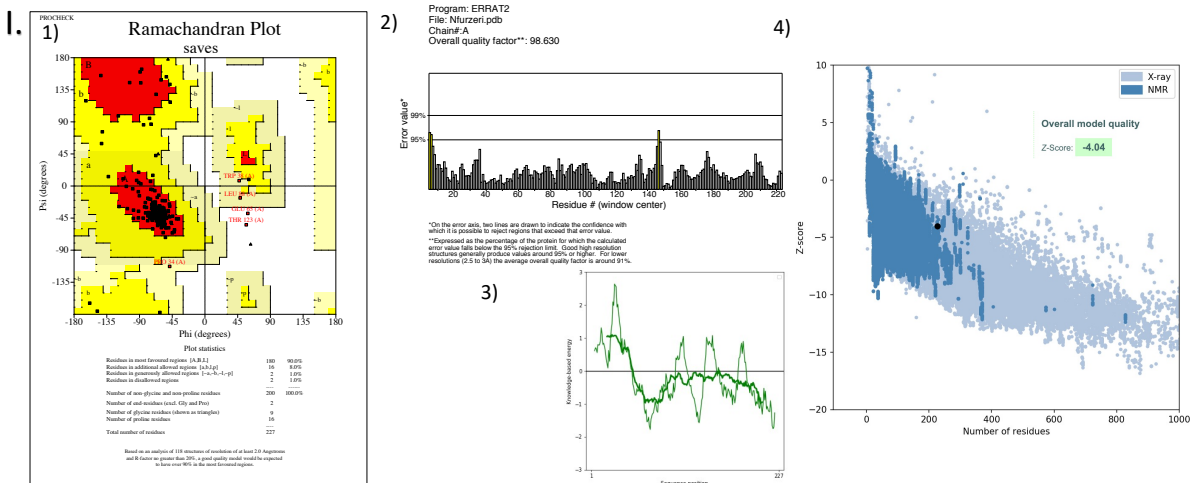

Supplementary Figure 2-3 . Protein structure evaluations of ATP6 for fish species *C. aceratus*, *C. gunnari*, C*. rastrospinosus*, *E. maclovinus*, *N. corriceps*, *T. bernacchii*, *D. rerio* and *N. furzeri* (A-I) using SAVES v6.0 (https://saves.mbi.ucla.edu/), using ERRAT[41], PROCHECK[42,43] and ProSA-web[44].

The structures are predicted models with 93-95% overall score for the model (ERRAT, the method provides an unbiased and statistically sound tool for identifying incorrectly built regions in protein models). The Ramachandran plot on average showed allowed regions from >85 %. An acceptable high-quality model will have allowed regions >90%, and this low percentage can be either attributed to either high active side residues that sometimes are found in disallowed regions or low resolution of the model that can have disallowed conformations (Supplementary Fig 3.).

Chapter 3 : Proteomes of icefish muscle mitochondria point to important differences in ATP synthase sub-units compared with closely related red blooded species

Proteomes of icefish muscle mitochondria point to important differences in ATP synthase sub-units compared with closely related red blooded species.

*Gunjan Katyal[1], Brad Ebanks[1], Freya Shephard[1], Chiara Papetti[2], Magnus Lucassen[3], Lisa Chakrabarti[1,4] *.*

[1]School of Veterinary Medicine and Science, University of Nottingham, Sutton Bonington, LE12 5RD, UK.

[2] Biology Department, University of Padova, via U. Bassi, 58/b, 35121, Padova, Italy.

[3] Alfred Wegener Institute, Bremerhaven, Germany.

[4] MRC-Versus Arthritis Centre for Musculoskeletal Ageing Research, UK.

* Corresponding author lisa.chakrabarti@nottingham.ac.uk

Abstract
Antarctic icefish are extraordinary in their ability to thrive without haemoglobin. We wanted to understand how the mitochondrial proteome has adapted to the loss of this protein. Metabolic pathways that utilise oxygen are most likely to be rearranged in these species. Here, we have defined the mitochondrial proteomes of both, the red and white muscle of two different icefish species (*Champsocephalus gunnari and Chionodraco rastrospinosus)* and compared these with two related red-blooded Notothenioids (*Notothenia rossii, Trematomus bernacchii*). Liquid Chromatography-Mass spectrometry (LC-MS/MS) was used to generate and examine the proteomic profiles of the two groups. We recorded a total of nighty-one differentially expressed proteins in the icefish red muscle mitochondria and eighty-nine in the white muscle mitochondria when compared with the red-blooded related species. The icefishes have a relatively higher abundance of proteins involved with Complex V of oxidative phosphorylation, RNA metabolism, and homeostasis, and fewer proteins for striated muscle contraction, haem, iron, creatine, and carbohydrate metabolism. Enrichment analyses showed that many important pathways were different in both red muscle and white muscle, including the citric acid cycle, ribosome machinery and fatty acid degradation. Life in the Antarctic waters poses extra challenges to the organisms that reside within them. The icefish have successfully inhabited this environment and we surmise that the species without haemoglobin uniquely maintain their physiology. Our study highlights the mitochondrial protein pathway differences between similar fish species according to their specific tissue oxygenation idiosyncrasies.

3.1 Introduction

Mitochondria are crucial organelles that produce ATP via oxidative phosphorylation, a process that involves the transfer of electrons between multi-subunit complexes (I to IV) of the electron transport chain (ETC) resulting in the reduction of molecular oxygen. These organelles are also known for their involvement in many vital cellular activities such as apoptosis, calcium homeostasis, and regulation of cell homeostasis. Due to this, there has been an increasing interest in the structure and function of mitochondrial proteins [1–4]. Efforts have been made to decipher the structure, assembly process, coupling mechanism, and associated pathologies of respiratory chain complexes [5,6].

Haemoglobin (Hb) synthesis requires a coordinated production of both haem and globin. Hb is a multi-subunit globular molecule made up of four polypeptide subunits, two alpha and two beta subunits. Each of the four subunits has a haem moiety that contains iron [7]. The prosthetic group haem is synthesised in a series of steps shuttling between the mitochondrion and the cytosol of immature erythrocytes [8]. To understand the role of haemoglobin it can be useful to examine eukaryotic systems that express this important protein at different levels. There is a wide range of evidence that suggests that Hb has dynamic locations in cell, neurons, endothelial cells, mitochondria, and vascular expression [9–13]. Previously, we have shown that haemoglobin proteins are located in the mitochondrion and both direct and indirect links have been established between mitochondria function and Hb expression [11,14,15].

Interestingly, a group of vertebrates known as Antarctic icefish are “null-mutants” for haemoglobin have some likely relevant cellular modifications, including a high mitochondrial density [16]. Antarctic icefish/white-blooded fish, (subfamily Channichthyidae, family Nototheniidae, suborder Notothenioidei [17]) are the only known vertebrates that do not possess functional haemoglobin genes and red blood cells (RBCs), in stark contrast to all the others that depend upon Hb to get oxygen to tissues and cells, via RBCs [18–20]. The loss of Hb in the Antarctic icefish is postulated to be a mutational process, resulting in the loss of the β-globin (hbb) gene and partial omission of the α-globin (hba) gene from α-/β-globin, causing the locus to become functionally inactive. Fifteen out of the sixteen icefish species are known to retain only a 3’ fragment of an α-globin gene [21]. The sixteenth species, *Neopagetopsis ionah*, retains an intact but unexpressed hba gene fused to two β-globin pseudogenes [22].

As might be expected, some proteins have been shown to be altered in the icefish and reasons have been suggested for these differences. Previously, studies have shown changes in the iron transporting proteins such as transferrin, ceruloplasmin, and ferritin [23]. All notothenioid species do not express myoglobin (Mb), an intracellular oxygen-binding protein in the muscle. In total, six of the sixteen icefish species don’t express Mb in their heart ventricles, a loss that occurred through four different mutational events [24]. Icefish have large hearts [25], which do not contain the mitochondrial creatine kinase [26]. They also have high mitochondrial densities which is postulated to counter the effects of cold temperature [27]. The high density of mitochondria rich in lipids serves as a pathway that enhances oxygen storage and diffusion which compensates for the lack of Hb and Mb [28] . An observed increase

in mitochondrial phospholipids may be due to an upregulation in the glycerol-lipid synthesis pathway, there is still a lot to be learned about protein networks and pathways in the icefish [29].

Proteomics can be used to identify protein-protein interactions which in turn influence protein expression or regulation [30]. In silico methods and web servers have been developed to predict the function and structure of proteins [31]. Although large-scale mitochondrial comparative proteomic data have been accumulated, mitochondrial proteomics still faces the challenge of how to investigate the functions of the identified mitochondrial proteins and how to build mitochondria specific signalling networks. An integrative network analysis approach can accommodate information from PPIs and proteomics and bridge that gap between the two. Hence using an interactive network approach could lay the foundation for a better understanding of the mitochondrial changes in the icefish [32].

Here, we establish for the first time the proteomes of red muscle mitochondria (RMM) and white muscle mitochondria (WMM) from four species of the suborder Notothenioidei: two icefish, *Champsocephalus gunnari* (*C. gunnari*) devoid of Hb and Mb (the loss of Hb and Mb completely) and *Chionodraco rastrospinosus (C. rastrospinosus*) devoid of Hb but with tissue specific expression of Mb, that is only expressed in the hearts of these species, are compared to their closely related red-blooded species *Notothenia rossii* (*N. rossii*) and *Trematomus bernacchii* (*T. bernacchii*), both the species belonging to the subfamily Nototheniidae, that express Hb and has tissue specific expression of Mb only heart ventricles. Mammalian skeleton muscles are mainly composed of two kinds of fibres, white-fast twitch type that makes the white muscle and red-slow twitch type that makes the red muscle [33]. White muscle requires a greater capacity for anaerobic energy production to meet the demands of the fast-twitch fibres [34].In contrast to mammalian white muscle tissue, the central regions of icefish red muscle contain numerous mitochondria [16]. In establishing these proteomes, we can understand how the mitochondrial proteome has adapted to the loss of this protein and potentially understand the role and interaction pathways of haemoglobin in the context of mitochondrial biology.

3.2 Methodology

3.2.1 Antarctic Fish Muscle tissue.

SVMS Clinical Ethical Review, University of Nottingham, (ref # 2744 190509). White and red muscle samples of Antarctic notothenioid fish, *N. rossii*, *T. bernacchii* (red-blooded species – Cruise PS112, Weddell Sea in 2013-2014), *C. gunnari* and *C. rastrospinosus* [icefish species – Cruise ANTXXVIII (PS79), Antarctic Peninsula in 2012]. *N. rossii* and *T. bernacchii* have 30-45 % of haematocrit and 18-28 % haematocrit respectively.

Ethics Statement

The proposal for the Antarctic Fish project was approved by Veterinary School's Clinical Ethical Review panel, University of Nottingham, with responses from at least four members of the panel. No ethical issues were raised by the panel. The Ethical project Number issued: 2744 190509.

3.2.2 Subcellular fractionation.

The white and red muscle tissues were stored at -80°C and while obtaining the fractions were put on ice throughout. The tissues were cut with a sterile blade and then homogenised using Dounce homogeniser, in 2 mL mitochondria extraction buffer (50 mM Tris-Cl pH 7.4, 100 mM KCl, 1.5 mM MgCl2, 1 mM EGTA, 50 mM HEPES and 100 mM sucrose). The homogenized mixture was centrifuged at 800 rpm for 10 minutes at 4°C to remove the insoluble fraction, and the first supernatant was centrifuged at 1000 rpm to pellet nuclear fraction. The supernatant obtained from the second centrifuge, was centrifuged at 10,500 rpm at 4°C for 30 minutes to obtain the mitochondrial fraction. The supernatant which contained the cytosolic fraction was transferred into a separate tube and the pellet contained the mitochondrial fraction. The quality of the crude fractions was confirmed using standard western blotting techniques with nuclear, mitochondrial and cytoplasmic markers (Histone H3, ab1791 (Abcam) Rb pAB; COX IV ab16056 (Abcam) Rb Ab; and GAPDH, Sigma G9545 Rb respectively) as described previously specific blots or this study can be found [15]. Majority of the proteins identified are associated with mitochondrial processes confirming the successful fractionation.

3.2.3 Liquid Chromatography-Mass spectroscopy proteomic analysis (LC-MS/MS).

Red Muscle: The extracted mitochondrial fractions of three specimens per species (C. gunnari: samples 639, 673, 690; C. rastrospinosus: sample 1005, 1020, 1355; N. rossii: 4-10, 4-27, 5-14; T. bernacchii: samples 7-23, 7-56, 8-24) were captured in gel and sent to the Metabolomics and Proteomics Lab (University of York, UK) for Liquid Chromatography-Mass spectroscopy (D-100) proteomic analysis. A label-free, intensity-based quantification for comparing relative protein amounts between samples approach was used. Mass spectrometry data were analysed using PEAKSX software. The mapped ion areas were used as metric for significance testing for changes in the abundances between groups by using the PEAKSQ interpretation of the significance of the B model. These were converted into relative percent of the total ion area for analysis. The PEAKSQ significance values have been multiply-test-corrected using the Hochberg and Benjamin FDR approach ($q<0.01$).

Protein identification: The spectra from PEAKSX studio were searched against the combined NCBI deposited proteins from *Notothenia coriiceps (*32,361 sequences; 15,554,893 residues)*, Chaenocephalus aceratus (*223 sequences; 59,314 residues)*, Dissostichus mawsoni (*210 sequences; 61,335 residues) and *Eleginops maclovinus (*193 sequences; 53,595 residues), in addition to 115 common proteomic contaminant proteins. Protein identifications were filtered to achieve <1% false discovery rate (FDR) as assessed against a reverse database. Identifications were further filtered to require a minimum of two unique peptide identifications per protein group.

White Muscle: The extracted mitochondrial fractions of three specimens per species (*C. gunnari*: 675, 708, 641 samples; *C. rastrospinosus*: 1006, 1021, 1386 samples; *T. bernacchii*: 7-37, 7-54, 8-22 samples; *N. rossii*: 4-25, 4-42, 4-59 samples) were captured in gel and sent to the Metabolomics and Proteomics Lab (University of York, UK) for Liquid Chromatography-Mass spectroscopy (D-270) proteomic analysis. The same approach was applied for analysing the mass spectrometry data for the white muscle mitochondria samples and was matched against the previously mentioned NCBI deposited proteins.

From the proteomic data, we used 'number of spectral matches' as it shows the best metric for the presence and absence of a predicted protein. For the quantitative analysis of the changes in protein proportions, we used the relative percent of total ion map area for comparison of the proteins.

Proteins that were individually low in abundance or higher in abundance for each species were characterised using the number of spectral matches and Ion Map Area (Supplementary Tables 1-12). The proteins from those lists present in species-specific quantities were grouped and used for comparing the abundance of proteins in red-blooded species (*N. rossii* & *T. bernacchii*) samples and with icefish species (*C. gunnari* & *C. rastrospinosus*) samples. This also took in account the proteins that followed a similar trend in their amounts i.e., more in abundance in icefish in comparison to red-blooded species and vice versa.

3.2.4 STRING Network analysis and Clustering.

The list of proteins that were found to follow a definite pattern in the proteome of the icefish in comparison to the red-blooded fish were checked as separate groups on STRING database (http://string-db.org). The protein IDs of the selected protein was extracted from the proteomics data and the respective FASTA sequences were extracted. The multiple FASTA sequence of the proteins was searched against the closest available species on the STRING db, *Danio rerio* (zebrafish) using the multiple sequence option. Network analyses were visualised in Cytoscape_v3.8.0 and to obtain the top hub proteins, a molecular complex detection plug-in (MCODE) was used to obtain the modules. The criteria used were Degree cut-off =2, node score cut-off=0.2, k-core=2 and max Depth= 100 [35]. The top modules were selected for graphical representation. Cytoscape with the GeneMANIA plugin was used to identify the genes most related to the groups of gene sets to form a network of functional genes based on their interaction, such as co-expression, physical-interaction, and shared protein domains. GeneMANIA, a plug-in for Cytoscape predicts the function of the identified gene sets by using a 'guilt-by-association' approach which is informed

by functional networks from multiple organisms [36]. The gene symbols for the proteins were inputted with default parameters using in-built *D. rerio* gene information, which have been collected from GEO, BioGRID and organism-specific functional genomic data sets. The pathway enrichment was analysed for GO terms 'biological significance' and 'associated metabolic pathways in KEGG'. The enrichment database fishENRICHR was run using gene symbols (**Table 1-4**), these were sorted according to the p values ($P < 0.05$, probability of any gene belonging to any set) [37,38].

Graphical representation. R package ggplot2 v.3.5.1. was used for generating heatmaps and volcano plots.

3.3 Results

3.3.1 LC/LC-MS Data for RMM and WMM

The purpose of the study was to identify mitochondrial and mitochondrial-associated proteins in the icefish and to understand how the loss of haemoglobin affects the proteome. LC-MS/MS data were analysed using PEAKSX for reliable matching to the available sequence database and the data were filtered to 1% false discovery rate by at least two unique peptides for each protein group (**Figure. 3-1 A1 & B1**). For red muscle mitochondria (RMM) 1148 proteins were identified belonging to unique protein groups this contrasts with white muscle mitochondria (WMM) where 429 proteins were identified. Haemoglobin α, β and γ were only identified in the red-blooded fish confirming sample specificity. The two types of muscle are faced with very different energetic demands, However, previously it has been shown that there are no big differences in mitochondrial protein expression when surveying different porcine muscle tissues [39].

Group 1 consisted of the proteins that were significantly more abundant, and group 2 consisted of less abundant proteins in the two icefish species when compared with the red-blooded species (**Tables 1-4**). The reported significance value is the –log10P value, with the null hypothesis being that protein is of equal abundance in all samples. The higher the significance value the greater the probability that the protein is not equal in abundance in all groups. The volcano plot distinctively shows the significant differentially expressed proteins (DEPs) ($q<0.05$) that were downregulated (green) and upregulated (red). The WMM had fewer proteins that weren't significant when compared to the RMM. A heat map that includes the differentially expressed proteins (DEPs) in red muscle (**Figure. 3-1 A2**) and white muscle (**Figure. 3-1 B2**) mitochondria illustrates that protein expression profiles are characteristic for the haemoglobin-less species when compared with red-blooded groups. The mapped ion areas were converted to relative percent values by weighting each protein equally to point out differences between groups.

There was a common increase in abundance in the complex V proteins and a group of ribosomal proteins (more evidently in the white muscle) in the icefish in both the muscle mitochondria tissues. A few mitochondrial import proteins were also seen increased such as ADP/ATP translocases, voltage-dependent anion channel, and heat shock proteins. A common decrease in abundance in the proteins for the icefish were seen in Hb and haem/Hb-associated proteins such as cytochrome c, transferrin, haem oxygenase 2 and hemopexin. Apart from those, a decrease in the abundance was seen in muscle proteins such as creatine kinase, troponin, titin, and myosin heavy chain.

The two groups of proteins from both the tissues RMM and WMM were mapped into protein-protein interaction (PPI) networks constructed using STRINGdb. The enrichment p-value for each of the three PPI networks is lesser than10^{-16} indicating that proteins share more interactions than would be expected for a random set of proteins of similar size drawn from the proteome suggesting at least partial biological connection as a group [40]. The network was retrieved and analysed

using Cytoscape software which allowed us to visualize and analyse molecular interaction networks [41] (**Figure. 3-2 & Figure. 3-4**) [36].

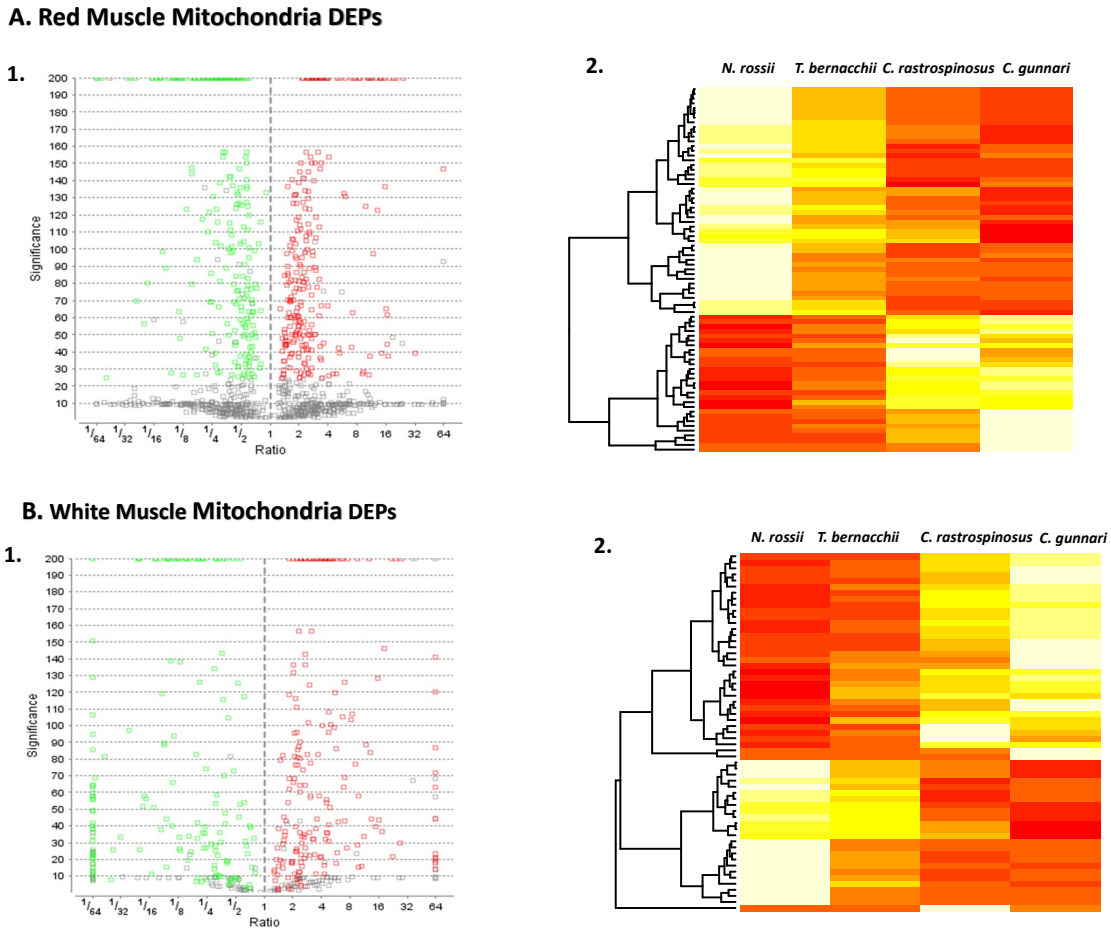

Figure 3-1 Volcano Plot and Heat Map of DEPs for the two tissue types. Volcano plot for differentially expressed proteins (A1. & B1.) The x axis depicts log fold change and Y axis depicts FDR; the lower genes are low p values; less significant. Genes that are upregulated are right side of the graph and those down regulate are left side of the graph (FDR>0.01). DEPs in red muscle mitochondria (A 2.) and white muscle mitochondria (B 2.) for the four species (Red is significantly more highly expressed). The heat maps are produced using the relative percent of total ion area that is used for comparing the change in abundance for the same protein from different samples. A clear distinction in the expression of the protein abundance among different species can be seen, red being more abundant and yellow being less (List of proteins Table 1-4).

3.4.1 Analysis of proteins more in abundance in icefish

Figure 3-2 Gene interaction networks for DEPs with increased abudance in icefish. A) RMM Analysis and B) WMM Analysis. A GeneMANIA gene–gene interaction network for protein abundance following the pattern N. rossii (+/+), T. bernacchii (+/+), C. rastrospinosus (-/+) and C. gunnari (-/-) in increasing order of their protein abundance, laid out and visualised with Cytoscape, showing interaction strength (edge thickness), interaction type (colour-bottom right), multiple edges between nodes, protein score (node size). Black nodes indicate query proteins, and grey nodes are neighbouring proteins with interactions as co-expressed, physical, or shared protein domains.

Forty-three proteins were differentially expressed with higher abundance in the RMM of the two icefishes compared to the red-blooded nonfamilial species. Fifty-seven proteins were significantly higher expressed in the WMM (**Tables 1 and 2**). Most proteins that were seen upregulated in both RMM and WMM were found to be part of the complex V, ribosomal and proteosome machineries in addition to a common upregulated expression of malate dehydrogenase and Fragile X mental retardation isoform 2 protein. In RMM components of complex V of the electron transport chain and proteins involved in transportation across mitochondria were observed. The upregulated proteins of WMM were involved in the citrate cycle and carbon metabolism.

GeneMANIA (based on zebrafish) analysis for interactions of the proteins with increased abundance in icefish produced one network per each muscle tissue (**Figure. 3-2 A & B**). In RMM, co-expression occupied 98.66% of the interactions seen in the network; shared protein domains occupied 1.13%; physical interaction 0.21%. The network showed shared domains among proteins, slc25a5, slc25a6, slc25a20, vdac3 and slc25a12, and, between atp5a1 and atp5b. The network showed physical interactions between atp5a1, atp5o, predicted cyc1 and coq9. In WMM, co-expression

occupied 98.46% of the interactions seen in the network; physical interactions occupied 1.431%; and shared protein domains occupied 0.11%. The network showed physical interactions between ribosomal proteins and separately also between proteasome proteins.

Table 1 - Differentially expressed proteins (DEPs) among the four species in RMM - higher abundance in icefish.

	Protein Abundance - Higher in icefish (Red Muscle)			Relative Percent of Total Ion Area (Mapped) - Converted from tptal sum of ion area to relative percent of totsl ion area				
S. No.	Protein Name	Gene Name	Quant Significance H&B multiple test corrected q-value	*N. rossii*	*T. bernacchii*	*C. rastrospinosus*	*C. gunnari*	Accession Number
1	26S protease regulatory subunit 4 isoform X1 & X2	psmc1a	1.26E-06	4.9	6.6	7	81.4	XP_010780333.1
2	Apolipoprotein B-100-like partial	apobb	3.76E-19	3.2	3.3	27.9	65.6	XP_010781933.1
3	NAD(P) transhydrogenase mitochondrial-like	nnt	2.96E-19	5.5	5.8	29.6	59.2	XP_010786020.1
4	Hyaluronan and proteoglycan link protein 1	hapln1	7.26E-20	9.1	5.2	30	55.7	XP_010767902.1
5	Sarcolemmal membrane-associated protein-like isoform X1 & X2	slmapa	9.74E-03	15.2	15.7	24	45.1	XP_010782086.1
6	ADP/ATP translocase 2-like	slc25a5	1.04E-18	13	6.2	36.5	44.3	XP_010765274.1
7	Dihydrolipoyllysine-residue acetyltransferase component of pyruvate dehydrogenase complex	dlat	9.10E-12	15.9	16.3	27.3	40.5	XP_010773292.1
8	Alpha-2-macroglobulin-like partial	a2ml	1.24E-04	14.7	22.1	23.1	40.1	XP_010771939.1
9	Inter-alpha-trypsin inhibitor heavy chain H4-like	itih3a.2	1.38E-11	12.1	12.7	35.9	39.3	XP_010793736.1
10	Stress-70 protein mitochondrial-like	hspa9	1.58E-05	20	18.3	33.7	28.1	XP_010766277.1
11	Epoxide hydrolase 1	ephx1l	3.80E-20	10.2	21.6	31.1	37.1	XP_010790338.1
12	Sorting and assembly machinery component 50 homolog	samm50	1.66E-19	17.4	8.9	37.3	36.4	XP_010773400.1
13	Calcium-binding mitochondrial carrier protein Aralar1	slc25a12	1.22E-19	23	7.8	32.8	36.4	XP_010768357.1
14	Long chain fatty acyl CoA synthetase	acsl1a	5.89E-07	2.6	19.1	42.1	36.1	AAK07470.1
15	Malonyl-CoA decarboxylase mitochondrial	mlycd	3.73E-20	10.9	18.7	34.7	35.6	XP_010792494.1
16	NADH dehydrogenase [ubiquinone] 1 beta subcomplex subunit 8 mitochondrial	ndufb8	6.63E-07	13.1	19.5	31.9	35.6	XP_010779169.1
17	60S ribosomal protein L27a isoform X1 & X2	rpl27a	5.18E-20	10.7	14.8	38.9	35.6	XP_010790259.1
18	Fatty acid binding protein H8-isoform	fabp3	2.44E-19	2.4	25.6	37.2	34.8	AAC60356.1
19	ATP-dependent 6-phosphofructokinase muscle type-like	pfkm	2.03E-10	22.3	12.5	31	34.2	XP_010794434.1
20	Carnitine/acylcarnitine carrier protein	slc25a20	1.20E-19	20	9.9	36.2	33.9	XP_010773584.1
21	ATP synthase subunit O	atp5o	4.06E-08	24.6	13.4	29.1	32.9	XP_010772138.1
22	Proliferation-associated protein 2G4-like	pa2g4b	4.31E-03	19	21.8	27.3	32	XP_010782747.1
23	ATP synthase subunit g mitochondrial	atp5l	2.26E-07	23.1	10.6	34.4	31.9	XP_010779232.1
24	Voltage-dependent anion-selective channel protein 3	vdac3	4.60E-19	13.2	12.1	43.2	31.6	XP_010782516.1
25	ATP synthase subunit alpha mitochondrial	atp5fa1	7.03E-09	22.2	14.9	31.7	31.2	XP_010779868.1
26	ATP synthase subunit beta mitochondrial	zgc:163069	1.07E-08	24.7	13.4	31.1	30.8	XP_010765728.1
27	ATP synthase subunit gamma mitochondrial isoform X1	atp5g	2.54E-14	18.3	10	41.5	30.1	XP_010778067.1
28	60S ribosomal protein L35	rpl35	2.93E-15	14.9	15.2	40.2	29.6	XP_010790499.1
29	ATP synthase F(0) complex subunit B1 mitochondrial	atp5pb	1.54E-15	23	11.6	36	29.5	XP_010786327.1
30	ATP synthase subunit delta mitochondrial	atp5d	6.63E-03	18.8	23.4	28.4	29.4	XP_010775450.1
31	Prothrombin partial	f2	5.96E-20	14.3	23.2	33.2	29.3	XP_010786167.1
32	ADP/ATP translocase 3	slc25a6	5.06E-12	23.5	13.6	33.9	29	XP_010784438.1
33	60S ribosomal protein L18a-like	rpl18a	3.98E-08	18.2	18.8	34.1	28.9	XP_010774792.1
34	ATP synthase subunit d mitochondrial	atp5pd	8.45E-20	25.2	8.6	37.5	28.7	XP_010766730.1
35	Malate dehydrogenase cytoplasmic-like partial	mdh1aa	7.88E-16	13.2	16.9	42.1	27.8	XP_010766317.1
36	Cytochrome c oxidase subunit 5A mitochondrial isoform X2	cox5a	5.67E-20	16.5	9.2	46.4	27.8	XP_010766309.1
37	60S ribosomal protein L23	rpl23	1.14E-12	15.9	20.4	37	26.7	XP_010783746.1
38	Prohibitin	phb	2.72E-06	18.1	18.4	39.1	24.5	XP_010773724.1
39	Ubiquinone biosynthesis protein COQ9	coq9	8.44E-11	17.2	17.6	42.1	23	XP_010793356.1
40	26S proteasome non-ATPase regulatory subunit 6	psmd6	3.76E-02	8.5	15	28.3	48.1	XP_010773228.1
41	Fragile X mental retardation syndrome-related protein 2	fxr2	7.07E-02	9.6	10.5	16.4	63.5	XP_010770797.1
42	Reticulon-4-interacting protein 1 homolog mitochondrial-like	rtn4ip1	1.05E-01	19.8	20.5	28.7	31	XP_010790805.1
43	Kininogen-1	kng1	1.28E-01	13.7	16.6	25.8	43.8	XP_010787469.1

Figure. 3-3 A shows PPI network generated using the FASTA sequences (corresponding NCBI IDs) for the proteins using STRING. The forty-three identified DEPs that were more abundant in RMM were analysed and connected with a PPI enrichment p-value < 1.0e-16, with 42 nodes (proteins RPL27 was not identified for organism *D. rerio*), 143 edges, and an average node-degree of 6.8. Four of forty-two DEPs (RTN4IP1, PFKMA, FRX2 and HAPLN1b) did not connect to any type of network (STRING interaction score=0.4). Thirty-eight of the remaining DEPs were connected to networks by complex relationships. RPL23, MDH1AA, ATP5B, and VDAC3 showed network hubs highly associated with other nodes in PPI. (**Supplementary Figure 3-7**). A single network was formed between DEPs ITIH4, A2ML, KNG1, F2 and APOBB. The highly connected proteins are majorly involved in energy metabolism and protein metabolism. Three distinctive clusters were seen for RMM upregulated proteins. Cluster 1 had proteins involved in ETC and oxidative phosphorylation, Cluster 2 proteins involved in cell signalling and Cluster 3 proteins involved in fatty acid biosynthesis (**Supplementary Figure 3-6**).
Functional enrichment analysis (FDR $<1.9 * 10^{-2)}$) showed proteins involved in TCA cycle, oxidative phosphorylation, degradation of RNA, cristae formation, mitochondrial

protein import and carbon metabolism (See **Figure. 3-3 A**) using the STRINGdb information provided under KEGG and Reactome pathways.
Using FishENRICHR [37,38], the most used GO Terms for different biological processes were: GO:0019674, NAD metabolic process; GO:0070306 lens fibre cell differentiation; GO:0006754 ATP biosynthesis; GO:0006839 mitochondrial transport; GO:0045898 regulation of RNA polymerase II transcriptional pre-initiation complex assembly. (See **Figure. 3-3 C 1 & 2**)

Red Muscle Mitochondria

A.

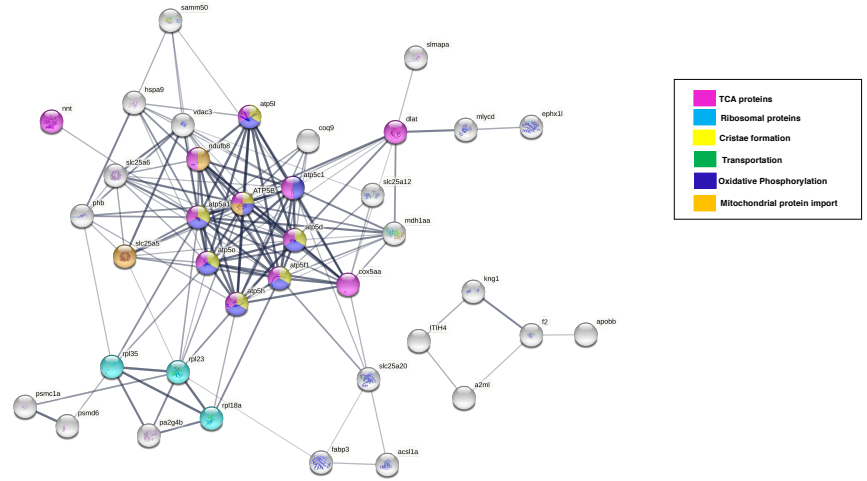

White Muscle Mitochondria

B.

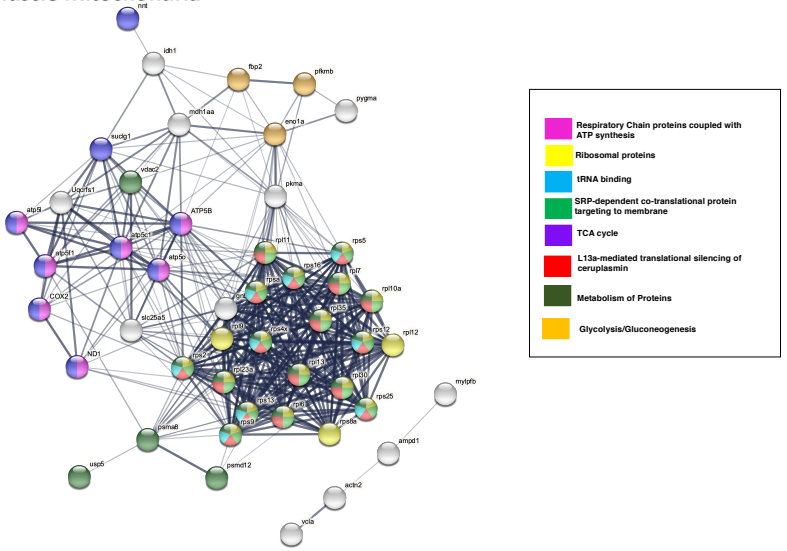

C.

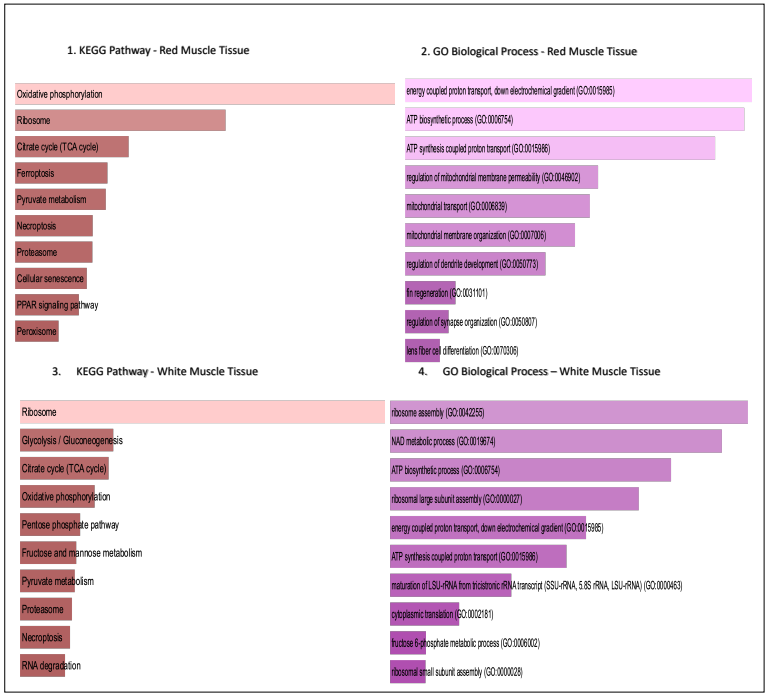

Figure 3-3. Network analysis of more highly abundant proteins in icefish mitochondria compared with closely related red-blooded species. A. RMM DEPs, number of nodes 42 with 143 edges, the average node degree is 6.8 and B. WMM, number of nodes 56 with 382 edges with an average node degree of 13.6. Network analysed using STRINGdb. The network highlights proteins involved in different pathways curated by STRINGdb from KEGG and Reactome databases. Nodes are coloured according to pathways. The edge shows type of interactions, experimentally determined interactions database derived, predicted interactions such as gene neighbourhood, gene co-occurrence, gene fusions respectively, co-expression interactions, text-mining interactions, and homology, thicker the edge higher the confidence obtained the mentioned sources. C. Using FishEnrichr [37,38] analyser KEGG Pathways and GO terms for Biological process showed proteins in different pathways. The length of the bar represents the significance of that specific gene-set or term. Brighter colours are highly significant.

Table 2 - DEPs between WMM with increased abundance in icefish specifically seen upregulated in icefish Champsocephalus gunnari

	Protein Abundance - Higher in icefish (White Muscle)			Relative Percent of Total Ion Area (Mapped) - Converted from tptal sum of ion area to relative percent of totsl ion area				
S. No.	Protein Name	Gene Name	Quant Significance H&B multiple test corrected q-value	*N. rossii*	*T. bernacchii*	*C. rastrospinosus*	*C. gunnari*	Accession Number
1	Myosin regulatory light chain 2 skeletal muscle isoform-like	mylpfb	3.42E-19	1	2.2	2.3	94.4	XP_010770965.1
2	Myozenin-1 isoform X1 & X2	myoz1b	1.55E-07	0	7.8	13.3	78.9	XP_010791910.1
3	Heat shock protein beta-1	hspb1	9.49E-05	9.9	4.1	11.5	74.6	XP_010788098.1
4	60S ribosomal protein L35	rpl35	4.58E-20	3.4	7.9	32.7	56	XP_010790499.1
5	40S ribosomal protein S16 isoform X1	rps16	9.30E-03	12.3	16.9	17.9	52.8	XP_010773777.1
6	60S ribosomal protein L7	rpl7	1.08E-06	6.9	7.8	33.1	52.3	XP_010770361.1
7	Fragile X mental retardation syndrome-related protein 2	fxr2	6.55E-04	4.6	11.6	32.2	51.6	XP_010770797.1
8	40S ribosomal protein S12	rps12	1.13E-04	8.4	13.8	27	50.8	XP_010783785.1
9	60S ribosomal protein L30	rpl30	8.33E-05	3.1	22.6	24	50.3	XP_010765856.1
10	60S ribosomal protein L12 isoform X2	rpl12	5.13E-20	9.9	11.7	28.5	49.8	XP_010779104.1
11	Reticulon	rtn1a	5.52E-20	14.9	13	22.7	49.4	XP_010790870.1
12	Palladin-like	palld	1.07E-14	2.7	15.9	32.1	49.2	XP_010785200.1
13	60S ribosomal protein L9	rpl9	4.71E-20	4.2	3.4	43.7	48.7	XP_010776310.1
14	AMP deaminase 1 isoform X1 & X2 [Notothenia coriiceps]	ampd1	1.65E-19	18.6	10.9	22.8	48.4	XP_010793467.1
15	ADP/ATP translocase 3	slc25a5	3.22E-10	7.8	10.6	33.7	47.8	XP_010784438.1
16	40S ribosomal protein S13 [Notothenia coriiceps]	rps13	9.88E-04	13.1	10.6	29.1	47.3	XP_010794693.1
17	40S ribosomal protein S8-like partial	rps8	2.92E-10	9.1	11.8	33	46	XP_010787537.1
18	Alpha-actinin-2	actn2	1.43E-08	12.1	18.2	23.6	46	XP_010791686.1
19	Kelch-like protein 41b	klhl41b	5.58E-20	4.2	11.6	38.5	45.7	XP_010774286.1
20	60S ribosomal protein L6	rpl6	4.54E-20	7	11.3	36.3	45.4	XP_010782543.1
21	40S ribosomal protein S5	rps5	7.75E-04	17	12.2	25.5	45.3	XP_010783741.1
22	Cytochrome c oxidase subunit II	mt-co2	5.92E-13	2.6	26.8	25.9	44.7	YP_004581500.1
23	40S ribosomal protein S25	rps25	6.64E-03	13	14.5	28.4	44.2	XP_010776714.1
24	60S ribosomal protein L11	rpl11	4.98E-20	15.6	11.7	29.1	43.7	XP_010779161.1
25	Voltage-dependent anion-selective channel protein 2	vdac2	8.77E-07	15.6	10.6	30.4	43.5	XP_010767141.1
26	40S ribosomal protein S4	rps4x	6.41E-20	7.5	16	33.6	43	XP_010792965.1
27	40S ribosomal protein S2	rps2	5.40E-20	6.8	11.4	39	42.8	XP_010783756.1
28	60S ribosomal protein L10a	rpl10a	2.26E-14	14.8	15.1	29.7	40.4	XP_010791484.1
29	40S ribosomal protein S9	rps9	4.40E-08	12.5	17.9	29.3	40.3	XP_010786813.1
30	ATP synthase subunit g	atp5l	4.66E-20	18.7	11.6	32.7	37	XP_010794136.1
31	Vinculin	vcla	1.15E-07	18.7	11.6	32.7	37	XP_010787927.1
32	60S ribosomal protein L13	rpl13	5.51E-11	8.2	16	39.4	36.5	XP_010789836.1
33	Fructose-1 6-bisphosphatase isozyme 2-like	fbp2	5.64E-20	9.8	26	28.1	36.1	XP_010781656.1
34	40S ribosomal protein SA isoform X2	rpsa	6.11E-20	10	17.7	37.1	35.3	XP_010768032.1
35	Succinyl-CoA ligase	suclg1	6.66E-11	5.5	10.2	49.4	35	XP_010778226.1
36	Tubulin alpha chain-like isoform X1 & X2	tuba8l2	4.49E-04	11.3	23.9	29.9	34.9	XP_010766070.1
37	60S ribosomal protein L23a	rpl23a	5.29E-08	3.5	9.8	56.9	34.8	XP_010791811.1
38	NADH-ubiquinone oxidoreductase	mt-nd1	8.22E-07	3.5	9.8	51.9	34.7	XP_010777506.1
39	Alpha-enolase-like	eno1a	4.27E-04	13	22.3	30.3	34.5	XP_010765339.1
40	Isocitrate dehydrogenase	idh1	1.22E-19	20.6	11	35.7	32.6	XP_010791048.1
41	26S proteasome non-ATPase regulatory subunit 12	psmd12	1.19E-03	10	11.8	47.6	30.6	XP_010777584.1
42	ATP synthase F(0) complex subunit B1	atp5pb	2.07E-10	19	6.4	44.2	30.2	XP_010786327.1
43	Peptidyl-prolyl cis-trans isomerase-like	pplb	1.03E-03	8	27.2	35.3	29.5	XP_010790691.1
44	Malate dehydrogenase	mdh1aa	1.71E-19	15.1	9	46.6	29.4	XP_010780749.1
45	ATP synthase subunit O	atp5o	5.16E-04	16.1	9.4	45.9	28.6	XP_010772138.1
46	NAD(P) transhydrogenase	nnt	5.81E-08	15.9	16.7	39	28.3	XP_010776087.1
47	Glycogen phosphorylase muscle form-like	pygma	8.47E-06	17.7	25.3	30	26.9	XP_010788355.1
48	Ubiquitin carboxyl-terminal hydrolase 5 isoform X1	usp5	4.80E-04	9.3	19.1	44.8	26.7	XP_010769500.1
49	Cytochrome b-c1 complex subunit 2	uqcrfs1	4.32E-04	11.7	10.4	52.9	25	XP_010784571.1
50	ATP synthase subunit gamma	atp5c1	1.42E-12	13.4	12.3	49.6	24.7	XP_010778067.1
51	ATP synthase subunit beta	zgc:163069	9.98E-16	17.5	12.4	46.2	23.8	XP_010765728.1
52	Pyruvate kinase PKM	pkma	5.13E-19	11	10.3	56	22.7	XP_010766216.1
53	Vitellogenin-1-like	vtg2	1.38E-02	0	2	93.6	4.4	XP_010779640.1
54	Proteasome subunit alpha type-7-like	psma8	1.97E-02	9.6	11.7	55.1	23.6	XP_010783619.1
55	Guanine nucleotide-binding protein subunit beta-2-like 1	gnb2l1	1.57E-02	13.2	21	29.6	36.2	XP_010780163.1
56	ATP-dependent 6-phosphofructokinase muscle type-like	pfkmb	1.84E-02	16.7	17.3	26.1	39.9	XP_010782695.1
57	Inter-alpha-trypsin inhibitor heavy chain H3-like	zgc:110377	1.92E-02	0	14.4	46.5	39.1	XP_010777740.1

Using the same steps as for RMM, a PPI network was generated for WMM DEPs (**Figure. 3-3 B**). As for the WMM the intra network connections were strongest (PPI enrichment p-value <1.0e^{-}16, with fifty-six nodes 382 edges and an average node-degree of 13.6). Nine of the fifty-six DEPs did not connect to any network (RTNA1, MYOZ1B, HSPB1, KLH41B, TUBA8L2, VTG2, ZGC:110377, PALLD, and FXR2-**Table 2**).

The remaining forty-seven of the differentially expressed proteins were connected to networks, where differentially expressed proteins ATP5B, GNB2L1, RPL11, RPL13, RPSA, PKMA, are the major protein-hubs (See **Supplementary Figure 3-8**). A single network was formed between DEPs MYLPFB, AMPD, ACTN2, and VCLA.

Three distinctive clusters were seen for WMM upregulated proteins similar to RMM. Cluster 1 had proteins of ribosome machinery, Cluster 2 proteins involved in ETC and TCA, and Cluster 3 proteins involved in fatty acid biosynthesis (**Supplementary Figure 3-6**).

Functional enrichment analysis (FDR $<1.4*10^{-2}$) showed proteins involved in TCA, ribosomal proteins, downstream signalling events of B cell receptors and L13a-mediated translational silencing of ceruloplasmin. The fishENRICHR identified, GO:0000463: “maturation of LSU-rRNA”, GO:0045727 and GO:0000470: “positive regulation of translation”, GO:0000027 and GO:0042273: “ribosomal large subunit assembly” as most common GO terms. Enriched KEGG pathways included ribosome, glycolysis and gluconeogenesis, and the pentose pathway (pathways sorted according to p-values) (**Figure 3-3. C 3 & 4**). The proteins involved in gluconeogenesis have previously been reported altered in their expression in rainbow trout. The study goes onto show an increase in the enzyme FB2 a key enzyme of gluconeogenesis to be increased in red muscle for the fish. On contrary we see FB2 to be increased fourfold in the white muscle tissue for the icefish rather than the red muscle [42].

The protein networks between RMM and WMM differ. In RMM, there is one quite dense cluster with some weak “satellites” and another cluster with similar connectivity as seen in WMM. In WMM there are three separate clusters with good and quite similar connection.

3.4.1 Proteins with lower abundance in icefish

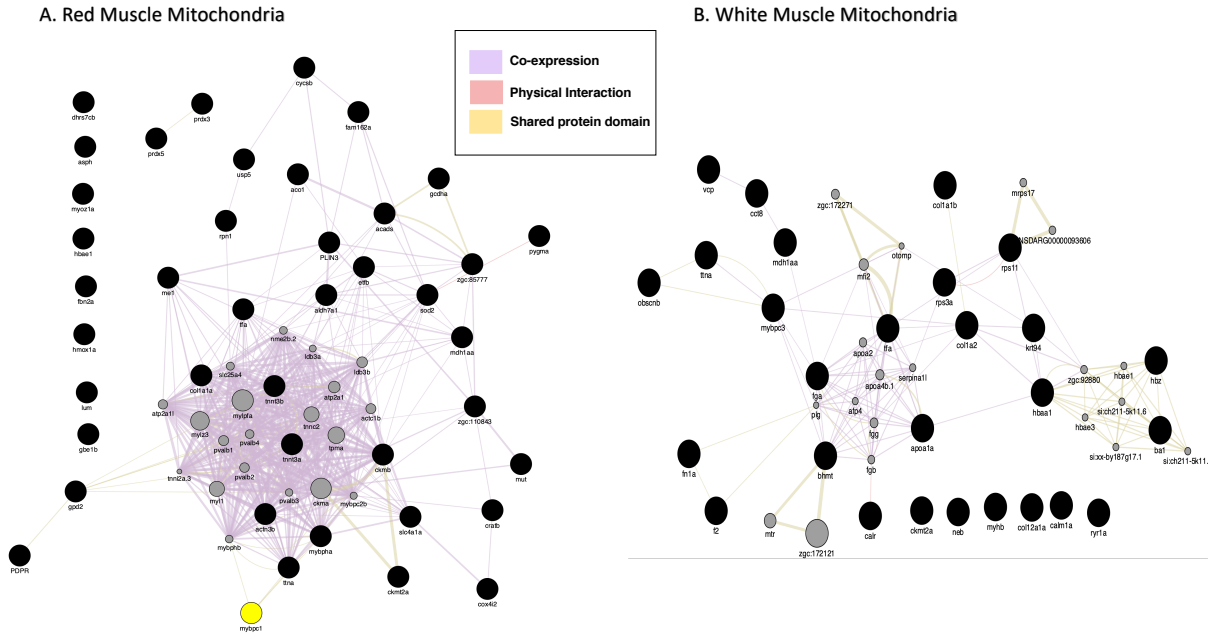

Figure 3-4. Gene interaction network for proteins with lower abundance in icefish A) RMM and B) WMM. A GeneMANIA gene–gene interaction network for protein abundance following the pattern N. rossii (+/+), T. bernacchii (+/+), C. rastrospinosus (-/+) and C. gunnari (-/-) in decreasing order of their protein abundance, laid out and visualised with Cytoscape, showing interaction strength (edge thickness), interaction type (colour-bottom right), multiple edges between nodes, protein score (node size) Black dots indicate query proteins, and grey dots depict neighbouring proteins.

Forty-eight proteins were found in lower quantities in RMM (ENSDARG00000030638, ca1, casq, gdh, mdh, pygm, rdh13, wu:fd55e03 were not recognised by GENEmania) and thirty-two proteins were differentially expressed in WMM in icefish compared to their red-blooded relatives (**Tables 3 & 4**). As before, GeneMANIA was used to analyse the interactions and produced one network per tissue (**Figure. 3-4 A & B**). In RMM, co-expression accounted for 96.14% of the total interactions seen in the network; and shared protein domains occupied 3.86%. In WMM, co-expression occupied 94.76%; physical interactions occupied 5.02%; and shared protein domains occupied 0.21%. The network showed physical interactions between ribosomal proteins and nebulin and this was predicted for the neighbouring protein tropomodulin.

Table 3 - DEPs in RMM with decreased abundance in icefish specifically seen downregulated in icefish Champsocephalus gunnari

	Protein Abundance - Lower in icefish (Red Muscle)			Relative Percent of Total Ion Area (Mapped) - Converted from tptal sum of ion area to relative percent of totsl ion area				
S. No.	Protein Name	Gene Name	Quant Significance H&B multiple test corrected q-value	*N. rossii*	*T. bernacchii*	*C. rastrospinosus*	*C. gunnari*	Accession Number
1	Hemoglobin subunit alpha-1	hbae1	1.88E-19	60	38.7	0.8	0.5	NP_001290227.1
2	Calsequestrin-1	casq1	6.09E-20	33.3	44.4	18.6	3.7	XP_010782377.1
3	Perilipin-3	plin3	1.53E-19	48.8	35.6	11.1	4.5	XP_010778108.1
4	creatine kinase S-type mitochondrial-like	ckmt2a	4.36E-19	71.4	22.4	1.4	4.8	XP_010772488.1
5	Transferrin	tfa	8.36E-20	34	54.2	17.3	5.5	CAL92189.1
6	Dehydrogenase/reductase SDR family member 7C	dhrs7cb	3.01E-09	68.9	18.2	7.1	5.7	XP_010784042.1
7	Myosin-binding protein H-like	mybpha	9.10E-20	66.6	20.7	5.9	6.8	XP_010764981.1
8	Band 3 anion transport protein	slc4a1	1.92E-08	39	52	2.1	6.9	XP_010785995.1
9	Cytochrome c oxidase subunit 4 isoform 2 mitochondrial-like	cox4i2	5.79E-20	60.1	22.5	9.6	7.7	XP_010770791.1
10	Titin-like	ttna	2.47E-11	50.9	21.6	19.4	8.1	XP_010787367.1
11	Glutaryl-CoA dehydrogenase mitochondrial-like	gcdh	4.93E-20	34	28.8	28.2	9	XP_010795730.1
12	Fibrillin-1-like isoform X1	fbn2a	5.14E-20	67.5	17.5	6	9	XP_010767938.1
13	heme oxygenase 2	hmox1	1.18E-04	48.5	20.6	21.3	9.7	XP_010786435.1
14	NADP-dependent malic enzyme	me1	1.29E-19	33.9	40.3	16	9.8	XP_010776993.1
15	Pyruvate dehydrogenase phosphatase regulatory subunit	pdpr	8.31E-09	24.9	48.6	15.4	11.1	XP_010773093.1
16	Dolichyl-diphosphooligosaccharide--protein glycosyltransferase subunit 1	rpn1	7.17E-12	38.5	30.1	20.2	11.2	XP_010777251
17	CDGSH iron-sulfur domain-containing protein 1	zgc:110843	4.55E-20	41	36	11.6	11.5	XP_010767760.1
18	Glutamate dehydrogenase	gdh	3.07E-19	29.9	48.6	11.1	11.9	P82264.1
19	Thioredoxin-dependent peroxide reductase mitochondrial	prdx3	6.47E-20	31.2	29.5	27.2	12.1	XP_010779546.1
20	malate dehydrogenase	mdh	1.18E-12	32.5	37	18.4	12.1	XP_010765488.1
21	Cytochrome c	cycsb	5.56E-20	42.8	28.7	16.1	12.5	XP_010792793.1
22	Troponin T fast skeletal muscle isoforms-like isoform X1 to X3	tnnt3a	4.90E-20	37.2	29.6	20.5	12.7	XP_010784864.1
23	Superoxide dismutase [Mn] mitochondrial	sod2	1.02E-10	42	33.4	11.5	13.1	XP_010771234.1
24	Carnitine O-acetyltransferase	crat	6.47E-13	29.1	38.8	19	13.1	XP_010795330.1
25	PDZ and LIM domain protein 7	ENSDARG00000030638	1.45E-08	45.5	21	20.3	13.3	XP_010765699.1
26	Protein FAM162B-like	fam162a	4.14E-04	41.5	32	13	13.6	XP_010783349.1
27	Aconitate hydratase mitochondrial	aco1	4.14E-19	45.3	26.8	14	14	XP_010781940.1
28	Retinol dehydrogenase 13-like isoform X1 & X2	wu:fd55e03	2.60E-13	42.1	26.2	17.6	14.1	XP_010791045.1
29	Myosin-binding protein C slow-type isoform X1 to X17	mybpc	2.39E-03	39.8	27.3	18.8	14.1	XP_010774860.1
30	Lumican	lum	2.21E-07	47.8	26.9	11.3	14.1	XP_010795529.1
31	Retinol dehydrogenase 13-like isoform X1	rdh13	2.60E-13	26.2	42.1	17.6	14.1	XP_010791045.1
32	PDZ and LIM domain protein 7-like isoform X2	ENSDARG00000030638	4.70E-20	40.6	26.1	18.9	14.4	XP_010785930.1
33	Glycogen phosphorylase	pygm	7.81E-20	30.6	44.1	10.9	14.4	XP_010788472.1
34	Alpha-aminoadipic semialdehyde dehydrogenase	aldh7a1	1.25E-19	36.3	28.9	20	14.7	XP_010772035.1
35	Myozenin-1-like	myoz1a	7.08E-20	46.5	26.8	12	14.7	XP_010764663.1
36	Collagen alpha-1(I) chain-like	col1a1a	9.41E-20	52.6	27.3	5.3	14.8	XP_010768975.1
37	Peroxiredoxin-5 mitochondrial	prdx5	8.33E-07	30.5	28.9	25.2	15.4	XP_010783999.1
38	Short-chain specific acyl-CoA dehydrogenase mitochondrial	acads	4.55E-08	32.5	26.7	25.1	15.8	XP_010779541.1
39	Troponin alpha-3 chain-like	tnnt3b	1.56E-19	36.9	35.9	11	16.1	XP_010771394.1
40	Creatine kinase M-type	ckmb	4.11E-05	34.8	25.6	23.3	16.3	XP_010791917.1
41	Glycerol-3-phosphate dehydrogenase mitochondrial	gpd2	1.14E-10	42.6	23.5	17	16.9	XP_010791177.1
42	electron transfer flavoprotein subunit beta	etfb	2.38E-05	33.9	24.8	24.2	17.1	XP_010791064.1
43	1 4-alpha-glucan-branching enzyme	gbe1b	2.21E-10	28.1	44.4	10.4	17.1	XP_010775191.1
44	Ubiquitin carboxyl-terminal hydrolase 5 isoform X1 & X2	usp5	8.41E-05	34.9	25.9	21.1	18	XP_010769508.1
45	Methylmalonyl-CoA mutase mitochondrial	mut	2.49E-04	33.7	26.7	21.5	18	XP_010784587.1
46	probable acyl-CoA dehydrogenase 6	zgc:85777	1.82E-03	31.3	26.9	23.2	18.6	XP_010772948.1
47	Alpha-actinin-3	actn3b	5.52E-19	39.5	28.5	13.3	18.7	XP_010784415.1
48	Carbonic anhydrase 1	ca1	7.89E-20	49.4	20	10.9	19.6	XP_010765900.1

In RMM, PPI networks include forty-eight protein nodes (**Figure. 3-5 A**), nine proteins (MUT, RPN1, CKMT2A, PDPR, DHRS7CB, ALDH7A1, WU:FD55e03, USP5, PLIN3) did not connect to any type of network (STRING interaction score=0.4). The PPI enrichment (p-value $<1.0e^{-16}$) had thirty-nine nodes and fifty-three edges and an average node degree of 2.52. The rest of the DEPs were connected to networks by complex relationships, where proteins ACTN3B, TTNA, CKMB, MYBPC1, TTNT3B, and CYCSB showed network hubs highly associated with many proteins (**Supplementary Figure 3-10**). Single networks were observed between FBN2A and TFA, SLC4A1A and HBAE1. Two distinctive clusters were seen for RMM. Cluster 1 had proteins involved in striated muscle contraction, and Cluster 2 proteins involved in oxidative stress (**Supplementary Figure 3-9**).

In WMM, six (ZGC:153629, HBZ, HBAA1, MYOM1A, EVA1BA and, MDH1AA) out of the thirty-two protein nodes in the network, did not connect to any type of network (**Figure. 3-5 B**). Proteins FGA, TFA, and TTNA represent network hubs, highly associated with other proteins (**Supplementary Figure 6**). The PPI enrichment (p-value $<3.49e^{-}12$) gave thirty-two nodes with forty-five edges and an average node-degree of 2.58. Three distinctive clusters were seen for WMM downregulated proteins. Cluster 1 had proteins of actin filament regulation, Cluster 2 proteins involved in muscle contraction, and Cluster 3 proteins involved with collagen (**Supplementary Figure 3-8 to 3-9**).

The functional enrichment analysis (FDR $<3.8*10^{-3}$) for RMM reduced proteins in icefish were involved in striated muscle contraction, erythrocytes absorbing oxygen,

fibrin clot formation hemostasias and haeme-associated proteins (**Figure. 3-5 A**). The following GO terms for biological processes were found overrepresented: GO:0006941 and GO:0006936: “striated muscle contraction” and GO:0045214: “sarcomere organisation”. The following KEGG pathways were affected: amino acid metabolism, fatty acid degradation, and peroxisome, glyoxylate, and dicarboxylate metabolism (**Figure. 3-5 C 1& 2**).

Table 4 - DEPs between WMM with decreased abundance in the icefish

	Protein Abundance - Lower in icefish (White Muscle)			Relative Percent of Total Ion Area (Mapped) - Converted from tptal sum of ion area to relative percent of totsl ion area				
S. No.	**Protein Name**	**Gene Name**	**Quant Significance H&B multiple test corrected q-value**	***N. rossii***	***T. bernacchii***	***C. rastrospinosus***	***C. gunnari***	**Accession Number**
1	Calreticulin	calr	5.73E-03	75.4	4.7	19.8	0	XP_010773398.1
2	Creatine kinase S-type mitochondrial-like	ckmt2a	1.19E-19	78.2	14.8	6.4	0.7	XP_010772488.1
3	Myosin heavy chain fast skeletal 13	zgc:66156	3.68E-03	37.8	34.7	26.6	0.9	XP_010791001.1
4	Prothrombin partial	f2	7.78E-04	37.3	30.3	31.2	1.1	XP_010786167.1
5	Fibronectin	fn1a	1.34E-05	33.1	30.2	34.9	1.8	XP_010794764.1
6	Transmembrane protease serine 2-like	LOC571565	6.81E-03	81.2	16.8	0	2	XP_010778161.1
7	Hemoglobin subunit zeta	hbz	2.99E-04	80.5	16.4	0.3	2.5	XP_010778322.1
8	Fibrinogen alpha chain-like	fga	2.67E-05	51.4	39.8	5.2	2.8	XP_010771898.1
9	Alpha globin	hbaa1	7.77E-20	79.6	16.5	0.4	3.3	AAC25100.1
10	Beta-globin	ba-1	7.45E-09	87.5	9.1	0	3.4	AAC60372.1
11	Haemoglobin	hb	7.33E-09	87.5	9.1	0	3.4	NP_001290226.1
12	Ryanodine receptor 1-	ryr1a	3.16E-04	54.5	19.7	21.1	4.5	XP_010787188.1
13	Keratin type I cytoskeletal 19-like	zgc:153629	8.84E-20	54.7	31.8	8.9	4.6	XP_010787448.1
14	Myosin heavy chain fast skeletal muscle-like	myhb	4.59E-12	46.7	27.6	19.2	6.5	NP_001290213.1
15	Malate dehydrogenase cytoplasmic	mdh1aa	5.57E-07	54.8	24.1	13.3	7.8	XP_010765488.1
16	Apolipoprotein A	apoa1	1.28E-19	54.4	20	16.1	9.3	XP_010792180.1
17	Myomesin-1-like	myom1	1.31E-19	31.1	29.8	21.8	17.3	XP_010789743.1
18	Betaine-homocysteine S-methyltransferase 1-like	bhmt	7.33E-20	53.1	20.8	14.4	11.6	XP_010794476.1
19	Collagen alpha-1(I) chain-like	col1a1b	6.56E-04	37.2	34.6	15.8	12.4	XP_010768975.1
20	Hemopexin	zgc:152945	3.14E-06	40.7	26.6	19.7	13	XP_010788340.1
21	T-complex protein 1 subunit theta	cct8	3.35E-06	60.6	18.2	7.4	13.9	NP_001290219.1
22	Transitional endoplasmic reticulum ATPase-like	vcp	3.11E-03	51.4	20.5	12.7	15.4	XP_010770092.1
23	40S ribosomal protein S11	rps11	8.27E-04	43.2	32.7	8.7	15.5	XP_010791578.1
24	Titin-like partial	ttna	1.66E-03	32.9	28.7	21.1	17.2	XP_010790363.1
25	Calmodulin	calm1a	1.20E-10	36.2	30.9	14	18.9	XP_010768524.1
26	40S ribosomal protein S3a	rps3a	9.93E-12	35.1	30.1	15.3	19.5	XP_010773841.1
27	Obscurin isoform X2	obscnb	2.11E-02	36.8	30.2	14.9	18.1	XP_010790854.1
28	Transferrin	tfa	3.15E-02	36.3	33.5	22.7	7.6	CAL92189.1
29	Collagen alpha-1(XII) chain isoform X1, X2, X3, X4 & X5	col12a1a	8.53E-02	68.8	18.2	8.5	4.5	XP_010777236.1
30	Nebulin-like isoform X4	neb	2.23E-01	54.2	23.8	9.2	12.7	XP_010772593.1
31	Myosin-binding protein C slow-type isoform X1 to X17	mybpc3	1.31E-01	45.6	26.9	12.6	14.9	XP_010774870.1
32	Collagen alpha-2(I) chain isoform X1	col1a2	2.91E-01	54.6	20.8	9.6	14.9	XP_010772950.1

The functional enrichment analysis (FDR <$2.5*10^{-4}$) for white muscle downregulated proteins in icefish identified multiple pathways, including translational silencing proteins and signal-recognition particle SRP-dependent co-translational protein targeting, the latter being involved in binding to the endoplasmic reticulum (ER) (**Figure. 5 B**).

Based on fishENRICHR analysis, the most used GO Terms for different biological processes were, GO:0019674 NAD metabolic process, GO:0060956 endocardial cell differentiation, GO:0020027 haemoglobin metabolic process, GO:1903512 endoplasmic reticulum to cytosol transport (**Figure. 3-5 C 4**). AGE-RAGE signalling pathway metabolism, glyoxylate, and dicarboxylate metabolism, amino acid metabolism, ECM-receptor interaction, and focal adhesion were identified by KEGG pathway analysis (See **Figure. 3-5 C 3**).

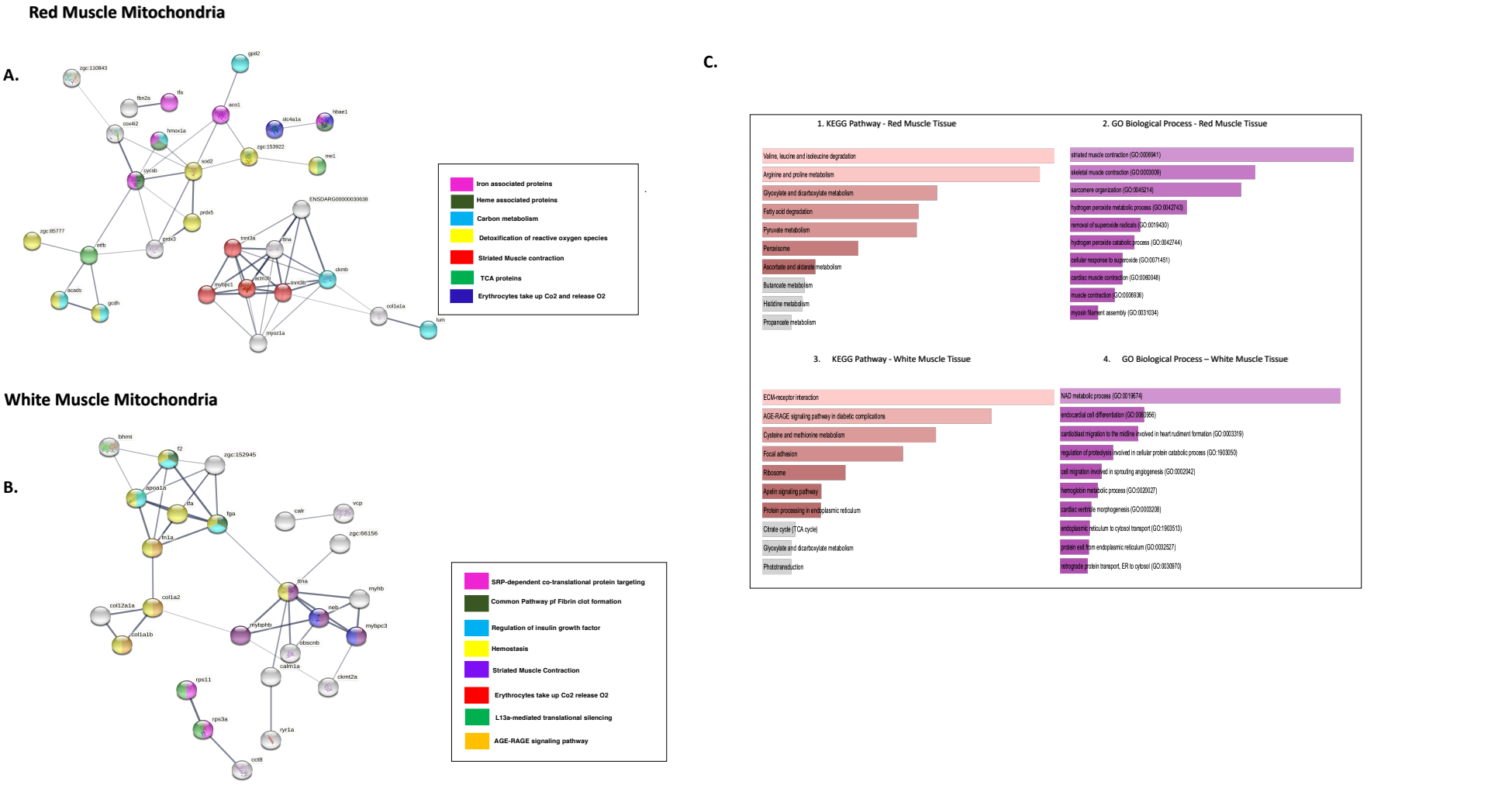

Figure 3-5. Network analysis of proteins lower expressed in icefish in comparison to closely related red-blooded species. A) RMM DEPs, number of nodes 48 with 53 edges, the average node degree is 2.52 and B) WMM, number of nodes 32 with 45 edges, the average node degree is 2.5. Network

analysed using STRINGdb. The network highlights proteins involved in different pathways curated by string from Reactome database. The nodes are coloured according to the pathways determined with Reactome Pathway Database. The edge shows type of interactions, experimentally determined interactions database derived, predicted interactions such as gene neighbourhood, gene co-occurrence, gene fusions respectively, co-expression interactions, text-mining interactions and homology, thicker the edge higher the confidence obtained the mentioned sources. C. Using FishEnrichr analyser KEGG Pathway and GO terms for biological process showed proteins involved in different pathways

3.5 Discussion

The paper presents the comparative analysis of the mitochondrial proteomes of white (WMM) and red muscle (RMM) of the icefish species that do not express haemoglobin protein to the closely related red-blooded species. We wanted to understand how the mitochondrial proteome has adapted to the loss of this protein. The differentially expressed proteins are identified using LC/LC-MS technique. The networks build using STRING database provided unbiased identification of network hubs as it builds all the networks entirely on external information. Network enrichment analysis provided several KEGG pathways that were linked to protein machinery, amino acid metabolism, energy production, and fatty acid metabolism.

Proteins involved in energy metabolism

The RMM and WMM tissues had a few proteins following a similar trend in their protein abundance in the icefish, The proteins involved in the ribosomal machinery, and cellular hypoxia were found to be commonly increased in the icefish (RMM: ATP5O, ATP5D ATP5B1, ATP5G; WMM: PSMD12, PSMA8). In cluster 1 of the red muscle tissue apart from involvement in hypoxia, some were also involved in the ETC, oxidative phosphorylation, and the TCA cycle (**Figure 3-3A**; increased abundance in icefish). ATP synthase subunit O (ATP5O), stress 70 protein (HSPA9), and malate dehydrogenase (MDH1AA) were found to be highly connected to the other nodes, and changes in any highly connected network proteins are likely to be lethal for an organism [43–45]. ATP5O is a component of the multi-subunit enzyme ATP synthase (complex V of the electron transport chain), which is located in the stalk that connects catalytic core (F_1) to membrane proton channel (F_O) [46]. The protein is known to influence the proton conductance by conformational changes [47]. ATP5O has also been found to interact directly with sirtuin 3 (SIRT3) that is significantly involved in energy production and stress responses [48]. ATP5O may contribute to the age-associated decline in association with SIRT3, mitochondria dysfunction, and diseases linked to mitochondrial homeostasis under hypoxia [48,49]. Another component of complex V, ATP synthase subunit gamma (ATPγ), which is also a part of the central stalk, was comparably high in the icefish cohort. ATPγ helps in the binding change mechanism by helping in the rotation of the β subunit. The icefish has been previously reported to show an increased coupling of proton transport and ATP synthase compared with the red-blooded notothenioids [50] and this could be correlated to the increase in the specific subunits of complex V that are directly involved in proton translocation . Previously, we have shown the ATP synthase subunit 6 of complex V to be sequentially and structurally different in the icefish *C. gunnari* when compared to its red-blooded related species [51].

One of the proteins densely connected in RMM (a hub node) in cluster 1 also involved in the TCA, was dihydrolipoyllysine-residue acetyltransferase component (DLAT). The increase in the abundance of this protein subunit in the icefish, component of pyruvate dehydrogenase complex (PDH), involved in the breakdown of pyruvate to acetyl-CoA that requires NAD^+ converting it to NADH, could be a response to moderate the pyruvate levels. This could be to prevent pyruvate being converted into acetyl-CoA for TCA and instead be used to meet the muscle energetic demands via anaerobic respiration [52,53]. The skeletal muscle is known to have metabolic flexibility in

meeting the energy demands of the tissue to respond and adapt to environmental changes [52,54]. The hearts and skeletal muscle of icefish have been suggested to have a dual oxidative-anaerobic metabolism to maintain the ATP levels [55–59]. An increase in the metabolites of fatty acid metabolism in the icefish have also been suggested previously [59]. This further could suggest that increase in DLAT is to maintain pyruvate levels, which could be converted to oxaloacetate for fatty acid cholesterol biosynthesis via glycolytic pathway [52]. PDH has been seen to be involved in metabolic rate depression in vertebrates which is a common element of anaerobiosis [60]. The regeneration of NAD^+ either happens aerobically via OxPhos or anaerobically by fermentation wherein lactate dehydrogenase (LDH) converts pyruvate to lactate. LDH enzyme has previously been reported to be highly increased in the icefish myocardium, which indicates involvement of anaerobic energetics in the icefish heart muscle [61]. LDH is regulated by the relative concentrations of its substrates, an increase in pyruvate could inhibit the enzyme [62–64].

Muscle-contraction proteins

A common decrease in the expression in the icefish for the proteins associated with biological processes, striated muscle contraction (RMM: MYBPC1, MYBPHA, NEB, TNA3, TTN3A, TNNT3A; WMM: MYBPC1, MYHB, MYBPC2A, MYBPC2B, MYBPC3, TTNA), creatine metabolism (RMM: CKMT2A, CKMB; WMM: CKMT2A), amino acid/protein metabolism (RMM: GCDH, OGDHA, BCKDHA, PSME2, CKMT2A; WMM: CCT8, VCP, TFA, RPS11, RPS3A) was observed in both RMM and WMM. Creatine kinase (CK) which has previously been shown by western blot to be absent in the hearts of the icefish did not appear in our protein lists from skeletal muscle mitochondria [65]. The mitochondria are enlarged in the oxidative muscle of icefish which decreases the distance for the diffusion of oxygen and for ATP between mitochondria and myofibrils which might reduce the demand for CK [29]. Mitochondrial CK helps maintain flux through the respiratory chain by maintaining low levels of ATP levels [66]. This is coherent with our observation of an increase in the abundance of proteins of complex V. Notothenioids lacking mtCK may compensate by increasing levels of ADP/ATP nucleotide translocases and voltage dependent anion-selective channel proteins (VDACs), as observed in our proteomics study as well, where VDAC3 is selectively seen higher. The lower levels or absence of this enzyme has previously been also reported to be an example of ‘paedomorphic trait’, a juvenile trait that persists into adulthood. This trait observed as a result of delayed development that has been seen as a common feature in the icefish, whether this is energetically efficient or not is still debatable [65,67].

A common muscle protein that was found to be downregulated both in RMM and WMM tissues, is myosin binding protein C isoforms (MYBPC) which encodes myosin binding protein C. MYBPC a thick filament associated protein that has both structural and regulatory roles in sarcomere assembly [68]. The protein was seen to decrease four folds in the icefish *C. gunnari* when compared to the red-blooded species, but the amount was comparable in in the icefish *C. rastrospinosus*. MYBPC mutations have been shown to increase the energetic cost of contraction in the muscle, and usually are found to act by reducing the protein content [69–71]. The downregulation of this protein in the icefish is in contrast to the study that has shown significant upregulation of MYBPC in colder temperatures, which is coherent to the observation of the amount

of this protein seen in their closely related red-blooded species [72]. Previously, mutations in MYBPC are seen to be involved in increased cardiac oxidative stress in the mouse model [73]. The other sarcomere protein that was seen significantly less in abundance in icefish was**,** myosin heavy chain b (MYBPH), the activity of this protein has been used as a model to explain the mechanism underlying that accompanies alterations in skeletal muscle contraction [74]. The ATPase reaction of a muscle fibre is determined by its myosin heavy chain composition, which might be altered with ageing seen previously in human skeletal muscle [75]. An impaired sarcomere energetics such as mutations in muscle contractions protein, can cause mitochondrial dysfunction due to Ca^{2+} imbalance or ROS accumulation impairing the oxidative phosphorylation capacity [76].The other proteins that were connected to MYBPH were titin, nebulin and CK. Titin, nebulin, and CK proteins have previously been seen to be downregulated under long term exposure to hypoxia in the zebrafish model [77]. **Chaperonin proteins, T-complex protein 1** encoded by CCT8 is known for its role in folding of cytoskeleton proteins upon ATP hydrolysis and changes in the protein can cause defects in the functioning of cytoskeleton and mitosis arrest. A study with *C. elegans* showed CCT8 as a candidate to sustain proteostasis during organismal ageing [78]. The decrease in the level of the protein is observed in human brain ageing and neurodegenerative diseases [79].

Redox

The proteins, GCDH- glutaryl-CoA dehydrogenase and Aldh7a1- Alpha aminoadipic semialdehyde dehydrogenase were remarkedly seen lower in the icefish *C. gunnari* specifically in WMM tissue. GCDH is a mitochondrial enzyme necessary for the metabolism of lysine/tryptophan and hydroxylysine. The absence of this enzyme is known to result in mitochondrial dysfunction. ALDH7A1 is an enzyme that metabolises betaine aldehyde to betaine, which is an important cellular osmolyte and methyl donor that helps in protecting the cell from oxidative stress. The enzyme is seen to be involved in lysine catabolism helps in maintaining the cellular nitrogen pool [80]. The changes in expression of these proteins might indicate the red-muscle tissue of *N. rossii* and *T. bernacchii* and even *C. rastrospinosus* (that has the expression mb) has enhanced defences against oxidative stress, which is coherent to the previous observation made in the cardiac mitochondrial protein expression data [81]. In WMM, we see that transmembrane protease serine 2-like is very reduced and perhaps missing in icefish. This protein has not been investigated very much to date and has not been reported as absent in these fish previously, the higher levels of it in the red-blooded fish suggest this difference may be of biological relevance.

Haem-associated proteins

Consistent with all the studies on the icefish, haemoglobin alpha and beta were solely identified in the red-blooded species. We also show that Hemopexin (Hx) protein is reduced in the WMM of icefish. It was previously shown that Hx transcription occurs at levels comparable to those in the red-blooded notothenioids, however, it seems possible that there is a discrepancy between transcript and protein levels of Hx [82]. Cytochrome c oxidase (CO) is an important haem-containing protein just like haemoglobin and in our study was also found to be much reduced in icefish RMM. As

this protein performs a multitude of functions, including cell apoptosis and energy metabolism, it remains to be seen what this reduced level means for the physiology of this tissue [83,84]. The oxygen-carrying capacity of their blood is only 10 % compared to that of red-blooded species. Cytochrome c oxidase is at first the terminal electron carrier of the respiratory chain, so lower protein expression may indicate a modification in redox metabolism in the icefish. Previously, it has also been shown that maximal capacities of CO and another mitochondrial enzyme citrate synthase activities to be higher in the red-blooded fish species in comparison to the icefish [85]. Transferrin was another protein that was found to be significantly reduced (5-fold) in the WMM of the icefish *C. gunnari*.

Ribosome Machinery in WMM

Overall, a striking finding in the samples we interrogated is the numbers of 26S, 40S and 60S ribosome proteins that are differentially (mostly) upregulated in icefish. There have been extensive studies on close interaction between mitochondria and the endoplasmic reticulum [86]. FXR2P, a ribosomal binding protein, was also measured at much higher levels in icefish muscle, it would be interesting to probe the connections between ribosome and mitochondrial biology in these organisms. FXR2P protein has not been found to be present in mammalian muscle and therefore its role in icefish muscle remains to be elucidated [87].

With this study, we have established biological pathways and proteins that can be used to understand the unique ‘haemoglobin-free’ biology of the icefish. We analysed samples directly taken from the field in the late summer season, ensuring that the pressures of a captive environment are not a factor. We show that muscle mitochondrial proteomes are distinct between the fish with different quantities of haemoglobin. We expect our contribution now directs researchers in this field to focus on the identified proteins and pathways that allow these remarkable and unique fish to survive and thrive in Antarctic waters.

ACKNOWLEDGEMENT

The authors would like to thank Nils Koschnick (Alfred Wegener Institute Helmholtz Centre for Polar and Marine Research, AWI, Bremerhaven, Germany) and the ship crew for their help in collecting samples onboard the R/V Polarstern. We need to add the funding at a later stage.

CONFLICTS OF INTEREST

The authors declare that they have no conflict of interest.

FUNDING

Gunjan Katyal was supported by Vice Chancellor's International Scholarship for Research Excellence, University of Nottingham (2018-2021). Brad Ebanks was supported by the Biotechnology and Biological Sciences Research Council [grant number BB/J014508/1]. This collaboration was made possible by a University of Nottingham International Research Collaboration Fund award.

Author Contributions

Conceptualization: Gunjan Katyal, Magnus Lucassen, Chiara Papetti, Lisa Chakrabarti.

Data curation: Gunjan Katyal, Brad Ebanks.

Formal analysis: Gunjan Katyal.

Funding acquisition: Lisa Chakrabarti.

Investigation: Gunjan Katyal.

Methodology: Gunjan Katyal, Lisa Chakrabarti.

Resources: Magnus Lucassen, Chiara Papetti.

Supervision: Lisa Chakrabarti.

Writing – original draft: Gunjan Katyal, Lisa Chakrabarti.

Writing – review & editing: Gunjan Katyal, Brad Ebanks, Magnus Lucassen, Chiara Papetti, Lisa Chakrabarti.

3.6 References:

1. Murphy MP. How mitochondria produce reactive oxygen species. Biochem J. 2009;417: 1–13. doi:10.1042/BJ20081386
2. Giorgi C, Agnoletto C, Bononi A, Bonora M, de Marchi E, Marchi S, et al. Mitochondrial calcium homeostasis as potential target for mitochondrial medicine. Mitochondrion. 2012;12: 77–85. doi:10.1016/j.mito.2011.07.004
3. Tait, S.W., and Green DR. Mitochondrial regulation of cell death. Cold Spring Harb. Perspect. Cold Spring Harb Perspect Biol. 2013; a008706. doi:10.1016/j.yapd.2006.04.010
4. Chu Q, Martinez TF, Novak SW, Donaldson CJ, Tan D, Vaughan JM, et al. Regulation of the ER stress response by a mitochondrial microprotein. Nat Commun. 2019;10: 1–13. doi:10.1038/s41467-019-12816-z
5. Azuma K, Ikeda K, Inoue S. Functional mechanisms of mitochondrial respiratory chain supercomplex assembly factors and their involvement in muscle quality. Int J Mol Sci. 2020;21: 1–17. doi:10.3390/ijms21093182
6. Guo R, Gu J, Zong S, Wu M, Yang M. Structure and mechanism of mitochondrial electron transport chain. Biomed J. 2018;41: 9–20. doi:10.1016/j.bj.2017.12.001
7. Perutz M, Rossmann M, Cullis AF, Muirhead H, Will G, North ACT. Structure of hoemoglobin. Nature. 1960;185: 416–422.
8. Heinemann IU, Jahn M, Jahn D. The biochemistry of heme biosynthesis. Arch Biochem Biophys. 2008;474: 238–251. doi:10.1016/j.abb.2008.02.015
9. Lechauve C, Butcher JT, Freiwan A, Biwer LA, Keith JM, Good ME, et al. Endothelial cell α-globin and its molecular chaperone α-hemoglobin-stabilizing protein regulate arteriolar contractility. J Clin Invest. 2018;128: 5073–5082. doi:10.1172/JCI99933
10. Brown N, Alkhayer K, Clements R, Singhal N, Gregory R, Azzam S, et al. Neuronal Hemoglobin Expression and Its Relevance to Multiple Sclerosis Neuropathology. J Mol Neurosci. 2016;59: 1–17. doi:10.1007/s12031-015-0711-6
11. Shephard F, Greville-Heygate O, Marsh O, Anderson S, Chakrabarti L. A mitochondrial location for haemoglobins—Dynamic distribution in ageing and Parkinson's disease. Mitochondrion. 2014;14: 64–72. doi:10.1016/J.MITO.2013.12.001
12. Corliss BA, Delalio LJ, Stevenson Keller TC, Keller AS, Keller DA, Corliss BH, et al. Vascular Expression of Hemoglobin Alpha in Antarctic Icefish Supports Iron Limitation as Novel Evolutionary Driver. Front Physiol. 2019;10. doi:10.3389/fphys.2019.01389
13. Straub AC, Butcher JT, Billaud M, Mutchler SM, Artamonov M V., Nguyen AT, et al. Hemoglobin α/eNOS coupling at myoendothelial junctions is required for nitric oxide scavenging during vasoconstriction. Arterioscler Thromb Vasc Biol. 2014;34: 2594–2600. doi:10.1161/ATVBAHA.114.303974
14. Chuang JY, Lee CW, Shih YH, Yang T, Yu L, Kuo YM. Interactions between amyloid-β and hemoglobin: Implications for amyloid plaque formation in alzheimer's disease. PLoS One. 2012;7. doi:10.1371/journal.pone.0033120
15. Shephard F, Greville-Heygate O, Liddell S, Emes R, Chakrabarti L. Analysis of Mitochondrial haemoglobin in Parkinson's disease brain. Mitochondrion. 2016;29: 45–52. doi:10.1016/j.mito.2016.05.001
16. Archer SD, Johnston IA. Density of Cristae and Distribution of Mitochondria in the Slow Muscle Fibers of Antarctic Fish. Physiol Zool. 1991;64: 242–258. doi:10.1086/physzool.64.1.30158522

17. Duhamel G, Hulley PA, Causse R, Koubbi P, Vacchi M, Pruvost P, et al. Chapter 7. Biogeographic Patterns of Fish. Biogeographic Atlas of the Southern Ocean. 2014.
18. Johan T. Ruud. Vertebrates without Erythrocytes and Blood Pigment. Nature. 1954;173: 848–850.
19. Kim BM, Amores A, Kang S, Ahn DH, Kim JH, Kim IC, et al. Antarctic blackfin icefish genome reveals adaptations to extreme environments. Nat Ecol Evol. 2019;3: 469–478. doi:10.1038/s41559-019-0812-7
20. Beers JM, Jayasundara N. Antarctic notothenioid fish: what are the future consequences of "losses" and "gains" acquired during long-term evolution at cold and stable temperatures? J Exp Biol. 2015;218: 1834–45. doi:10.1242/jeb.116129
21. Di Prisco G, Cocca E, Parker SK, Detrich HW. Tracking the evolutionary loss of hemoglobin expression by the white-blooded Antarctic icefishes. Gene. 2002;295: 185–191. doi:10.1016/S0378-1119(02)00691-1
22. Near TJ, Parker SK, Detrich HW. A genomic fossil reveals key steps in hemoglobin loss by the Antarctic icefishes. Mol Biol Evol. 2006;23: 2008–2016. doi:10.1093/molbev/msl071
23. Scudiero R, Trinchella F, Riggio M, Parisi E. Structure and expression of genes involved in transport and storage of iron in red-blooded and hemoglobin-less antarctic notothenioids. Gene. 2007. doi:10.1016/j.gene.2007.03.003
24. Borley KA, Sidell BD. Evolution of the myoglobin gene in Antarctic Icefishes (Channichthyidae). Polar Biol. 2011;34: 659–665. doi:10.1007/s00300-010-0921-x
25. Wujcik JM, Wang G, Eastman JT, Sidell BD. Morphometry of retinal vasculature in Antarctic fishes is dependent upon the level of hemoglobin in circulation. J Exp Biol. 2007;210: 815–824. doi:10.1242/jeb.001867
26. O'Brien KM, Mueller IA, Orczewska JI, Dullen KR, Ortego M. Hearts of some Antarctic fishes lack mitochondrial creatine kinase. Comp Biochem Physiol -Part A Mol Integr Physiol. 2014;178: 30–36. doi:10.1016/j.cbpa.2014.08.003
27. Sidell BD, O'Brien KM. When bad things happen to good fish: The loss of hemoglobin and myoglobin expression in Antarctic icefishes. J Exp Biol. 2006;209: 1791–1802. doi:10.1242/jeb.02091
28. Sidell BD. Intracellular oxygen diffusion: the roles of myoglobin and lipid at cold body temperature. J Exp Biol. 1998;201: 1119–1128.
29. O'Brien KM, Mueller IA. The unique mitochondrial form and function of antarctic channichthyid icefishes. Integr Comp Biol. 2010;50: 993–1008. doi:10.1093/icb/icq038
30. Lu H, Zhou Q, He J, Jiang Z, Peng C, Tong R, et al. Recent advances in the development of protein–protein interactions modulators: mechanisms and clinical trials. Signal Transduct Target Ther. 2020;5. doi:10.1038/s41392-020-00315-3
31. Rachlin J, Cohen DD, Cantor C, Kasif S. Biological context networks: A mosaic view of the interactome. Mol Syst Biol. 2006;2: 1–12. doi:10.1038/msb4100103
32. Marín M, Esteban FJ, Ramírez-Rodrigo H, Ros E, Sáez-Lara MJ. An integrative methodology based on protein-protein interaction networks for identification and functional annotation of disease-relevant genes applied to channelopathies. BMC Bioinformatics. 2019;20: 1–13. doi:10.1186/s12859-019-3162-1
33. Baldwin KM, Winder WW, Terjung RL, Holloszy JO. Glycolytic enzymes in different types of skeletal muscle: adaptation to exercise. Am J Physiol Content. 1973;225: 962–966. doi:10.1152/ajplegacy.1973.225.4.962
34. Huang YC, Dennis RG, Baar K. Cultured slow vs. fast skeletal muscle cells differ in

physiology and responsiveness to stimulation. Am J Physiol - Cell Physiol. 2006;291: 11–17. doi:10.1152/ajpcell.00366.2005
35. Pruitt KD, Hogue CW, Groll M, Hartmann C, Huber R, Fields S. Mcode. Nucleic Acids Res. 2001;29: 137–140. Available: https://academic.oup.com/nar/article-lookup/doi/10.1093/nar/29.1.137
36. Franz M, Rodriguez H, Lopes C, Zuberi K, Montojo J, Bader GD, et al. GeneMANIA update 2018. Nucleic Acids Res. 2018;46: W60–W64. doi:10.1093/nar/gky311
37. Chen EY, Tan CM, Kou Y, Duan Q, Wang Z, Meirelles G V., et al. Enrichr: Interactive and collaborative HTML5 gene list enrichment analysis tool. BMC Bioinformatics. 2013;14. doi:10.1186/1471-2105-14-128
38. Kuleshov M V., Jones MR, Rouillard AD, Fernandez NF, Duan Q, Wang Z, et al. Enrichr: a comprehensive gene set enrichment analysis web server 2016 update. Nucleic Acids Res. 2016;44: W90–W97. doi:10.1093/nar/gkw377
39. Glancy B, Balaban RS. Protein composition and function of red and white skeletal muscle mitochondria. Am J Physiol Cell Physiol. 2011;300: C1280-90. doi:10.1152/ajpcell.00496.2010
40. Szklarczyk D, Gable AL, Lyon D, Junge A, Wyder S, Huerta-Cepas J, et al. STRING v11: Protein-protein association networks with increased coverage, supporting functional discovery in genome-wide experimental datasets. Nucleic Acids Res. 2019;47: D607–D613. doi:10.1093/nar/gky1131
41. Doncheva NT, Assenov Y, Domingues FS, Albrecht M. Topological analysis and interactive visualization of biological networks and protein structures. Nat Protoc. 2012;7: 670–685. doi:10.1038/nprot.2012.004
42. Magnoni LJ, Crespo D, Ibarz A, Blasco J, Fernández-Borràs J, Planas J V. Effects of sustained swimming on the red and white muscle transcriptome of rainbow trout (Oncorhynchus mykiss) fed a carbohydrate-rich diet. Comp Biochem Physiol - A Mol Integr Physiol. 2013;166: 510–521. doi:10.1016/j.cbpa.2013.08.005
43. Raman K, Damaraju N, Joshi GK. The organisational structure of protein networks: Revisiting the centrality-lethality hypothesis. Syst Synth Biol. 2014;8: 73–81. doi:10.1007/s11693-013-9123-5
44. He X, Zhang J. Why do hubs tend to be essential in protein networks? PLoS Genet. 2006;2: 0826–0834. doi:10.1371/journal.pgen.0020088
45. Zotenko E, Mestre J, O'Leary DP, Przytycka TM. Why do hubs in the yeast protein interaction network tend to be essential: Reexamining the connection between the network topology and essentiality. PLoS Comput Biol. 2008;4. doi:10.1371/journal.pcbi.1000140
46. Devenish RJ, Prescott M, Boyle GM, Nagley P. The oligomycin axis of mitochondrial ATP synthase: OSCP and the proton channel. J Bioenerg Biomembr. 2000;32: 507–515. doi:10.1023/A:1005621125812
47. Devenish RJ, Prescott M, Boyle GM, Nagley P. The oligomycin axis of mitochondrial ATP synthase: OSCP and the proton channel. J Bioenerg Biomembr. 2000;32: 507–515. doi:10.1023/a:1005621125812
48. Yang W, Nagasawa K, Münch C, Xu Y, Satterstrom K, Jeong S, et al. Mitochondrial Sirtuin Network Reveals Dynamic SIRT3-Dependent Deacetylation in Response to Membrane Depolarization. Cell. 2016;167: 985-1000.e21. doi:10.1016/j.cell.2016.10.016
49. Okada H, Goldhaber JI, Ross RS, Okada H, Lai NC, Kawaraguchi Y, et al. Integrins protect cardiomyocytes from ischemia / reperfusion injury Find the latest version : Integrins

protect cardiomyocytes from ischemia / reperfusion injury. 2013;123: 4294–4308. doi:10.1172/JCI64216.4294
50. Mueller IA, Grim JM, Beers JM, Crockett EL, O'Brien KM. Inter-relationship between mitochondrial function and susceptibility to oxidative stress in red-And white-blooded Antarctic notothenioid fishes. J Exp Biol. 2011;214: 3732–3741. doi:10.1242/jeb.062042
51. Katyal G, Ebanks B, Lucassen M, Papetti C. Sequence and structure comparison of ATP synthase F0 subunits 6 and 8 in notothenioid fish. 2021.
52. Zhang S, Hulver MW, McMillan RP, Cline MA, Gilbert ER. The pivotal role of pyruvate dehydrogenase kinases in metabolic flexibility. Nutr Metab. 2014;11: 1–9. doi:10.1186/1743-7075-11-10
53. Biomedical P. Pyruvate kinase f r o m oplophorus g r a c i l i r o s t r i s muscle. 1976;55: 475–478.
54. Goodpaster BH, Sparks LM. Metabolic Flexibility in Health and Disease. Cell Metab. 2017;25: 1027–1036. doi:10.1016/j.cmet.2017.04.015
55. Feller G, Goessens G, Gerday C, Bassleer R. Heart structure and ventricular ultrastructure of hemoglobin- and myoglobin-free icefish Channichthys rhinoceratus. Cell Tissue Res. 1985;242: 669–676. doi:10.1007/BF00225436
56. Feller G, Gerday C. Metabolic pattern of the heart of haemoglobin- and myoglobin-free Antarctic fish Channichthys rhinoceratus. Polar Biol. 1987;7: 225–229. doi:10.1007/BF00287418
57. Feller G, Pauly J-P, Smal A, O'Carra P, Gerday C. The lactate dehydrogenase of the icefish heart: biochemical adaptations to hypoxia tolerance. Biochim Biophys Acta - Protein Struct Mol Enzymol. 1991;1079: 343–347. doi:https://doi.org/10.1016/0167-4838(91)90079-F
58. citations-20220104T191622.
59. Feller G, Gerday C. Adaptations of the hemoglobinless Antarctic icefish (Channichthyidae) to hypoxia tolerance. Comp Biochem Physiol - A Physiol. 1997;118: 981–987. doi:10.1016/S0300-9629(97)86786-2
60. Storey KB, Storey JM. Metabolic rate depression in animals: Transcriptional and translational controls. Biol Rev Camb Philos Soc. 2004;79: 207–233. doi:10.1017/S1464793103006195
61. Feller G, Gerday C. Metabolic pattern of the heart of haemoglobin- and myoglobin-free Antarctic fish Channichthys rhinoceratus. Polar Biol. 1987;7: 225–229. doi:10.1007/BF00287418
62. June FL. Volume 3, number 5 FEBS LETTERS June 1969. FEBS Lett. 2000;3: 3–7.
63. Arriaga DE. Inhibition of Lactate blakesleeanus: 1981;362: 357–362.
64. Hewitt CO, Eszes CM, Sessions RB, Moreton KM, Dafforn TR, Takei J, et al. A general method for relieving substrate inhibition in lactate dehydrogenases. Protein Eng. 1999;12: 491–496. doi:10.1093/protein/12.6.491
65. O'Brien KM, Mueller IA, Orczewska JI, Dullen KR, Ortego M. Hearts of some Antarctic fishes lack mitochondrial creatine kinase. Comp Biochem Physiol -Part A Mol Integr Physiol. 2014;178: 30–36. doi:10.1016/j.cbpa.2014.08.003
66. Wallimann T, Wyss M, Brdiczka D, Nicolay K, Eppenberger HM. Intracellular compartmentation, structure and function of creatine kinase isoenzymes in tissues with high and fluctuating energy demands: The "phosphocreatine circuit" for cellular energy homeostasis. Biochem J. 1992;281: 21–40. doi:10.1042/bj2810021

67. Albertson RC, Yan YL, Titus TA, Pisano E, Vacchi M, Yelick PC, et al. Molecular pedomorphism underlies craniofacial skeletal evolution in Antarctic notothenioid fishes. BMC Evol Biol. 2010;10. doi:10.1186/1471-2148-10-4
68. Kraker J, Viswanathan SK, Knöll R, Sadayappan S. Recent advances in the molecular genetics of familial hypertrophic cardiomyopathy in South Asian descendants. Front Physiol. 2016;7. doi:10.3389/fphys.2016.00499
69. Witjas-Paalberends ER, Güclü A, Germans T, Knaapen P, Harms HJ, Vermeer AMC, et al. Gene-specific increase in the energetic cost of contraction in hypertrophic cardiomyopathy caused by thick filament mutations. Cardiovasc Res. 2014;103: 248–257. doi:10.1093/cvr/cvu127
70. Barefield D, Kumar M, de Tombe PP, Sadayappan S. Contractile dysfunction in a mouse model expressing a heterozygous MYBPC3 mutation associated with hypertrophic cardiomyopathy. Am J Physiol - Hear Circ Physiol. 2014;306: 807–815. doi:10.1152/ajpheart.00913.2013
71. Van Dijk SJ, Dooijes D, Remedios C Dos, Michels M, Lamers JMJ, Winegrad S, et al. Cardiac myosin-binding protein C mutations and hypertrophic ardiomyopathy haploinsufficiency, deranged phosphorylation, and cardiomyocyte dysfunction. Circulation. 2009;119: 1473–1483. doi:10.1161/CIRCULATIONAHA.108.838672
72. Dimitriadi A, Beis D, Arvanitidis C, Adriaens D, Koumoundouros G. Developmental temperature has persistent, sexually dimorphic effects on zebrafish cardiac anatomy. Sci Rep. 2018;8: 1–10. doi:10.1038/s41598-018-25991-8
73. Lynch TL, Sivaguru M, Velayutham M, Cardounel AJ, Michels M, Barefield D, et al. Oxidative Stress in Dilated Cardiomyopathy Caused by MYBPC3 Mutation. Oxid Med Cell Longev. 2015;2015. doi:10.1155/2015/424751
74. Han YS, Proctor DN, Geiger PC, Sieck GC. Reserve capacity for ATP consumption during isometric contraction in human skeletal muscle fibers. J Appl Physiol. 2001;90: 657–664. doi:10.1152/jappl.2001.90.2.657
75. Klitgaard H, Zhou M, Schiaffino S, Betto R, Salviati G, Saltin B. Ageing alters the myosin heavy chain composition of single fibres from human skeletal muscle. Acta Physiol Scand. 1990;140: 55–62. doi:10.1111/j.1748-1716.1990.tb08975.x
76. Van Der Velden J, Tocchetti CG, Varricchi G, Bianco A, Sequeira V, Hilfiker-Kleiner D, et al. Metabolic changes in hypertrophic cardiomyopathies: Scientific update from the working group of myocardial function of the European Society of Cardiology. Cardiovasc Res. 2018;114: 1273–1280. doi:10.1093/cvr/cvy147
77. Marques IJ, Leito JTD, Spaink HP, Testerink J, Jaspers RT, Witte F, et al. Transcriptome analysis of the response to chronic constant hypoxia in zebrafish hearts. J Comp Physiol B Biochem Syst Environ Physiol. 2008;178: 77–92. doi:10.1007/s00360-007-0201-4
78. Noormohammadi A, Khodakarami A, Gutierrez-Garcia R, Lee HJ, Koyuncu S, Konig T, et al. Somatic increase of CCT8 mimics proteostasis of human pluripotent stem cells and extends C. elegans lifespan. Nat Commun. 2016;7. doi:10.1038/ncomms13649
79. Brehme M, Voisine C, Rolland T, Wachi S, Soper JH, Zhu Y, et al. A chaperome subnetwork safeguards proteostasis in aging and neurodegenerative disease. Cell Rep. 2014;9: 1135–1150. doi:10.1016/j.celrep.2014.09.042
80. Brocker C, Lassen N, Estey T, Pappa A, Cantore M, Orlova V V., et al. Aldehyde dehydrogenase 7A1 (ALDH7A1) is a novel enzyme involved in cellular defense against hyperosmotic stress. J Biol Chem. 2010;285: 18452–18463. doi:10.1074/jbc.M109.077925

81. O'Brien KM, Rix AS, Egginton S, Farrell AP, Crockett EL, Schlauch K, et al. Cardiac mitochondrial metabolism may contribute to differences in thermal tolerance of red- and white-blooded Antarctic notothenioid fishes. J Exp Biol. 2018;221: jeb177816. doi:10.1242/jeb.177816
82. Bilyk KT, Zhuang X, Murphy KR, Christina Cheng CH. A tale of two genes: Divergent evolutionary fate of haptoglobin and hemopexin in hemoglobinless Antarctic icefishes. J Exp Biol. 2019;222. doi:10.1242/jeb.188573
83. Cai J, Yang J, Jones DP. Mitochondrial control of apoptosis: The role of cytochrome c. Biochim Biophys Acta - Bioenerg. 1998;1366: 139–149. doi:10.1016/S0005-2728(98)00109-1
84. Santucci R, Sinibaldi F, Cozza P, Polticelli F, Fiorucci L. Cytochrome c: An extreme multifunctional protein with a key role in cell fate. International Journal of Biological Macromolecules. Elsevier B.V.; 2019. pp. 1237–1246. doi:10.1016/j.ijbiomac.2019.06.180
85. O'Brien KM, Skilbeck C, Sidell BD, Egginton S. Muscle fine structure may maintain the function of oxidative fibres in haemoglobinless Antarctic fishes. J Exp Biol. 2003;206: 411–421. doi:10.1242/jeb.00088
86. Marchi S, Patergnani S, Pinton P. The endoplasmic reticulum-mitochondria connection: One touch, multiple functions. Biochim Biophys Acta - Bioenerg. 2014;1837: 461–469. doi:10.1016/j.bbabio.2013.10.015
87. Bakker CE, De Diego Otero Y, Bontekoe C, Raghoe P, Luteijn T, Hoogeveen AT, et al. Immunocytochemical and biochemical characterization of FMRP, FXR1P, and FXR2P in the mouse. Exp Cell Res. 2000;258: 162–170. doi:10.1006/excr.2000.4932

3.7 APENDIX B: Chapter 3

Results:

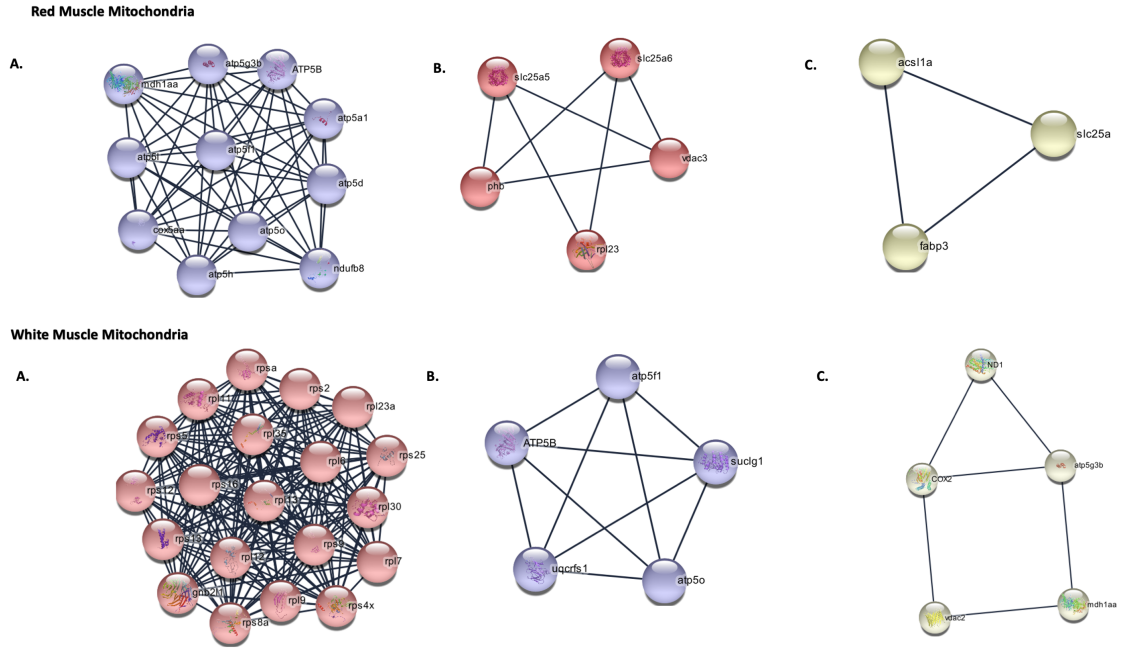

Supplementary Figure 3-6. Top modules obtained from the PPI network using Cytoscape's plugin MCODE for Red muscle tissue network (C) and white muscle tissue network (D) for upregulated proteins in the icefish in comparison to red-blooded species. There are common modules seen in both RMM and WMM for complex V subunits.

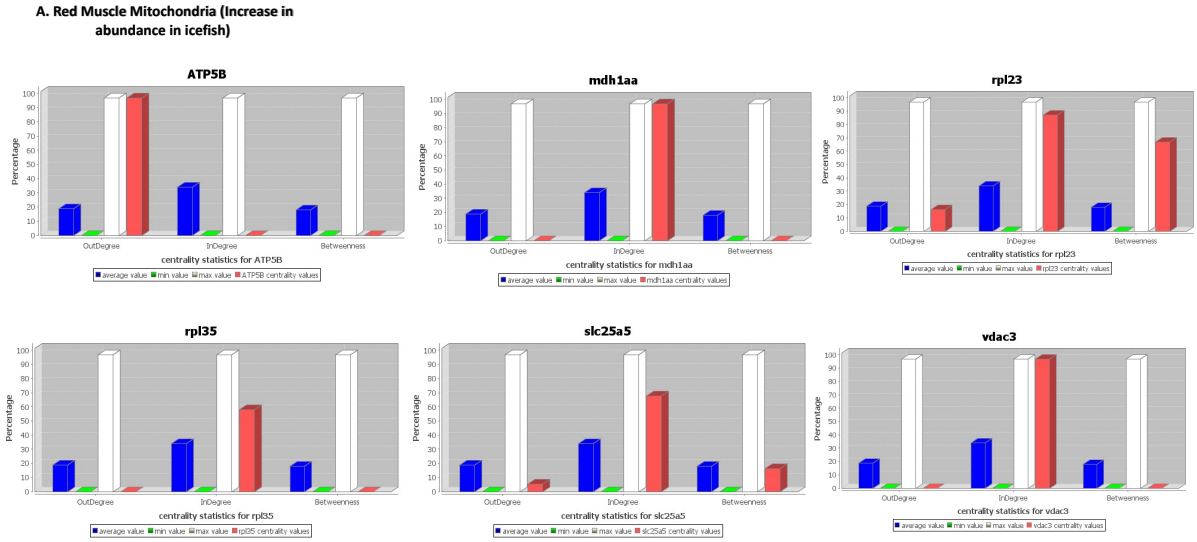

Supplementary Figure 3-7. Highly connected protein nodes for RMM PPI using CentiScaPe, Cytoscape plugin. ATP5B had the highest percentage of OutDegree whereas MDH1AA has the highest percentage of indegree with VDAC3, RPL23 and SLC25A5 following the trend.

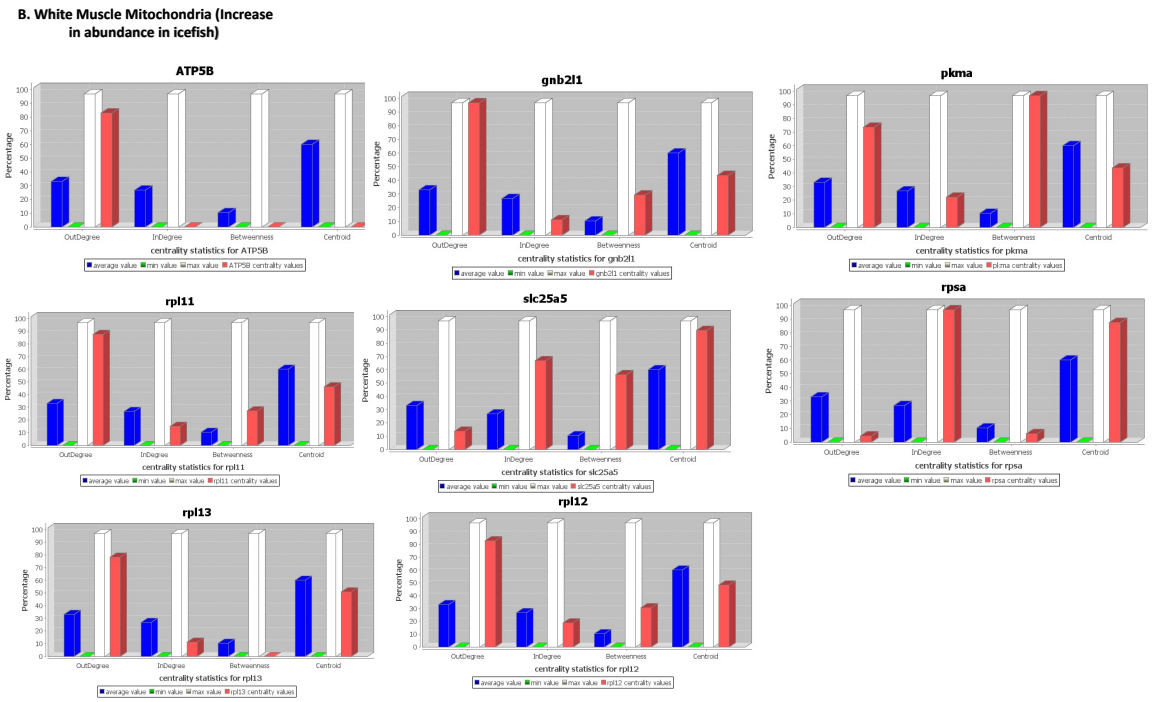

Supplementary Figure 3-8. Highly connected protein nodes for WMM PPI. Protein GNB2L1 followed by ATP5B (also seen in RMM), RP11 and PKMA have the highest percentage of outdegree. Proteins RPSA, followed by ribosomal proteins RP13 and RP12 and SLC25A5 have the highest percentage of inDegree.

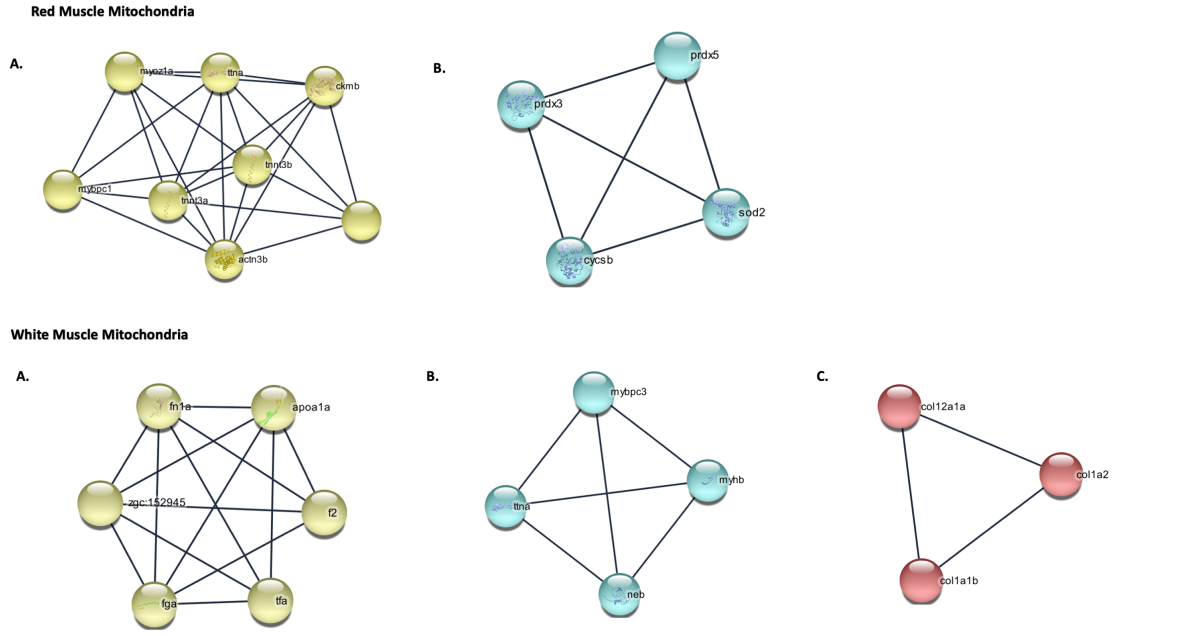

Supplementary Figure 3-9. Top modules obtained from the PPI network using Cytoscape's plugin MCODE for Red muscle tissue network (C) and white muscle tissue network (D) for upregulated proteins in the icefish in comparison to red-blooded species. Genes with the highest degree of connectivity obtained from the PPI network with Cytoscape.

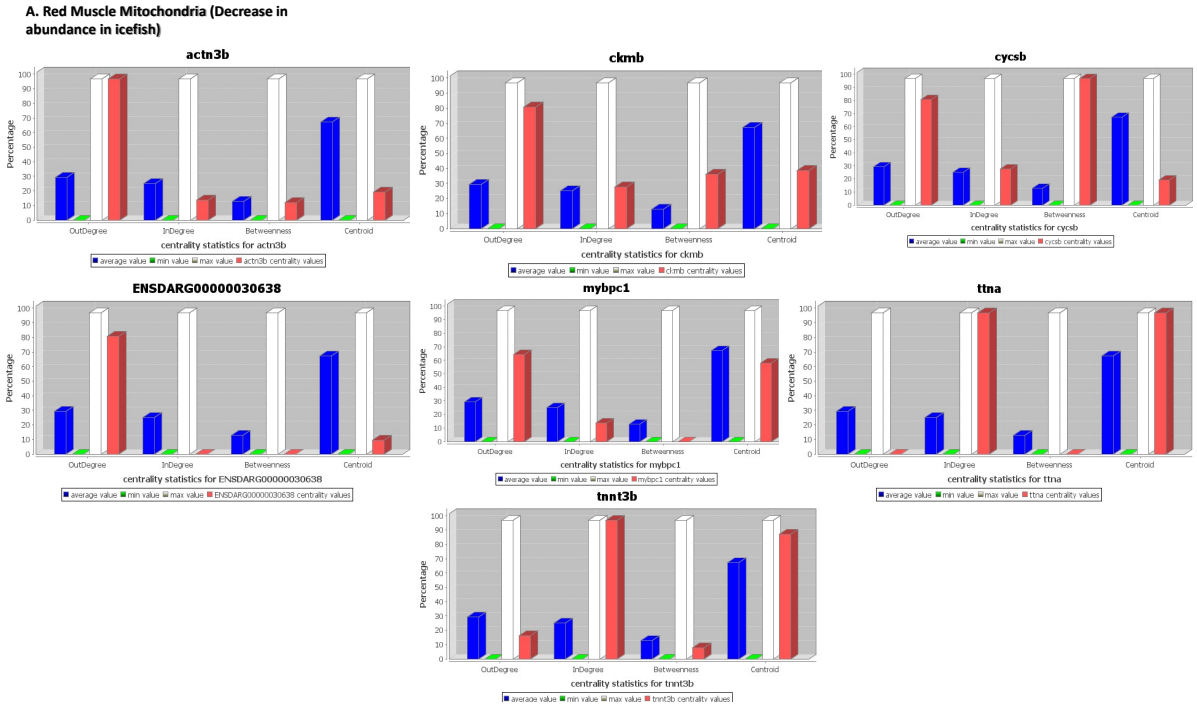

Supplementary Figure 3-10. Highly connected protein nodes for RMM PPI. Proteins ACTN3B, followed by CKMB, CYSB and MYBPC1 have high percentage of OutDegree. Proteins TTNA and TNNT3B have the highest percentage of InDegree.

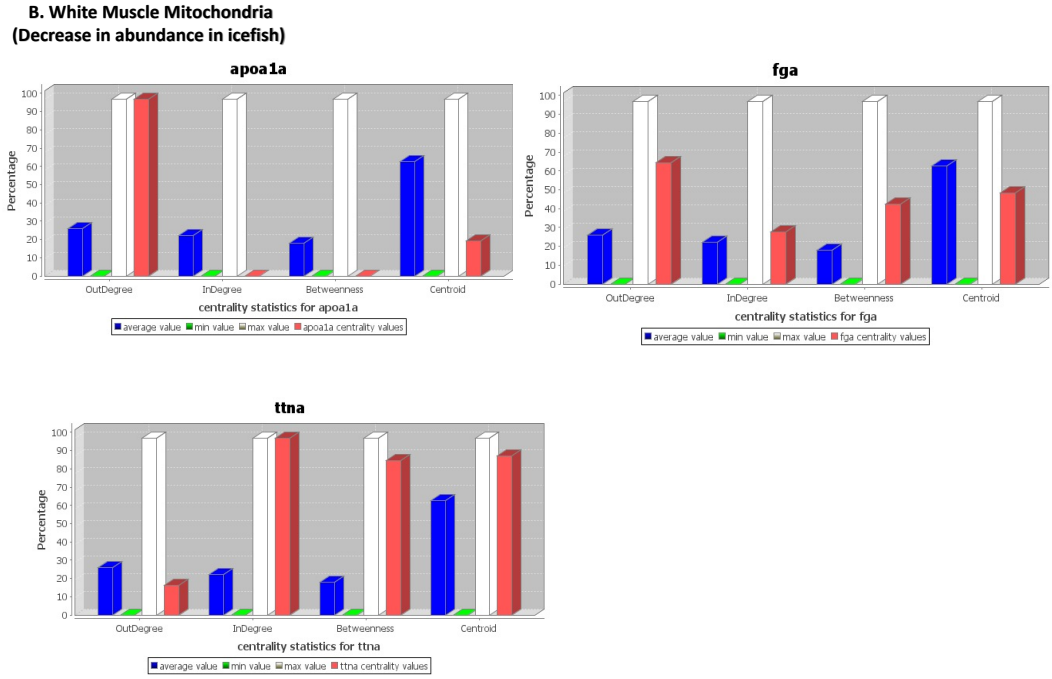

Supplementary Figure 3-11. Highly connected protein nodes for WMM PPI. Protein APOA1A followed by FGA have the highest percentage of outdegree. Protein TTNA has the highest percentage of inDegree.

Proteomics protein trend across species.

3.7.1 Red Muscle Mitochondria

Supplementary Table 1. Proteins higher in abundance in *N. rossii*

Accession Id's	Protein Name	Relative percentage of Total Ion Area
CAC27776.1	Myosin heavy chain	33.8
XP_010777618.1	myosin heavy chain fast skeletal	66.6
AAO21697.1	alpha actin	47.9
XP_010792310.1	actin cytoplasmic 3	32.4
XP_010784415.1	alpha-actinin-3	39.5
XP_010794573.1	desmin	71.8
AAO24741.1	creatine kinase mitochondrial isoform	41.7
XP_010776201.1	titin	60.2
XP_010791686.1	alpha-actinin-2	48.2
XP_010777287.1	tropomyosin alpha-1 chain	37.3
XP_010792180.1	apolipoprotein A-I	30.9

XP_010794773.1	myomesin-2	38.0
AAC25100.1	alpha globin	60.0
AAC59671.1	alpha-1 globin	60.0
XP_010781418.1	isocitrate dehydrogenase [NADP]	32.6
XP_010784569.1	Cytochrome b-c1 complex subunit 2	64.7
XP_010767505.1	myosin regulatory light chain 2	41.6
XP_010771394.1	tropomyosin alpha-3 chain	36.9
XP_010778108.1	perilipin-3	48.8
XP_010774927.1	histone H2AX	30.8
XP_010774355.1	myomesin-1	32.4
XP_010776993.1	NADP-dependent malic enzyme	33.9
XP_010765036.1	aspartate aminotransferase	28.5
XP_010772035.1	alpha-aminoadipic semialdehyde dehydrogenase	36.3
XP_010777712.1	cytochrome b-c1 complex subunit 1	33.6
XP_010770990.1	troponin I	39.1
XP_010768648.1	nebulin	58.7
XP_010765900.1	carbonic anhydrase 1 [	49.4
XP_010788472.1	glycogen phosphorylase	30.6
XP_010771131.1	NADH dehydrogenase [ubiquinone] iron-sulphur protein 7	33.8
XP_010788098.1	heat shock protein beta 1	49.4
XP_010768865.1	cytochrome c oxidase subunit 5B	31.8
XP_010770791.1	cytochrome c oxidase subunit 4 isoform 2	60.1
XP_010766259.1	NADH dehydrogenase [ubiquinone] 1 alpha subcomplex subunit 7	39.2
XP_010792793.1	cytochrome c	42.8
XP_010767026.1	cytochrome c oxidase subunit NDUFA4	75.3
XP_010765537.1	glutaryl-CoA dehydrogenase	33.1
XP_010767938.1	fibrillin-1 isoform X1	67.5
XP_010795730.1	glutaryl-CoA dehydrogenase	34.0
XP_010776996.1	mitochondrial pyruvate carrier 2	36.7
XP_010767760.1	CDGSH iron-sulphur domain-containing protein 1	41.0
XP_010766700.1	palladin	52.7
XP_010794954.1	calcium/calmodulin-dependent protein kinase type II subunit beta	49.8
XP_010769019.1	NADH dehydrogenase [ubiquinone] 1 beta subcomplex subunit 5	33.0
XP_010773120.1	apolipoprotein O	40.0
XP_010791045.1	retinol dehydrogenase 13 isoform X1	42.1
XP_010766696.1	enoyl-CoA delta isomerase 2	42.8
XP_010783831.1	alanine aminotransferase 1	51.3
XP_010771234.1	superoxide dismutase [Mn]	42.0
XP_010795670.1	3-hydroxyisobutyrate dehydrogenase	43.5
XP_010781417.1	1-acyl-sn-glycerol-3-phosphate acyltransferase gamma	75.8
XP_010772950.1	collagen alpha-2 (I) chain isoform X1	39.6
XP_010784042.1	dehydrogenase/reductase SDR family member 7C	68.9
XP_010788327.1	nebulin	57.4

XP_010778895.1	long-chain specific acyl-CoA dehydrogenase	57.8
XP_010779324.1	mitochondrial import inner membrane translocase subunit Tim21	70.4
XP_010778764.1	alanine aminotransferase 2	40.5
NP_001290228.1	fatty acid-binding protein	72.5
XP_010773093.1	Pyruvate dehydrogenase phosphatase regulatory subunit	24.9

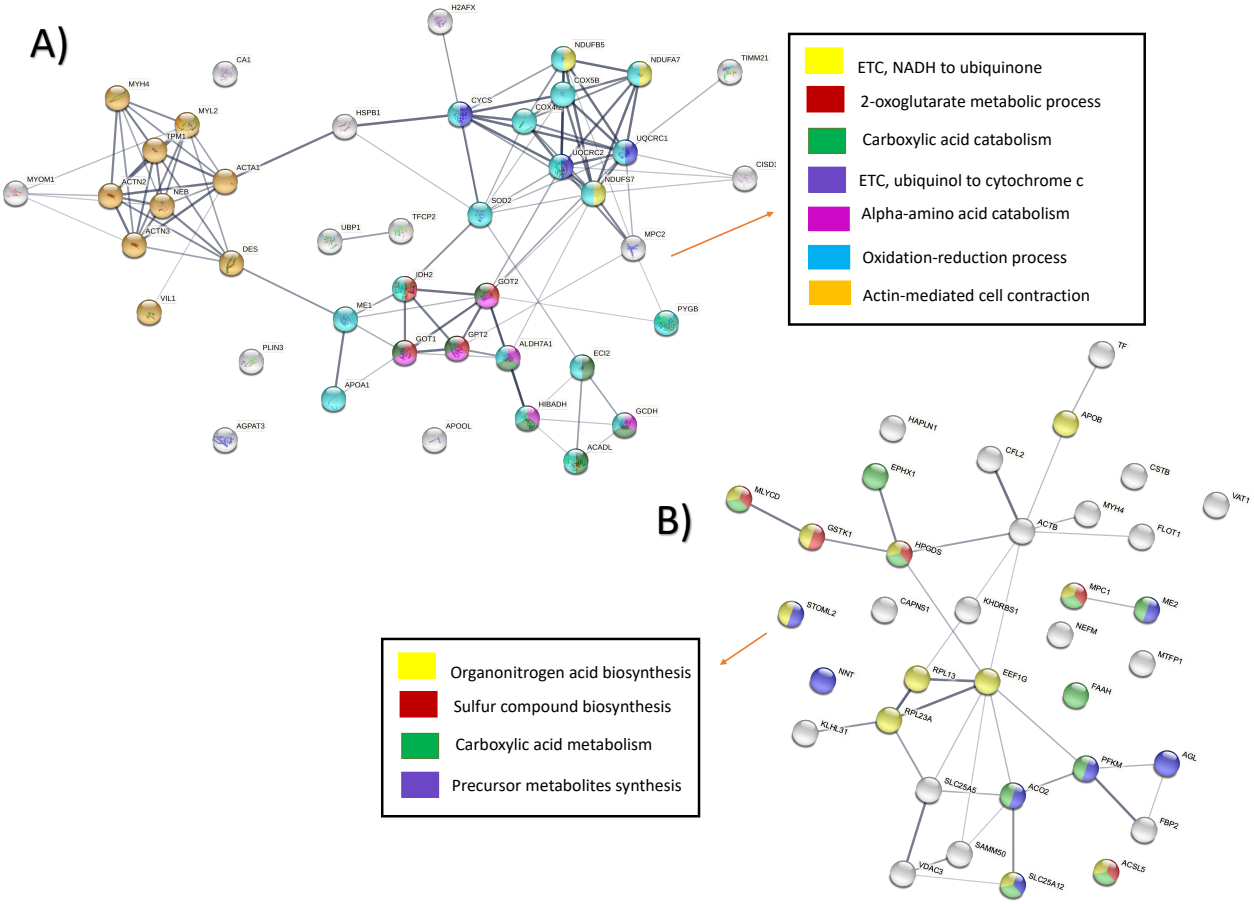

Figure 3-12. PPI networks generated by STRINGdb for proteins in RMM for *N. rossii* A) Increased protein abundance. B) Decreased protein abundance.

PPI network for differentially expressed proteins in RMM in *N. rossii* are seen in Supplementary Table 1 & supplementary table 2. **Figure 3-12** shows the network with more abundant proteins (A) and decreased abundance of proteins (B). The increased proteins PPI (relative ion area >25) has 42 protein nodes with 110 number of edges and a PPI enrichment p-value < 1.0e-16. Functional enrichment of the proteins showed, more abundant proteins belonging to complex I, amino acid metabolism, complex III, and muscle proteins. The less abundant PPI (relative ion area <20) has 35 protein nodes and 33 edges, with a PPI enrichment p-value < 7.39e-06 and the functional enrichment analysis showed proteins involved in sulphur compound metabolism, organonitrogen biosynthesis and carboxylic acid metabolism.

Supplementary Table 2. **Proteins lower in abundance in *N. rossii***

Accession Id's	Relative percentage of Total Ion Area	Protein Name
CAC27777.1	7.9	MyoHC-A3
XP_010765274.1	13.0	ADP/ATP translocase 2
AGN90720.1	14.8	beta-actin
XP_010776110.1	14.8	actin cytoplasmic 1
XP_010782516.1	13.2	voltage-dependent anion-selective channel protein 3
XP_010786020.1	5.5	NAD (P) transhydrogenase
AAC60356.1	2.4	fatty acid binding protein H8-isoform
XP_010772744.1	15.2	calcium-binding mitochondrial carrier protein Aralar1
XP_010773400.1	17.4	sorting and assembly machinery component 50 homolog
XP_010782695.1	9.3	ATP-dependent 6-phosphofructokinase
XP_010773584.1	20.0	mitochondrial carnitine/acylcarnitine carrier protein
XP_010771546.1	6.5	apolipoprotein B-100
XP_010768502.1	16.0	sodium/potassium-transporting ATPase subunit alpha-3
XP_010789292.1	21.0	eukaryotic initiation factor 4A-I
XP_010780086.1	6.2	NAD-dependent malic enzyme
CAL92187.1	4.0	transferrin
XP_010767902.1	9.1	hyaluronan and proteoglycan link protein 1
XP_010790586.1	3.9	KH domain-containing RNA-binding signal transduction-associated protein 1
XP_010786167.1	14.3	prothrombin
XP_010774874.1	16.3	neurofilament medium polypeptide
XP_010778213.1	15.2	pyruvate dehyrogenase phosphatase catalytic subunit 1
XP_010766309.1	16.5	cytochrome c oxidase subunit 5A isoform X2
XP_010786726.1	19.0	glutathione S-transferase kappa 1
XP_010782566.1	12.5	elongation factor 1-gamma
XP_010780100.1	13.1	stomatin protein 2
XP_010766151.1	14.9	elongation factor 1-gamma
XP_010790260.1	10.7	60S ribosomal protein L27a isoform X2
XP_010790259.1	10.7	60S ribosomal protein L27a isoform X1
XP_010772921.1	14.1	kelch protein 31
XP_010781656.1	14.1	fructose-1 6-bisphosphatase isozyme 2
XP_010793467.1	16.1	AMP deaminase 1 isoform X2
XP_010782071.1	16.5	vitellogenin-2
XP_010771562.1	13.4	glycogen debranching enzyme
XP_010773277.1	17.7	cystatin-B

XP_010782228.1	17.3	mitochondrial fission process protein 1
XP_010792412.1	9.3	stomatin protein 2
XP_010791811.1	8.4	60S ribosomal protein L23a
XP_010795420.1	18.5	synaptic vesicle membrane protein VAT-1 homolog
XP_010774286.1	18.6	kelch protein 41b
XP_010787572.1	18.3	methenyltetrahydrofolate synthase domain-containing protein isoform X1
XP_010778366.1	17.7	ATP-dependent Clp protease proteolytic subunit
XP_010784742.1	6.7	calpain small subunit 1
XP_010779525.1	7.5	aconitate hydratase
XP_010773293.1	9.0	histone H1
XP_010776100.1	17.3	mitochondrial pyruvate carrier 1
XP_010792543.1	6.7	flotillin-1
XP_010789836.1	14.4	60S ribosomal protein L13
XP_010790338.1	10.2	epoxide hydrolase 1
XP_010793737.1	16.9	fatty-acid amide hydrolase 1
XP_010792494.1	10.9	malonyl-CoA decarboxylase
XP_010792115.1	12.0	glutathione S-transferase A
XP_010766317.1	13.2	malate dehydrogenase
XP_010796013.1	1.4	myosin heavy chain fast
XP_010782096.1	6.8	14-3-3 protein beta/alpha-1
AAK07470.1	2.6	long chain fatty acyl CoA synthetase
XP_010780333.1	4.9	26S protease regulatory subunit 4 isoform X1
XP_010766277.1	20	Stress-70 protein mitochondrial-like
XP_010772138.1	24.6	ATP synthase subunit O
XP_010779232.1	23.1	ATP synthase subunit g mitochondrial
XP_010779868.1	22.2	ATP synthase subunit alpha mitochondrial
XP_010765728.1	24.7	ATP synthase subunit beta mitochondrial
XP_010778067.1	18.3	ATP synthase subunit gamma mitochondrial isoform X1
XP_010786327.1	23	ATP synthase F (0) complex subunit B1 mitochondrial
XP_010775450.1	18.8	ATP synthase subunit delta mitochondrial
XP_010784438.1	23.5	ADP/ATP translocase 3
XP_010783746.1	15.9	60S ribosomal protein L23
XP_010793356.1	17.2	Ubiquinone biosynthesis protein COQ9

Supplementary Table 3. **Proteins higher in abundance in *C. rastrospinosus***

Accession Id's	Relative percentage of Total Ion Area	Protein Name
XP_010765274.1	36.5	ADP/ATP translocase 2
XP_010774339.1	39.3	ADP/ATP translocase 1
XP_010782516.1	43.2	voltage-dependent anion-selective channel protein 3
XP_010777287.1	30.4	tropomyosin alpha-1 chain isoform X1
AAC60356.1	37.2	fatty acid binding protein H8-isoform
XP_010770006.1	37.2	NADH dehydrogenase [ubiquinone] iron-sulfur protein 2
XP_010772744.1	42	calcium-binding mitochondrial carrier protein Aralar1
XP_010773400.1	37.3	sorting and assembly machinery component 50 homolog
XP_010790716.1	33.5	NADH dehydrogenase [ubiquinone] flavoprotein 1
XP_010789886.1	33.7	cytochrome c1 heme protein mitochondrial
XP_010774927.1	42.5	histone H2AX
XP_010794136.1	34.4	ATP synthase subunit g
XP_010785217.1	36.2	NADH dehydrogenase [ubiquinone] iron-sulfur protein 3
XP_010768357.1	32.8	calcium-binding mitochondrial carrier protein Aralar1
XP_010773584.1	36.2	mitochondrial carnitine/acylcarnitine carrier protein
XP_010768822.1	38	NADH dehydrogenase [ubiquinone] flavoprotein 2
XP_010792996.1	40.5	histone H4
XP_010766804.1	32	sideroflexin-1
XP_010794867.1	36.9	sodium/potassium-transporting ATPase subunit alpha-1
XP_010769976.1	44.2	myosin-binding protein H
XP_010765220.1	38.3	NADH dehydrogenase [ubiquinone] 1 alpha subcomplex subunit 12
XP_010789215.1	45.7	NADH dehydrogenase [ubiquinone] 1 alpha subcomplex subunit 9
XP_010785201.1	31.9	titin
XP_010789292.1	43.4	eukaryotic initiation factor 4A-I
XP_010766730.1	37.5	ATP synthase subunit d
XP_010773903.1	50.1	cytochrome b-c1 complex subunit Rieske
XP_010766290.1	42.6	elongation factor Tu
XP_010778686.1	38.8	isocitrate dehydrogenase [NAD] subunit alpha
CAL92187.1	40.5	transferrin
XP_010780431.1	38.9	cytochrome b-c1 complex subunit 8
XP_010772963.1	38.2	NADH dehydrogenase [ubiquinone] 1 beta subcomplex subunit 4
XP_010768865.1	35.4	cytochrome c oxidase subunit 5B
XP_010775725.1	43	NADH dehydrogenase [ubiquinone] 1 alpha subcomplex subunit 5
XP_010783386.1	38.7	EH domain-containing protein 2 isoform X2

XP_010784582.1	35.8	NADH dehydrogenase [ubiquinone] 1 alpha subcomplex subunit 9
XP_010793340.1	46.4	obg ATPase 1
XP_010778644.1	36.9	NADH dehydrogenase [ubiquinone] 1 beta subcomplex subunit 3
XP_010766309.1	46.4	cytochrome c oxidase subunit 5Al isoform X2
XP_010766259.1	30.1	NADH dehydrogenase [ubiquinone] 1 alpha subcomplex subunit 7
XP_010770879.1	40.8	NADH dehydrogenase [ubiquinone] 1 alpha subcomplex subunit 8
XP_010771148.1	30.2	troponin C
XP_010786726.1	45	glutathione S-transferase kappa 1
XP_010782566.1	45.1	elongation factor 1-gamma
XP_010780100.1	43.6	stomatin protein 2
XP_010766151.1	40	elongation factor 1-gamma
XP_010790260.1	38.9	60S ribosomal protein L27a isoform X2
XP_010790259.1	38.9	60S ribosomal protein L27a isoform X1
XP_010792329.1	39.6	NADH dehydrogenase [ubiquinone] 1 beta subcomplex subunit 6
XP_010782228.1	49.4	mitochondrial fission process protein 1
XP_010792412.1	47.1	stomatin protein 2
XP_010791811.1	37.2	60S ribosomal protein L23a
XP_010784618.1	37.8	NADH dehydrogenase [ubiquinone] 1 alpha subcomplex subunit 6
XP_010779525.1	72.8	aconitate hydratase
XP_010773293.1	57.3	histone H1
XP_010776100.1	45.7	mitochondrial pyruvate carrier 1
XP_010789836.1	43.3	60S ribosomal protein L13
XP_010766317.1	42.1	malate dehydrogenase
XP_010786327.1	36	ATP synthase F (0) complex subunit B1 mitochondrial
XP_010765152.1	36.9	NADH dehydrogenase [ubiquinone] 1 alpha subcomplex subunit 10
XP_010788090.1	42	complement component 1 Q subcomponent-binding
XP_010774413.1	44.8	adenylosuccinate synthetase isozyme 1
XP_010787501.1	37.1	60S ribosomal protein L5
XP_010791295.1	39.4	pyruvate dehydrogenase (acetyl-transferring) kinase isozyme 2
XP_010786834.1	37.2	60S ribosomal protein L18
XP_010784234.1	39.5	NADH-cytochrome b5 reductase 3
XP_010764848.1	37.1	moesin isoform X1
XP_010792965.1	39.4	40S ribosomal protein S4
XP_010792689.1	42.5	cytochrome b-c1 complex subunit 1
XP_010782003.1	34.2	carnitine O-palmitoyltransferase 1
XP_010764516.1	69.8	nucleolar protein 56
XP_010783746.1	37	60S ribosomal protein L23
XP_010788817.1	33.3	phosphoglucomutase-1

XP_010764118.1	33.6	probable 2-oxoglutarate dehydrogenase E1 component DHKTD1
XP_010766620.1	35	proteasome subunit alpha type-5
XP_010788586.1	33.5	nucleolin
XP_010792044.1	41.2	isocitrate dehydrogenase [NAD] subunit beta isoform X2
XP_010785528.1	31.6	annexin A6 isoform X1
XP_010785529.1	31.6	annexin A6 isoform X2
XP_010793356.1	42.1	ubiquinone biosynthesis protein COQ9
XP_010788727.1	35.4	heat shock protein HSP 90-alpha 1
XP_010786454.1	36.9	heat shock protein 75 kDa
XP_010776005.1	39.7	transmembrane emp24 domain-containing protein 10
XP_010795693.1	33.3	60S ribosomal protein L4
XP_010767141.1	30.9	voltage-dependent anion-selective channel protein 2
XP_010787333.1	39.1	voltage-dependent anion-selective channel protein 1
XP_010783785.1	38.5	40S ribosomal protein S12
XP_010779868.1	31.7	ATP synthase subunit alpha
XP_010779103.1	33.4	60S ribosomal protein L12 isoform X1
XP_010779104.1	33.4	60S ribosomal protein L12 isoform X2
XP_010788657.1	27.9	60S ribosomal protein L7a
XP_010778828.1	34.2	26S protease regulatory subunit 8
XP_010777506.1	30.4	NADH-ubiquinone oxidoreductase 75 kDa
XP_010774792.1	34.1	60S ribosomal protein L18a
XP_010772138.1	29.1	ATP synthase subunit O
XP_010782878.1	34.4	40S ribosomal protein S18
XP_010774669.1	36.1	voltage-dependent anion-selective channel protein 2
XP_010772721.1	35.6	succinyl-CoA ligase [ADP-forming] subunit beta
XP_010788571.1	30.6	T-complex protein 1 subunit gamma
XP_010773777.1	38.3	40S ribosomal protein S16 isoform X1
XP_010769328.1	31.9	phosphoglycerate mutase 2
XP_010795246.1	35.8	elongation factor 1-beta
XP_010773724.1	39.1	prohibitin
XP_010777155.1	32.8	thioredoxin-related transmembrane protein 1
XP_010790696.1	36.6	mitochondrial import receptor subunit TOM40 homolog
XP_010774042.1	27.6	FK506-binding protein 1
XP_010795081.1	30	annexin A4
XP_010765060.1	33.9	60S ribosomal protein L21
XP_010774335.1	35.6	fatty acid-binding protein
XP_010774833.1	36.2	eukaryotic translation initiation factor 2 subunit 1
XP_010789111.1	29.3	glyceraldehyde-3-phosphate dehydrogenase

XP_010766874.1	34.7	40S ribosomal protein S20
XP_010779594.1	53.4	proteasome subunit alpha type-2
XP_010773596.1	31.8	succinate dehydrogenase [ubiquinone] iron-sulfur subunit
XP_010776147.1	30.6	40S ribosomal protein S3
XP_010795570.1	91.7	ryanodine receptor 1
XP_010773129.1	49.5	transferrin receptor protein 1
XP_010786813.1	42.5	40S ribosomal protein S9
XP_010777993.1	45.8	ATP synthase subunit s
XP_010765492.1	44.8	UTP--glucose-1-phosphate uridylyltransferase
XP_010786020.1	29.6	NAD (P) transhydrogenase mitochondrial-like
XP_010782086.1	24	Sarcolemmal membrane-associated protein
XP_010773292.1	27.3	Dihydrolipoyllysine-residue acetyltransferase component of pyruvate dehydrogenase
XP_010766277.1	33.7	Stress-70 protein
XP_010775450.1	28.4	ATP synthase subunit delta mitochondrial
XP_010781933.1	27.9	Apolipoprotein B-100-like partial
XP_010783388.1	40.7	26S proteasome non-ATPase regulatory subunit 8

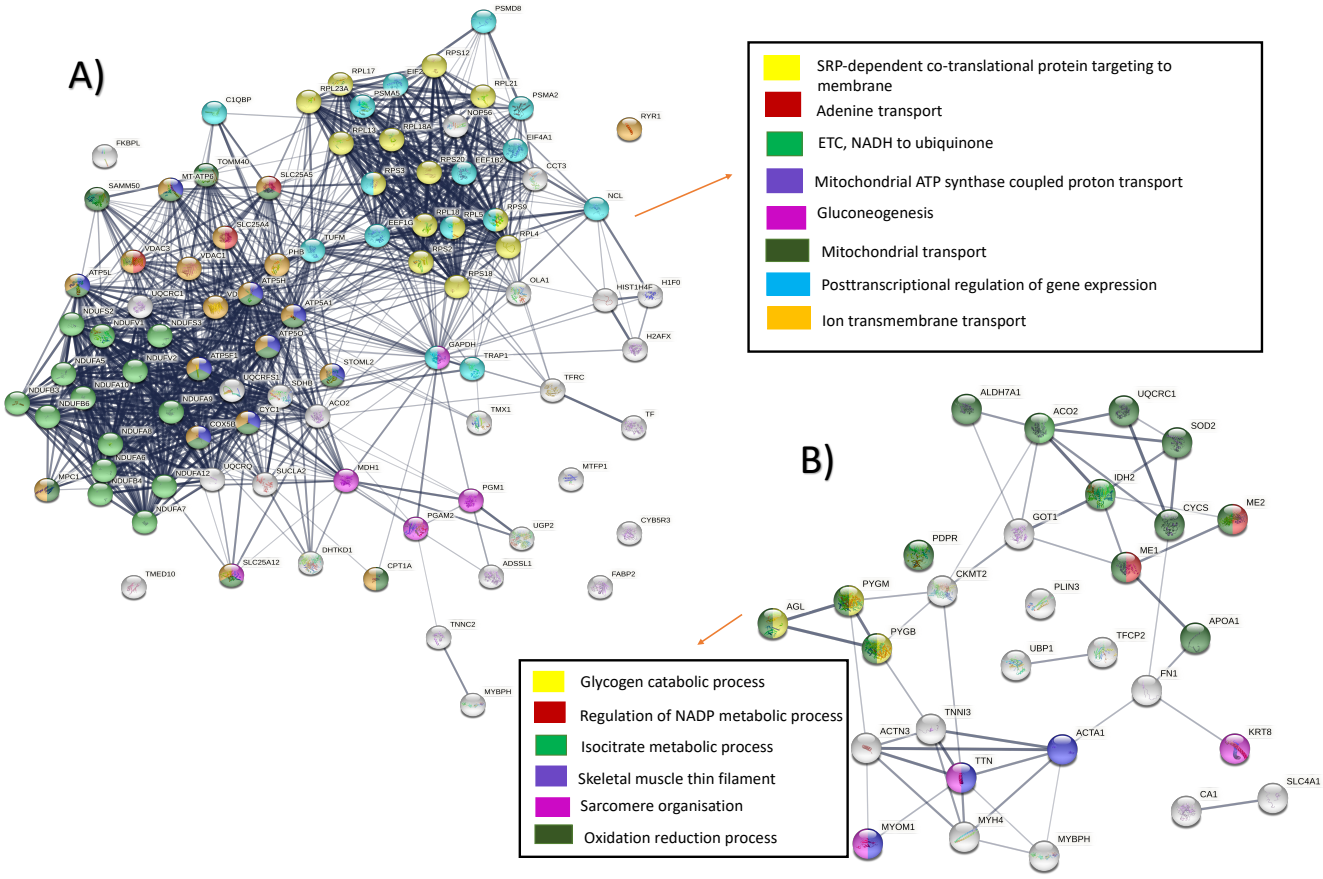

Figure 3-13. PPI networks generated by STRINGdb for proteins in RMM for icefish *C. rastrospinosus* A) Increased protein abundance. B) Decreased protein abundance.

PPI network for differentially expressed proteins in RMM in *C. rastrospinosus* are seen in **Supplementary Table 3 & 4**. **Figure 3-13** shows the network with more abundant proteins (A) and decreased abundance of proteins (B). The increased proteins PPI (relative ion area >30) had 89 protein nodes with 9861 number of edges and a PPI enrichment p-value < 1.0e-16. *C. rastrospinosus* has the greatest number of proteins that were seen increased. Functional enrichment of the proteins showed, more abundant proteins belonging to SRP-dependent co-translational, complex I, complex III, and complex V and mitochondrial transport. The less abundant PPI (relative ion area <20) had 29 protein nodes and 48 edges, with a PPI enrichment p-value < 1.0e-16 and the functional enrichment analysis showed proteins involved in glycogen metabolism, regulation of NADP metabolic process, sarcomere organisation, and isocitrate metabolism.

Supplementary Table 4. **Proteins lower in abundance in *C. rastrospinosus***

Accession Id's	Relative percentage of Total Ion Area	Protein Name
CAC27776.1	1.4	myosin heavy chain
CAC27777.1	1.9	MyoHC-A3
AAO21697.1	8.7	alpha actin
XP_010784415.1	13.3	alpha-actinin-3
XP_010794573.1	8.6	desmin
AAO24741.1	2.3	creatine kinase mitochondrial isoform
XP_010772488.1	1.4	creatine kinase S-type
XP_010781940.1	14.0	aconitate hydratase
XP_010793425.1	0.7	myosin-7 isoform X1
XP_010791227.1	12.1	myosin-binding protein C fast-type isoform X2
XP_010776201.1	11.1	titin
XP_010792180.1	15.3	apolipoprotein A-I
XP_010794773.1	10.5	myomesin-2
XP_010785535.1	13.1	keratin type II cytoskeletal 8
AAC25100.1	0.8	alpha globin
AAC59671.1	0.8	alpha-1 globin
XP_010781418.1	17.2	isocitrate dehydrogenase [NADP]
XP_010784569.1	12.4	cytochrome b-c1 complex subunit 2 isoform X1
XP_010771394.1	11.0	tropomyosin alpha-3 chain
XP_010778108.1	11.1	perilipin-3
XP_010774355.1	8.8	myomesin-1
XP_010776993.1	16.0	NADP-dependent malic enzyme
XP_010765036.1	21.7	aspartate aminotransferase cytoplasmic
XP_010772035.1	20.0	alpha-aminoadipic semialdehyde dehydrogenase
XP_010777712.1	6.8	cytochrome b-c1 complex subunit 1
XP_010767025.1	11.5	plectin isoform X1
XP_010791816.1	15.3	fructose-bisphosphate aldolase C-B
XP_010768648.1	5.2	nebulin
XP_010765900.1	10.9	carbonic anhydrase 1
XP_010788472.1	10.9	glycogen phosphorylase
XP_010780086.1	17.0	NAD-dependent malic enzyme
XP_010773075.1	6.6	M-protein striated muscle
XP_010794764.1	10.1	fibronectin
XP_010792793.1	16.1	cytochrome c
XP_010767026.1	12.6	cytochrome c oxidase subunit NDUFA4
XP_010782071.1	12.9	vitellogenin-2
XP_010771562.1	9.2	glycogen debranching enzyme
XP_010787466.1	14.0	methylcrotonoyl-CoA carboxylase subunit alpha isoform X1
XP_010788355.1	19.3	glycogen phosphorylase
XP_010771234.1	11.5	superoxide dismutase [Mn]
XP_010791177.1	17.0	glycerol-3-phosphate dehydrogenase
XP_010770992.1	12.5	troponin I
XP_010773093.1	15.4	pyruvate dehydrogenase phosphatase regulatory subunit
XP_010785995.1	2.1	band 3 anion transport protein

XP_010786435.1	21.3	heme oxygenase 2
XP_010784864.1	20.5	Troponin T fast skeletal muscle isoforms-like isoform X1 to X3
XP_010765699.1	20.3	PDZ and LIM domain protein 7
XP_010772035.1	20	Alpha-aminoadipic semialdehyde dehydrogenase
XP_010791917.1	23.3	Creatine kinase M-type
XP_010769508.1	21.1	Ubiquitin carboxyl-terminal hydrolase 5 isoform X1 & X2
XP_010784587.1	21.5	Methylmalonyl-CoA mutase

Supplementary Table 5**. Proteins more in abundance in *C. gunnari***

Accession Id's	Relative percentage of Total Ion Area	Protein Name
NP_001290213.1	69.7	myosin heavy chain
XP_010765274.1	44.3	ADP/ATP translocase 2
XP_010781933.1	65.6	apolipoprotein B-100
NP_001290222.1	33.9	long-chain-fatty-acid--CoA ligase 1
XP_010782516.1	31.6	voltage-dependent anion-selective channel protein 3
XP_010786020.1	59.2	NAD (P) transhydrogenase
XP_010788987.1	30.8	titin
AAC60356.1	34.8	fatty acid binding protein H8-isoform
XP_010773400.1	36.4	sorting and assembly machinery component 50 homolog
XP_010794136.1	31.9	ATP synthase subunit g
XP_010777712.1	32.5	cytochrome b-c1 complex subunit 1
XP_010768357.1	36.4	calcium-binding mitochondrial carrier protein Aralar1
XP_010773584.1	33.9	mitochondrial carnitine/acylcarnitine carrier protein
XP_010771546.1	83.3	apolipoprotein B-100
XP_010766804.1	34.0	sideroflexin-1
XP_010767902.1	55.7	hyaluronan and proteoglycan link protein 1
XP_010772963.1	27.7	NADH dehydrogenase [ubiquinone] 1 beta subcomplex subunit 4
XP_010786167.1	29.3	prothrombin
XP_010770879.1	29.8	NADH dehydrogenase [ubiquinone] 1 alpha subcomplex subunit 8
XP_010766151.1	31.1	elongation factor 1-gamma
XP_010790260.1	35.6	60S ribosomal protein L27a isoform X2
XP_010790259.1	35.6	60S ribosomal protein L27a isoform X1
XP_010771562.1	31.8	glycogen debranching enzyme
XP_010774059.1	33.7	AFG3 protein 2
XP_010776936.1	43.8	60S ribosomal protein L28
XP_010790338.1	37.1	epoxide hydrolase 1
XP_010766317.1	27.8	malate dehydrogenase
XP_010786327.1	29.5	ATP synthase F (0) complex subunit B1
XP_010778067.1	30.1	ATP synthase subunit gamma X1

XP_010773598.1	35.0	ATPase family AAA domain-containing protein 3A
XP_010770997.1	42.4	dynamin-1 protein
XP_010768163.1	64.7	adenylate kinase 4
XP_010793736.1	39.3	inter-alpha-trypsin inhibitor heavy chain H4
XP_010794434.1	34.2	ATP-dependent 6-phosphofructokinase
XP_010767276.1	31.0	ATP-binding cassette sub-family B member 7
XP_010765728.1	30.8	ATP synthase subunit beta
XP_010774792.1	28.9	60S ribosomal protein L18a
XP_010772138.1	32.9	ATP synthase subunit O
XP_010779169.1	35.6	NADH dehydrogenase [ubiquinone] 1 beta subcomplex subunit 8
XP_010780333.1	81.4	26S protease regulatory subunit 4 isoform X1
XP_010780334.1	81.4	26S protease regulatory subunit 4 isoform X2
XP_010765060.1	39.8	60S ribosomal protein L21
XP_010772504.1	39.8	voltage-dependent anion-selective channel protein 2 isoform X2
XP_010775450.1	29.4	ATP synthase subunit delta
XP_010771726.1	30.4	cytochrome c oxidase subunit 4 isoform 1 isoform X1
XP_010771732.1	30.4	cytochrome c oxidase subunit 4 isoform 1 isoform X2
XP_010790855.1	34.2	obscurin isoform X3
XP_010790853.1	34.2	obscurin isoform X1
XP_010790854.1	34.2	obscurin isoform X2
XP_010781840.1	40.8	transitional endoplasmic reticulum ATPase
XP_010780029.1	52.3	ATP-binding cassette sub-family F member 2
XP_010773228.1	48.1	26S proteasome non-ATPase regulatory subunit 6
XP_010770797.1	63.5	fragile X mental retardation syndrome-related protein 2
XP_010768595.1	37.7	stress-70 protein
XP_010790499.1	29.6	60S ribosomal protein L35
XP_010786327.1	29.5	ATP synthase F (0) complex subunit B1 mitochondrial
XP_010775450.1	29.4	ATP synthase subunit delta
XP_010784438.1	29.0	ADP/ATP translocase 3
XP_010786167.1	29.3	Prothrombin partial
XP_010774792.1	28.9	60S ribosomal protein L18a-like
XP_010766730.1	28.7	ATP synthase subunit d
XP_010766317.1	27.8	Malate dehydrogenase
XP_010766309.1	27.8	Cytochrome c oxidase subunit 5A
XP_010783746.1	26.7	60S ribosomal protein L23
XP_010773724.1	24.5	Prohibitin
XP_010793356.1	23	Ubiquinone biosynthesis protein

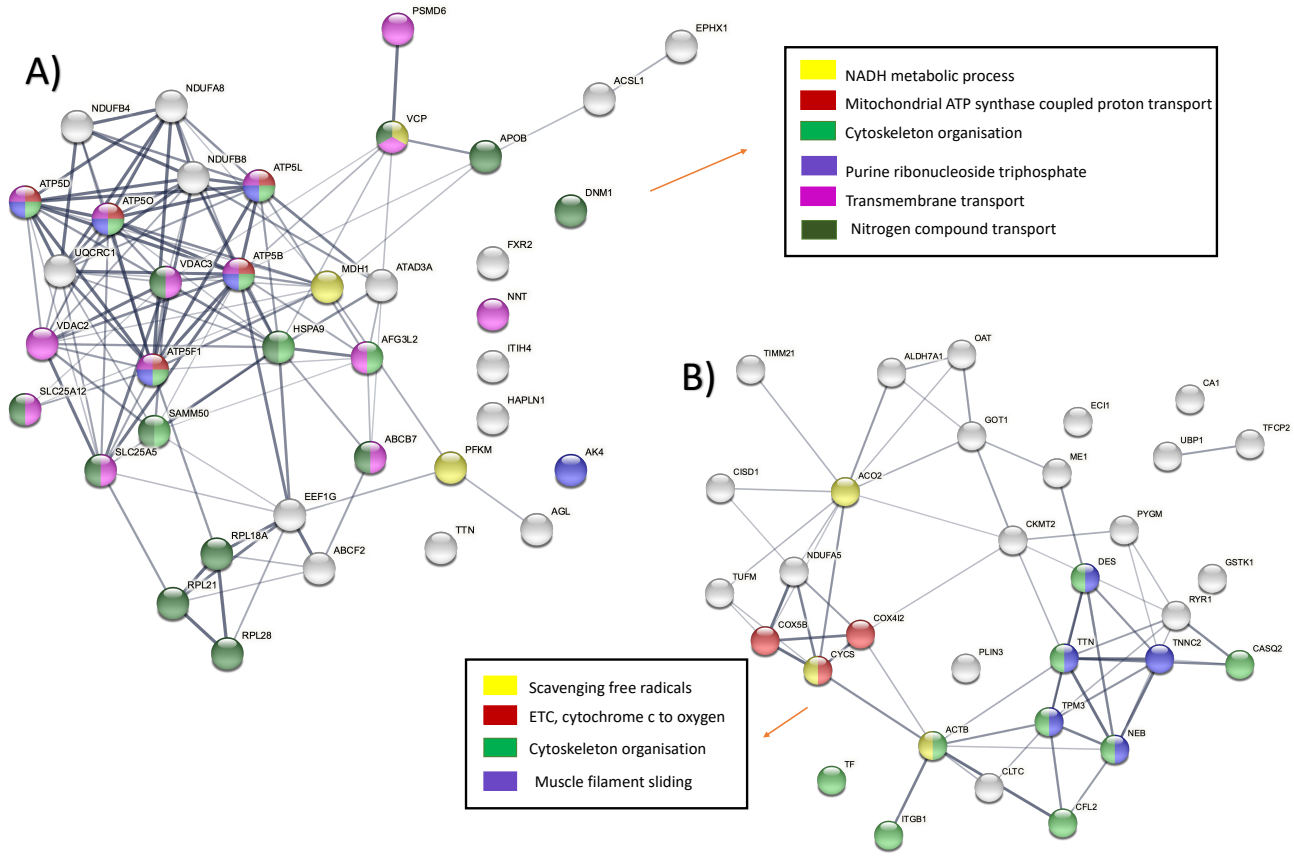

Figure 3-14. PPI networks generated by STRINGdb for proteins in RMM for *C. gunnari* A) Increased protein abundance. B) Decreased protein abundance.

PPI network for differentially expressed proteins in RMM in *C. gunnari* are seen in **Supplementary Table 5 & 6. Figure 3-14** shows the network with more abundant proteins (A) and decreased abundance of proteins (B). The increased proteins PPI (relative ion area >30) had 38 protein nodes with 119 number of edges and a PPI enrichment p-value < 1.0e-16. Functional enrichment of the proteins showed, more abundant proteins belonging NADH metabolic process, ATP synthase coupled transport, cytoskeleton organisation, and transmembrane transport. The less abundant PPI (relative ion area <20) had 32 protein nodes and 59 edges, with a PPI enrichment p-value < 1.0e-16 and the functional enrichment analysis showed proteins involved in scavenging free radicals, complex III, sarcomere organisation, and muscle filament sliding

Supplementary Table 6. **Proteins less in abundance in *C. gunnari***

Accession Id's	Relative percentage of Total Ion Area	Protein Name
AGN90720.1	12.1	beta-actin
XP_010776110.1	12.1	actin cytoplasmic 1
XP_010794573.1	9.9	desmin
XP_010772488.1	4.8	creatine kinase S-type
XP_010781940.1	14.0	aconitate hydratase

XP_010793425.1	3.9	myosin-7 isoform X1
AAC25100.1	0.5	alpha globin
AAC59671.1	0.5	alpha-1 globin
XP_010767505.1	8.1	myosin regulatory light chain 2
XP_010771394.1	16.1	tropomyosin alpha-3 chain
XP_010778108.1	4.5	perilipin-3
XP_010776993.1	9.8	NADP-dependent malic enzyme
XP_010765036.1	15.4	aspartate aminotransferase
XP_010772035.1	14.7	alpha-aminoadipic semialdehyde dehydrogenase
XP_010768975.1	14.8	collagen alpha-1 (I) chain
XP_010785475.1	10.5	titin
XP_010791816.1	11.8	fructose-bisphosphate aldolase C-B
XP_010768648.1	15.2	nebulin
CAL92189.1	5.5	transferrin
NP_001290225.1	5.5	serotransferrin precursor
XP_010765900.1	19.6	carbonic anhydrase 1
XP_010788472.1	14.4	glycogen phosphorylase
XP_010772394.1	14.7	titin
XP_010766290.1	12.4	elongation factor Tu
XP_010778686.1	12.6	isocitrate dehydrogenase [NAD] subunit alpha
XP_010768865.1	12.2	cytochrome c oxidase subunit 5B
XP_010775725.1	22.1	NADH dehydrogenase [ubiquinone] 1 alpha subcomplex subunit 5
XP_010782377.1	3.7	calsequestrin-1
XP_010770791.1	7.7	cytochrome c oxidase subunit 4 isoform 2
XP_010792793.1	12.5	cytochrome c
XP_010771148.1	9.9	troponin C
XP_010786726.1	15.5	glutathione S-transferase kappa 1
XP_010767938.1	9.0	fibrillin-1 isoform X1
XP_010784864.1	12.7	troponin T fast skeletal muscle isoforms isoform X4
XP_010767760.1	11.5	CDGSH iron-sulphur domain-containing protein 1
XP_010765498.1	10.4	ornithine aminotransferase
XP_010790914.1	13.5	flotillin-2 isoform X1
XP_010776148.1	13.2	enoyl-CoA delta isomerase 1
XP_010795570.1	3.2	ryanodine receptor 1
XP_010779324.1	10.0	mitochondrial import inner membrane translocase subunit Tim21
XP_010774135.1	6.2	clathrin heavy chain 1
XP_010765900.1	19.6	Carbonic anhydrase 1
XP_010784415.1	18.7	Alpha-actinin-3
XP_010772948.1	18.6	probable acyl-CoA dehydrogenase 6
XP_010783999.1	15.4	Peroxiredoxin-5
XP_010771394.1	16.1	Troponin alpha-3 chain-like
XP_010779541.1	15.8	Short-chain specific acyl-CoA dehydrogenase
XP_010791917.1	16.3	Creatine kinase M-type
XP_010791177.1	16.9	Glycerol-3-phosphate dehydrogenase
XP_010791064.1	17.1	electron transfer flavoprotein subunit beta

XP_010775191.1	17.1	1 4-alpha-glucan-branching enzyme
XP_010769508.1	18	Ubiquitin carboxyl-terminal hydrolase 5 isoform X1 & X2
XP_010784587.1	18	Methylmalonyl-CoA mutase

3.7.2 White Muscle Mitochondria (WMM)

Supplementary Table 7. **Proteins more in abundance in *N. rossii***

Accession Id's	Relative percentage of Total Ion Area	Protein Name
CAC27776.1	49.0	myosin heavy chain
XP_010768010.1	44.1	titin
XP_010785479.1	40.6	titin
XP_010791917.1	37.8	creatine kinase M-type
XP_010778896.1	41.0	myosin light chain 1/3
XP_010782377.1	41.0	calsequestrin-1
XP_010792180.1	54.5	apolipoprotein A-I
XP_010772488.1	78.2	creatine kinase S-type
XP_010787448.1	54.7	keratin type I cytoskeletal 19
AAC25100.1	79.7	alpha globin
AAC59671.1	79.7	alpha-1 globin
XP_010794476.1	53.1	betaine--homocysteine S-methyltransferase 1
XP_010788362.1	38.3	annexin A1
XP_010781921.1	49.0	histidine-rich glycoprotein
XP_010764663.1	35.3	myozenin-1
XP_010764532.1	45.1	ryanodine receptor 1
XP_010771614.1	29.0	tropomyosin alpha-1 chain isoform X3
XP_010773841.1	35.1	40S ribosomal protein S3a
XP_010794954.1	9.5	calcium/calmodulin-dependent protein kinase type II subunit beta
AAC60372.1	87.5	beta-globin
XP_010781066.1	41.2	aspartate aminotransferase
XP_010783999.1	47.5	peroxiredoxin-5
XP_010765488.1	54.8	malate dehydrogenase
XP_010778325.1	40.2	haemoglobin subunit beta-C
XP_010788340.1	40.7	hemopexin
XP_010775215.1	62.6	collagen alpha-3 (VI) chain
XP_010791819.1	60.6	T-complex protein 1 subunit theta isoform X1
XP_010785995.1	64.3	band 3 anion transport protein
XP_010771898.1	51.4	fibrinogen alpha chain
XP_010778322.1	80.6	haemoglobin subunit zeta

XP_010791578.1	43.2	40S ribosomal protein S11
XP_010778161.1	81.2	transmembrane protease serine 2
XP_010776993.1	95.0	NADP-dependent malic enzyme
CAL92189.1	36.3	transferrin
NP_001290225.1	36.3	serotransferrin precursor
XP_010778035.1	58.2	succinate dehydrogenase [ubiquinone] flavoprotein

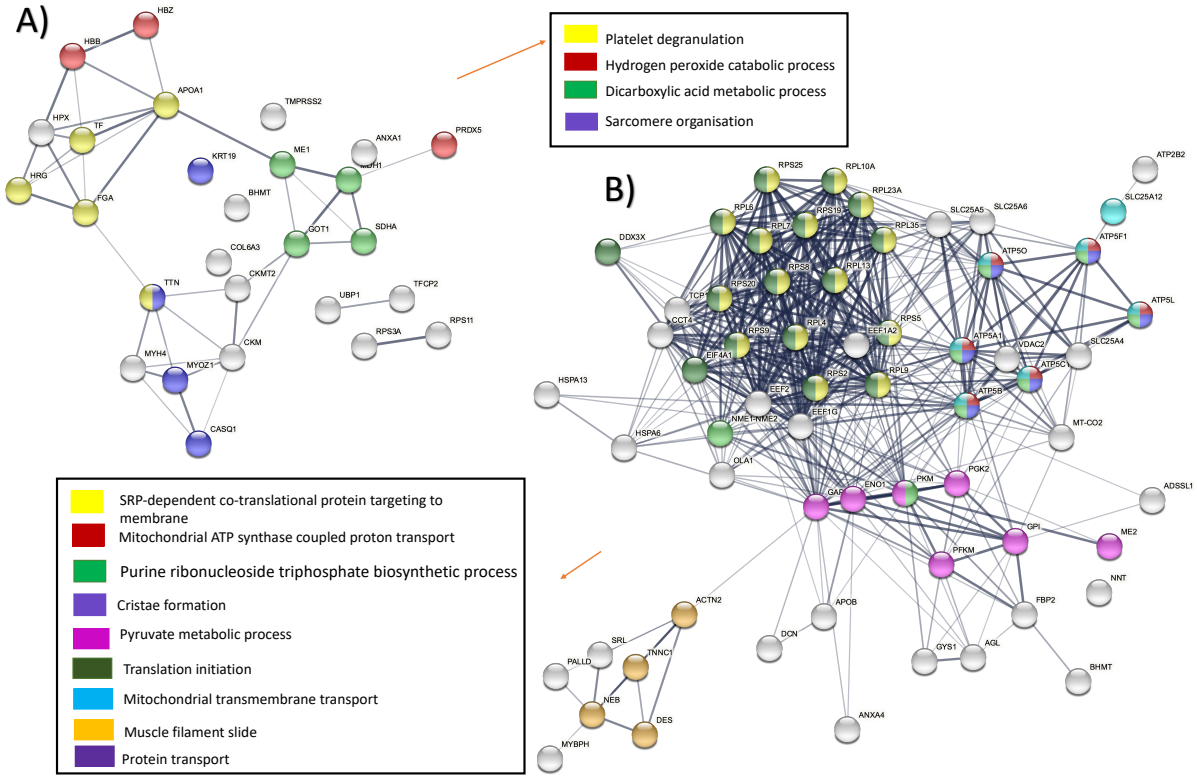

Figure 3-15. PPI networks generated by STRINGdb for proteins in WMM for *N. rossii* A) Increased protein abundance. B) Decreased protein abundance.

PPI network for differentially expressed proteins in WMM in *N. rossii* are seen in Supplementary **Table 7** & **Table 8**. shows the network with more abundant proteins (A) and decreased abundance of proteins (B). The increased proteins PPI (relative ion area >30) has 27 protein nodes with 39 number of edges and a PPI enrichment p-value < 1.0e-16. Functional enrichment of the proteins showed, more abundant proteins belonging to hydrogen peroxide metabolism, sarcomere organisation, platelet degranulation. The less abundant PPI (relative ion area <20) has 62 protein nodes and 498 edges, with a PPI enrichment p-value < 1.0e-16 and the functional enrichment analysis showed proteins involved in ATP synthase coupled proton transport, cristae formation, pyruvate metabolism, transmembrane transport.

Supplementary Table 8. **Proteins less in abundance in *N. rossii***

Accession Id's	Relative percentage of Total Ion Area	Protein Name

XP_010766216.1	11.0	pyruvate kinase PKM
XP_010781933.1	4.2	apolipoprotein B-100
XP_010779868.1	19.0	ATP synthase subunit alpha
XP_010794573.1	15.8	desmin
XP_010770965.1	1.0	myosin regulatory light chain 2
XP_010794434.1	7.1	ATP-dependent 6-phosphofructokinase
XP_010785886.1	22.3	nucleoside diphosphate kinase B
XP_010769976.1	8.4	myosin-binding protein H
XP_010764264.1	16.0	elongation factor 2
XP_010774339.1	20.6	ADP/ATP translocase 1
XP_010788727.1	10.9	heat shock protein HSP 90-alpha 1
XP_010782071.1	9.6	vitellogenin-2
XP_010774413.1	9.7	adenylosuccinate synthetase isozyme 1
XP_010766317.1	2.8	malate dehydrogenase
XP_010777526.1	17.7	nebulin
XP_010789292.1	5.9	eukaryotic initiation factor 4A-I
XP_010793340.1	11.8	obg ATPase 1
XP_010792965.1	7.5	40S ribosomal protein S4
XP_010766151.1	5.7	elongation factor 1-gamma
XP_010773292.1	7.9	dihydrolipoyllysine-residue acetyltransferase component of pyruvate dehydrogenase complex
XP_010771231.1	9.8	T-complex protein 1 subunit alpha
XP_010768032.1	10.0	40S ribosomal protein SA isoform X2
XP_010781656.1	9.8	fructose-1 6-bisphosphatase isozyme 2
XP_010774286.1	4.2	kelch protein 41b
XP_010783756.1	6.8	40S ribosomal protein S2
XP_010785174.1	8.5	T-complex protein 1 subunit delta
XP_010779161.1	15.6	60S ribosomal protein L11 isoform X2
XP_010776310.1	4.2	60S ribosomal protein L9
XP_010794136.1	18.7	ATP synthase subunit g
XP_010793781.1	12.7	phosphoglycerate kinase
XP_010790499.1	3.4	60S ribosomal protein L35
XP_010782543.1	7.0	60S ribosomal protein L6
XP_010765728.1	17.5	ATP synthase subunit beta
XP_010779184.1	12.4	elongation factor 1-alpha
XP_010771942.1	12.3	vitellogenin-1
XP_010785200.1	2.7	palladin
XP_010791484.1	14.8	60S ribosomal protein L10a
AAL99930.1	0.0	IgM heavy chain secretory form
BAV53298.1	2.6	cytochrome c oxidase subunit II
XP_010782566.1	7.1	elongation factor 1-gamma
XP_010778067.1	13.4	ATP synthase subunit gamma
XP_010793954.1	15.8	plasma membrane calcium-transporting ATPase 2
XP_010789836.1	8.2	60S ribosomal protein L13
XP_010778226.1	5.5	succinyl-CoA ligase [ADP/GDP-forming] subunit alpha

XP_010794954.1	9.5	calcium/calmodulin-dependent protein kinase type II subunit beta
XP_010771562.1	16.3	glycogen debranching enzyme
XP_010786327.1	19.2	ATP synthase F (0) complex subunit B1
XP_010787537.1	9.1	40S ribosomal protein S8
XP_010784438.1	7.8	ADP/ATP translocase 3
XP_010772744.1	8.9	calcium-binding mitochondrial carrier protein Aralar1
XP_010788735.1	15.4	glucose-6-phosphate isomerase
XP_010778188.1	10.0	sarcalumenin
AAC60356.1	7.7	fatty acid binding protein H8-isoform
XP_010795693.1	3.8	60S ribosomal protein L4
XP_010789111.1	18.0	glyceraldehyde-3-phosphate dehydrogenase
XP_010764689.1	3.5	ATP-dependent RNA helicase DDX3X
XP_010791686.1	12.1	alpha-actinin-2
XP_010765741.1	19.1	heat shock 70 kDa protein
XP_010786813.1	12.5	40S ribosomal protein S9
XP_010791811.1	5.6	60S ribosomal protein L23a
XP_010776087.1	15.9	NAD (P) transhydrogenase
XP_010765274.1	12.1	ADP/ATP translocase 2
XP_010767141.1	15.6	voltage-dependent anion-selective channel protein 2
XP_010781251.1	8.2	26S protease regulatory subunit 6A
XP_010770361.1	6.9	60S ribosomal protein L7
XP_010764414.1	1.5	troponin C
XP_010796172.1	14.1	40S ribosomal protein S19
XP_010766874.1	9.1	40S ribosomal protein S20
XP_010768357.1	9.8	calcium-binding mitochondrial carrier protein Aralar1
XP_010766286.1	3.5	glycogen [starch] synthase
XP_010795485.1	2.6	fragile X mental retardation syndrome-related protein 1 isoform X3
XP_010784570.1	11.7	cytochrome b-c1 complex subunit 2 isoform X2
XP_010765339.1	13.0	alpha-enolase
XP_010769508.1	9.3	ubiquitin carboxyl-terminal hydrolase 5 isoform X2
XP_010772138.1	16.1	ATP synthase subunit O
XP_010783741.1	17.0	40S ribosomal protein S5
XP_010773196.1	5.9	betaine--homocysteine S-methyltransferase 1
XP_010776714.1	13.0	40S ribosomal protein S25
XP_010795528.1	17.7	decorin
XP_010795081.1	3.3	annexin A4
XP_010769990.1	9.2	heat shock 70 kDa protein 6
XP_010791048.1	20.6	Isocitrate dehydrogenase

Supplementary Table 9. **Proteins less in abundance in *C. rastrospinosus***

Accession Id's	Relative percentage of Total Ion Area	Protein Name
XP_010794573.1	5.7	desmin
XP_010770965.1	2.3	myosin regulatory light chain 2
ACN49202.1	4.7	parvalbumin
XP_010782377.1	11.6	calsequestrin-1
XP_010782071.1	11.1	vitellogenin-2
AAC25100.1	0.4	alpha globin
AAC59671.1	0.4	alpha-1 globin
XP_010794476.1	11.6	betaine--homocysteine S-methyltransferase 1
XP_010771942.1	2.5	vitellogenin-1
XP_010771614.1	15.8	tropomyosin alpha-1 chain isoform X3
XP_010794954.1	9.5	calcium/calmodulin-dependent protein kinase type II subunit beta
XP_010768524.1	14.0	calmodulin
AAC60358.1	3.7	fatty acid binding protein H8-isoform
AAC60372.1	0.0	beta-globin
AAD56588.1	0.0	beta globin
XP_010765488.1	7.8	malate dehydrogenase
XP_010764414.1	1.9	troponin C
XP_010787278.1	12.1	angiotensinogen
XP_010788340.1	13.0	hemopexin
XP_010793059.1	5.7	fibrinogen gamma chain
XP_010778322.1	0.3	haemoglobin subunit zeta
XP_010778161.1	2.0	transmembrane protease serine 2
XP_010771900.1	9.9	fibrinogen beta chain
XP_010785851.1	12.0	protein disulphide-isomerase
XP_010776993.1	5.0	NADP-dependent malic enzyme
CAL92189.1	7.6	transferrin
NP_001290225.1	7.6	serotransferrin precursor
XP_010773398.1	19.8	Calreticulin
XP_010791001.1	26.6	Myosin heavy chain fast skeletal 13
XP_010787188.1	21.1	Ryanodine receptor 1
XP_010790363.1	21.1	Titin-like partial
CAL92189.1	22.7	Transferrin

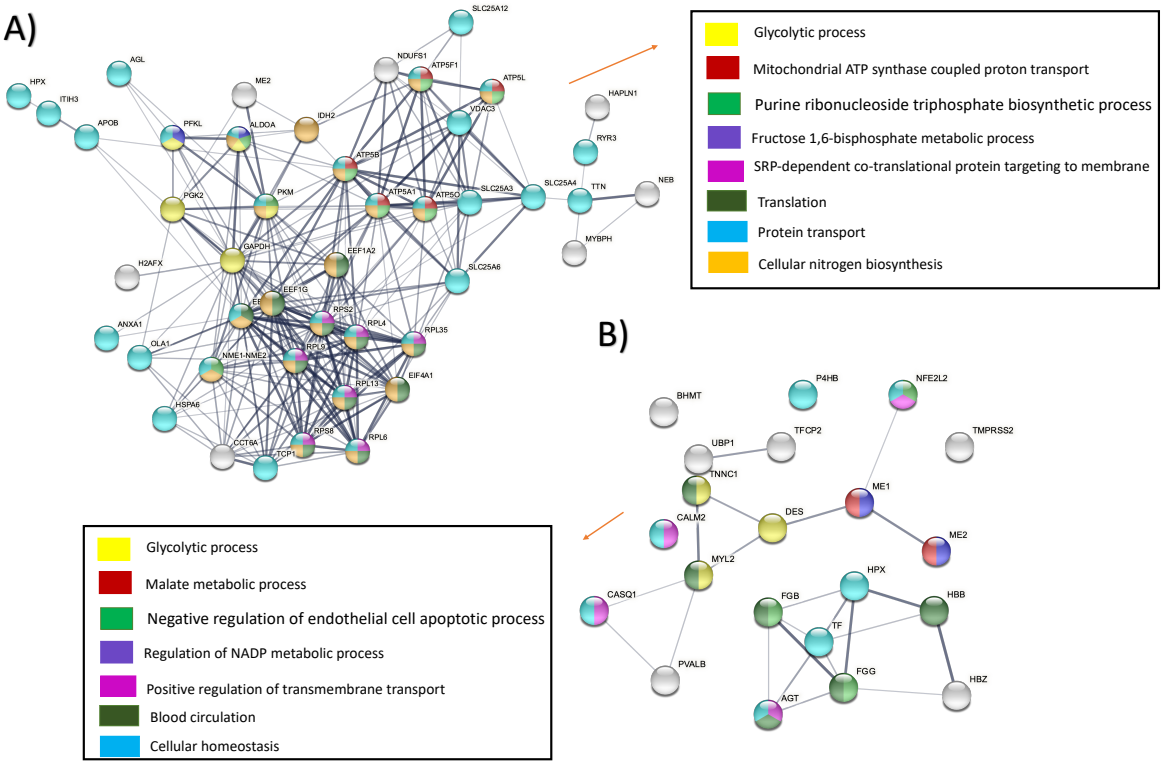

Figure 3-16. PPI networks generated by STRINGdb for proteins in WMM for *C. rastrospinosus* A) Increased protein abundance. B) Decreased protein abundance.

PPI network for differentially expressed proteins in WMM in *C. rastrospinosus* are seen in Table 9 & Table 10. **Figure 3-16** shows the network with more abundant proteins (A) and decreased abundance of proteins (B). The increased proteins PPI (relative ion area >30) had 45 protein nodes with 254 number of edges and a PPI enrichment p-value < 1.0e-16. Functional enrichment of the proteins showed, more abundant proteins belonging to SRP-dependent co-translational, glycolytic process, and complex V and protein transport. The less abundant PPI (relative ion area <20) had 21 protein nodes and 23 edges, with a PPI enrichment p-value < 1.23e-14 and the functional enrichment analysis showed proteins involved in regulation of NADP metabolic process, malate metabolic process, muscle filament sliding, transmembrane transport and isocitrate cellular homeostasis.

Supplementary Table 10. Proteins more in abundance in *C. rastrospinosus*

Accession Id's	Relative percentage of Total Ion Area	Protein Name
XP_010785279.1	33.2	myosin heavy chain fast skeletal muscle
XP_010776201.1	27.8	titin
AAO24738.1	64.0	creatine kinase muscle isoform 1
XP_010766208.1	56.0	pyruvate kinase PKM
XP_010781933.1	61.4	apolipoprotein B-100
XP_010779868.1	42.2	ATP synthase subunit alpha

XP_010794434.1	42.2	ATP-dependent 6-phosphofructokinase
XP_010785886.1	26.1	nucleoside diphosphate kinase B
XP_010769976.1	44.6	myosin-binding protein H
XP_010764264.1	35.1	elongation factor 2
XP_010774339.1	54.6	ADP/ATP translocase 1
XP_010788727.1	51.1	heat shock protein HSP 90-alpha 1
XP_010780749.1	46.6	malate dehydrogenase
XP_010774927.1	45.5	histone H2AX
XP_010791048.1	35.7	isocitrate dehydrogenase [NADP]
XP_010783416.1	34.3	ryanodine receptor 3
XP_010774282.1	73.6	immunoglobulin and fibronectin type III domain-containing protein 1 isoform X4
XP_010766317.1	34.5	malate dehydrogenase
XP_010782516.1	58.4	voltage-dependent anion-selective channel protein 3
XP_010788362.1	36.4	annexin A1
XP_010789292.1	42.1	eukaryotic initiation factor 4A-I
XP_010793340.1	49.8	obg ATPase 1
XP_010792965.1	33.6	40S ribosomal protein S4
XP_010766151.1	45.2	elongation factor 1-gamma
XP_010773292.1	43.9	dihydrolipoyllysine-residue acetyltransferase component of pyruvate dehydrogenase complex
XP_010771231.1	46.8	T-complex protein 1 subunit alpha
XP_010768032.1	37.1	40S ribosomal protein SA isoform X2
XP_010768026.1	37.1	40S ribosomal protein SA isoform X1
XP_010773064.1	47.8	phosphate carrier protein
XP_010783756.1	39.0	40S ribosomal protein S2
XP_010788327.1	67.6	nebulin
XP_010776310.1	43.7	60S ribosomal protein L9
XP_010794136.1	32.7	ATP synthase subunit g
XP_010793781.1	41.9	phosphoglycerate kinase
XP_010790499.1	32.7	60S ribosomal protein L35
XP_010782543.1	36.3	60S ribosomal protein L6
XP_010765728.1	46.2	ATP synthase subunit beta
XP_010779184.1	48.7	elongation factor 1-alpha
XP_010767902.1	59.4	hyaluronan and proteoglycan link protein 1
XP_010778067.1	49.6	ATP synthase subunit gamma isoform X1
XP_010778068.1	49.6	ATP synthase subunit gamma isoform X2
XP_010789836.1	39.4	60S ribosomal protein L13
XP_010778226.1	49.4	succinyl-CoA ligase [ADP/GDP-forming] subunit alpha
XP_010771562.1	32.6	glycogen debranching enzyme
XP_010786327.1	44.2	ATP synthase F (0) complex subunit B1 mitochondrial
XP_010787537.1	33.0	40S ribosomal protein S8
XP_010784438.1	33.7	ADP/ATP translocase 3
XP_010772744.1	60.2	calcium-binding mitochondrial carrier protein Aralar1
XP_010795693.1	51.1	60S ribosomal protein L4
XP_010777506.1	45.8	NADH-ubiquinone oxidoreductase 75 kDa subunit
XP_010772746.1	82.8	plasminogen activator inhibitor 1 RNA-binding protein isoform X2
XP_010768357.1	58.1	calcium-binding mitochondrial carrier protein Aralar1
XP_010782556.1	33.6	fructose-bisphosphate aldolase A
XP_010795485.1	46.0	fragile X mental retardation syndrome-related protein 1 isoform X3
XP_010772138.1	45.9	ATP synthase subunit O

XP_010784946.1	41.6	T-complex protein 1 subunit zeta
XP_010777740.1	39.1	inter-alpha-trypsin inhibitor heavy chain H3
QBF53709.1	85.1	hemopexin
XP_010766540.1	31.7	glyceraldehyde-3-phosphate dehydrogenase
XP_010769990.1	86.2	heat shock 70 kDa protein 6
XP_010783785.1	27	40S ribosomal protein S12
XP_010765856.1	24	60S ribosomal protein L30
XP_010779104.1	28.5	60S ribosomal protein L12 isoform X2
XP_010790870.1	22.7	Reticulon
XP_010793467.1	22.8	AMP deaminase 1 isoform X1 & X2 [Notothenia coriiceps]
XP_010794693.1	29.1	40S ribosomal protein S13 [Notothenia coriiceps]
XP_010783741.1	25.5	40S ribosomal protein
YP_004581500.1	25.9	Cytochrome c oxidase subunit II
XP_010776714.1	28.4	40S ribosomal protein S25
XP_010779161.1	29.1	60S ribosomal protein L11
XP_010791484.1	29.7	60S ribosomal protein L10a
XP_010786813.1	29.3	40S ribosomal protein S9
XP_010781656.1	28.1	Fructose-1 6-bisphosphatase isozyme 2-like

. Proteins more in abundance in *C. gunnari*

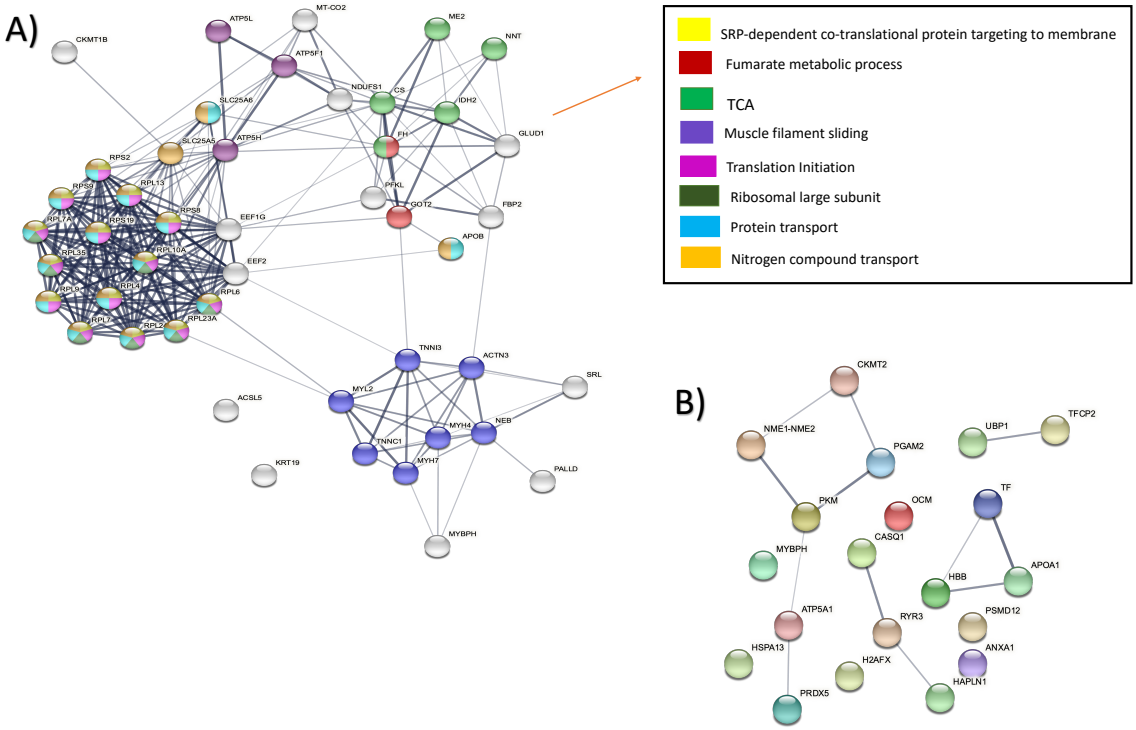

Figure 3-17. PPI networks generated by STRINGdb for proteins in WMM for *C. gunnari* A) Increased protein abundance. B) Decreased protein abundance.

PPI network for differentially expressed proteins in WMM in *C. gunnari* are seen in Supplementary **Table 11** & **Table 12**. **Figure 3-17** shows the network with more abundant proteins (A) and decreased abundance of proteins (B). The increased proteins PPI (relative ion area >30) had 46 protein nodes with 242 number of edges and a PPI enrichment p-value < 1.0e-16. Functional enrichment of the proteins showed, more abundant proteins belonging Sr-dependent co-translational, TCA, muscle filament, translation initiation, and protein transport. The less abundant PPI (relative ion area <20) had 32 protein nodes and 59 edges, with a PPI enrichment p-value= 0.000341, which is low and hence there wasn't any functional enrichment analysis for these set of proteins.

Supplementary Table 11. Proteins more in abundance in *C. gunnari*

Accession Id's	Relative percentage of Total Ion Area	Protein Name
XP_010770965.1	Myosin regulatory light chain 2 skeletal muscle isoform-like	94.4
XP_010791910.1	Myozenin-1 isoform X1 & X2	78.9
XP_010788098.1	Heat shock protein beta-1	74.6
XP_010790499.1	60S ribosomal protein L35	56

XP_010773777.1	40S ribosomal protein S16 isoform X1	52.8
XP_010770361.1	60S ribosomal protein L7	52.3
XP_010770797.1	Fragile X mental retardation syndrome-related protein 2	51.6
XP_010783785.1	40S ribosomal protein S12	50.8
XP_010765856.1	60S ribosomal protein L30	50.3
XP_010779104.1	60S ribosomal protein L12 isoform X2	49.8
XP_010790870.1	Reticulon	49.4
XP_010785200.1	Palladin-like	49.2
XP_010776310.1	60S ribosomal protein L9	48.7
XP_010793467.1	AMP deaminase 1 isoform X1 & X2 [Notothenia coriiceps]	48.4
XP_010784438.1	ADP/ATP translocase 3	47.8
XP_010794693.1	40S ribosomal protein S13 [Notothenia coriiceps]	47.3
XP_010787537.1	40S ribosomal protein S8-like partial	46
XP_010791686.1	Alpha-actinin-2	46
XP_010768845.1	Ryanodine receptor 3-like	32.9
XP_010791686.1	Alpha-actinin-2	46
XP_010774286.1	Kelch-like protein 41b	45.7
XP_010782543.1	60S ribosomal protein L6	45.4
XP_010783741.1	40S ribosomal protein S5	45.3
YP_004581500.1	Cytochrome c oxidase subunit II	44.7
XP_010776714.1	40S ribosomal protein S25	44.2
XP_010779161.1	60S ribosomal protein L11	43.7
XP_010767141.1	Voltage-dependent anion-selective channel protein 2	43.5
XP_010764830.1	40S ribosomal protein S26	32.7
XP_010792965.1	40S ribosomal protein S4	43
XP_010783756.1	40S ribosomal protein S2	42.8
XP_010791484.1	60S ribosomal protein L10a	40.4
XP_010786813.1	40S ribosomal protein S9	40.3
XP_010782695.1	ATP-dependent 6-phosphofructokinase muscle type-like	39.9
XP_010777740.1	Inter-alpha-trypsin inhibitor heavy chain H3-like	39.1
XP_010794136.1	ATP synthase subunit g	37
XP_010787927.1	Vinculin	37
XP_010789836.1	60S ribosomal protein L13	36.5
XP_010780163.1	Guanine nucleotide-binding protein subunit beta-2-like 1	36.2
XP_010781656.1	Fructose-1 6-bisphosphatase isozyme 2-like	36.1

XP_010768032.1	40S ribosomal protein SA isoform X2	35.3
XP_010778226.1	Succinyl-CoA ligase	35
XP_010766070.1	Tubulin alpha chain-like isoform X1 & X2	34.9
XP_010791811.1	60S ribosomal protein L23a	34.8
XP_010777506.1	NADH-ubiquinone oxidoreductase	34.7
XP_010765339.1	Alpha-enolase-like	34.5
XP_010791048.1	Isocitrate dehydrogenase	32.6
XP_010777584.1	26S proteasome non-ATPase regulatory subunit 12	30.6
XP_010786327.1	ATP synthase F (0) complex subunit B1	30.2
XP_010790691.1	Peptidyl-prolyl cis-trans isomerase-like	29.5
XP_010780749.1	Malate dehydrogenase	29.4
XP_010772138.1	ATP synthase subunit O	28.6
XP_010785896.1	Glycine-rich RNA-binding protein GRP2A-like	28.4
XP_010776087.1	NAD (P) transhydrogenase	28.3
XP_010788355.1	Glycogen phosphorylase muscle form-like	26.9
XP_010769500.1	Ubiquitin carboxyl-terminal hydrolase 5 isoform X1	26.7
XP_010784571.1	Cytochrome b-c1 complex subunit 2	25
XP_010778067.1	ATP synthase subunit gamma	24.7
XP_010765728.1	ATP synthase subunit beta	23.8
XP_010783619.1	Proteasome subunit alpha type-7-like	23.6
XP_010766216.1	Pyruvate kinase PKM	22.7
XP_010774042.1	FK506-binding protein 1	28.1
XP_010774927.1	histone H2AX	45.5
XP_010794764.1	fibronectin	34.9

Supplementary Table 12. Proteins less in abundance in *C. gunnari*

Accession Id's	Relative percentage of Total Ion Area	Protein Name
XP_010766216.1	22.7	pyruvate kinase PKM
XP_010779868.1	9.8	ATP synthase subunit alpha
XP_010785886.1	13.3	nucleoside diphosphate kinase B
XP_010788727.1	16.1	heat shock protein HSP 90-alpha 1

XP_010764982.1	6.2	myosin-binding protein H
XP_010770129.1	0.5	parvalbumin beta
XP_010774927.1	13.4	histone H2AX
XP_010782377.1	3.9	calsequestrin-1
XP_010782071.1	8.0	vitellogenin-2
XP_010792180.1	9.4	apolipoprotein A-I
XP_010772488.1	14.8	creatine kinase S-type
XP_010769328.1	11.8	phosphoglycerate mutase 2
XP_010786426.1	12.3	sarcalumenin isoform X2
XP_010783416.1	10.6	ryanodine receptor 3
AAC25100.1	3.4	alpha globin
AAC59671.1	3.4	alpha-1 globin
XP_010788362.1	8.1	annexin A1
XP_010771942.1	1.2	vitellogenin-1
AAL99930.1	0.2	IgM heavy chain secretory form
CAL92187.1	2.8	transferrin
XP_010767902.1	4.9	hyaluronan and proteoglycan link protein 1
AAC60372.1	3.4	beta-globin
XP_010765741.1	16.9	heat shock 70 kDa protein
XP_010783999.1	12.0	peroxiredoxin-5
XP_010778322.1	2.6	haemoglobin subunit zeta
XP_010777584.1	11.8	26S proteasome non-ATPase regulatory subunit 12
XP_010792310.1	4.8	actin cytoplasmic 3
XP_010768524.1	18.9	Calmodulin
XP_010773841.1	19.5	40S ribosomal protein S3a
XP_010790854.1	18.1	Obscurin isoform X2

Chapter 4 : Unconventional role of Haemoglobin alpha

Abstract:

The conventional role of haemoglobin (Hb) only as an oxygen and carbon dioxide transporter is being challenged by researchers due to enough evidence of its presence in different organelles [1–4] The protein was previously found to have enzymatic activity as it has structural similarity with other haem proteins. Even in the haemoglobin-less icefish within the Channichthyidae family, all species have retained the 3'truncated haemoglobin alpha (HbA) protein. Many mitochondrial changes have been observed in these fish including tight coupling of the mitochondria. ATPase inhibitor (ATPIF1), a mitochondrial enzyme, is involved in the regulation of the catalytic activity of ATP synthase (ATPase). Apart from interacting with ATPases, ATPIF1 has previously reported in interacting with a membrane protein other than ATPase [5]. The current study is aimed at understanding the sequential and structural changes in the haemoglobin alpha protein in the icefish compared to that of their closely related red-blooded fish and other well studied vertebrate species. We speculated whether HbA and ATPIF1 interact using in silico approaches of docking and molecular dynamics simulations. A change in expression of the protein ATPIF1 was also observed in the red muscle tissue of Antarctic icefish when compared to red-blooded species.

4.1 Introduction

The Antarctic fish, of perciform order Notothenioidei is very diverse due to evolutionary adaptations to survive in a challenging environment. The sub-order has eight known families under its name, Bovichtidae, Pseudaphritidae, Eleginopsidae, Nototheniidae, Harpagiferidae, Bathydraconidae and Channichthyidae. Notothenioidei have acquired traits for survival such as the expression of antifreeze glycoproteins [6], they have also undergone losses like the heat shock response [7] and of the protein haemoglobin (Hb/Hbs) which is absent in the Channichthyidae family, also known as the icefish (species from this family are referred to as icefish in this manuscript from hereon) [8]. The absence of Hb has been attributed to a single deletional event, where the fish lost the globin genes, retaining just the 3'end of alpha-globin (HbA/α-globin) [9,10]. The remnants of the α-globin gene contain the 3' portion of intron 2, exon 3, and the 3' untranslated region of α-globin gene [11]. Myoglobin is absent in the oxidative skeletal muscle of all icefish, but the absence of myoglobin in cardiac muscle has only been reported in the six species of Channichthyinae[12,13]. The red-blooded species have also evolved physiological and molecular adaptations, with a decrease in the concentration of Hb and its affinity for oxygen[14]. The reduced haematocrit in these fish has led to decrease in the elemental iron[15] . Though there are subtle differences the α-globin gene of the red-blooded species is very similar to that of other vertebrates[11].The remnant α-globin genes from icefish *Chionodraco rastrospinosus* (*C. rastrospinosus*) and *Chaenocephalus aceratus* (*C. aceratus*) show 96.4% and 95.1% similarity respectively, with the overlapping regions of the gene from *Notothenia corriceps* (*N. corriceps*), a red-blooded species from the family Nototheniidae[11]. The loss of Hb and Mb in the icefish is related to increased levels of nitric oxide (NO) levels compared with the red-blooded species[16]. The fish *C. gunnari* has been an exception for most of its adaptation. Even with nitric oxide (NO) steady state levels all icefish have higher steady state levels of NO except *C. gunnari*, that has an NO concentration similar to that of red-blooded species[17]. Previously, we reported changes we found in mitochondrial encoded protein ATP6, a key subunit of the F0 component of ATP synthase complex (ATPase/complex V) in the icefish *C. gunnari*[18].

The structure of haemoglobin was elucidated in 1966 by Nobel Laureate Dr. Max F Perutz[19]. The protein has four subunits, with each having one polypeptide chain, alpha of 141 amino acids and beta of 146 amino acids in humans, and one haeme group. The alpha chain of all human Hbs remains the same throughout adult life unlike the beta chain which switches from foetal to adult HbB, that is developmentally regulated[20]. Hb is synthesised in a complex series of steps, where the haem moiety is partially synthesised in mitochondria and cytosol, and globin proteins are synthesised by ribosomes in the cytosol[21,22]. Conventionally Hb, is known as a two-way respiratory carrier, transporting oxygen and carbon dioxide. At a low pH, the cooperative oxygen binding capacity of Hb is decreased due to significant conformational changes in its structure[23,24]. Hbs are highly sensitive to temperature and the structure and function could be influenced by its environmental conditions encountered by its species. Amino-acid substitutions can be attributed to many the functional differences in the vertebrate Hbs in correlation with species-adaptation theory by Perutz[25].

The concept that Hb is only responsible for carrying oxygen and carbon dioxide is being challenged by new research around the protein. As it stands, the protein shares structure similarities with other haemoproteins which corresponds to its enzymatic activities. It has been seen to play protective roles against oxidative and nitrostative stresses[26]. The deoxy structure of Hb has a higher affinity for protons, chloride, and organic phosphate than oxygen. In high Antarctic notothenioids the presence of single Hb in contrast to the normal multiplicity or several globin gene highlights its reduced role as an oxygen-carrier [14]. Several studies have shown the binding of adenosine nucleotides to haemoglobin[27–30]. HbA, specifically has been assigned roles other than that of oxygen transport, such as in vascular remodelling through endothelial nitric oxide signalling[1,31]. The structure analysis of the remnant HbA in the icefish has shown that all the haem binding sites are excluded from the fragment[4]. These evidence suggests that Hb could be having a role other than that of transporting gases. The genome of *Notothenia corriceps* (*N. corriceps*) shows that Hb and some mitochondrial proteins have adapted to increase the efficiency of aerobic cellular respiration for these Antarctic species and support the oxidative phosphorylation mechanism[32].

In vertebrates the majority of energy requirements are met by the ATP produced through the oxidative phosphorylation pathway. Complex V is responsible for the production of intracellular ATP from ADP and inorganic phosphate, the final step of oxidative phosphorylation. ATPase is a multi-subunit complex where each subunit is directly or indirectly involved in mitochondrial protein interactions and facilitates mitochondrial function[33]. The activity of proton pumping in complex V is regulated by ADP, proton motive force and by its natural inhibitor Inhibitory Factor 1 (IF1). To advance our understanding of the protein interactome within mitochondria, it is important to detect, dynamic or/and transient interaction between different membrane proteins. Cellular functions rely on protein-protein interactions. A lot of literature is available on protein-ligand interactions, but macromolecular interactions have come to light only recently[34,35]. Previously, Hb in neurons has been shown to act as a sensor of energy status, where Hb is linked to ATP concentration and mitochondria function[36].
The ATPase inhibitory factor 1 (ATPIF1/IF1), is a natural regulator of ATP synthase activity. It is a protein of 84 amino acids, regulates proton motive force via mitochondrial influx of H+ ions, mitochondrial structure, and ATP synthesis. When the membrane potential is low the reverse action of ATPase, that is hydrolysis of ATP is favoured. This hydrolysis is inhibited by IF1, and a restoration of the membrane potential displaces IF1 from ATPase interacting with its γ subunit of F1 domain. At pH 6.5 the hydrolase activity of ATPase is inhibited and is dimeric, at pH 8 it forms a tetramer. The residues between position 32 and 43 are necessary for a tetramer formation and are pH dependent. The protein dimerises in antiparallel α-helical fashion and inhibits the hydrolysis activity of ATPase and, in its tetrameric form the inhibitory regions are masked. In the conditions of low oxygen or an uncoupler of oxidative phosphorylation, ATP hydrolysis is favoured, and glycolysis becomes the only source of ATP. Due to this the cytosolic pH decreases that subsequently decreases the pH of mitochondrial matrix where ATP is made, promoting the action of IF1[37]. The question that still is unanswered is where does the unbound tetrameric IF1 go in the mitochondrion? A study conducted in 1993 suggested that the mitochondrial inhibitor protein IF1

docks to a membrane protein other than that of ATP synthase[5]. This binding to a small protein of 5-6 kDa hampers the activity of IF1 as an inhibitor of ATPase[5]. Interestingly, a zebrafish non-lethal mutant for gene pinotage (*pnt*) was found to be anaemic despite normal expression of the β-globin and another erythroid cell marker, band-3. The candidate gene found for the pnt locus was ATPIF1, further the results showed a reduced level of expression of atpif1a[38]. The teleosts have a gene duplication for atpif1[39]. However, on conducting a nucleotide BLAST search with atpif1 nucleotide sequence from zebrafish against the Notothenioidei (taxid:8205) species we found a similarity of 76.98% with the atp5if1a with the red-blooded species *Trematomus bernacchii* (*T. bernacchii*) and *Notothenia corriceps* (*N. corriceps*) and 72.63% and 72.98 for atp5if1b respectively for the two species. The BLAST search for atp5if1b resulted 76.11% and 75.83 with atp5if1b from *N. corriceps* and *T. bernacchi*i, and 70.04 % for atp5if1a for both the species. The zebrafish study also went on to show that a knockdown of atpif1a lacked haemoglobinized cells[38]. A possible role of atpif1a is suggested in haeme synthesis, as the protein was seen increased in expression with other proteins required for haeme synthesis such as ferrochelatase and mitoferrin in developing erythroblasts[38].

In this work we combine sequence and structure analysis to understand the conservation and variation in the remnant HbA sequence of the icefish aligned with other notothenioid species as well as vertebrate species. We also investigate a previously raised question whether the remnant C-terminal peptide of HbA in the two icefish and subsequently the protein, has an alternative role in the cellular machinery. We have used molecular docking and molecular dynamics (MD) to decipher if the ATP complex inhibitor interacts with haemoglobin. By employing dynamic refinement using MD simulations the aim is to find the lowest macromolecular association complex energy of the docked proteins.

4.2 Methodology

4.2.1 Multiple Sequence Alignment

The list of protein sequences were obtained from the National Centre for Biotechnology Information (NCBI) protein database search, we chose only the Refseq (provides a comprehensive, integrated, non-redundant, well-annotated set of sequences, including genomic DNA, transcripts, and proteins) sequence queries (https://www.ncbi.nlm.nih.gov/ lMSast searched:4th March 2021). Though these sequences have been taken from highly reliable Refseq database [40] validated by different sources it is important to recognise they could still be prone to error. (-/-) Indicates absence of both haemoglobin and myoglobin genes, whereas (-/+) indicates absence of haemoglobin but presence of myoglobin. The sequences for the Notothenioidei suborder species *C. rastrospinosus* (-/+), *C. aceratus* (-/-), red-blooded Antarctic fish, *T. newnesi*, *T. bernacchii*, *N. corriceps*, *N. angustata*, *N. neglecta*, *P. borchgrevinki*, *D. mawsoni*, *G. acuticeps*, *C. mawsoni*, *G. gibberifrons*, and sub-Antarctic species, *E. maclovinus*, five fish species including, *S. trutta*, *O. mykiss*, *S. namacyus*, *D. rerio*, and *N. furzeri* as an outgroup, mammalian species, *H. glaber*, *M. musculus*, *B. taurus*, *P. Anubis* and *H. sapiens*. CLUSTAL [41] were used for the initial alignment of ATP6 protein under the criteria of the presence and the absence of haemoglobin and myoglobin proteins in the species, the alignments were also verified using the other two progressive methods, MAFFT [42] and MUSCLE. The same method was applied for protein ATP8. The MSA was visualised and edited using JALVIEW [43]. The selection of these different species shows the conservation of these mitochondrial proteins across vertebrate species, including H. sapiens.

4.2.2 Comparison of properties of amino acids for HbA among the species.

Using the ExPASy [44] tool ProtScale, different amino acid properties such as the molecular weight of amino acids across the sequence, hydrophobicity trend of amino acids, α--helix forming amino acids, average flexibility trend and mutability for the protein HbA were compared graphically for all the species. (https://web.expasy.org/protscale/).

4.2.3 Structure prediction and structure alignment for protein sequences.

Structures for HbA in the Antarctic species were created using the structure prediction tool I-TASSER [45] (Iterative Threading ASSEmbly Refinement) a hierarchical approach to protein structure and function prediction (https://zhanglab.ccmb.med.umich.edu/I-TASSER/). The structures were validated using SAVES v6.0 (https://saves.mbi.ucla.edu/), using ERRAT, PROCHECK [46] and ProSA-web [47]. (Figures in supplementary files). The structure for the 3'HbA fragment for *C. rastrospinosus* was aligned with the red-blooded species, D. mawsoni, sub-Antarctic species *E. maclovinus*, fish species, *S. trutta* and *D. rerio*, mammalian species, *M. musculus* (PDB:3HRW) and *H. sapiens* (PDB:4HHB) using TM-Align suite (https://zhanggroup.org/TM-align/).

4.2.4 Structures from PDB for investigation.

The ATPIF1 3D structure was extracted from its X-ray resolved complex with ATP synthase complex from *B. taurus (*cow) (PDB ID: 1GMJ) and was used for docking simulations. The choice of the selection of the organism is due to the fact that *B. taurus* is the only verified structure from mammals available. The haemoglobin structure was taken from 3D structure of haemoglobin from *B. taurus (*PDB ID:6II1), to keep the consistency in the choice of organism and was prepared for docking as tetrameric, dimeric, and monomeric forms (only HbA). All protein structures were minimised before proceeding with docking.

4.2.5 Protein-protein docking.

Patch dock protein-protein[48] docking (bioinfo3d.cs.tau.ac.il/ PatchDock/) server was used for different dockings a) ATPIF1 to ATPase complex. B) ATPIF1 monomer to Hb all chains no ligands. C) ATPIF1 dimer to Hb all chains no ligands. D) ATPIF1 monomer with HB dimer E) ATPIF1 dimer to Hb dimer. F) ATPIF1 with HbA chains A and C. G) Voxelotor inhibitor for Hb. The results obtained from this server were further improved with submission to associate refinement server FireDock [49]. The poses were selected based on Global energy. The PDBsum interaction analysis represents interaction residues on either chain with residues shown in different colours based on their properties and the coloured lines joining these residues representing the type of interaction between these residues [50]. The docked proteins were analysed and visualised using UCSF Chimera [51]. The proteins were docked using different webservers for comparison, HDOCK [52] and ClusPro[53] (Supplementary Figure 3). All proteins were minimised using Chimera [51].

Molecular dynamics of protein–protein complexes and MM/ PBSA calculation

Protein–protein complexes were subsequently prepared for MD simulation with GROMACS ('S2352711015000059', no date) by generating topology files and coordinate files. Simulation boxes of 11.88 × 11.88 × 11.88 nm (Hb All chains-IF1), 11.89× 11.89 × 11.89 nm (HbA – IF1), were initially set, with the protein complex centred inside. spc216.gro solvent configuration was used to add water molecules together with the addition of NaCl to neutralize the entire system. The resulting models were parametrised using AMBER99SB-ILDNP Force Field [55,56] implemented in the GROMACS 5.0 software package. A robust energy minimization protocol was applied consisting of 50 000 cycles with the Steepest Descent minimization algorithm (Fmax < 1500 kJ mol−1) was reached. Velocity was generated using a V-rescale thermostat,48 according to a Maxwell distribution at 310 K, with a short 200 ps run in the NVT ensemble. Position restraints were applied to the protein with a force constant of 1000 kJ mol−1, for the whole NVT run. The accurate leap-frog algorithm was used as the MD integrator for the whole dynamics using 0.002 fs as the time step for integration. Periodic boundary conditions were applied in all directions (pbc = XYZ). The LINCS algorithm was used to constrain the stretching of all bonds. Electrostatic interactions were calculated applying the Particle Mesh Ewald (PME) algorithm and a cut-off at 1.2 nm.49 The same cut-off (1.2 nm) was also chosen for switching off the van der Waals potential. Changing the ensemble to the NPT one required an 8 ns equilibration run with the Parrinello–Rahman algorithm for

pressure coupling under isotropic conditions and V-rescale was still used for temperature coupling. MD analysis was mostly performed using Pymol[57] and CHIMERA[51].
We used a similar approach to the docking as mentioned in the protein-protein interaction of human glyoxalase II paper[58].

4.2.6 Western Blotting.

Antarctic Fish Muscle tissue samples. This Antarctic fish project was approved by Veterinary School's Clinical Ethical Review panel, University of Nottingham, with responses from at least four members of the panel. No ethical issues were raised by the panel and assigned #2744 190509. White muscle and red muscle samples of notothenioid Antarctic fish, Red-Blooded fish species – N. rossii, T. bernacchhii (Cruise PS112) and Icefish species- C. gunnari, C. rastorspinosus (Cruise ANTXXVIII) were obtained from Dr. Magnus Lucassen of the Alfred-Wegener-Institut, Helmholtzzentrum für Polar- und Meeresforschung - Integrative Ecophysiology Institute. N. rossii and T. bernacchhii have 30-45 % haematocrit and 18-28 % haematocrit respectively. Both icefish species lack haemoglobin, whereas C. gunnari lacks myoglobin as well. Each sample weighed about 200-300mg. Summary of samples given in Table 1.

Species	Tissue	Sample No
N. rossii	Red muscle	4-27
T. bernacchii	Red muscle	5-12
C. rastrospinosus	Red muscle	1355
C. gunnari	Red muscle	690

Whole cell fractions were prepared with buffer (100 mM dithiothreitol, LDS) and boiled for 10 min. Protein samples were resolved by SDS-PAGE, transferred to nitrocellulose membrane (Thermo Scientific), and blocked in 3% milk (w/v) in tris Buffered Saline-Tween 20 (TBS-T) for 1 hour at room temperature. The membrane was probed with primary antibody ATPIF1 rabbit polyclonal (sigma SAB2100188) 1:1000 dilution, overnight at 4 C, blocked in 3% BSA (w/v) in TBS-T. Washed with TBS-T 5mins x 3. Immunoblots were then probed with horseradish peroxidase-coupled anti-rabbit antibodies (abcam ab6721) at 1:5000 dilution and developed with Enhanced Chemiluminescent Plus reagent (Pierce Thermofisher) and incubated for 5 minutes on the roller at room temperature. Bands were visualised using the ChemiDoc visualizer using the chemiluminescence and colorimetry option.

4.3 Results

4.3.1 Protein sequence and structure alignment of HbA

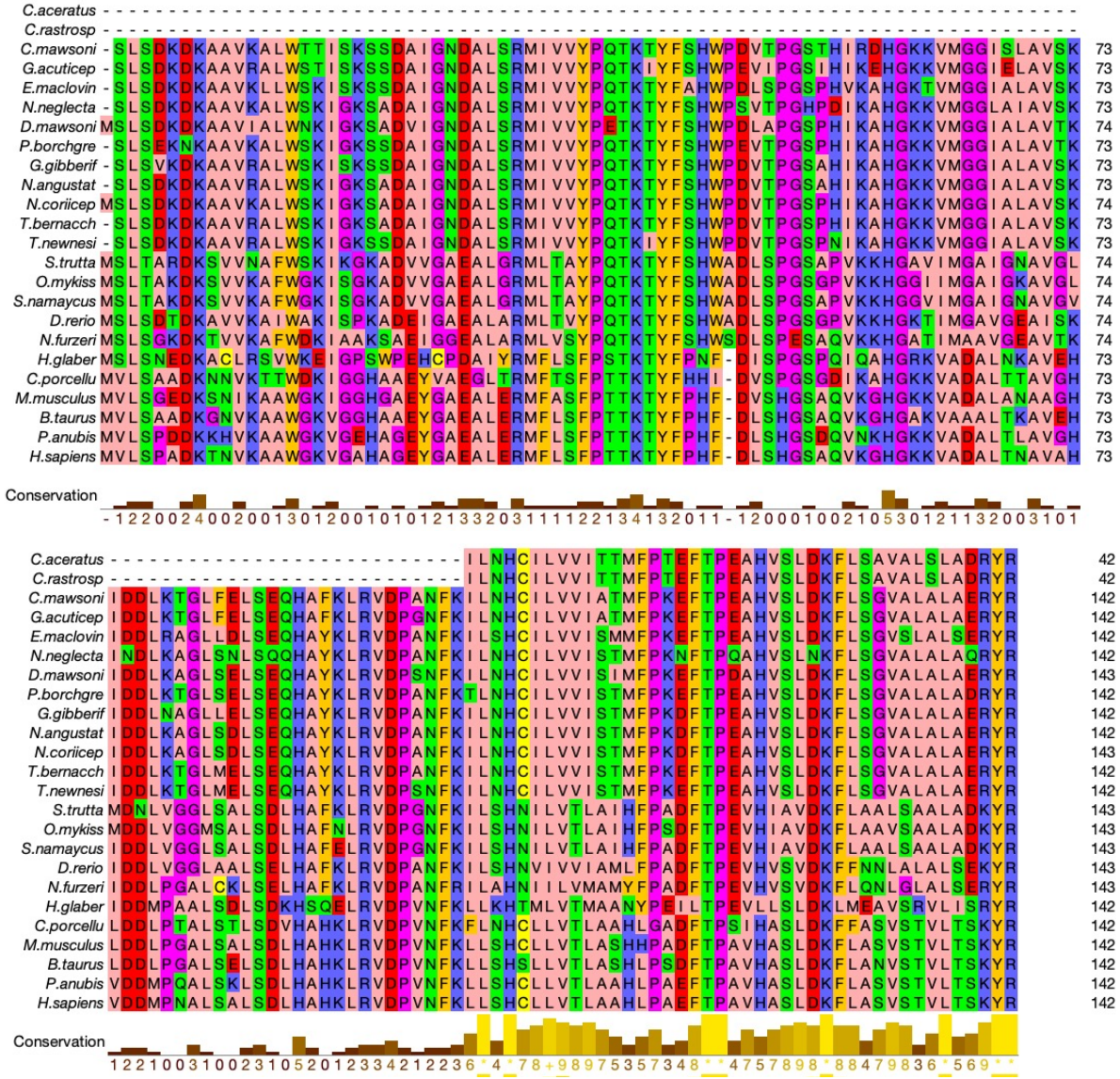

Figure 4-1. Multiple Sequence Alignment of haemoglobin subunit alpha sequences. The HbA protein sequences were aligned using Clustal omega and visualised using zappo colour scheme in JalView. (Colours according to physio-chemical properties of amino acids; Aliphatic/hydrophobic-A, I, L, M, V- light pink; Aromatic-F, W, Y- mustard; Conformationally special-Glycine, P- magenta; C-yellow; Hydrophilic- N, Q, S, Q, T- light green; Negatively charged/D,E-Red; Positively charged/R,H,K-Blue) in jalview. The bar-graphs below represent a quantitative measure of conservation at each position. The figure was created using JalView. The conservation bargraph shows how each residue is conserve for that position in the given alignment.

The complete HbA sequences were aligned for twenty-four vertebrate species showing conserved sequences across the species based on identity and similarity (**Figure 4-1**). Fifteen out of the sixteen species of icefish from the subfamily Channichthyinae, have retained only a 3' fragment of an α-globin gene. Figure 1 shows the alignment of two icefish, *C. rastrospinosus* & *C. gunnari*, α-globin fragment, with five closely related red-blooded Antarctic fish, *T. newnesi*, *T.*

bernacchii, *N. corriceps*, *N. angustata*, *N. neglecta*, *P. borchgrevinki, D. mawsoni*, *G. acuticeps, C. mawsoni*, *G. gibberifrons*, and sub-Antarctic species, *E. maclovinus*, five fish species including, *S. trutta*, *O. mykiss*, *S. namacyus*, D. rerio, and N. furzeri also as an outgroup, mammalian species, *H. glaber*, *M. musculus*, *B. taurus*, *P. Anubis* and *H. sapiens*. The protein sequence for HbA is highly conserved across the twenty-four vertebrate species, including the C-terminal fragment of the two icefish species. The C-terminal end of HbA is relatively more hydrophobic in comparison to the whole protein sequence (Figure 2 B). The icefish HbA remnant is identical to the rest of the closely Antarctic fish species. Previously it has been suggested that 3' truncated HbA that was not eliminated genetically might be still expressed as a protein influencing the cellular machinery of these fish[4] . Preservation of a deleterious trait even when these fish have adapted to a diffusion-based oxygen transport which has a higher energetic cost[59], suggests an alternate role to the protein as seen in previous studies[1,31].

A conservation of residues, Ile-Leu-Arg-His-Cys-Ile-Leu-Val-Val-Ile-x-x-Meth-Phe-Pro-Lys-AspA/GluA-Phe-Thr-Pro-GluA-Ala-His-Val-Ser-Leu-AspA-Lys-Phe-Leu-Gly-Val-Ala-Leu-Ala-Glu-Arg-Trp-Arg is seen for all the species. The icefish have two distinctive changes in their 3'truncated HbA sequence, one at position 136/137 where all species except the icefish have an alanine whereas the icefish has a serine residue. The other is the presence of alanine at the position 132/133 instead of glycine as in all their closely related red-blooded Antarctic and sub-Antarctic species. A glycine to alanine or vice-versa change can interfere with the conformation and flexibility of the protein, this is because conventionally alanine is bigger than glycine due to an additional methyl group. This has been seen before for mitochondrial protein cytochrome b [60],even single change of Gly to Ala may have pathological significance [61]. Having a Gly residue instead of alanine brings down the stability in small peptide[62]. Sometimes adaptive changes in structure happens away from its active site which could affect the thermal stability and energy changes associated with it, one such trend is having glycine clusters[63].

Position 139 is occupied by serine for all mammalian species whereas the other species have either glutamic acid or aspartic acid for the same position with an exception to this in notothenioid species *N. neglecta* that has glutamine in that position. Serine is often mutated to glutamic acid and/or sometimes to aspartic acid to mimic phosphorylation of the serine. The conserved residue lysine at positions 102 and 137 are predicted to be a binding site by I-TASSER structure and function prediction tool.

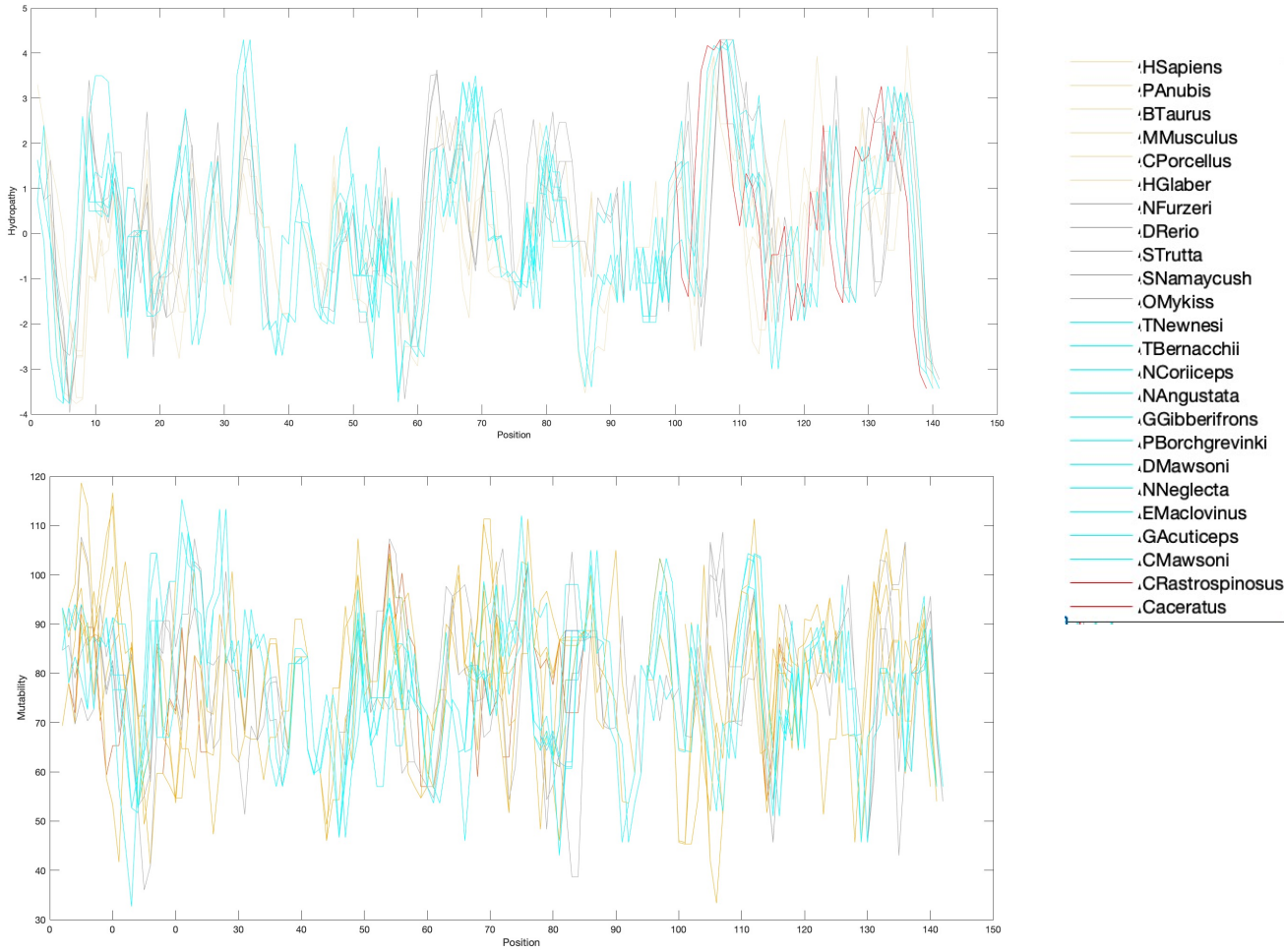

Figure 4-2. Primary sequence features of HbA across the twenty-four vertebrate species.

When comparing the amino acid properties of such as hydrophobicity and mutability (**Figure 4-2**), the Hb sequences are quite conserved across vertebrate species, where the C-terminal is hydrophobic with a hydrophilic tail of three amino residues. The mutability graph (graph 2) shows a likelihood of variability at the N-terminal end than C-terminal end for HbA, also seen in the alignment (**Figure 4-1**), the conservation bar graph.

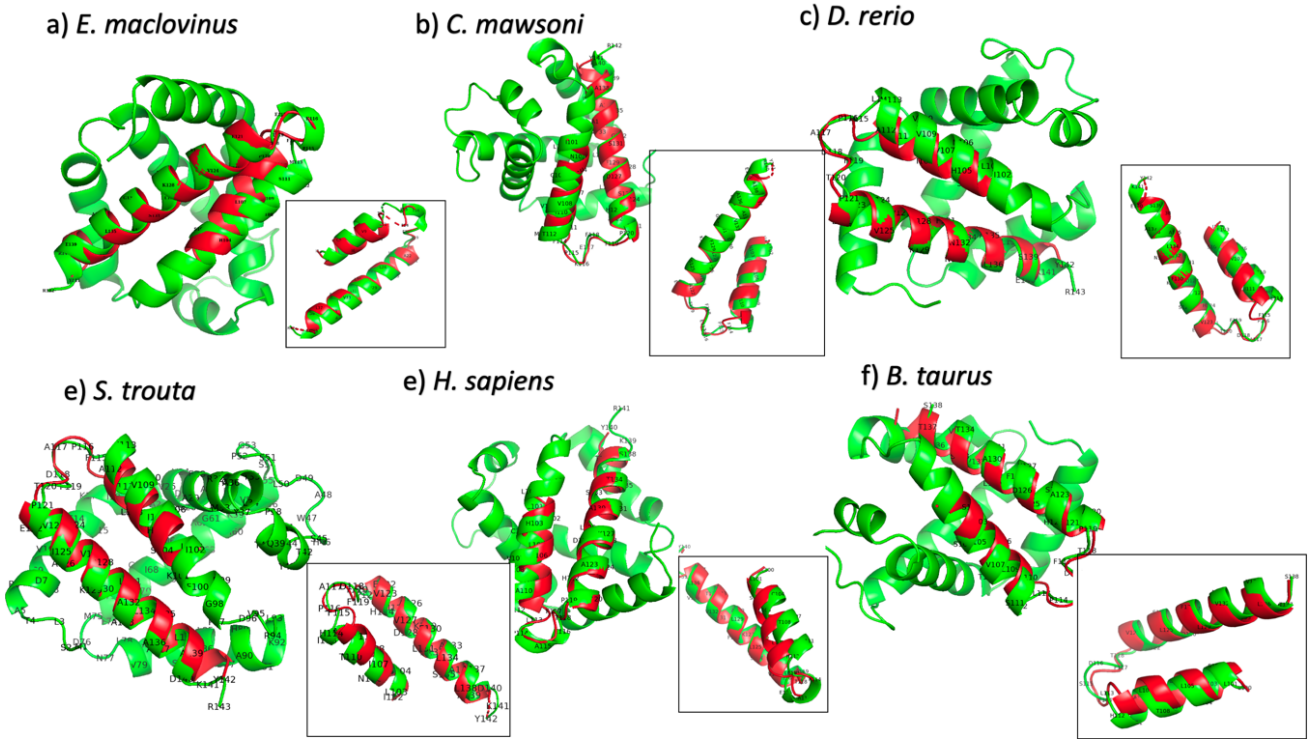

Figure 4-3. Truncated HbA protein structure (red) from icefish *C. aceratus* (structure obtained using I-TASSER) aligned to HbA sequences (green) of related red-blooded species *C. mawsoni*, sub-Antarctic species E. maclovinus, two fish species, *D. rerio* and *S. trutta,* and mammalian species, *H. sapiens* (PDB ID: 4HHB) and *B. taurus* (PDB ID: 6II1) using TM-ALIGN.

We mapped the truncated 3'HbA fragment from the icefish *C. aceratus* (structure produced using I-TASSER from NCBI ID sequence: AAC25098.1) with HbA sequences from sub-Antarctic species, E. maclovinus, closely related red-blooded species *C. mawsoni*, fish species *D. rerio* and *S. trutta* and mammalian species, *H. sapiens* and *B. taurus*. The predicted alignment showed that the icefish has retained predicted ligand binding sites, 102 and 137 (Hit PDB ID: 3KMF).

The truncated HbA sequence was used to model a structure for the peptide in the icefish *C. aceratus* (I-TASSER[45]) and structurally aligned to the sub-Antarctic species, *E. maclovinus*, closely related red-blooded species, *C. mawsoni*, fish species, *D. rerio* and *S. trouta* and, mammalian species, *H. sapiens* and *B. taurus* aligned using TM-Align ((**Figure 4-3**). As can be seen, the residues involved haem group stabilisation and O2 binding ability are missing in the truncated HbA sequence[4]. The truncated HbA from icefish has two helices, a truncated smaller helix and C-terminal helix. The larger helix aligns structurally perfectly for all the species. A slight difference in the structure of the truncated helix is observed.

4.3.2 Westerns ATP-IF1 Notothenioid tissues

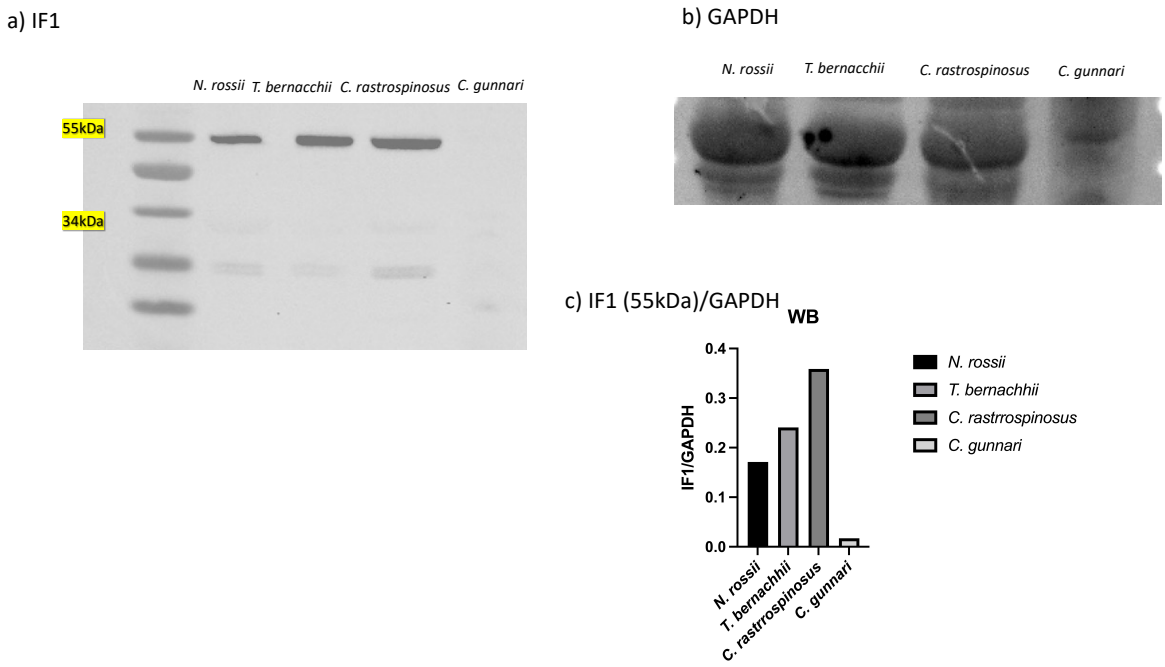

Figure 4-4. Western analysis of ATP synthase complex inhibitory factor 1 (ATPIF1) in whole cell lysate from red muscle tissue of notothenioid fish. ATPIF1 is seen reduced in icefish *C. gunnari* (a, c). The GAPDH control shows the presence of the proteins (b) in the lysate for *C. gunnari*.

The bands for ATP-IF1 appear at a larger weight that is predicted. The predicted band size is Bands were observed at 34kDa and 55kDa (**Figure 4-4**). The expression of protein was seen highest in icefish, *C. rastrospinosus*. The antibody Is seen to have bands at 50kDa and 10kDa previously, the higher band observed was as the gel was run for a shorter duration of 25 mins instead of 35 mins. No or low expression was observed for *C. gunnari*, but by seeing the intensity of bands of the control, GAPDH, there might be low protein loaded, and the expression might be lower and not completely absent. A co-immunoprecipitation with ATPIF1 antibody with *N. rossii* red muscle tissue lysate was performed followed by western analysis for the final eluted proteins and last wash buffer proteins with, antibodies HbA and HbB. Interestingly, a faint HbA band was observed in the last wash buffer protein lane (Appendix C **Figure 4-12**). No band was observed for HbB for any of the protein extractions. To further this investigation, we performed docking and MD simulations for Hb and ATPIF1, as discussed in the subsequent sections.

4.3.3 Docking ATPIF1 to Haemoglobin

Table 4-1 Docking scores from PatchDock and FireDock for Haemoglobin alpha chain and ATP-IF1. Global energy calculated by FireDock is the binding energy of the compound in solution. Score calculated by PatchDock represents the geometric shape complementary, higher the score lesser the stearic clashes. Area shows in approximate interface area of the complex. ACE is the atomic contact energy, the energy required transfer from water to protein site. Attractive van der Waals (VdW) indicate specific binding of the protein in that pose.

S. No. (FireDock)	Solution Number (PatchDock)	Global Energy (kcal/mol)	Attractive VdW (kcal/mol)	Repulsive VdW (kcal/mol)	ACE (kcal/mol)	Score	Area
1	8	-37.84	-27.85	13.77	3.13	11588	1356.50
2	3	-20.75	-18.22	6.18	2.50	11988	1706.30
3	34	-19.64	-33.34	24.33	10.24	10584	1428.20
4	25	-10.15	-28.12	15.34	6.04	10824	1323.70
5	43	-5.36	-37.07	30.53	18.52	10296	1449.80
6	31	-5.14	-27.18	7.12	12.45	10608	1849.70
7	2	-3.89	-28.98	7.95	5.50	12304	1659.30
8	5	-2.64	-18.48	2.52	6.48	11966	1606.50

The work is focused on the protein-protein interactions involved in possible Hb-ATPIF1. We have used the well-established structures of haemoglobin (PDB ID-6II1) and ATP-IF1 (PDB ID- 1GMJ) for organisms *Bos taurus*. PatchDock is an online webserver for protein-protein docking accurately predicting residue-residue contacts in the target interaction[48]. It uses a scoring function that considers both geometric fit and atomic desolvation energy with a final application of RMSD (root mean square deviation) to remove redundant solutions. Table 1 and Table 2 have the geometric score, interface area size and normalised desolvation energy from PatchDock and subsequently FireDock tools for docking of ATPIF1 with Hb all chains and HbA respectively. FireDock server provides flexible refinement and scoring. The different docking poses revealed that if ATPIF1 were to interact with Hb, it interacts with the c-terminal end of the alpha globin chain. This was also seen with other automated servers HDOCK[52] and ClusPro (Appendix C **Figure 4-14**). Docking was performed for minimised structure of Hb with all chains and no ligands and for HbA chain C with ATPIF1 chain. The docking of known inhibitor of Hb, voxelotor, was also performed using PatchDock to compare it to the docking with ATPIF1 (Appendix C **Figure 4-13**).

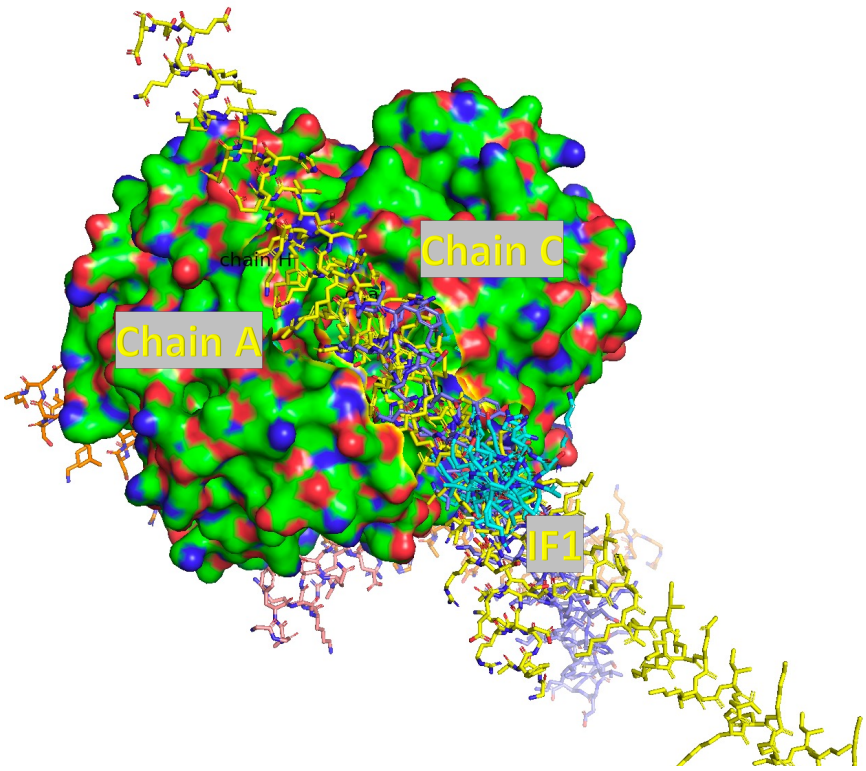

Figure 4-5. Top 10 best ranked Docking results for Hb-all chains and IF1. Hb is represented by a molecular green surface, the IF1 structures are represented by different colours

On docking the IF1-monomer to Hb-all chains tetramer, we chose 50 docking conformations ranked based on their PatchDock scores and then submitted to Firedock refinement. The top 10 were selected based on global energy (**Figure 4-5**). After assessing the structures using Ramachandran plot to validate the docking pose, we chose FireDock solution number 1 (solution 8 of PatchDock), the conformation that had high global energy, attractive van der Waals and low repulsive van der Waals (**Table 4-1**). A high global energy indicates robust binding of two proteins. Solution 8 docked pose showed interactions of IF1 with Hb chains A and C (**Figure 4-6**). More interactions with Chain C of HbA were seen (**Figure 4-7**), Chain C was then used as a monomer to dock with IF1 again using PatchDock and FireDock (**Figure 4-8**). The subsequent best docked score also showed that the IF1 interacts with the c-terminal end residues of HbA (**Figure 4-16)**.

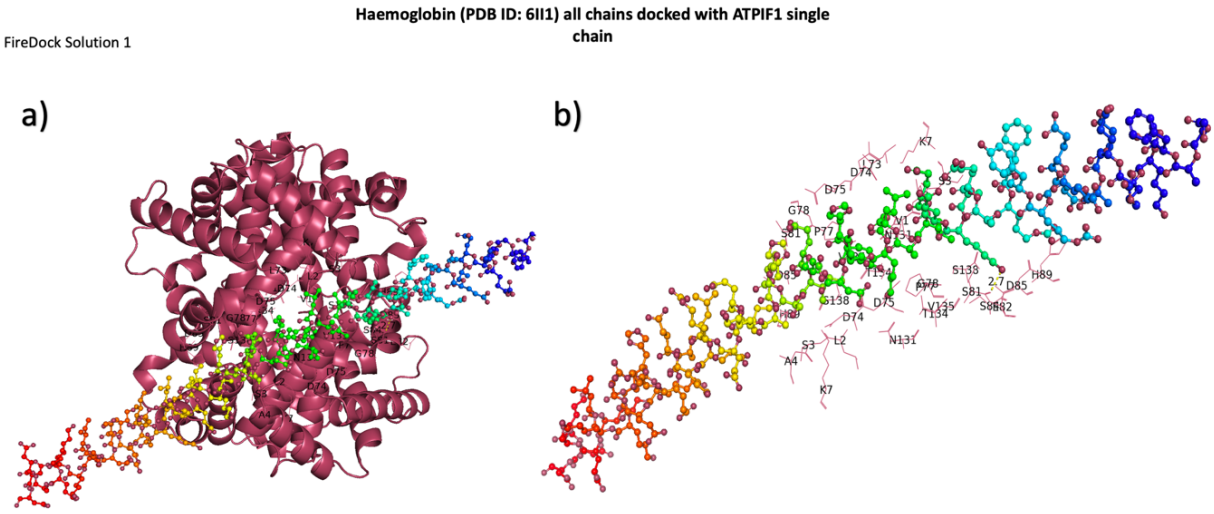

Figure 4-6. The interacting residues of haemoglobin with ATPIF1 best docked pose using PatchDock (Schneidman-Duhovny *et al.*, 2005) and FireDock (Andrusier, Nussinov and Wolfson, 2007) refinement tool. (Hb PDB ID:6II1; ATPIF1 PDB ID: 1GMJ).

Docking the minimised structure of Hb (including all chains, AC chains HbA and BD chains corresponding HbB) with minimised structure of IF1 (chain H), the best refined-docked structure showed contacts between the two alpha chains of Hb with IF1.

The possible interaction of IF1 (monomer) with Hb all chains (**Figure 4-6**) and only HbA chains (**Figure 4-8**) was assessed. The previous study that has suggested that IF1 binds to a membrane protein may maintain the protein monomer form while binding to the unknown membrane protein[5] . The bovine IF1 is 84 amino acids in length. IF1 attaches to F1 catalytic subunit of ATPase to inhibit its hydrolysis activity when conditions are unfavourable such as absence of oxygen. At that point the IF1 forms a dimer, and its N-terminal region is free to be inserted in the F1 heads. The binding depends on the presence of MgATP.

The energy stable computational structures produced by PatchDock showed residues 35-60 of IF1 interacting with Hb (all chain) residues (**Figure 4-6 & Figure 4-7**). Residues between 32-43 contains amino acid that are involved in pH dependent interconversion in the states from dimer to tetramer for IF1[37]. Residue 39, lysine in IF1 chain makes a polar hydrogen bond with Serine 81 of Hb Chain A of HbA.

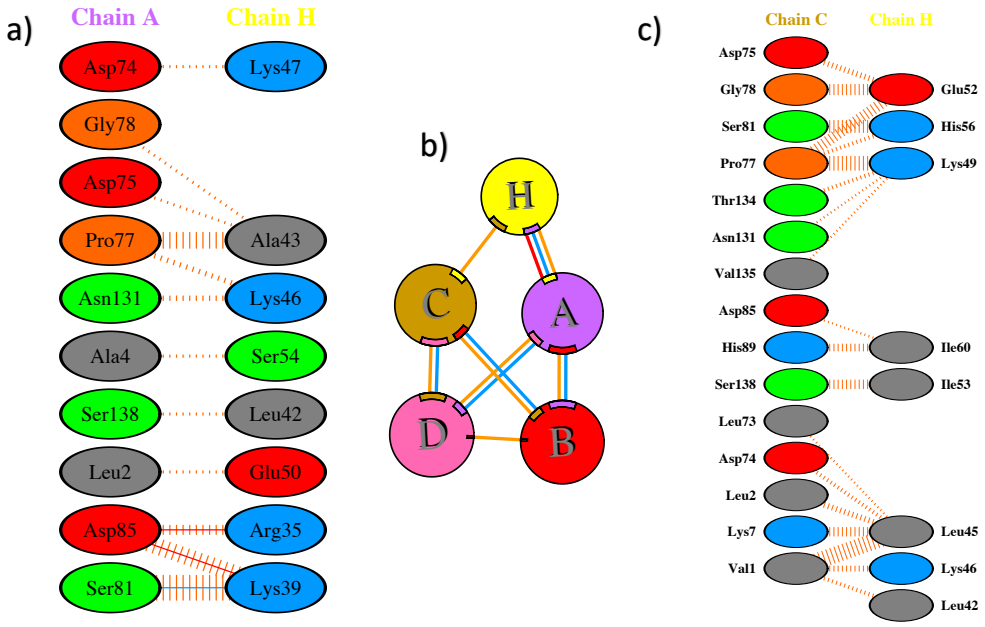

Figure 4-7. Graphical representation of interacting residues of protein chains for (Figure 4-6**)** dock pose generated using PDBsum (Laskowski *et al.*, 2018). Interacting chains are joined by coloured lines representing different kind of interactions; red- salt bridges, yellow- disulphide bonds, blue-hydrogen bonds, orange-non bonded contacts. Each amino acid residue colour represents different properties; blue- positively charged (H,K,R), red-negatively charged (D,E), green- neutral (S,T,N,Q), grey-aliphatic (A,V,L,I,M), magenta-aromatic (F,Y,W), mustard-P & G, yellow-cysteine.

Table 4-2 Docking scores from PatchDock and FireDock for Haemoglobin alpha chain and ATP-IF1

S. No. (FireDock)	Solution Number (PatchDock)	Global Energy (kcal/mol)	Attractive VdW (kcal/mol)	Repulsive VdW (kcal/mol)	ACE (kcal/mol)	Score	Area
1	30	-27.01	29.93	11.49	7.74	8696	1125.90
2	19	-16.10	-25.88	13.35	11.48	8852	1081.70
3	44	-15.84	-28.74	26.23	5.54	8340	1267.10
4	15	-12.18	-29.70	13.98	8.57	9022	1087.50
5	38	-8.08	-18.35	14.55	5.09	8464	1444.70
6	7	-6.67	-33.25	18.06	15.48	9368	1154.40
7	11	-4.14	-6.10	2.72	4.76	9132	1123.70
8	25	-0.54	-26.40	13.84	10.61	8814	1202.00
9	36	-0.33	-19.90	7.34	4.43	8502	1368.90

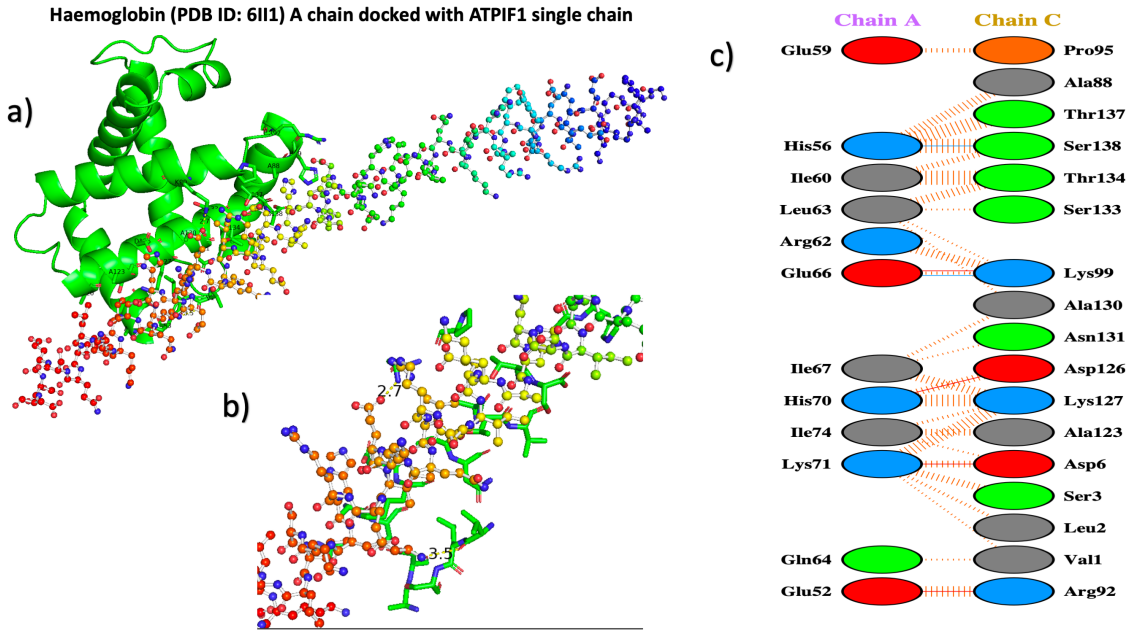

Figure 4-8. Interacting residues of only α globin chain with IF1 residues. C) Graphical representation of interacting residues of protein chains for generated using PDBsum (Laskowski *et al.*, 2018). Interacting chains are joined by coloured lines representing different kind of interactions; red- salt bridges, yellow- disulphide bonds, blue-hydrogen bonds, orange-non bonded contacts. Each amino acid residue colour represents different properties; blue- positively charged (H,K,R), red-negatively charged (D,E), green- neutral (S,T,N,Q), grey-aliphatic (A,V,L,I,M), magenta-aromatic (F,Y,W), mustard-P & G, yellow-cysteine.

On docking, only the alpha globin peptide of haemoglobin (Chain C) with ATPIF1 (Chain A), it showed two polar contacts between the two molecules (5 Å) between residues Glu66 of ATPIF1 protein and Lys99 of HbA bond length 2.7 Å and, His56 of ATPIF1 and Ser138 of HbA of a 3.5 Å (See Figure 6. b & c). The isolated HbA chain interacted with residues 52-74 (c-terminal end) of IF1. The interacting residues of Hb in common between the two docking were Val1, Leu2, Asn131, Thr134, Thr137, Ser 138 (**Table 4-3**).

4.3.4 MD Simulation (8 ns)

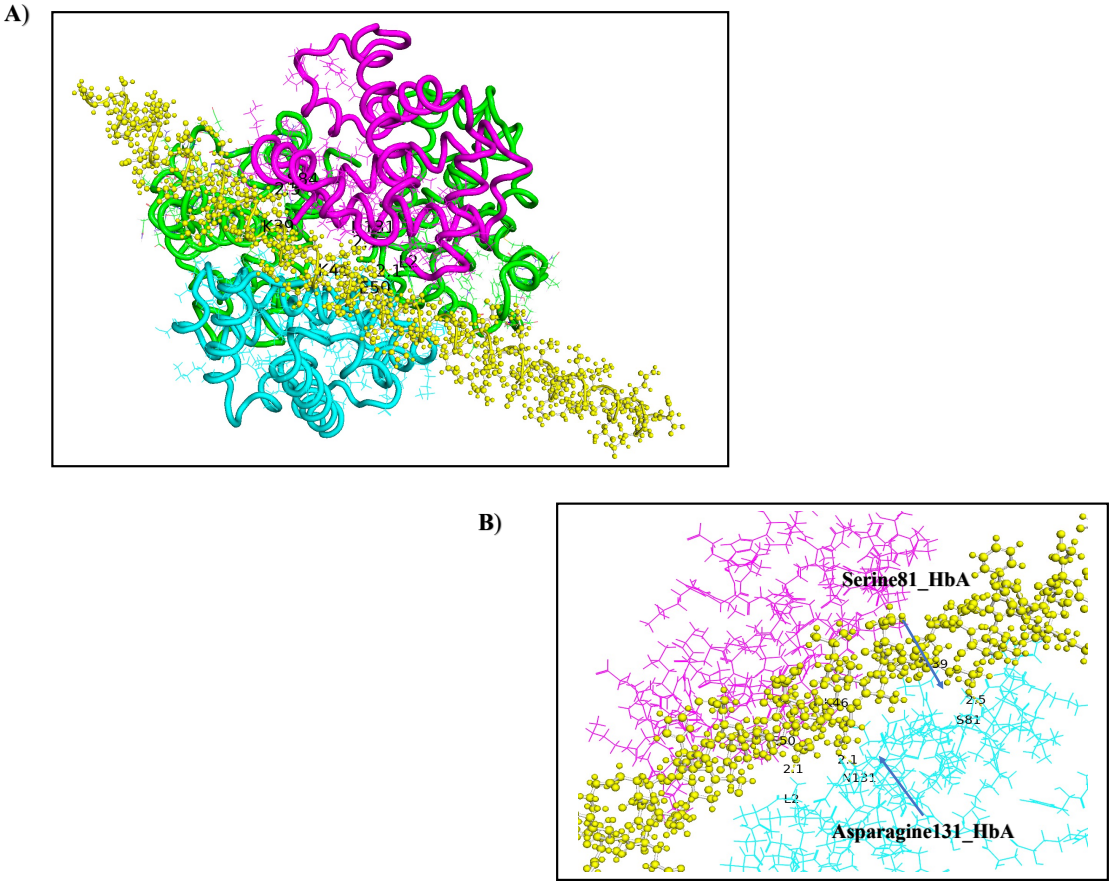

Figure 4-9. Hb-IF1 association after 8 ns MD simulation: A) IF1 docked in the cleft of two alpha chains of Hb (Pink- Chain A, light blue- Chain C, yellow-IF1). B) Shows interaction of Hb residues with IF1 residues where residues Serine84 and Asparagine131 of HbA show polar contacts with IF1.

The best docked conformation (solution 8, **Table 4-1**) was chosen according to the global energy of the docked compound. The docked protein was prepared creating a topology file that contains all the information of the structure. AMBER99SB-ILDN (Lindorff-Larsen)[64] forcefield was applied on the complex. The choice of force field is very important for relevant and accurate conformations for protein energetics. The information given by the forcefield includes addition of hydrogen atoms to an amino acid residue taking in account the molecular geometry and selected properties of tested structures. The AMBER99SB-IL forcefield is tailored for amino acids specifically as it improves backbone and side chain torsion potentials[64]. The system was equilibrated at 305K constant temperature, density, and pressure (**Appendix C Figure 4-18-2,3,4**) The structure was relaxed using energy minimisation (**Appendix C Figure 4-18-1**).

The quality of simulated structure is checked using root-mean-square deviation over the simulation time (8 ns) a common technique to verify the stability of MD simulation. **Figure 4-10** shows that the system was approximately stable somewhere between 4 ns to 7 ns. Therefore, it can be concluded that the structure did not deviate much and was stable over the simulation. The radius of gyration (Rg) is an important parameter in protein stability during simulation. If

the protein was stable during the simulation, the radius of gyration would be reasonably invariant in its compact form (**Figure 4-10**). The accepted range of Rg for a tetramer and globular protein of a similar molecular weight about is 2.5-2.6nm at a temperature 300-350K [65,66] which was seen in the simulation (2.52nm) for the Hb-IF1 complex.

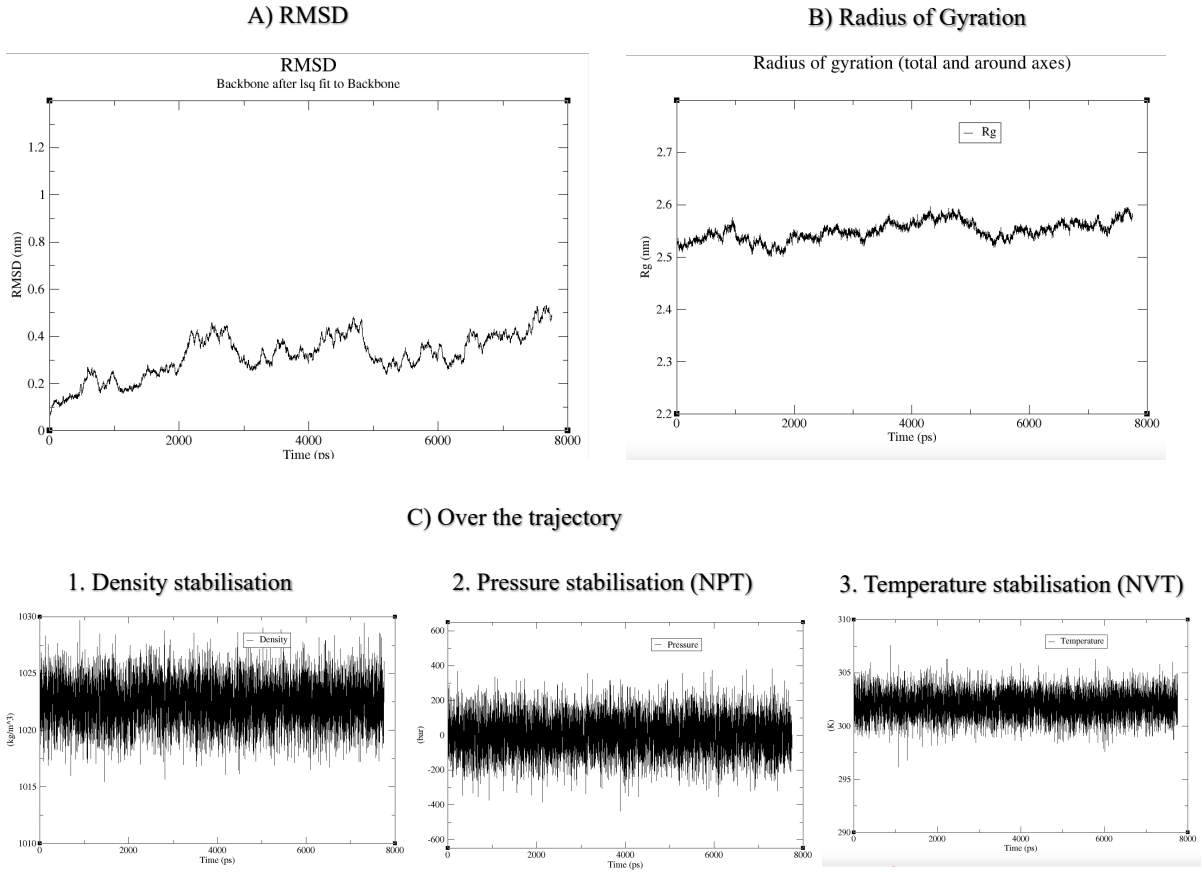

Figure 4-10. Quantitative quality check for the MD run. A) RMSD B) Radius of Gyration shows a reasonable invariant Rg values (2.5-26nm) across the MD run of 8ns indicating the protein remains very stable. C) The thermodynamic factors such as density, pressure and temperature are very stable across the MD run.

Figure 4-9 shows the IF1 bound to Hb after the MD simulation run of 8 ns. Most of the interactions that were present at the start of the MD run, that is the best docked complex were seen at the end of the MD stabilisation as well (**Table 4-3**). An additional hydrogen bond was seen between Asn131 and Lys46, with a measured distance of 2.1 Å. The residue Ser81 of Hb was seen to make hydrogen bond with Lys39 both before and after MD stabilisation. Another polar contact observed was Leu2 of Hb with Glu50 of IF1, a measured distance of 2.1 Å. All the other interacting residues within 4 Å of the protein, that were seen before the MD simulation were also seen after MD run (**Table 4-3**), suggesting stable binding.

Table 4-3. IF1 interacting residues with Hb. The first part of the table shows residues interacting between IF1 and HbA, and IF1 and Hb all chains from the FireDock best docking pose. Second half of the table shows stable interacting residues that remained through the MD trajectory.

Before simulation				After simulation		
IF1	**HbA**	**Hb-all chains**		**IF1**	**Hb-all chains**	
	Chain C	Chain A	Chain C		Chain A	Chain C
Arg35		Asp85		Arg35	Asp85	
Lys39		Asp85, Ser81		Lys39	Ser81, Asp85	
Leu42		Ser138	Val1	Leu42	Ser138	Val1
Ala43		Gly78, Asp75, Pro77		Ala43	Gly78, Asp75	
Leu45			Leu73, Asp74, Leu2, Lys7, Val1	Leu45		Leu2, Asp74, Lys7, Val1
Lys46		Pro77, Asn131	Val1	Lys46	Pro77, Asn131, Val135	Val1
Lys47		Asp74		Lys47	Asp74	
Lys49			Pro77, Thr134, Asn131, Val135	Lys49		Pro77, Thr134
Glu50		Leu2		Glu50	Leu2	
Glu52	Arg92		Asp75, Gly78, Pro77	Glu52		Asp75, Pro7
Ile53			Ser138	Ile53		Ser138
Ser54		Ala4		Ser54	Ser3, Ala4, Leu2	
His56	Ala88, Thr137, Ser138		Ser81, Pro77	His56		Ser81
Ala57				Ala57	Ser3	
Glu59	Pro95			Glu59		
Ile60	Thr134, Ser138		His89, Asp85	Ile60		
Arg62	Lys99			Arg62		
Leu63	Lys99, Thr134, Ser133, Ala130			Leu63		
Gln64	Val1			Gln64		
Glu66	Lys99			Glu66		
Ile67	Ala130, Asn131, Lys127			Ile67		
His70	Asp126, Lys127			His70		
Lys71	Lys127, Asp6, Ser3, Leu2			Lys71		
Ile74	Lys127, Ala123, Asp6			Ile74		

4.4 Discussion

Changes have been observed in the protein haemoglobin in neurodegenerative diseases[67–70] and its role as a drug receptor has been argued previously[71]. This has led to the speculation whether the protein has a role other than transporting gases oxygen and carbon dioxide in the blood. There is evidence describing the dynamic location of the protein. The fish in the waters of the Southern Ocean, Antarctic fish, give us the opportunity to study the protein closely. The ice fish have undergone many adaptations, such as a reduced red blood cells (RBCs) concentration to total loss of RBCs and loss of two globins, haemoglobin and myoglobin, in the icefish. The preservation of the 3'truncated fragment of HbA has previously been suggested to have a vascular function[4] and there is evidence for HbA to influence vascular remodelling through nitric oxide signalling in the endothelial [1,31]. It has been seen to colocalise in the mitochondria[72,73], which made us hypothesise whether it has a mitochondrial-specific function, specifically in the energy mechanism.

The main proteins involved in the energy mechanism in the mitochondria are the OxPhos complexes, mainly Complex I, II, III, IV of the electron transport chain (ETC) and the final complex V. The final step of ATP synthesis is catalysed by the multiple subunit complex, ATP synthase, whose enzyme activity is modulated by its natural inhibitor ATP synthase inhibitory factor 1 (ATPIF1/ IF1). The binding of IF1 to the F1 complex of ATPase occurs only in a pH below neutrality and in de-energised inner mitochondrial membrane in response to low oxygen levels[74]. Yet, it is still not known where IF1 binds in the inner membrane when it is not bound to ATP synthase that is under the aerobic conditions it is poorly understood. It has been speculated that the protein binds to a small protein other than that of the ATP synthase, in the inner mitochondria membrane[5].

IF1 knock out has been previously reported to correlate with anaemia in zebra fish despite the normal expression of HbB. HbA was reported to be localised in the inner membrane of the mitochondria. Due to these pieces of indirect evidence, we questioned whether a part of HbA interacts with IF1 protein in the inner-mitochondrial membrane when it's not bound to the ATP synthase, this might be signalled by the protons (**Figure 4-11**).

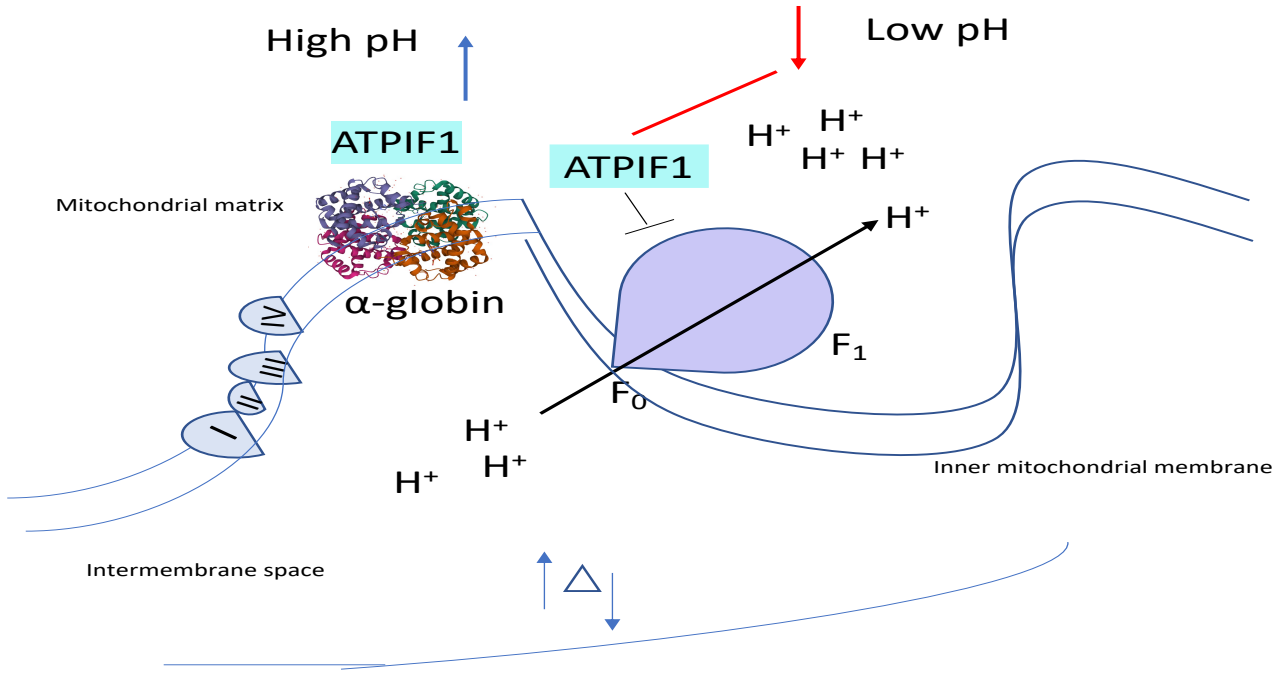

Figure 4-11. A schematic representation of HbA interacting with IF1- modulating energy status in mitochondria.

To check if there were differences at sequence level for the Antarctic species, we aligned the sequences of truncated 3'HbA from the icefish *C. rastrospinosus* and *C. aceratus* with the other species of sub-order Notothenioidei that have complete sequences of HbA. We included temperate water species, *D. rerio*, *S. trutta*, *O. mykiss*, *S. namacyus,* and *N. furzeri* as an outgroup. HbA is relatively well conserved across the species examined however the variation in sequence is still high considering its single canonical function.
Certain anaemias are caused due to defects in the mitochondrial enzyme, ferrochelatase, involved in haem biosynthesis[75–77]. Investigation of interdependence functions of regulators of mitochondria, such as, IF1 and the enzymes responsible in haem synthesis showed IF1 regulates the catalytic activity of enzyme ferrochelatase to synthesise haem. Hence, a loss of Atpif1 impairs haemoglobin synthesis in zebrafish, mouse, and human models of anaemia because of elevated mitochondrial pH[38]. IF1 is known to inhibit the reversal, that is the hydrolysis, of ATP synthase enzyme and also has a role in maintaining the membrane potential and proton motive force[78,79]. The Antarctic fish stands as a natural model for drastic reduction in haemoglobin content in the red-blooded fish[14] and the condition is seen extreme in the icefish by complete loss of haemoglobin[80].

We wanted to see how the protein expression for ATPIF1 might be in the different species of the Antarctic fish in the red-blooded, *N. corriceps*, *T. bernacchii*, and icefish *C. rastrospinosus* and *C. gunnari* where we had samples from red muscle. There was as significant lower expression of ATPIFI observed in Hb-less *C. gunnari*. The co-immunoprecipitation (co-IP) with anti-IF1 antibody showed pulled down of HbA by IF1 though the HbA band observed was very faint which could be due to the fact a

monoclonal IF1 antibody was used for the co-IP. This association was investigated by docking and MD simulations.

IF1 a key regulator of the ATP synthase[81], also has a protective role from hypoxia in tissues that require high energy[82]. The other roles of IF1 include, regulation of stem cell differentiation[83], haem synthesis[38], cell proliferation and programmed cell death[84,85]. The IF1 interacts with the γ subunit of ATP synthase by its N-terminus in a super coiled helix form, between the catalytic interface of α and β subunits of ATP synthase, which is empty[86]. After the hydrolysis of two ATP molecules, that represents two rotations of γ subunit, α β adopt a closed conformation, rearranging the IF1 moiety[87]. The rearrangement causes changes in the IF1 protein itself. An increase in pH makes IF1 stickier and it forms a tetramer masking the inhibitory region of IF1 at its N-terminus [37,88,89].

The N-terminal region of IF1 has been seen to interact with the C-terminal of calmodulin in a Ca^{2+} and pH dependent way [90,91]. IF1 when not bound to ATP synthase, is an intrinsically disordered protein, such proteins are important components of cell signalling and make transient interactions with other proteins[92]. Yet it is not known where the unbound protein resides in the mitochondria. There is a suggestion that it binds to a membrane receptor but not to the subunits of ATP synthase[5]. Though IF1 is predominantly compartmentalised inside the mitochondrial matrix it has also been reported in cytosol, plasma membrane[93], serum[94], and in the extracellular environment, involved in modulation of activity of endothelial cells[95]. This all supports roles for IF1 in addition to modulating ATP synthase[94,95].

Using a reliable docking protocol combined with MD simulation, we investigated bovine IF1-monomer interactions with bovine Hb tetramer. The interacting residues for the best docked structure, solution 8, ranked 1 using FireDock refinement showed interacting residues Pro77, Gly78, Asp85, Ser81, Asn131, Ser138, Pro77, Thr134, Val 135 of HbA. The important interacting residues seen in IF1 were residues 35-75. The activity of IF1 is regulated by pH by its five key histidine residues, His48, 49, 55, 56 and 70, that are also evolutionary conserved. The residues 44-84 in IF1 are involved in dimerization of the protein, while in its tetrameric form it is extended to residues 32-84 [37]. The residue E30 in IF1 has been previously reported to form a salt bridge with the β subunit of ATP synthase. Changes in its Ser39 can stop the interaction and inhibitory activity of IF1 on the ATP synthase.
From our docking results IF1 seems to interact from the central residues (35-70) and towards C-terminal end of the protein with haemoglobin. The residues 48-70 are involved in the pH sensing mechanism of IF1[96]. At pH < 6.5 the protein is a dimer, at pH 6.5 protein dimers and oligomers are in equilibrium, at pH 7-8, the dimers can exist as inactive tetramers or higher oligomers involving residues 32-44. Even though a monomer form of IF1 was reported in human serum using SDS PAGE, western blotting, and mass spectrometry[94]. In the same study they speculated interaction of If1 with other proteins[94].
IF1 comes into play when electrochemical gradient collapses, under anaerobic conditions, matrix pH decreases and the proton gradient favourable for ATP synthesis declines. The role of Hb as a regulator of stress response could be attributed to the fact it modulates ATP concentration[36] through its interaction with IF1. As seen with our docking results, IF1 has been seen to interact with several inner mitochondrial membrane proteins with its c-terminal end [5,97–99] where HbA is also seen to be

localised in intermembrane space of mitochondrial membrane[100]. Thus, like the interactions of IF1 with other proteins from its c-terminal end, we speculate that IF1 could be interacting with HbA with its c-terminal end.

Throughout these studies all observations needed validation to increase the probability of the predictions being correct, so the simulations were validated with RMSD and ROG. The RMSD between structures created in the simulation in the time dimension was an appropriate criterion to ensure the stability of the dynamic molecular simulation[65,101]. In addition, the gyration radius is an important factor that indicates the amount of protein folding. If a protein is folded well, the gyration radius for that protein is fixed during simulation[102]. This factor provides useful information about the distribution of proteins in the spherical form[102]. Thus, changes in the structure of a protein can be examined by taking into consideration the gyration radius. Both RMSD and ROG were stable during the simulation, indicating the first docked pose was very stable throughout the simulation.

After the MD simulations all the interacting residues that were present before the simulation remained after the simulation, showing stable interactions. The polar contacts between Asparagine 131 of HbA with Lysine 46 of IF1, and Serine 81 of HbA with Lys39 were seen after the MD simulation as well. Changes in potential energy, pressure, temperature, and density for each of the structures through the equilibration phase were examined to ensure the stability of the simulations. Each provided acceptable sustainability in the best docked structures for the two proteins, the computational results showed a high stabilization of the complexes. The role of Hb as an energy modulator[103] and stress response[36] has been previously reported. With the current data we also suggest a possible interaction of HbA and ATPIF1 for the modulation of energy mechanism in mitochondria. Further, in vitro investigation, such as yeast two-hybrid assay a repetition of co-IP or reverse co-IP whether HbA pull-down ATPIF1 would be required to validate this finding.

4.5 References:

1. Straub AC, Lohman AW, Billaud M, Johnstone SR, Dwyer ST, Lee MY, et al. Endothelial cell expression of haemoglobin α regulates nitric oxide signalling. Nature. 2012;491: 473–477. doi:10.1038/nature11626
2. Shephard F, Greville-Heygate O, Marsh O, Anderson S, Chakrabarti L. A mitochondrial location for haemoglobins—Dynamic distribution in ageing and Parkinson's disease. Mitochondrion. 2014;14: 64–72. doi:10.1016/J.MITO.2013.12.001
3. Shephard F, Greville-Heygate O, Liddell S, Emes R, Chakrabarti L. Analysis of Mitochondrial haemoglobin in Parkinson's disease brain. Mitochondrion. 2016;29: 45–52. doi:10.1016/j.mito.2016.05.001
4. Corliss BA, Delalio LJ, Stevenson Keller TC, Keller AS, Keller DA, Corliss BH, et al. Vascular Expression of Hemoglobin Alpha in Antarctic Icefish Supports Iron Limitation as Novel Evolutionary Driver. Front Physiol. 2019;10. doi:10.3389/fphys.2019.01389
5. LOPEZ-MEDIAVILLA C, VIGNY H, GODINOT C. Docking the mitochondrial inhibitor protein IF1 to a membrane receptor different from the F1-ATPase β subunit. Eur J Biochem. 1993;215: 487–496. doi:10.1111/j.1432-1033.1993.tb18058.x
6. L. DA, E. WD. Freezing Resistance in Some Antarctic Fishes. Science (80-). 1969;163: 1073–1075. doi:10.1126/science.163.3871.1073
7. Hofmann GE, Buckley BA, Airaksinen S, Keen JE, Somero GN. Heat-shock protein expression is absent in the antarctic fish Trematomus bernacchii (family Nototheniidae). J Exp Biol. 2000;203: 2331–2339. doi:10.1242/jeb.203.15.2331
8. Barber DL, Mills Westermann JE, White MG. The blood cells of the Antarctic icefish Chaenocephalus aceratus Lönnberg: light and electron microscopic observations. J Fish Biol. 1981;19: 11–28. doi:https://doi.org/10.1111/j.1095-8649.1981.tb05807.x
9. Zhao Y, Ratnayake-Lecamwasam M, Parker SK, Cocca E, Camardella L, di Prisco G, et al. The major adult alpha-globin gene of antarctic teleosts and its remnants in the hemoglobinless icefishes. Calibration of the mutational clock for nuclear genes. J Biol Chem. 1998;273: 14745–14752. doi:10.1074/jbc.273.24.14745
10. di Prisco G, Cocca E, Parker SK, Detrich HW. Tracking the evolutionary loss of hemoglobin expression by the white-blooded Antarctic icefishes. Gene. 2002;295: 185–191. doi:https://doi.org/10.1016/S0378-1119(02)00691-1
11. Zhao Y, Ratnayake-Lecamwasam M, Parker SK, Cocca E, Camardella L, Di Prisco G, et al. The major adult α-globin gene of antarctic teleosts and its remnants in the hemoglobinless icefishes. Calibration of the mutational clock for nuclear genes. J Biol Chem. 1998;273: 14745–14752. doi:10.1074/jbc.273.24.14745
12. Sidell BD, Vayda ME, Small DJ, Moylan TJ, Londraville RL, Yuan ML, et al. Variable expression of myoglobin among the hemoglobinless Antarctic icefishes. Proc Natl Acad Sci U S A. 1997;94: 3420–3424. doi:10.1073/pnas.94.7.3420
13. Small DJ, Moylan T, Vayda ME, Sidell BD. The myoglobin gene of the Antarctic icefish, Chaenocephalus aceratus, contains a duplicated TATAAAA sequence that interferes with transcription. J Exp Biol. 2003;206: 131–139. doi:10.1242/jeb.00067
14. Verde C, Parisi E, di Prisco G. The evolution of thermal adaptation in polar fish.

Gene. 2006;385: 137–145. doi:10.1016/j.gene.2006.04.006
15. Andrews NC. Iron homeostasis: insights from genetics and animal models. Nature reviews. Genetics. England; 2000. pp. 208–217. doi:10.1038/35042073
16. Beers JM, Borley KA, Sidell BD. Relationship among circulating hemoglobin, nitric oxide synthase activities and angiogenic poise in red- and white-blooded Antarctic notothenioid fishes. Comp Biochem Physiol - A Mol Integr Physiol. 2010;156: 422–429. doi:10.1016/j.cbpa.2010.03.027
17. Beers JM, Borley KA, Sidell BD. Relationship among circulating hemoglobin, nitric oxide synthase activities and angiogenic poise in red- and white-blooded Antarctic notothenioid fishes. Comp Biochem Physiol - A Mol Integr Physiol. 2010;156: 422–429. doi:10.1016/j.cbpa.2010.03.027
18. Katyal G, Ebanks B, Lucassen M, Papetti C, Chakrabarti L. Sequence and structure comparison of ATP synthase F0 subunits 6 and 8 in notothenioid fish. PLoS One. 2021;16: e0245822. doi:10.1371/journal.pone.0245822
19. Perutz M, Rossmann M, Cullis AF, Muirhead H, Will G, North ACT. Structure of hoemoglobin. Nature. 1960;185: 416–422.
20. Sankaran VG, Xu J, Orkin SH. Advances in the understanding of haemoglobin switching: Review. Br J Haematol. 2010;149: 181–194. doi:10.1111/j.1365-2141.2010.08105.x
21. Nilsson R, Schultz IJ, Pierce EL, Soltis KA, Naranuntarat A, Ward DM, et al. Discovery of Genes Essential for Heme Biosynthesis through Large-Scale Gene Expression Analysis. Cell Metab. 2009;10: 119–130. doi:10.1016/j.cmet.2009.06.012
22. Dailey HA, Dailey TA, Gerdes S, Jahn D, Jahn M, O'Brian MR, et al. Prokaryotic Heme Biosynthesis: Multiple Pathways to a Common Essential Product. Microbiol Mol Biol Rev. 2017;81. doi:10.1128/mmbr.00048-16
23. Kristinsson HG, Hultin HO. Changes in Trout Hemoglobin Conformations and Solubility after Exposure to Acid and Alkali pH. J Agric Food Chem. 2004;52: 3633–3643. doi:10.1021/jf034563g
24. Kristinsson HG, Hultin HO. The Effect of Acid and Alkali Unfolding and Subsequent Refolding on the Pro-oxidative Activity of Trout Hemoglobin. J Agric Food Chem. 2004;52: 5482–5490. doi:10.1021/jf035062y
25. Perutz MF. Species adaptation in a protein molecule. Mol Biol Evol. 1983;1: 1–28. doi:10.1093/oxfordjournals.molbev.a040299
26. Straub AC, Butcher JT, Billaud M, Mutchler SM, Artamonov M V., Nguyen AT, et al. Hemoglobin α/eNOS coupling at myoendothelial junctions is required for nitric oxide scavenging during vasoconstriction. Arterioscler Thromb Vasc Biol. 2014;34: 2594–2600. doi:10.1161/ATVBAHA.114.303974
27. Lo HH, Schimmel PR. Interaction of human hemoglobin with adenine nucleotides. J Biol Chem. 1969;244: 5084–5086. doi:10.1016/s0021-9258(18)94313-9
28. Cashon R, Bonaventura C, Bonaventura J, Focesi A. The nicotinamide adenine dinucleotides as allosteric effectors of human hemoglobin. J Biol Chem. 1986;261: 12700–12705. doi:10.1016/s0021-9258(18)67148-0
29. Banerjee M, Chakrabarti A, Basu S. Oxidative interaction between OxyHb and ATP: A spectroscopic study. J Phys Chem B. 2012;116: 6150–6157. doi:10.1021/jp302899t
30. Gupta RK, Benovic JL, Rose ZB. Magnetic resonance studies of the binding of ATP and cations to human hemoglobin. J Biol Chem. 1978;253: 6165–6171. doi:10.1016/s0021-9258(17)34594-5
31. Lechauve C, Butcher JT, Freiwan A, Biwer LA, Keith JM, Good ME, et al.

Endothelial cell α-globin and its molecular chaperone α-hemoglobin-stabilizing protein regulate arteriolar contractility. J Clin Invest. 2018;128: 5073–5082. doi:10.1172/JCI99933
32. Shin SC hu., Ahn DH wa., Kim SJ i., Pyo CW o., Lee H, Kim MK, et al. The genome sequence of the Antarctic bullhead notothen reveals evolutionary adaptations to a cold environment. Genome Biol. 2014;15: 468. doi:10.1186/s13059-014-0468-1
33. Schägger H, Pfeiffer K. Supercomplexes in the respiratory chains of yeast and mammalian mitochondria. EMBO J. 2000;19: 1777–1783. doi:https://doi.org/10.1093/emboj/19.8.1777
34. Velours C, Aumont-Nicaise M, Uebel S, England P, Velazquez-Campoy A, Stroebel D, et al. Macromolecular interactions in vitro, comparing classical and novel approaches. Eur Biophys J. 2021;50: 313–330. doi:10.1007/s00249-021-01517-5
35. Simon I. Macromolecular interactions of disordered proteins. Int J Mol Sci. 2020;21. doi:10.3390/ijms21020504
36. Codrich M, Bertuzzi M, Russo R, Francescatto M, Espinoza S, Zentilin L, et al. Neuronal hemoglobin affects dopaminergic cells' response to stress. Cell Death Dis. 2018;8: e2538–e2538. doi:10.1038/cddis.2016.458
37. Cabezon E, Butler PJG, Runswick MJ, Walker JE. Modulation of the oligomerization state of the bovine F1-ATPase inhibitor protein, IF1, by pH. J Biol Chem. 2000;275: 25460–25464. doi:10.1074/jbc.M003859200
38. Shah DI, Takahashi-Makise N, Cooney JD, Li L, Schultz IJ, Pierce EL, et al. Mitochondrial Atpif1 regulates haem synthesis in developing erythroblasts. Nature. 2012;491: 608–612. doi:10.1038/nature11536
39. Postlethwait JH, Yan YL, Gates MA, Horne S, Amores A, Brownlie A, et al. Vertebrate genome evolution and the zebrafish gene map. Nat Genet. 1998;18: 345–349. doi:10.1038/ng0498-345
40. O'Leary NA, Wright MW, Brister JR, Ciufo S, Haddad D, McVeigh R, et al. Reference sequence (RefSeq) database at NCBI: Current status, taxonomic expansion, and functional annotation. Nucleic Acids Res. 2016;44: D733–D745. doi:10.1093/nar/gkv1189
41. McWilliam H, Li W, Uludag M, Squizzato S, Park YM, Buso N, et al. Analysis Tool Web Services from the EMBL-EBI. Nucleic Acids Res. 2013;41: 597–600. doi:10.1093/nar/gkt376
42. Rozewicki J, Li S, Amada KM, Standley DM, Katoh K. MAFFT-DASH: Integrated protein sequence and structural alignment. Nucleic Acids Res. 2019;47: W5–W10. doi:10.1093/nar/gkz342
43. Waterhouse AM, Procter JB, Martin DMA, Clamp M, Barton GJ. Jalview Version 2-A multiple sequence alignment editor and analysis workbench. Bioinformatics. 2009;25: 1189–1191. doi:10.1093/bioinformatics/btp033
44. Gasteiger E, Gattiker A, Hoogland C, Ivanyi I, Appel RD, Bairoch A. ExPASy: The proteomics server for in-depth protein knowledge and analysis. Nucleic Acids Res. 2003;31: 3784–3788. doi:10.1093/nar/gkg563
45. Yang J, Zhang Y. I-TASSER server: New development for protein structure and function predictions. Nucleic Acids Res. 2015;43: W174–W181. doi:10.1093/nar/gkv342
46. Laskowski RA, MacArthur MW, Moss DS, Thornton JM. PROCHECK: a program to check the stereochemical quality of protein structures. J Appl Crystallogr. 1993;26: 283–291. doi:10.1107/s0021889892009944
47. Wiederstein M, Sippl MJ. ProSA-web: Interactive web service for the

recognition of errors in three-dimensional structures of proteins. Nucleic Acids Res. 2007;35: 407–410. doi:10.1093/nar/gkm290
48. Schneidman-Duhovny D, Inbar Y, Nussinov R, Wolfson HJ. PatchDock and SymmDock: Servers for rigid and symmetric docking. Nucleic Acids Res. 2005;33: 363–367. doi:10.1093/nar/gki481
49. Andrusier N, Nussinov R, Wolfson HJ. FireDock: Fast interaction refinement in molecular docking. Proteins Struct Funct Bioinforma. 2007;69: 139–159. doi:https://doi.org/10.1002/prot.21495
50. Laskowski RA, Jabłońska J, Pravda L, Vařeková RS, Thornton JM. PDBsum: Structural summaries of PDB entries. Protein Sci. 2018;27: 129–134. doi:10.1002/pro.3289
51. Pettersen EF, Goddard TD, Huang CC, Couch GS, Greenblatt DM, Meng EC, et al. UCSF Chimera--a visualization system for exploratory research and analysis. J Comput Chem. 2004;25: 1605–1612. doi:10.1002/jcc.20084
52. Yan Y, Tao H, He J, Huang S-Y. The HDOCK server for integrated protein-protein docking. Nat Protoc. 2020;15: 1829–1852. doi:10.1038/s41596-020-0312-x
53. Desta IT, Porter KA, Xia B, Kozakov D, Vajda S. Performance and Its Limits in Rigid Body Protein-Protein Docking. Structure. 2020;28: 1071-1081.e3. doi:10.1016/j.str.2020.06.006
54. S2352711015000059.
55. Aliev AE, Kulke M, Khaneja HS, Chudasama V, Sheppard TD, Lanigan RM. Motional timescale predictions by molecular dynamics simulations: case study using proline and hydroxyproline sidechain dynamics. Proteins. 2014;82: 195–215. doi:10.1002/prot.24350
56. Weiner SJ, Kollman PA, Case DA, Singh UC, Ghio C, Alagona G, et al. A new force field for molecular mechanical simulation of nucleic acids and proteins. J Am Chem Soc. 1984;106: 765–784. doi:10.1021/ja00315a051
57. Janson G, Zhang C, Prado MG, Paiardini A. PyMod 2.0: improvements in protein sequence-structure analysis and homology modeling within PyMOL. Bioinformatics. 2017;33: 444–446. doi:10.1093/bioinformatics/btw638
58. Galeazzi R, Laudadio E, Falconi E, Massaccesi L, Ercolani L, Mobbili G, et al. Protein-protein interactions of human glyoxalase II: findings of a reliable docking protocol. Org Biomol Chem. 2018;16: 5167–5177. doi:10.1039/c8ob01194j
59. Sidell BD, O'Brien KM. When bad things happen to good fish: The loss of hemoglobin and myoglobin expression in Antarctic icefishes. J Exp Biol. 2006;209: 1791–1802. doi:10.1242/jeb.02091
60. Fisher N, Meunier B. Re-examination of inhibitor resistance conferred by Qo-site mutations in cytochrome b using yeast as a model system. Pest Manag Sci. 2005;61: 973–978. doi:https://doi.org/10.1002/ps.1066
61. Xiao J, Cheng H, Silva T, Baum J, Brodsky B. Osteogenesis imperfecta missense mutations in collagen: Structural consequences of a glycine to alanine replacement at a highly charged site. Biochemistry. 2011;50: 10771–10780. doi:10.1021/bi201476a
62. Serrano L, Neira J-L, Sancho J, Fersht AR. Effect of alanine versus glycine in α-helices on protein stability. Nature. 1992;356: 453–455. doi:10.1038/356453a0
63. Johns GC, Somero GN. Evolutionary Convergence in Adaptation of Proteins to Temperature: A4-Lactate Dehydrogenases of Pacific Damselfishes (Chromis spp.). Mol Biol Evol. 2004;21: 314–320. doi:10.1093/molbev/msh021
64. Lindorff-Larsen K, Piana S, Palmo K, Maragakis P, Klepeis JL, Dror RO, et al.

Improved side-chain torsion potentials for the Amber ff99SB protein force field. Proteins. 2010;78: 1950–1958. doi:10.1002/prot.22711
65. Arnittali M, Rissanou AN, Harmandaris V. Structure of Biomolecules Through Molecular Dynamics Simulations. Procedia Comput Sci. 2019;156: 69–78. doi:10.1016/j.procs.2019.08.181
66. Smilgies D-M, Folta-Stogniew E. Molecular weight-gyration radius relation of globular proteins: a comparison of light scattering, small-angle X-ray scattering and structure-based data. J Appl Crystallogr. 2015;48: 1604–1606. doi:10.1107/S1600576715015551
67. Shephard F, Greville-Heygate O, Liddell S, Emes R, Chakrabarti L. Analysis of Mitochondrial haemoglobin in Parkinson's disease brain. Mitochondrion. 2016;29: 45–52. doi:10.1016/j.mito.2016.05.001
68. Chuang JY, Lee CW, Shih YH, Yang T, Yu L, Kuo YM. Interactions between amyloid-β and hemoglobin: Implications for amyloid plaque formation in alzheimer's disease. PLoS One. 2012;7. doi:10.1371/journal.pone.0033120
69. Atti AR, Palmer K, Volpato S, Zuliani G, Winblad B, Fratiglioni L. Anaemia increases the risk of dementia in cognitively intact elderly. Neurobiol Aging. 2006;27: 278–284. doi:https://doi.org/10.1016/j.neurobiolaging.2005.02.007
70. Pandav RS, Chandra V, Dodge HH, DeKosky ST, Ganguli M. Hemoglobin Levels and Alzheimer Disease: An Epidemiologic Study in India. Am J Geriatr Psychiatry. 2004;12: 523–526. doi:https://doi.org/10.1097/00019442-200409000-00011
71. Perutz MF, Fermi G, Abraham DJ, Poyart C, Bursaux E. Hemoglobin as a receptor of drugs and peptides: x-ray studies of the stereochemistry of binding. J Am Chem Soc. 1986;108: 1064–1078. doi:10.1021/ja00265a036
72. Shephard F, Greville-Heygate O, Liddell S, Emes R, Chakrabarti L. Analysis of Mitochondrial haemoglobin in Parkinson's disease brain. Mitochondrion. 2016;29: 45–52. doi:10.1016/j.mito.2016.05.001
73. Shephard F, Greville-Heygate O, Marsh O, Anderson S, Chakrabarti L. A mitochondrial location for haemoglobins-Dynamic distribution in ageing and Parkinson's disease. Mitochondrion. 2014;14: 64–72. doi:10.1016/j.mito.2013.12.001
74. Di Pancrazio F, Mavelli I, Isola M, Losano G, Pagliaro P, Harris DA, et al. In vitro and in vivo studies of F 0F 1ATP synthase regulation by inhibitor protein IF 1 in goat heart. Biochim Biophys Acta - Bioenerg. 2004;1659: 52–62. doi:10.1016/j.bbabio.2004.07.009
75. Nordmann Y, Beuzard Y, Deybacht J. Erythropoietic Protoporphyria in the House Mouse. J Clin Invest. 1991;88: 1730–1736.
76. Rüfenacht UB, Gouya L, Schneider-Yin X, Puy H, Schäfer BW, Aquaron R, et al. Systematic analysis of molecular defects in the ferrochelatase gene from patients with Erythropoietic protoporphyria. Am J Hum Genet. 1998;62: 1341–1352. doi:10.1086/301870
77. Lyoumi S, Abitbol M, Andrieu V, Henin D, Robert E, Schmitt C, et al. Increased plasma transferrin, altered body iron distribution, and microcytic hypochromic anemia in ferrochelatase-deficient mice. Blood. 2007;109: 811–818. doi:10.1182/blood-2006-04-014142
78. Walker JE. The regulation of catalysis in ATP synthase. Curr Opin Struct Biol. 1994;4: 912–918. doi:https://doi.org/10.1016/0959-440X(94)90274-7
79. Campanella M, Parker N, Tan CH, Hall AM, Duchen MR. IF1: setting the pace of the F1Fo-ATP synthase. Trends Biochem Sci. 2009;34: 343–350. doi:https://doi.org/10.1016/j.tibs.2009.03.006

80. Johan T. Ruud. Vertebrates without Erythrocytes and Blood Pigment. Nature. 1954;173: 848–850.
81. Faccenda D, Campanella M. Molecular Regulation of the Mitochondrial F_1F_o-ATPsynthase: Physiological and Pathological Significance of the Inhibitory Factor 1 (IF_1). Filomeni G, editor. Int J Cell Biol. 2012;2012: 367934. doi:10.1155/2012/367934
82. Matic I, Strobbe D, Frison M, Campanella M. Controlled and Impaired Mitochondrial Quality in Neurons: Molecular Physiology and Prospective Pharmacology. Pharmacol Res. 2015;99: 410–424. doi:10.1016/j.phrs.2015.03.021
83. Sánchez-Aragó M, García-Bermúdez J, Martínez-Reyes I, Santacatterina F, Cuezva JM. Degradation of IF1 controls energy metabolism during osteogenic differentiation of stem cells. EMBO Rep. 2013;14: 638–644. doi:https://doi.org/10.1038/embor.2013.72
84. Faccenda D, Tan CH, Seraphim A, Duchen MR, Campanella M. IF1 limits the apoptotic-signalling cascade by preventing mitochondrial remodelling. Cell Death Differ. 2013;20: 686–697. doi:10.1038/cdd.2012.163
85. Formentini L, Sánchez-Aragó M, Sánchez-Cenizo L, Cuezva JM. The Mitochondrial ATPase Inhibitory Factor 1 Triggers a ROS-Mediated Retrograde Prosurvival and Proliferative Response. Mol Cell. 2012;45: 731–742. doi:https://doi.org/10.1016/j.molcel.2012.01.008
86. Cabezón E, Montgomery MG, Leslie AGW, Walker JE. The structure of bovine F1-ATPase in complex with its regulatory protein IF1. Nat Struct Biol. 2003;10: 744–750. doi:10.1038/nsb966
87. Bason J V., Montgomery MG, Leslie AGW, Walker JE. Pathway of binding of the intrinsically disordered mitochondrial inhibitor protein to F1-ATPase. Proc Natl Acad Sci U S A. 2014;111: 11305–11310. doi:10.1073/pnas.1411560111
88. Gordon-Smith DJ, Carbajo RJ, Yang JC, Videler H, Runswick MJ, Walker JE, et al. Solution structure of a C-terminal coiled-coil domain from Bovine IF1: The inhibitor protein of F1 ATPase. J Mol Biol. 2001;308: 325–339. doi:10.1006/jmbi.2001.4570
89. Cabezón E, Runswick MJ, Leslie AGW, Walker JE. The structure of bovine IF1, the regulatory subunit of mitochondrial F-ATPase. EMBO J. 2001;20: 6990–6996. doi:https://doi.org/10.1093/emboj/20.24.6990
90. Contessi S, Haraux F, Mavelli I, Lippe G. Identification of a conserved calmodulin-binding motif in the sequence of F0F1ATPsynthase inhibitor protein. J Bioenerg Biomembr. 2005;37: 317–327. doi:10.1007/s10863-005-8643-4
91. Pagnozzi D, Birolo L, Leo G, Contessi S, Lippe G, Pucci P, et al. Stoichiometry and topology of the complex of the endogenous ATP synthase inhibitor protein IF1 with calmodulin. Biochemistry. 2010;49: 7542–7552. doi:10.1021/bi100447t
92. Wright PE, Dyson HJ. Intrinsically disordered proteins in cellular signalling and regulation. Nat Rev Mol Cell Biol. 2015;16: 18–29. doi:10.1038/nrm3920
93. Cortés-Hernández P, Domínguez-Ramírez L, Estrada-Bernal A, Montes-Sánchez DG, Zentella-Dehesa A, de Gómez-Puyou MT, et al. The inhibitor protein of the F1F0-ATP synthase is associated to the external surface of endothelial cells. Biochem Biophys Res Commun. 2005;330: 844–849. doi:https://doi.org/10.1016/j.bbrc.2005.03.064
94. Genoux A, Pons V, Radojkovic C, Roux-Dalvai F, Combes G, Rolland C, et al. Mitochondrial inhibitory factor 1 (IF1) is present in human serum and is

positively correlated with HDL-cholesterol. PLoS One. 2011;6. doi:10.1371/journal.pone.0023949
95. Burwick NR, Wahl ML, Fang J, Zhong Z, Moser TL, Li B, et al. An inhibitor of the F1 subunit of ATP synthase (IF1) modulates the activity of angiostatin on the endothelial cell surface. J Biol Chem. 2005;280: 1740–1745. doi:10.1074/jbc.M405947200
96. Green DW, Grover GJ. The IF1 inhibitor protein of the mitochondrial F1Fo-ATPase. Biochim Biophys Acta - Bioenerg. 2000;1458: 343–355. doi:https://doi.org/10.1016/S0005-2728(00)00085-2
97. Minauro-Sanmiguel F, Bravo C, García JJ. Cross-linking of the endogenous inhibitor protein (IF1) with rotor (γ, ε) and stator (α) subunits of the mitochondrial ATP synthase. J Bioenerg Biomembr. 2002;34: 433–443. doi:10.1023/A:1022514008462
98. Ichikawa N, Nakabayashi K, Hashimoto T. A Yeast Mitochondrial ATPase Inhibitor Interacts with Three Proteins That Are Easy to Dissociate from the Mitochondrial Inner Membrane. J Biochem. 2002;132: 649–654. doi:10.1093/oxfordjournals.jbchem.a003269
99. Shen L, Zhi L, Hu W, Wu MX. IEX-1 targets mitochondrial F1Fo-ATPase inhibitor for degradation. Cell Death Differ. 2009;16: 603–612. doi:10.1038/cdd.2008.184
100. Shephard F, Greville-Heygate O, Marsh O, Anderson S, Chakrabarti L. A mitochondrial location for haemoglobins-Dynamic distribution in ageing and Parkinson's disease. Mitochondrion. 2014. pp. 64–72. doi:10.1016/j.mito.2013.12.001
101. Kufareva I, Abagyan R. Methods of protein structure comparison. Methods Mol Biol. 2012;857: 231–257. doi:10.1007/978-1-61779-588-6_10
102. Lobanov MY, Bogatyreva NS, Galzitskaya O V. Radius of gyration as an indicator of protein structure compactness. Mol Biol. 2008;42: 623–628. doi:10.1134/S0026893308040195
103. Brown N, Alkhayer K, Clements R, Singhal N, Gregory R, Azzam S, et al. Neuronal Hemoglobin Expression and Its Relevance to Multiple Sclerosis Neuropathology. J Mol Neurosci. 2016;59: 1–17. doi:10.1007/s12031-015-0711-6

4.6 APENDIX C: Chapter 4

4.6.1 C.1 Methods:

Dynabeads M-270 epoxy (suspended in C1 solution 10mg/ml), were weighed 10µg and washed with 500µL of C1 in 1.5 ml Eppendorf tubes. The tube was then placed on the disinfected magnet for 1 min allowing the beads to collect at the tube wall, and supernatant was removed. The 10µL of C1 and 40µL IF1 antibody (abcam ab110277 mouse monoclonal) solution was mixed by gentle pipetting and then C2 was added to the solution making the total volume 100µL mixing it by gentle pipetting. The solution was incubated on the roller overnight at room temperature. The tube with solution was put on magnet for 1 min, allowing the beads to collect on the tube wall, and supernatant was removed. The tube was removed from the magnet and 400µL of HB was added for washing. Repeat the magnet step and remove he supernatant. The step was repeated with 400µL of LB and the supernatant was removed. The step was repeated twice with 400µL of SB wash and the supernatant was removed. The SB wash was added again, and the tube was incubated for 15 mins on the roller and the supernatant was removed thereafter. The tube was removed from the magnet and resuspended with 100µL of SB per mg of the beads. Meanwhile cell lysate was prepared using 100 µL Co-IP extraction buffer, red muscle tissue (mass=0.2g), from red-blooded Antarctic species, *N. rossii* sample number 4-33 (Antarctic Fish Muscle tissue. SVMS Clinical Ethical Review, University of Nottingham, (ref # 2744 190509). Red muscle samples of Antarctic notothenioid fish (red-blooded species – Cruise PS112, Weddell Sea in 2013-2014)). The homogenised tissue was centrifuged at 850g for 10 minutes at 4 deg. Celsius to clear debris. The co-immunoprecipitation protein samples were prepared using 2mL of Extraction buffer (1x IP) and 200µL of Last wash buffer (1x LWB). The antibody coupled Dynabeads were washed with 900µL of EB and was placed on the tube containing solution for 1min, and the supernatant was removed. The antibody coupled Dynabeads were then resuspended in the prepared cell lysate and incubated on a roller at room temperature for 30 mins. The tube was then put on the magnet for 1 min and the supernatant was transferred to 'unbound' labelled tube. The tube was removed from the magnet and the solution was washed with 200µL of 1X IP by gentle pipetting. The tube was put on the magnet for 1 min and the supernatant was transferred to tube labelled IP1. This step was repeated twice, and the supernatant was transferred to tubes labelled IP2 and IP3. After the transfer of last supernatant, the Dynabeads were washed in 200µL of LWB, mixed by gentle pipetting and left on the roller at room temperature for 5 mins. The solution was kept on the magnet and the supernatant was transferred to LWB labelled tube. After the transfer the tube was removed from the magnet and the Dynabeads were suspended in 60µL of Elution Buffer (EB) and incubated on the roller for 5mins at room temperature. The tube was placed on the magnet and the supernatant contained the purified protein complex that was prepared for Western Blot, with UB as control and LWB as well. UB was prepared with 2µL of UB solution 10µL of phosphate buffer saline (PBS) mixed with 6µL DTT and 6 µL LDS and, EB and LWB were prepared with 2µL of sample mixed in 6µL of DTT and LDS each. All the samples were boiled at 70 deg. Celsius. The westerns were followed as mentioned in the methodology before. The primary antibodies used were HbA (abcam ab 227552 rabbit polyclonal) at a dilution 1:1000 and HbB (abcam ab82871 rabbit polyclonal) at a dilution 1:1000. The

secondary antibody was peroxidase conjugate goat anti-rabbit for 1h at room temp, at a 1:5000 dilution.

4.6.2 C.1 Results:

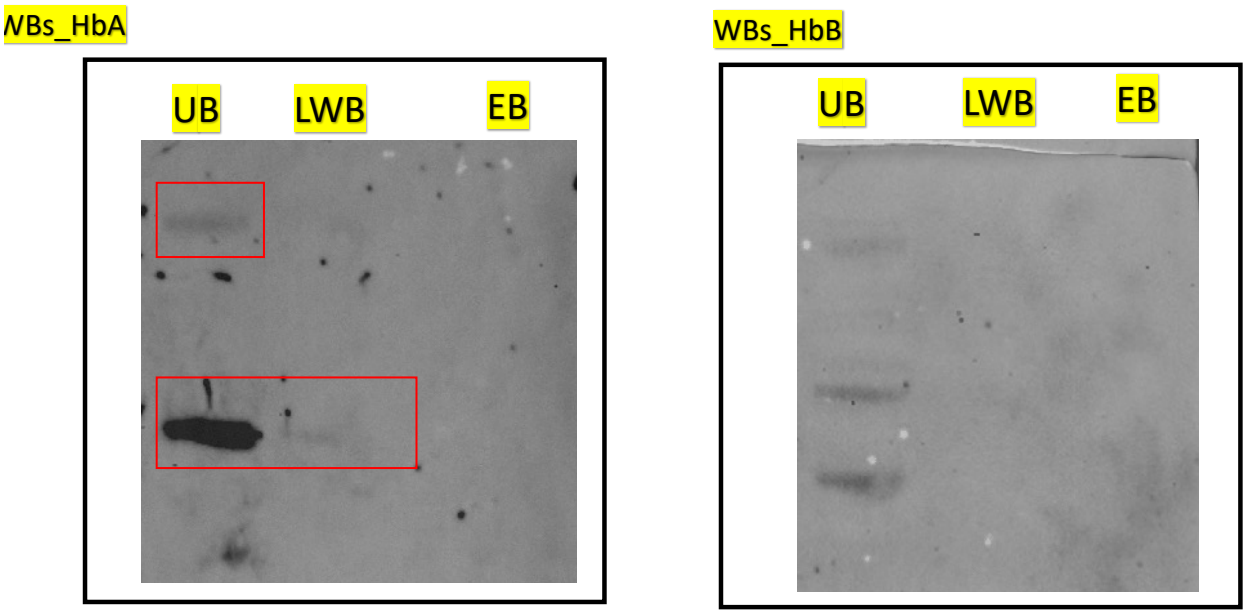

Figure 4-12. Co-immunoprecipitations' fractions were immunoblotted with HbA and HbB. A faint HbA antibody band was observed in the LWB lane (UB- unbound protein lane, EB-Eluted Buffer protein lane, LWB-Last wash buffer protein lane).

The red-muscle tissue cell lysate from *N. rossii* was used for co-immunoprecipitation with IF1 monoclonal antibody. The resulting fractions, unbound proteins used as a control, LWB and EB were used for western blots. The fractions were immunoblotted using HbA polyclonal (rabbit) and HbB polyclonal (rabbit) antibodies. The results showed HbA and HbB in the control lanes for the antibodies. A faint band of HbA was observed in the EB lane. No bands were observed for HbB antibody in LWB or EB lanes. The western blot will be repeated for confirming the HbA association with IF1 protein.

4.6.3 C.2 Methods:

The docking was done using the Patchdock and FireDock protein-protein docking protocol described before in the methodology for chapter 4.

4.6.4 C.2 Results:

This comparison docking of Hb with its known drug voxelotor, a small drug compound used for treating sickle-cell anaemia, which forms a bond with N-terminal end of α-chain of Hb. This was done as a relative test to see if the global energy were comparable. Since IF1 is a 80 residues protein yet, it showed a comparable global energy when compared to the small compound voxelotor.

a) Docking with Hb drug Voxelotor

b) Docking with atpif1

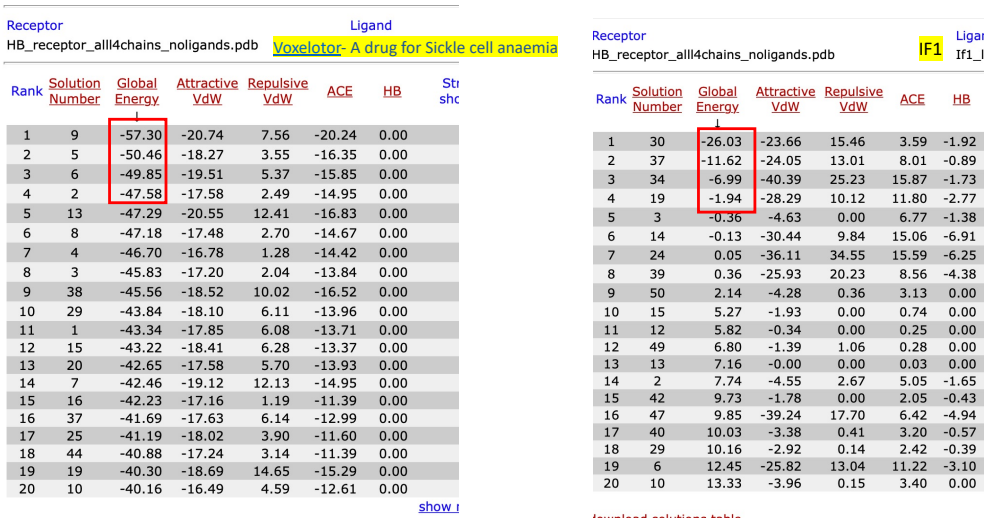

Receptor: HB_receptor_alll4chains_noligands.pdb | Ligand: Voxelotor- A drug for Sickle cell anaemia

Rank	Solution Number	Global Energy	Attractive VdW	Repulsive VdW	ACE	HB
1	9	-57.30	-20.74	7.56	-20.24	0.00
2	5	-50.46	-18.27	3.55	-16.35	0.00
3	6	-49.85	-19.51	5.37	-15.85	0.00
4	2	-47.58	-17.58	2.49	-14.95	0.00
5	13	-47.29	-20.55	12.41	-16.83	0.00
6	8	-47.18	-17.48	2.70	-14.67	0.00
7	4	-46.70	-16.78	1.28	-14.42	0.00
8	3	-45.83	-17.20	2.04	-13.84	0.00
9	38	-45.56	-18.52	10.02	-16.52	0.00
10	29	-43.84	-18.10	6.11	-13.96	0.00
11	1	-43.34	-17.85	6.08	-13.71	0.00
12	15	-43.22	-18.41	6.28	-13.37	0.00
13	20	-42.65	-17.58	5.70	-13.93	0.00
14	7	-42.46	-19.12	12.13	-14.95	0.00
15	16	-42.23	-17.16	1.19	-11.39	0.00
16	37	-41.69	-17.63	6.14	-12.99	0.00
17	25	-41.19	-18.02	3.90	-11.60	0.00
18	44	-40.88	-17.24	3.14	-11.39	0.00
19	19	-40.30	-18.69	14.65	-15.29	0.00
20	10	-40.16	-16.49	4.59	-12.61	0.00

show

Receptor: HB_receptor_alll4chains_noligands.pdb | Ligand: IF1

Rank	Solution Number	Global Energy	Attractive VdW	Repulsive VdW	ACE	HB
1	30	-26.03	-23.66	15.46	3.59	-1.92
2	37	-11.62	-24.05	13.01	8.01	-0.89
3	34	-6.99	-40.39	25.23	15.87	-1.73
4	19	-1.94	-28.29	10.12	11.80	-2.77
5	3	-0.36	-4.63	0.00	6.77	-1.38
6	14	-0.13	-30.44	9.84	15.06	-6.91
7	24	0.05	-36.11	34.55	15.59	-6.25
8	39	0.36	-25.93	20.23	8.56	-4.38
9	50	2.14	-4.28	0.36	3.13	0.00
10	15	5.27	-1.93	0.00	0.74	0.00
11	12	5.82	-0.34	0.00	0.25	0.00
12	49	6.80	-1.39	1.06	0.28	0.00
13	13	7.16	-0.00	0.00	0.03	0.00
14	2	7.74	-4.55	2.67	5.05	-1.65
15	42	9.73	-1.78	0.00	2.05	-0.43
16	47	9.85	-39.24	17.70	6.42	-4.94
17	40	10.03	-3.38	0.41	3.20	-0.57
18	29	10.16	-2.92	0.14	2.42	-0.39
19	6	12.45	-25.82	13.04	11.22	-3.10
20	10	13.33	-3.96	0.15	3.40	0.00

Figure 4-13. Comparison of overall docking scores of Hb and its known drug voxelotor and Hb and ATPIF1 using PatchDock docking and FireDock refinement tools.

4.6.5 C.3 Methods:

The docking was done using the HDOCK (Yan *et al.*, 2020) and ClusPro (protein-protein docking protocol using HbA alpha chain for the HDOCK and HB-all chains for ClusPro with IF1 minimised structure for both.

4.6.6 C.3 Results:

The docking with two automated protein-protein docking tool HDOCK that provides ab initio template free docking (**Supplementary Figure 3 A**). Since the tool only takes one peptide as an input, it was tested to see if it binds to HbA c-terminal residues. Interesting IF1 binds to residues seen in the docking with PatchDock best scored model for HbA and IF1. Similarly, ClusPro, taking Hb all chains as an input showed that IF1 interacts with HbA chains of haemoglobin and interacting with c-terminal end of HbA (**Supplementary Figure 3 A**). This supports the docking pose selection.

a) HDOCK docking tool

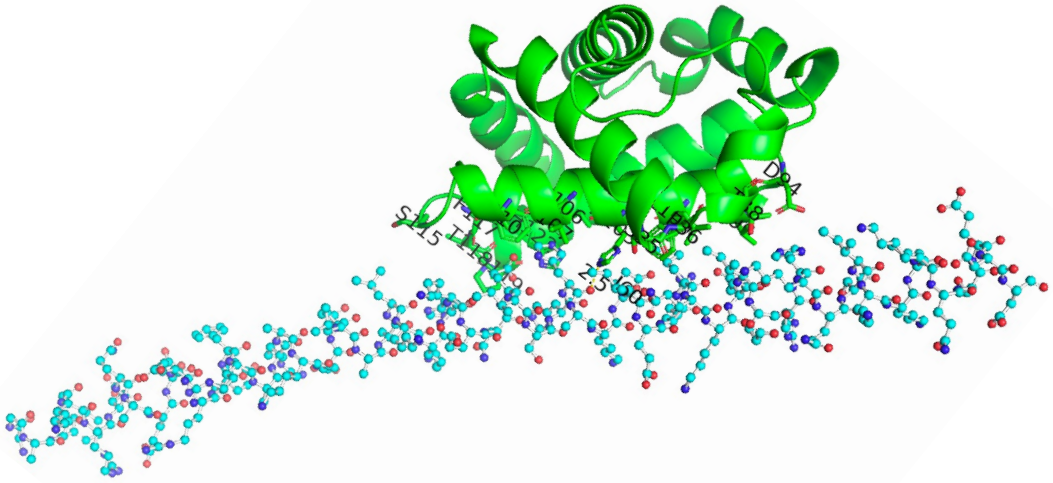

b) ClusPro docking tool

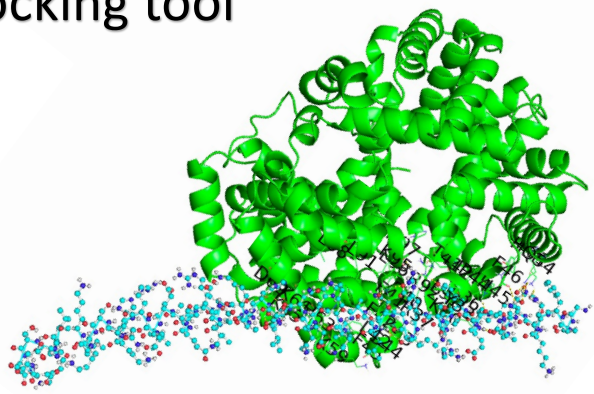

Figure 4-14. Best dock poses from servers HDOCK and ClusPro showing ATP-IF1 interacting with the c-terminal end residues of HbA (70-09).

4.6.7 Results

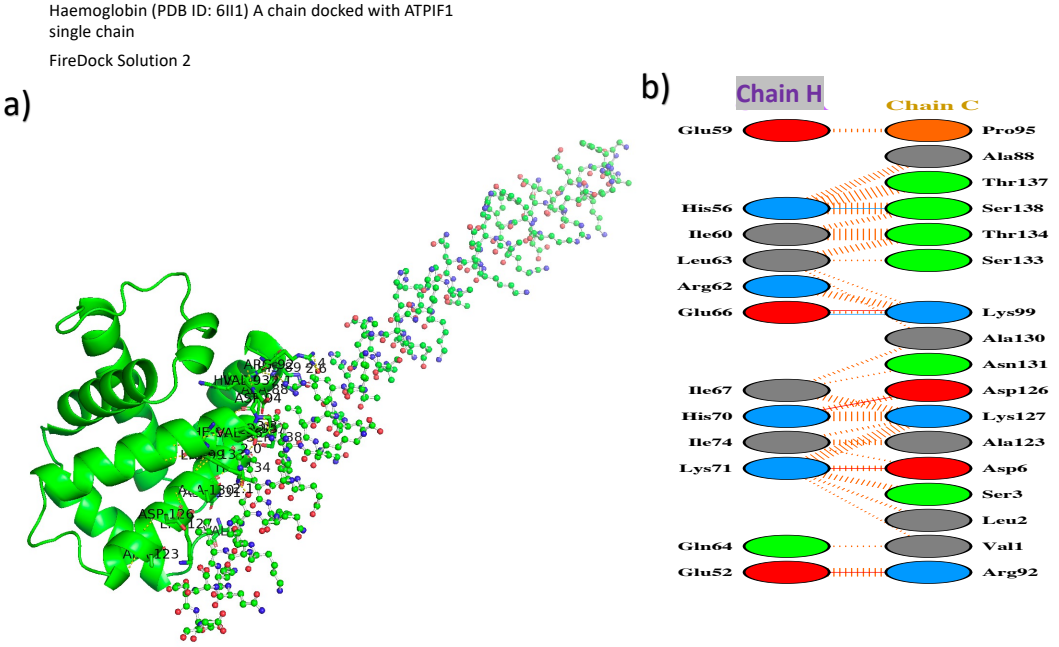

Figure 4-15. A) FireDock solution 2 HbA and ATPIF1. B) The interacting residues of second best docked pose using FireDock (Andrusier, Nussinov and Wolfson, 2007) refinement tool. (Hb PDB ID:6II1; ATPIF1 PDB ID: 1GMJ); Chain H-ATPIF1, Chain C-HbA.

Figure 4-16 shows the second-best docked pose of HbA and ATPIF1, where again the complex V inhibitor is seen to interact with IF1 residues at the C-terminal end. Interestingly, it also shows residues 1-3 & 6 of the N-terminal, these interacting residues were seen after the MD simulation run.

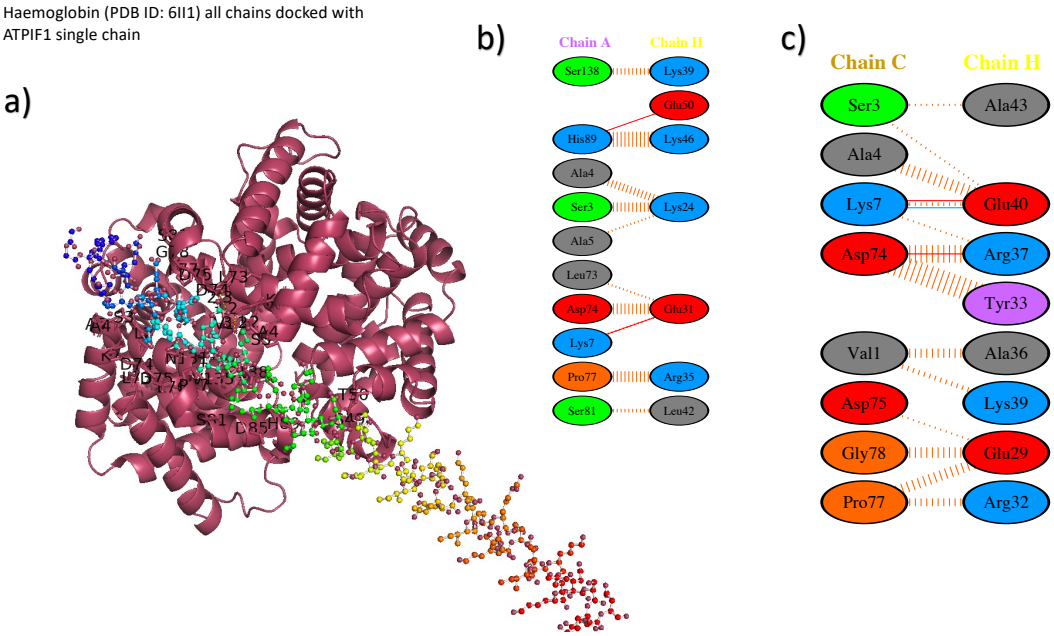

Figure 4-16. FireDock solution 3 Hb all chains and ATPIF1. B) The interacting residues of docked pose using FireDock (Andrusier, Nussinov and Wolfson, 2007) refinement tool. (Hb PDB ID:6II1; ATPIF1 PDB ID: 1GMJ); Chain H-ATPIF1, Chain C-HbA.

Figure 4-16, was the third solution from the FireDock (Andrusier, Nussinov and Wolfson, 2007) refinement tool, for Hb all chains and ATPIF1. The interacting residues were again very consistent as seen in the best docked structure and stabilised structure after the MD run. **Figure 4-17** was the second-best docked structure from FireDock results, and one of the two where ATPIF1 was seen interacting with a few residues at the centre of HbA and also the D chain of HbB. The other docked protein showing interactions with HbB and HbA was docked pose 10 which had high global energy (positive). This can be further confirmed by doing an MD run with docked pose 2 and see if the protein-complex is stable throughout the MD run or the interactions change back to our MD run.

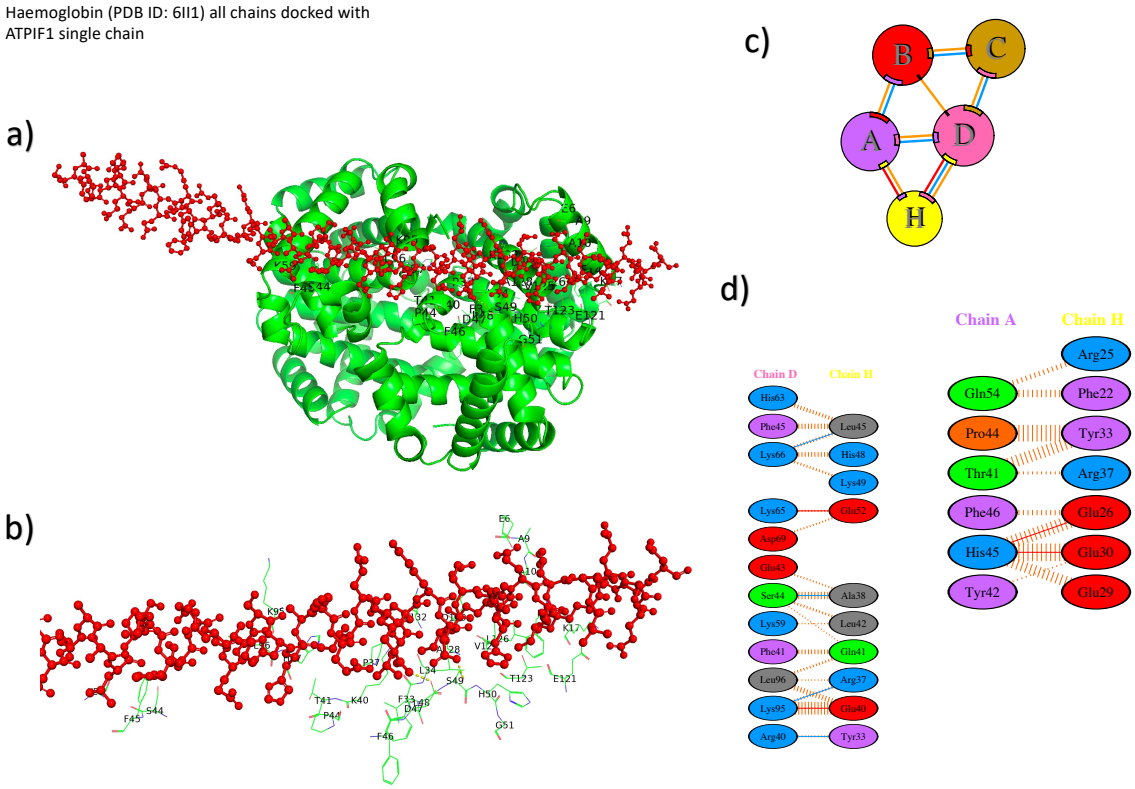

Figure 4-17. FireDock solution 8 Hb all chains and ATPIF1. B) The interacting residues of the docked pose using FireDock (Andrusier, Nussinov and Wolfson, 2007) refinement tool. (Hb PDB ID:6II1; ATPIF1 PDB ID: 1GMJ); Chain H-ATPIF1, Chain C-HbA, Chain D-HbB.

4.6.8 RESULTS

The equilibration plots show that the system prepared for MD run was stabilised at 305 K temperature, constant pressure, and density, where the whole system was minimised using robust steepest descent energy minimisation algorithm. The 8ns MD interaction of protein IF1 and Hb can be seen in the video.

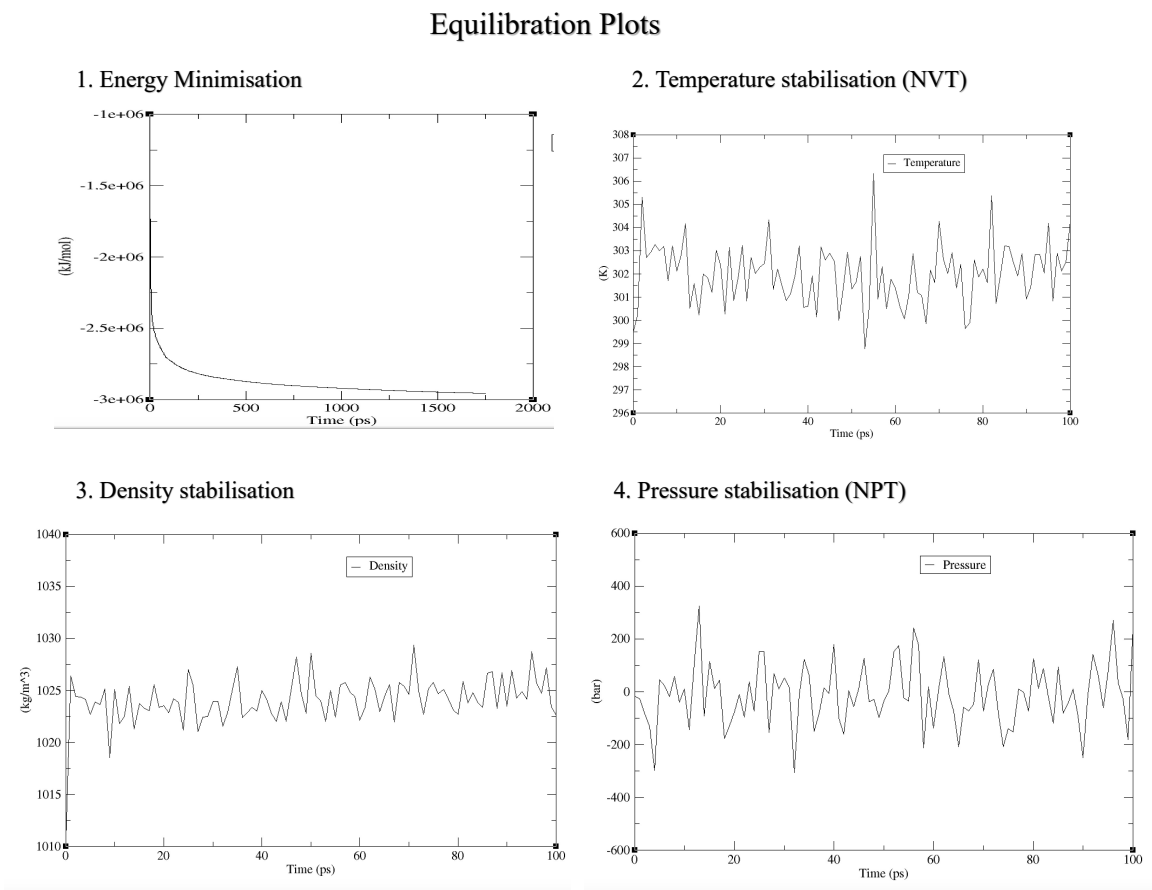

Figure 4-18. MD Simulation for Hb and IF1. a) Energy Minimisation of the system, demonstrating a nice steady convergence of potential energy. b) Temperature equilibration (NVT), the plot shows that temperature ranges 302-306 K (average temperature 305 K). c) Pressure equilibration, the pressure fluctuates but in the expected range maintaining the average value. d) Density equilibration, the density plot is very close to the expected values and is stable over time.

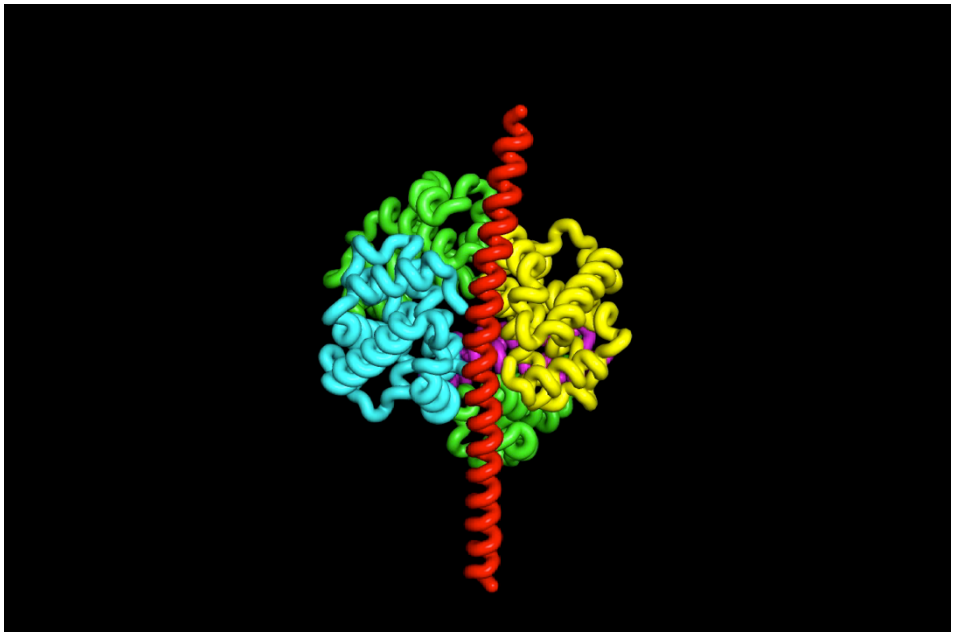

An Mpg video of 8ns simulation showing the interaction of ATPIF1 with Haemoglobin.

Chapter 5 : DISCUSSION

5.1 Discussion

Life evolved from single cell to multi-cellular organisms, is dependent on the highly specialised molecular machines, that we know as proteins and their functional interactions.
The protein-protein interactions occur at both inter and intra-cellular levels making it complex and essential for an overall analysis of their mechanism to understand various cellular functions. Mitochondria are essential for several cellular processes, yet many of the mitochondrial proteins are either uncharacterised or fully annotated [1]. A consistent effort of large-scale proteomics and computational tools have helped in establishing mitochondrial proteome much more efficiently. This has helped to understand many dysfunctions of these organelles to be associated with many diseases and disorders [2]. Many transient interactions that take place in the cell modifying the behaviour of the proteins and modulating different pathways [3,4]. The dynamic localisation of protein Hb in different cellular compartments could be argued against that its only role is in transporting oxygen and carbon dioxide.

All vertebrates have haemoglobin (Hb) in their blood but the exception to this is a small family of fish living in the cold waters of Antarctica, the unique Antarctic icefish, of the Channichthyidae family of the sub-order Notothenioidei. Haemoglobin is an important protein that predates the origin of animals and links many species. It has been suggested that changes in the molecule was seen in neurodegenerative diseases and argued its role as a drug receptor. Neurodegeneration is directly affected by a rather fundamental yet inevitable phenomenon of ageing as discussed previously and direct and indirect evidence have shown mitochondria dysfunction as one of the hallmarks of the neurodegenerative diseases.

The theory behind this project is that oxygen carrying haemoglobin is localised in the mitochondria where its presence might influence other proteins situated there. The icefish that are the only organisms without Hb and can act as a perfect model to understand the differences observed in the presence/absence of this protein. This can be done by recording subtle changes that occur at cellular level and answer a long-standing question of proteins use information about their surroundings to make adaptive responses. The data generated in this thesis is to help understand the role of mitochondrial haemoglobin and its interacting partners (protein) which might help shed light on how these fish survive and indirectly help understand haemoglobin's role apart from carrying oxygen especially in the studies of ageing and neurodegeneration.

Protein function and protein-protein interactions are highly dependent on their primary sequence, structure, their dynamics, and stability. A number of research suggests that Hb has a dynamic location [5–9] and is not just found in the red-blood cells as previously believed. The presence of Hb in in the mitochondria could influence its machinery, specifically oxidative phosphorylation. Previously there have been studies connecting haemoglobin and neurodegeneration. There has been enough evidence on change in expression of Hb as discussed in our introduction.

Mitochondrial ATP production via the OxPhos system is the main source of energy in cells for intracellular metabolic pathways. The complex V or ATP synthase (ATPase) is the fifth multi-subunit enzyme of the OxPhos system. The complex consists of two components, the F_1, catalytic part and, the F_o component, that is the motor part.

Complex V is composed of 15 structural and two assembly subunits encoded by both the nuclear and mitochondrial genomes.

5.1.1 Chapter 2 - ATP6 of the proton pump

In the first chapter of this thesis, we have looked at the two subunits of Fo component of ATP synthase, ATP6, also known as subunit a, and ATP8. The aim was to see whether there were sequential or structural changes in the proteins of the haemoglobin-less fish for these proteins. The mitochondria of these fish have significant modifications, such as tight coupling of the mitochondria to facilitate sustained oxygen and hence we wanted to see the proteins that are directly involved in proton translocation. ATP6 and ATP8 are two mitochondrial encoded proteins that are overlapping in the genome. Subunit a, encoded by gene ATP6, contains the proton channel that releases the proton gradient established across the inner mitochondrial membrane. There have been numerous studies that have reported mutations in the mitochondrial encoded protein ATP6 that have directly associated with mitochondrial diseases [10–12] in humans including neurodegenerative diseases [13–16]. Simple four-point mutations in the gene can lead to a disease [13–15]. A mutation in the gene for ATP6 doesn't necessarily impact the inherent activity of the enzyme but rather has a direct functional impairment of the coupling of proton pumping and ATP synthesis [12,17–20]. Interestingly about 45 years ago it was reported that Hb has ATP binding sites and changes have been observed in the phosphate groups of the ATP in the presence and absence of Hb [21] and there has been evidence for Hb to modulate energy mechanism in high demanding tissues such as neurons [22].

This led our interest to investigate if there were any sequential changes in the gene/protein for ATP6 in the icefish and other notothenioid fish. Since the protein is prone to single mutations manifesting into a physiological or pathological change for the protein it was important to check the genomic sequence for ATP6. Our first observation with the genomic sequences was there was an addition of 12 nucleotides (nt) at the N-terminal end of the gene for the five Antarctic fish species, of the sub-order Notothenioidei, including the red-blooded *N. corriceps*, *T. bernacchii*, sub-Antarctic red-blooded species, *E. maclovinus* and the two icefish *C. rastrospinosus* (devoid of Hb and has Mb) *C. aceratus* (devoid of Hb, has remnant 3' fragment of HbA, do not express Mb but have a nearly identical gene to that of *C. rastrospinosus* for Mb). The only exception, is the icefish *C. gunnari* which is an extreme case of complete loss of Hb and Mb that does not have the addition of 12 nucleotide. Interestingly, length of nt in *C. gunn*ari is the same as the other vertebrates, including mammals such as *H. sapiens* (humans) and *C. porcellus* (guinea pig). The change observed in the gene length could be attributed an altered variation of the gene for this fish. The other observation that was important to the study was these additional nucleotide sequences start with an alternative codon "GTG", which has been previously observed more in recent studies for the mitochondrial genome. Again, the exception to this was *C. gunnari* icefish like the other vertebrate species. Alternative codons have come into light in the recent years where for very long only "ATG" was an accepted start codon. As explained previously an alternate initiation codon for protein ATP6 can suggest a common parallel evolution translation machinery. The favouring of GTG as a start codon can indicate higher stability of the protein as GC base pair due to its higher thermal stability. This raises the question whether the red-blooded counter parts of

the Antarctic icefish have evolved more to retain the globins whereas *C. gunnari* is just another fish that lost its haemoglobin due to environmental factors. Another important observation was made with codon alignment of the genes that serine encoded by codon TCT/TCC at position 39 for all species except *C. gunnari* that had GCT instead, which codes for the amino acid serine. As previously mentioned, point mutations in ATP6 has led to altered pathology more regarding the proton pumping activity of ATP synthase. An alanine in this position seems like a mutation non-synonymous base substitution of thymine to guanine at N1 position, from TCT serine to GCT alanine.

5.1.2 Chapter 3- Differential expression of Mitochondrial proteins.

Protein-protein interactions (PPI) are important for many biological processes including cell signalling, metabolic pathways and development [23]. The PPI knowledge and data has expanded in recent years with technologies like mass spectrometry, two-hybrid systems, and phage display to name a few [24]. In the second chapter of my thesis, we employed liquid chromatography with tandem mass spectrometry (LC-MS/MS) for mitochondria fractions from skeletal muscle tissues, red muscle tissue, and white muscle tissue of Antarctic fish species, the red-blooded fish, *N. rossii*, *T. bernacchii* (the controls for experiment), and icefish *C. rastrospinosus* (has Mb expression only in cardiac myocytes, and 3' remnant of HbA), and *C. gunnari*, previously discussed the extreme case of no Hb or Mb [25,26]. The purpose of this experiment was to find and understand the changes that might have occurred in the mitochondria, at protein expression level, in these fish without Hb. It has been previously reported that the icefish has an exceptionally high mitochondrial density that helps in oxygen storage [27]. The question that arises with this is: does Hb help in storage of oxygen in mitochondria when the need arises and hence icefish requires an extreme modification for their mitochondria?

We chose the two different muscle tissues, the red muscle is a slow-twitch fibre where the major source of energy comes from OxPhos, and white muscle is a fast-twitch fibre where anaerobic energy is utilised to meet the demands of fast-twitch fibre [28]. Both the tissues contain numerous mitochondria to support our study [29]. Cellular respiration is the primary means of energy production in the Antarctic fishes as they have reduced anaerobic capacity when compared to their temperate teleost. As we know ATP production is the primary function of skeletal muscle mitochondria and it has been observed during acclimation that aerobic enzymes are notably high for the organism [30,31]. It has been suggested that a higher demand for mitochondria biogenesis might be present in the icefish which could be achieved by increased supply of mitochondrial components through mutations at genetic levels and selective increase or decrease of mitochondrial protein's expression level [32]. This has been tested previously at transcriptomic level for icefish *Chionodraco hamatus* [32] but not for protein expression until now. Hence a comparative approach was chosen to find differentially expressed proteins in the icefish while comparing to their closely related species that has haemoglobin. The expression of Hb was found only in the red-blooded species and not in the icefish.

In the study we observed eighty-two differentially expressed proteins (DEPs) in the mitochondria of the red muscle tissue for the icefish. A total number of seventy DEPs were recorded for the mitochondria of white muscle tissue for the icefish. In the red muscle mitochondria (RMM), the proteins that were seen significantly higher in number in the icefish when compared to the red-blooded closely related species, were proteins involved in energy metabolism, specifically complex V of the OxPhos were seen as a compact cluster. The subunits ATP synthase, gamma (γ), subunit O, subunit b1 (F0 complex), subunit delta, subunit g and subunit d were seen comparatively higher in the icefish. The subunit gamma during ATP synthesis, the proton movement rotates the assembly of γ, with other two subunits c and ε, changing the conformation of catalytic sites to release ATP. The other subunits d, b1, g is part of the transmembrane rotatory motor F0 and helps in proton translocation. The other proteins that were seen significantly increased were, proteins involved protein transport,
ADP/ATP translocase 2 and ADP/ATP translocase 3, Aralar, a calcium binding mitochondrial, carnitine/acylcarnitine carrier translocase protein, and VDAC/VDAC3 another protein to transport ATP and other metabolites. The activity of these translocases depends on availability of ADP/ATP or/and the membrane potential and act as contact points between the inner and outer mitochondrial membrane. Previously, it has been seen in pyramidal neurons, that HbB interacts with ADP/ATP translocase, acting as an energy sensor, which might indicate a selective increase of these proteins as a response to absence of HbB in the icefish [33]. A comparable increase in some ribosomal proteins was observed in the icefish mitochondria.

The protein network of down-regulated in the icefish in both red-muscle mitochondria and white muscle mitochondria showed hub-proteins: NEB, CKMB, MYBPC1, MYBPC2B, TTN and CYCSB. All these proteins are part of muscle assembly and contraction. The muscle proteins include structural and contractile proteins (actins, myosin, and troponin) as well as soluble muscle protein enzymes (creatine kinase). A common decrease of protein creatine kinase was observed, which plays a role in maintaining ATP levels, this could be attributed to enlarged mitochondria in the icefish which might decrease the distance for the diffusion of oxygen and for ATP between mitochondria and myofibril which might reduce the demand for CK [34]. The complete loss of expression of the enzyme is observed previously in the heart ventricle of icefish, *C. aceratus* and *C. gunnari*, where these species rely majorly on fatty acid oxidation for cardiac energy requirements [35,36]. Notothenioids lacking mtCK may compensate by increasing levels of ADP/ATP nucleotide translocases and VDACs, as observed in our proteomics study as well. The other proteins that were seen to be lowered in the icefish involved in redox metabolism, GCDH and Aldh7aq. All the haem associated proteins were significantly lower in the mitochondria of the icefish.

5.1.3 Chapter 4- HbA has a role in modulating IF1?

Many studies suggest that haemoglobin has variety of roles in the endothelium In vertebrates such as vascular remodelling through endothelial nitric oxide signalling [5,6]. Studies have also shown Hb playing a role as an energy sensor, as discussed previously [33]. There also have been links between neuronal expression of Hb in regulating stress response in relative to ATP concentration and mitochondrial function [22]. ATP synthase Inhibitor Factor 1 (ATPIF1) is a natural regulator of ATP synthesis and hydrolysis activities of the complex V, and hence keeps the ATP levels and membrane potential intact in the mitochondria. ATPIF1 is previously reported as a regulator of haem synthesis indicating interdependence of mitochondrial homeostasis and haem synthesis [37]. It is still unclear where the inactive ATPIF1 binds when it is not bound to ATP synthase subunits, with one study directly suggesting it binds to an unknown inner membrane protein [38]. A few studies have also shown it to interact with other inner mitochondrial proteins [39–41] supporting roles for IF1 in addition to modulating ATP synthase. We wanted to see whether ATPIF1 interacts with Hb using docking studies. Hb showed relative affinity for IF1 when compared to an already known drug inhibitor, voxelotor. To further this, we used MD simulations to see the stability of the docked structures of IF1 and Hb, where HbA shown interacting with IF1 residues mainly 35-70 of the c-terminal end. Further experimental studies would require confirming this hypothesis.

5.1 Conclusions

In conclusion, mitochondria are crucial organelles for most of the energy production of the cell. As discussed previously mitochondria are significantly compromised/altered in ageing, neurodegeneration, and cancer [42,43]. The role of haemoglobin for transporting O_2 is established, but it's presence in mitochondria [44,45] is very novel and can contribute to our basic understanding of mitochondrial biology in science and medicine. The haemoglobin interactome would change are view of mitochondrial specific networks and could be targeted for therapeutics in ageing, neurodegeneration and cancer diseases. Point mutations in *mt*DNA encoded proteins can be seen more extensively. The changes in protein expression observed in the muscle tissues of icefish highlight pathways modulated in the absence of Hb, which can further be explored as therapeutic targets to support mitochondria in health and disease. Lastly, interaction of the natural inhibitor of Complex V of OxPhos, ATPIF1 with mitochondrial Hb can help us delve into deeper understanding of the energy mechanism, which is at the heart of the mitochondria. Hence the thesis adds onto substantiate our understanding of mitochondrial Hb and its putative role.

5.2 Future Work

Further experimental studies would be required to confirm this hypothesis. Experimental techniques such as far western blot can be used for mitochondrial extracts from different species to support and establish direct contacts between mitochondrial protein and mitochondrial Hb. Further the sub-mitochondrial location of these interactions can also be established by subcellular fractionation and immunoblotting techniques. Techniques involving globin knock-downs specifically in organisms such as *Caenorhabditis elegans* using RNAi constructs and observe changes in their mitochondria and compare it with our already established proteomes in the icefish. ATP production assays can be further employed to measure ATP and cell viability.

5.3 Reference:

1. Calvo SE, Clauser KR, Mootha VK. MitoCarta2.0: an updated inventory of mammalian mitochondrial proteins. Nucleic Acids Res. 2016;44: D1251–D1257. doi:10.1093/nar/gkv1003
2. Nunnari J, Suomalainen A. Mitochondria: in sickness and in health. Cell. 2012;148: 1145–1159. doi:10.1016/j.cell.2012.02.035
3. Higurashi M, Ishida T, Kinoshita K. Identification of transient hub proteins and the possible structural basis for their multiple interactions. Protein Sci. 2008;17: 72–78. doi:https://doi.org/10.1110/ps.073196308
4. Singh GP, Ganapathi M, Dash D. Role of intrinsic disorder in transient interactions of hub proteins. Proteins Struct Funct Bioinforma. 2007;66: 761–765. doi:https://doi.org/10.1002/prot.21281
5. Straub AC, Lohman AW, Billaud M, Johnstone SR, Dwyer ST, Lee MY, et al. Endothelial cell expression of haemoglobin α regulates nitric oxide signalling. Nature. 2012;491: 473–477. doi:10.1038/nature11626
6. Lechauve C, Butcher JT, Freiwan A, Biwer LA, Keith JM, Good ME, et al. Endothelial cell α-globin and its molecular chaperone α-hemoglobin-stabilizing protein regulate arteriolar contractility. J Clin Invest. 2018;128: 5073–5082. doi:10.1172/JCI99933
7. Shephard F, Greville-Heygate O, Marsh O, Anderson S, Chakrabarti L. A mitochondrial location for haemoglobins-Dynamic distribution in ageing and Parkinson's disease. Mitochondrion. 2014;14: 64–72. doi:10.1016/j.mito.2013.12.001
8. Shephard F, Greville-Heygate O, Liddell S, Emes R, Chakrabarti L. Analysis of Mitochondrial haemoglobin in Parkinson's disease brain. Mitochondrion. 2016;29: 45–52. doi:10.1016/j.mito.2016.05.001
9. Corliss BA, Delalio LJ, Stevenson Keller TC, Keller AS, Keller DA, Corliss BH, et al. Vascular Expression of Hemoglobin Alpha in Antarctic Icefish Supports Iron Limitation as Novel Evolutionary Driver. Front Physiol. 2019;10. doi:10.3389/fphys.2019.01389
10. Jesina P, Tesarová M, Fornůsková D, Vojtísková A, Pecina P, Kaplanová V, et al. Diminished synthesis of subunit a (ATP6) and altered function of ATP synthase and cytochrome c oxidase due to the mtDNA 2 bp microdeletion of TA at positions 9205 and 9206. Biochem J. 2004;383: 561–571. doi:10.1042/BJ20040407
11. Alila-Fersi O, Chamkha I, Majdoub I, Gargouri L, Mkaouar-Rebai E, Tabebi M, et al. Co segregation of the m.1555A>G mutation in the MT-RNR1 gene and mutations in MT-ATP6 gene in a family with dilated mitochondrial cardiomyopathy and hearing loss: A whole mitochondrial genome screening. Biochem Biophys Res Commun. 2017;484: 71–78. doi:10.1016/j.bbrc.2017.01.070
12. Hao X, Liu S, Wu X, Hao Y, Chen Y. Infantile mitochondrial disorder associated with subclinical hypothyroidism is caused by a rare mitochondrial DNA 8691A>G mutation: a case report. Neuroreport. 2015;26: 588–592. doi:10.1097/WNR.0000000000000392
13. Pfeffer G, Blakely EL, Alston CL, Hassani A, Boggild M, Horvath R, et al. Adult-onset spinocerebellar ataxia syndromes due to MTATP6 mutations. J Neurol Neurosurg Psychiatry. 2012;83: 883–886. doi:10.1136/jnnp-2012-302568

14. Pitceathly RDS, Murphy SM, Cottenie E, Chalasani A, Sweeney MG, Woodward C, et al. Genetic dysfunction of MT-ATP6 causes axonal Charcot-Marie-Tooth disease. Neurology. 2012;79: 1145–1154. doi:10.1212/WNL.0b013e3182698d8d
15. Verny C, Guegen N, Desquiret V, Chevrollier A, Prundean A, Dubas F, et al. Hereditary spastic paraplegia-like disorder due to a mitochondrial ATP6 gene point mutation. Mitochondrion. 2011;11: 70–75. doi:https://doi.org/10.1016/j.mito.2010.07.006
16. Duno M, Wibrand F, Baggesen K, Rosenberg T, Kjaer N, Frederiksen AL. A novel mitochondrial mutation m.8989G>C associated with neuropathy, ataxia, retinitis pigmentosa - the NARP syndrome. Gene. 2013;515: 372–375. doi:10.1016/j.gene.2012.12.066
17. Burrage LC, Tang S, Wang J, Donti TR, Walkiewicz M, Luchak JM, et al. Mitochondrial myopathy, lactic acidosis, and sideroblastic anemia (MLASA) plus associated with a novel de novo mutation (m.8969G>A) in the mitochondrial encoded ATP6 gene. Mol Genet Metab. 2014;113: 207–212. doi:10.1016/j.ymgme.2014.06.004
18. Honzik T, Tesarova M, Magner M, Mayr J, Jesina P, Vesela K, et al. Neonatal onset of mitochondrial disorders in 129 patients: clinical and laboratory characteristics and a new approach to diagnosis. J Inherit Metab Dis. 2012;35: 749–759. doi:10.1007/s10545-011-9440-3
19. López-Gallardo E, Solano A, Herrero-Martín MD, Martínez-Romero I, Castaño-Pérez MD, Andreu AL, et al. NARP syndrome in a patient harbouring an insertion in the MT-ATP6 gene that results in a truncated protein. J Med Genet. 2009;46: 64–67. doi:10.1136/jmg.2008.060616
20. Vázquez-Memije ME, Shanske S, Santorelli FM, Kranz-Eble P, DeVivo DC, DiMauro S. Comparative biochemical studies of ATPases in cells from patients with the T8993G or T8993C mitochondrial DNA mutations. J Inherit Metab Dis. 1998;21: 829–836. doi:10.1023/a:1005418718299
21. Costello AJR, Marshall WE, Omachi A, Henderson TO. (Received November 8th, 1976). 1977;491: 469–472.
22. Codrich M, Bertuzzi M, Russo R, Francescatto M, Espinoza S, Zentilin L, et al. Neuronal hemoglobin affects dopaminergic cells' response to stress. Cell Death Dis. 2018;8: e2538–e2538. doi:10.1038/cddis.2016.458
23. Braun P, Gingras A-C. History of protein-protein interactions: from egg-white to complex networks. Proteomics. 2012;12: 1478–1498. doi:10.1002/pmic.201100563
24. Pan A, Lahiri C, Rajendiran A, Shanmugham B. Computational analysis of protein interaction networks for infectious diseases. Brief Bioinform. 2016;17: 517–526. doi:10.1093/bib/bbv059
25. Johan T. Ruud. Vertebrates without Erythrocytes and Blood Pigment. Nature. 1954;173: 848–850.
26. Sidell BD, Vayda ME, Small DJ, Moylan TJ, Londraville RL, Yuan ML, et al. Variable expression of myoglobin among the hemoglobinless Antarctic icefishes. Proc Natl Acad Sci U S A. 1997;94: 3420–3424. doi:10.1073/pnas.94.7.3420
27. O'Brien KM, Mueller IA. The unique mitochondrial form and function of antarctic channichthyid icefishes. Integr Comp Biol. 2010;50: 993–1008. doi:10.1093/icb/icq038
28. Huang YC, Dennis RG, Baar K. Cultured slow vs. fast skeletal muscle cells differ in physiology and responsiveness to stimulation. Am J Physiol - Cell Physiol. 2006;291: 11–17. doi:10.1152/ajpcell.00366.2005
29. Archer SD, Johnston IA. Density of Cristae and Distribution of Mitochondria in

the Slow Muscle Fibers of Antarctic Fish. Physiol Zool. 1991;64: 242–258. doi:10.1086/physzool.64.1.30158522
30. Lucassen M, Koschnick N, Eckerle LG, Pörtner H-O. Mitochondrial mechanisms of cold adaptation in cod (Gadus morhua L.) populations from different climatic zones. J Exp Biol. 2006;209: 2462–2471. doi:10.1242/jeb.02268
31. Orczewska JI, Hartleben G, O'Brien KM. The molecular basis of aerobic metabolic remodeling differs between oxidative muscle and liver of threespine sticklebacks in response to cold acclimation. Am J Physiol Regul Integr Comp Physiol. 2010;299: R352-64. doi:10.1152/ajpregu.00189.2010
32. Coppe A, Agostini C, Marino IAM, Zane L, Bargelloni L, Bortoluzzi S, et al. Genome evolution in the cold: Antarctic icefish muscle transcriptome reveals selective duplications increasing mitochondrial function. Genome Biol Evol. 2013;5: 45–60. doi:10.1093/gbe/evs108
33. Brown N, Alkhayer K, Clements R, Singhal N, Gregory R, Azzam S, et al. Neuronal Hemoglobin Expression and Its Relevance to Multiple Sclerosis Neuropathology. J Mol Neurosci. 2016;59: 1–17. doi:10.1007/s12031-015-0711-6
34. O'Brien KM, Mueller IA. The unique mitochondrial form and function of antarctic channichthyid icefishes. Integr Comp Biol. 2010;50: 993–1008. doi:10.1093/icb/icq038
35. Crockett EL, Sidell BD. Some Pathways of Energy Metabolism Are Cold Adapted in Antarctic Fishes. Physiol Zool. 1990;63: 472–488. doi:10.1086/physzool.63.3.30156223
36. O'Brien KM, Mueller IA, Orczewska JI, Dullen KR, Ortego M. Hearts of some Antarctic fishes lack mitochondrial creatine kinase. Comp Biochem Physiol - Part A Mol Integr Physiol. 2014;178: 30–36. doi:10.1016/j.cbpa.2014.08.003
37. Shah DI, Takahashi-Makise N, Cooney JD, Li L, Schultz IJ, Pierce EL, et al. Mitochondrial Atpif1 regulates haem synthesis in developing erythroblasts. Nature. 2012;491: 608–612. doi:10.1038/nature11536
38. LOPEZ-MEDIAVILLA C, VIGNY H, GODINOT C. Docking the mitochondrial inhibitor protein IF1 to a membrane receptor different from the F1-ATPase β subunit. Eur J Biochem. 1993;215: 487–496. doi:10.1111/j.1432-1033.1993.tb18058.x
39. Ichikawa N, Nakabayashi K, Hashimoto T. A Yeast Mitochondrial ATPase Inhibitor Interacts with Three Proteins That Are Easy to Dissociate from the Mitochondrial Inner Membrane. J Biochem. 2002;132: 649–654. doi:10.1093/oxfordjournals.jbchem.a003269
40. Shen L, Zhi L, Hu W, Wu MX. IEX-1 targets mitochondrial F1Fo-ATPase inhibitor for degradation. Cell Death Differ. 2009;16: 603–612. doi:10.1038/cdd.2008.184
41. Minauro-Sanmiguel F, Bravo C, García JJ. Cross-linking of the endogenous inhibitor protein (IF1) with rotor (γ, ε) and stator (α) subunits of the mitochondrial ATP synthase. J Bioenerg Biomembr. 2002;34: 433–443. doi:10.1023/A:1022514008462
42. López-Otín C, Blasco MA, Partridge L, Serrano M, Kroemer G. The Hallmarks of Aging. Cell. 2013;153: 1194–1217. doi:https://doi.org/10.1016/j.cell.2013.05.039
43. Sun N, Youle RJ, Finkel T. The Mitochondrial Basis of Aging. Mol Cell. 2016;61: 654–666. doi:10.1016/j.molcel.2016.01.028
44. Shephard F, Greville-Heygate O, Liddell S, Emes R, Chakrabarti L. Analysis of Mitochondrial haemoglobin in Parkinson's disease brain. Mitochondrion.

2016;29: 45–52. doi:10.1016/j.mito.2016.05.001
45. Shephard F, Greville-Heygate O, Marsh O, Anderson S, Chakrabarti L. A mitochondrial location for haemoglobins—Dynamic distribution in ageing and Parkinson's disease. Mitochondrion. 2014;14: 64–72. doi:10.1016/J.MITO.2013.12.001